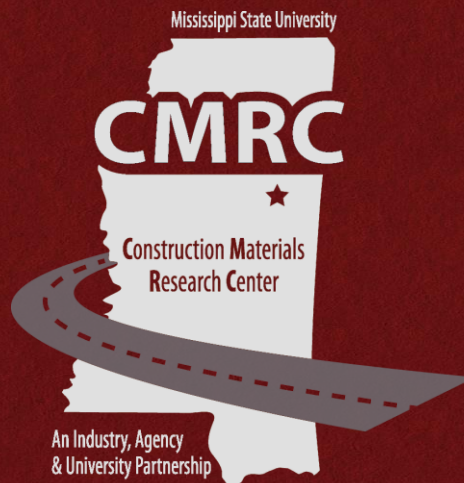


Columbus Mississippi Field Aging and Laboratory Conditioning Study: Plant Mixed and Laboratory Compacted Asphalt Mixtures

Report Written and Performed By:

Isaac L. Howard – Mississippi State University
Rabeea W. Bazuhair – Mississippi State University
Carl V. Pittman – Mississippi State University
Braden T. Smith – Mississippi State University

Final Report
FHWA/MS-DOT-RD-18-266/270-Volume 3
December 2018



Technical Report Documentation Page

1. Report No. FHWA/MS-DOT-RD-18-266/270-Volume 3	2. Government Accession No.	3. Recipient's Catalog No.	
4. Title and Subtitle Columbus Mississippi Field Aging and Laboratory Conditioning Study: Plant Mixed and Laboratory Compacted Asphalt Mixtures		5. Report Date December 2018	
		6. Performing Organization Code	
7. Author(s) <i>Isaac L. Howard</i> , Materials and Construction Industries Chair, MSU <i>Rabeea W. Bazuhair</i> , Graduate Research Assistant, MSU <i>Carl V. Pittman</i> , Alumni, MSU <i>Braden T. Smith</i> , Alumni, MSU		8. Performing Organization Report No.	
9. Performing Organization Name and Address Mississippi State University (MSU) Civil and Environmental Engineering Department 501 Hardy Road: P.O. Box 9546 Mississippi State, MS 39762		10. Work Unit No. (TRAIS)	
		11. Contract or Grant No.	
12. Sponsoring Agency Name and Address Mississippi Department of Transportation (MDOT) Research Division P.O. Box 1850 Jackson, MS 39215-1850		13. Type of Report and Period Covered Final Report March 2013 to June 2018	
		14. Sponsoring Agency Code	
Supplementary Notes: Work was performed under Mississippi State University projects titled: Asphalt Mixture Field Aging Study Preliminary Testing (Project No. 106526 101000), Field Aging Effects on Asphalt Mixed at Different Temperatures and Hauled Different Distances (State Study 266), and Laboratory Conditioning and Field Aging of Asphalt Mixtures (State Study 270). All work performed for this report was under principal investigator Isaac L. Howard. Two additional reports were performed as part of Project 106526 101000, State Study 266, and State Study 270, which were designated FHWA/MS-DOT-RD-18-266/270-Volume 1 and FHWA/MS-DOT-RD-18-266/270-Volume 2. Both additional volumes deal with field aging of asphalt mixtures and all three reports complement each other.			
16. Abstract The main objective of this report was to characterize asphalt containing warm mix technologies at various levels of field aging and laboratory conditioning in terms of mixture and binder properties encompassing the temperature range expected in Mississippi. The primary data sets collected for this overall body of work are from full-scale constructed test sections where cores were collected over time (Volume 2), and from plant mixed asphalt containing warm mix technology that was field aged for four years or laboratory conditioned (Volume 3). Approximately 5,100 mixture specimens were tested as part of this three volume set of reports. When rounded to the nearest hundred mixture specimens, 300 were tested for Volume 1, 3,400 were tested for Volume 2, and 1,400 were tested for Volume 3. Binder testing was also performed in support of mixture testing. A primary recommendation of this work is to use Cantabro Mass Loss (CML) for assessment of environmental effects, and in particular combined effects of oxidation, moisture, and freeze-thaw (FT). The default recommendation is to compact an asphalt specimen, then expose this specimen to 5 days of 85 °C air, followed by 14 days submerged in 64 °C water, and 1 FT cycle before testing for CML. Based on findings from this collective body of work (Volumes 1 to 3), this appears to simulate 4.0 to 5.5 years of aging in the Mississippi climate. It is also recommended that all three warm mix technologies evaluated in this paper be allowed for consideration to optimize a given project. This recommendation was based on none of the technologies holistically behaving better or worse than the others, while also not being dramatically different than hot mixed asphalt that was also evaluated in this report.			
17. Key Words WMA, Aging, Cantabro, Sasobit, Evotherm, Foam, Fracture Energy		18. Distribution Statement No distribution restrictions.	
19. Security Classif. (of this report) Unclassified	20. Security Classif. (of this page) Unclassified	21. No. of Pages 144	22. Price

NOTICE

The contents of this report reflect the views of the author, who is responsible for the facts and accuracy of the data presented herein. The contents do not necessarily reflect the views or policies of the Mississippi Department of Transportation or the Federal Highway Administration. This report does not constitute a standard, specification, or regulation.

This document is disseminated under the sponsorship of the Department of Transportation in the interest of information exchange. The United States Government and the State of Mississippi assume no liability for its contents or use thereof.

The United States Government and the State of Mississippi do not endorse products or manufacturers. Trade or manufacturer's names appear herein solely because they are considered essential to the object of this report.

TABLE OF CONTENTS

LIST OF FIGURES	vi
LIST OF TABLES	viii
ACKNOWLEDGEMENTS	x
LIST OF SYMBOLS AND ACRONYMS	xi
CHAPTER 1 - INTRODUCTION.....	1
1.1 General and Background Information	1
1.2 Objectives and Scope	1
1.3 Summary of Asphalt Mixture Considered	2
CHAPTER 2 – LITERATURE REVIEW	6
2.1 Overview of Literature Review	6
2.2 Definition of Warm Mixed Asphalt	6
2.3 Performance and Behaviors of Warm Mixed Asphalt Technologies	7
2.3.1 Field Aging of Warm Mix Asphalt	10
2.3.2 Laboratory Aging of Warm Mix Asphalt	14
2.4 Replicating Field Aging with Laboratory Conditioning	19
2.5 Test Methods to Detect Environmental Damage	24
CHAPTER 3 – EXPERIMENTAL PROGRAM	26
3.1 Overview of Experimental Program	26
3.2 Specimens Tested and Test Matrices	26
3.3 Asphalt Mixtures Tested	28
3.4 Specimen Preparation	30
3.4.1 Laboratory Compaction	30
3.4.2 Laboratory Conditioning	30
3.4.2.1 Oven Conditioning	31
3.4.2.2 Hot Water Conditioning	31
3.4.2.3 Freeze-Thaw Conditioning	33

3.4.3	Field Aging	34
3.4.4	Specimen Slicing	38
3.5	Mixture Testing.....	39
3.5.1	Cantabro Testing.....	39
3.5.2	Indirect Tensile Testing	40
3.5.3	Fracture Energy Testing.....	41
3.5.4	Asphalt Pavement Analyzer Testing.....	42
3.5.5	Hamburg Loaded Wheel Testing.....	42
3.6	Recovered Binder Testing.....	43
3.6.1	Binder Extraction and Recovery	43
3.6.2	Dynamic Shear Rheometer Testing	44
3.6.3	Bending Beam Rheometer Testing	45
3.6.4	Penetration Testing	46
3.6.5	Fourier Transform Infrared Spectroscopy Testing	46
CHAPTER 4 – RESULTS		48
4.1	Overview of Results.....	48
4.2	Mixture Properties	48
4.2.1	Cantabro Mass Loss (CML) Results.....	50
4.2.2	Indirect Tensile Strength (IDT) Results.....	52
4.2.3	20°C Fracture Energy (FE ₊₂₀) Results	55
4.2.4	-10°C Fracture Energy (FE ₋₁₀) Results	57
4.3	Wheel-Tracking Tests.....	59
4.3.1	Hamburg Loaded Wheel Tracker (HLWT) Results.....	64
4.3.2	Asphalt Pavement Analyzer (APA) Results	66
4.4	Binder Properties	68
4.4.1	Penetration (<i>Pen.</i>) Results.....	71
4.4.2	Intermediate Temperature Dynamic Shear Rheometer (DSR _{8mm}) Results...73	
4.4.3	High Temperature Dynamic Shear Rheometer (DSR _{25mm}) Results.....	75
4.4.4	Bending Beam Rheometer (BBR) Results.....	77
4.4.5	Fourier Transform Infrared Spectroscopy (FTIR) Results	82

CHAPTER 5 – CONDITIONING PROTOCOL AND TEST METHOD COMBINATIONS TO DETECT MIXTURE DAMAGE.....	85
5.1 Overview.....	85
5.2 Results and Discussion	86
5.2.1 Oxidation Effects	90
5.2.2 Moisture Effects.....	91
5.2.3 Combined Effects of Oxidation and Moisture	91
 CHAPTER 6 – INFLUENCE OF WMT TYPE ON MIXTURE AND BINDER RESPONSE TO LABORATORY INDUCED DAMAGE	 92
6.1 Overview of Results.....	92
6.2 Oxidation Effects	96
6.3 Moisture Effects.....	99
6.4 Moisture and Freeze-Thaw Effects.....	101
6.5 Combined Oxidation, Moisture, and Freeze-Thaw Effects	105
 CHAPTER 7 – FIELD AGING TEST RESULTS.....	 108
7.1 Overview of Field Aging Results	108
7.2 Tests Methods Evaluation for Field Aged Data.....	109
7.3 Statistical Comparison of Mixture Types	112
7.4 Mixture Properties	113
7.4.1 Low Temperature properties.....	113
7.4.2 Intermediate Temperature	114
7.4.3 High Temperature Properties.....	116
7.5 Binder Properties	117
7.5.1 Low Temperature properties.....	119
7.5.2 Intermediate Temperature Properties	120
7.5.3 High Temperature Properties.....	121
7.5.4 Binder Chemical Properties	122
7.6 Convergence of WMA and HMA Properties with Field Aging	123

CHAPTER 8 – SIMULATION OF FIELD AGING WITH LABORATORY CONDITIONING PROTOCOLS	125
8.1 Overview	125
8.2 Replicating Field Aging of Asphalt Mixture	126
8.2.1 Conditioning Protocols in Conjunction with Cantabro Mass Loss.....	127
8.2.2 Conditioning Protocols in Conjunction with Indirect Tensile	128
8.2.3 Conditioning Protocols in Conjunction with Fracture Energy	130
8.2.4 Conditioning Protocols in Conjunction with Asphalt Pavement Analyzer	131
8.3 Summary of Overall Field Aging Time Simulations	131
 CHAPTER 9 – SUMMARY, CONCLUSIONS, AND RECOMMENDATIONS.....	 133
9.1 Summary	133
9.2 Conclusions.....	133
9.2.1 Chapter 5 Conclusions	133
9.2.2 Chapter 6 Conclusions	133
9.2.3 Chapter 7 Conclusions	134
9.2.4 Chapter 8 Conclusions	134
9.3 Recommendations.....	134
 CHAPTER 10 – REFERENCES	 135

LIST OF FIGURES

Figure 3.1	Stacked Asphalt Buckets Prior to Testing	29
Figure 3.2	Pine AFGC 125X SGC	30
Figure 3.3	Example Oven Conditioning Photograph	31
Figure 3.4	Example of Water Conditioning.	32
Figure 3.5	Example Freeze-thaw Conditioning Photograph	33
Figure 3.6	Freeze-Thaw Temperature of Trial 13	34
Figure 3.7	Compacted Specimens During Field Aging	35
Figure 3.8	Cumulative Weather Summary	38
Figure 3.9	Specimen Slicing Process for Binder and Fracture Energy Specimens	39
Figure 3.10	Cantabro Testing Examples	40
Figure 3.11	Non-Instrumented IDT Test.....	40
Figure 3.12	Instrumented IDT Testing Process.....	41
Figure 3.13	APA Testing Equipment and Specimen	42
Figure 3.14	HLWT Testing Equipment and Specimens	43
Figure 3.15	Binder Extraction and Recovery Equipment	44
Figure 3.16	DSR Equipment	45
Figure 3.17	BBR Equipment	46
Figure 3.18	<i>Pen.</i> Testing Equipment.....	46
Figure 3.19	Nicolet 380 FT-IR Analyzer	47
Figure 4.1	CML Field Aged Results	50
Figure 4.2	CML Laboratory Conditioned Equality Plots.....	52
Figure 4.3	IDT Field Aged Results	53
Figure 4.4	IDT Laboratory Conditioned Equality Plots.....	54
Figure 4.5	FE ₊₂₀ Field Aged Results	56
Figure 4.6	FE ₊₂₀ Laboratory Conditioned Results	57
Figure 4.7	FE ₋₁₀ Field Aged Results.....	58
Figure 4.8	FE ₋₁₀ Lab Conditioned Results.....	59
Figure 4.9	HLWT Field Aged Results	65
Figure 4.10	HLWT Laboratory Conditioned Results.....	66
Figure 4.11	APA Field Aged Results	67
Figure 4.12	APA Laboratory Conditioned Results	68
Figure 4.13	<i>Pen.</i> Field Aged Results.....	72
Figure 4.14	<i>Pen.</i> Laboratory Conditioned Results	73
Figure 4.15	DSR _{8mm} Field Aged Results.....	74
Figure 4.16	DSR _{8mm} Laboratory Conditioned Results	75
Figure 4.17	DSR _{25mm} Field Aged Results	76
Figure 4.18	DSR _{25mm} Laboratory Conditioned Results.....	77
Figure 4.19	BBR m-value Field Aged Results.....	78
Figure 4.20	BBR Stiffness Field Aged Results.....	80
Figure 4.21	BBR m-value Laboratory Conditioned Results	81
Figure 4.22	BBR Stiffness Laboratory Conditioned Results	82
Figure 4.23	FTIR Field Aged Results	83
Figure 4.24	FTIR Laboratory Conditioned Results.....	84

Figure 5.1	Mixture-Environmental Effects Hypothesis Diagram	86
Figure 5.2	Test Property Correlations	88
Figure 5.3	ML (%) and S_t (kPa) Equality Plots	89
Figure 6.1	Effects of Oxidative Conditioning on Asphalt Mixture and Binder Properties	97
Figure 6.2	Effects of Moisture Conditioning on Asphalt Mixture and Binder Properties	100
Figure 6.3	Effects of Moisture with FT Conditioning on Asphalt Mixture and Binder Properties	103
Figure 6.4	Effects of Combined Oxidation and Moisture with FT Conditioning on Asphalt Mixture and Binder Properties	106
Figure 7.1	Relative Responses Based on Mixture Test Results	111
Figure 7.2	FE ₋₁₀ Field Aged Results.....	114
Figure 7.3	CML Field Aged Results	114
Figure 7.4	IDT Field Aged Results	115
Figure 7.5	FE ₊₂₀ Field Aged Results	116
Figure 7.6	APA Field Aged Results	116
Figure 7.7	Relative Binder Responses	118
Figure 7.8	BBR m -value Field Aged Results.....	119
Figure 7.9	BBR Stiffness Field Aged Results.....	120
Figure 7.10	$Pen.$ Field Aged Results.....	120
Figure 7.11	DSR _{8mm} Field Aged Results.....	121
Figure 7.12	DSR _{25mm} Field Aged Results	122
Figure 7.13	FTIR Field Aged Results	123
Figure 8.1	Correlating Field Aging and Laboratory Conditioning for CML at 4% V_a	128
Figure 8.2	Correlating Field Aging and Laboratory Conditioning for CML at 7% V_a	128
Figure 8.3	Correlating Field Aging and Laboratory Conditioning for IDT at 4% V_a	129
Figure 8.4	Correlating Field Aging and Laboratory Conditioning for IDT at 7% V_a	129
Figure 8.5	Correlating Field Aging and Laboratory Conditioning for FE ₊₂₀ at 7% V_a	130
Figure 8.6	Correlating Field Aging and Laboratory Conditioning for FE ₋₁₀ at 7% V_a	131
Figure 8.7	Correlating Field Aging and Laboratory Conditioning for APA at 7% V_a	131

LIST OF TABLES

Table 1.1	Mixture Volumetric Properties Utilized During Research Program.....	3
Table 1.2	Mixture Components Information Utilized During Research Program.....	4
Table 1.3	Mixture Gradations Utilized During Research Program	5
Table 2.1	General Behaviors of Warm Mix Technologies	8
Table 2.2	Summary of Field Aging of WMA Pavements (Mixture Testing)	11
Table 2.3	Summary of Field Aging of WMA Pavements (Binder Testing)	12
Table 2.4	Summary of Field Aging of WMA Pavements (Field Surveys).....	13
Table 2.5	Effects of Laboratory Oxidative Conditioning on Warm Mix Technologies	16
Table 2.6	Effects of Laboratory Moisture Conditioning on Warm Mix Technologies	17
Table 2.7	Correlation of Field Aging and Laboratory Conditioning of Asphalt Mixtures.	21
Table 2.8	Test Method Evaluations in Literature	25
Table 3.1	Summary of Mixture Testing Plan.....	27
Table 3.2	Summary of Binder Testing Plan.....	28
Table 3.3	G _{mm} Measurements for Mixtures M17 to M20.....	29
Table 3.4	Laboratory Conditioning Protocols.....	31
Table 3.5	Water Bath Conditioning Trials.....	32
Table 3.6	Year 1 Weather Summary (November 2012 to October 2013)	36
Table 3.7	Year 2 Weather Summary (November 2013 to October 2014)	36
Table 3.8	Year 3 Weather Summary (November 2013 to October 2014)	37
Table 3.9	Year 4 Weather Summary (November 2015 to October 2016)	37
Table 4.1	CML, IDT, and FE Test Results for All Specimen Types.....	49
Table 4.2	HLWT Results for 0-yr Control and 1-yr Field Aged Specimens	60
Table 4.3	HLWT Results for Laboratory Conditioned Specimens.....	61
Table 4.4	APA Results for 0-yr and Field Aged Specimens	62
Table 4.5	APA Results for 7% V _a Laboratory Conditioned Specimens.....	63
Table 4.6	Binder Results for 0-yr and Field Aged Specimens.....	69
Table 4.7	Binder Results for Laboratory Conditioned Specimens	70
Table 5.1	Relative Mixture and Binder Data	87
Table 5.2	Statistical Assessment of Mixture Test Results	90
Table 6.1	Asphalt Mixture Testing Data.....	93
Table 6.2	Asphalt Binder Testing Data.....	94
Table 6.3	Initial ANOVA of Certain Mixture Properties	95
Table 6.4	Summary of Isolated Oxidation Observations	98
Table 6.5	Relation of Oxidation Observations to Literature.....	98
Table 6.6	Summary of Isolated Moisture Observations	101
Table 6.7	Relation of Moisture Observations to Literature	101
Table 6.8	Summary of Moisture with FT Observations	104
Table 6.9	Relation of Moisture with FT Observations to Literature	104
Table 6.10	Summary of Combined Oxidation and Moisture with FT Observations.....	107
Table 6.11	Relation of Oxidation and Moisture with FT Observations to Literature.....	107
Table 7.1	Mixture Test Results	108
Table 7.2	Binder Test Results	109
Table 7.3	<i>t</i> -grouping Test for Mixture Properties with Respect to Field Aging Time	110

Table 7.4	<i>t</i> -grouping Test for Mixture Properties Based on Mixture Type	112
Table 7.5	<i>t</i> -grouping Test for Binder Properties Based on Mixture Type	113
Table 7.6	Time in Years for Mixtures to Converge (Mixture Properties)	124
Table 7.7	Time in Years for Mixtures to Converge (Binder Properties)	124
Table 8.1	Field Aged Mixture Test Results	125
Table 8.2	Laboratory Conditioned Mixture Test Results	126
Table 8.3	Simulation of Field Aging in Years for Asphalt Mixture Test Methods	132

ACKNOWLEDGEMENTS

Thanks are due to many for the successful completion of this report. The MDOT Research Division is owed special thanks for funding State Study 266 and State Study 270. James Watkins served as State Research Engineer at the beginning of this project, with Cindy Smith serving as State Research Engineer at the conclusion of this project. The MDOT Project Engineer was Alex Middleton.

APAC Mississippi supported the field aging test section. The Ergon Asphalt & Emulsions Student Support Initiative in Construction Materials was also beneficial for asphalt activities during a portion of the time frame of this project. Paragon Technical Services, Inc (PTSi) supported all binder testing activities. The Engineer Research and Development Center (ERDC) provided the plant mixed asphalt that served as the basis for this report. Several current and former Mississippi State University (MSU) students assisted this project in a variety of manners, mostly as research assistants.

Individuals deserving thanks for the work of State Study 266 and State Study 270 include Gaylon Baumgardner, Mike Bogue, Justin Cooper, Ben C. Cox, Will Crawley, Codrin Daranga, Jesse Doyle, Web Floyd, Westin Graves, Mike Hemsley, Chase Hopkins, Robert James, Trey Jordan, Patrick Kuykendall, Garrison Lipscomb, Drew Moore, Rae Ann Otts (Lawrence), Sonia Serna, and Donald Young.

LIST OF SYMBOLS AND ACRONYMS

AASHTO	American Association of State and Highway Transportation Officials
ABSP	Absorbance Peak
AFB	Air Force Base
ANOVA	Analysis of Variance
APA	Asphalt Pavement Analyzer
APB	Airfields and Pavements Branch
ASTM	American Society for Testing and Materials
B	Bottom
BBR	Bending Beam Rheometer
CAFB	Columbus Air Force Base
CDD ^{high}	High Temperature Cumulative Degree Days
CD ^{fluctuation}	Cumulative Days of Temperature Fluctuation
CFI	Cumulative Freezing Index
CI	Carbonyl Index
CML	Cantabro Mass Loss
CMRC	Construction Materials Research Center
COV	Coefficient of Variation
CP	Control Protocol
CPPC	Cyclic Pore Pressure Conditioning
D	Specimen Diameter
DDC	Deformation Differential Curve
DSR	Dynamic Shear Rheometer
DSR _{25mm}	High Temperature DSR Testing
DSR _{8mm}	Intermediate Temperature DSR Testing
E/R	Extracted and Recovered
ERDC	Engineer Research and Development Center
F1	Freezer 1
F2	Freezer 2
FE	Fracture Energy
FE ₊₂₀	Fracture Energy at 20°C
FE ₋₁₀	Fracture Energy at -10°C
FHWA	Federal Highway Administration
FT	Freeze-Thaw
FTIR	Fourier Transformation Infrared Spectroscopy
G*	Complex Shear Modulus
G _{mb}	Mixture Bulk Specific Gravity
G _{mm}	Maximum Specific Gravity
G _{sa}	Apparent Specific Gravity
G _{sb}	Bulk Specific Gravity
G _{se}	Effective Specific Gravity
GTR	Ground Tire Rubber
HL	Hydrated Lime
HLWT	Hamburg Loaded Wheel Tracking
HMA	Hot Mixed Asphalt

IDT	Indirect Tensile Strength
LA	Los Angeles
LM	Loose Mixture
LMLC	Laboratory Mixed and Laboratory Compacted
LTOA	Long Term Oven Aging
M_1	Mass Before Cantabro Testing
M_2	Mass After Cantabro Testing
MDOT	Mississippi Department of Transportation
ML	Mass Loss
M_R	Resilient Modulus
MSU	Mississippi State University
M_t	Slope of Field Aging Trendline for Specific Test Method
NAPA	National Asphalt Pavement Association
NCAT	National Center for Asphalt Technology
NCHRP	National Cooperative Highway Research Program
NMAS	Nominal Maximum Aggregate Size
P_1	Test Result for the Specification Value for Property at T1
P_2	Test Result for the Specification Value for Property at T2
P_{200}	Percent of Material Finer Than 0.075 mm
P_b	Asphalt Binder Content
$P_{ba(mix)}$	Absorbed Asphalt Binder Content on a Total Mix Mass Basis
P_{be}	Effective Asphalt Binder Content
<i>Pen.</i>	Penetration
PG	Performance Grade
P_{max}	Maximum Load
PMFC	Plant Mixed and Field Compacted
PMLC	Plant Mixed and Laboratory Compacted
P_s	Specification Value for Property
PURWheel	Purdue University Laboratory Wheel Tracking Device
RAP	Reclaimed Asphalt Pavement
RAS	Recycled Asphalt Shingles
RD_{APA}	APA Rut Depth
RD_{HLWT}	HLWT Rut Depth
S	Stiffness
s	Standard Deviation
SAS	Single Aggregate Source
SGC	Superpave Gyratory Compactor
SI	Sulfoxide Index
SIP	Stripping Inflection Point
SS266	State Study 266
SS270	State Study 270
S_t	Indirect Tensile Strength
STOA	Short Term Oven Aging
t	Specimen Thickness
T	Top
T_1	Lower of the Two Test Temperatures

T_2	Higher of the Two Test Temperatures
T_c	Critical Temperature
T_{c-m}	Critical Temperatures from M-Value
T_{c-s}	Critical Temperatures from Creep Stiffness
T_{design}	Design Temperature
T_{dhigh}	Maximum Daily Temperature
T_{dlow}	Minimum Daily Temperature
t_F	Time in the Field
$T_{production}$	Production Temperature
t_{SF}	Simulated Field Aging Time
TSR	Tensile Strength Ratio
$t_{warm-up}$	Time for Water Bath to Reach Setpoint Temperature
US	United States
USACE	United States Army Corps of Engineers
V_a	Air Void
V_{be}	Volume of Effective Asphalt Binder
V_i	Average Test Method Value for CP
VMA	Voids in mineral aggregate
WMA	Warm Mixed Asphalt
WMT	Warm Mix Technology
X_i	Test Value of a Given Test
X_{max}	Higher Test Value of a Given Test
X_{min}	Lower Test Value of a Given Test
Y_i	Normalized Value of X_i
Y_t	Y Intercept of Field Aging Trendline for Specific Test Method
δ	Phase Angle

CHAPTER 1-INTRODUCTION

1.1 General and Background Information

Field aging of asphalt mixtures has been studied for several decades. Several binder testing and conditioning protocols have been developed since the 1950s, and have led to improved understanding of aging. Over the past decade, warm mixed asphalt (WMA) has been one of the biggest advancements to asphalt paving in the US (WMA is also used in many other parts of the world and originated in Europe), and with those advancements have come questions regarding how to predict WMA behaviors such as aging compared to hot mixed asphalt (HMA), relative behavior between warm mix technologies, and how characterize combined effects of environmental exposure.

WMA technology can be applied through foamed asphalt, or several additives. WMA is a technology increasingly being used in place of HMA due to its potential economic and environmental benefits. As such, improved understanding is needed regarding the differences in WMA aging and HMA aging. A formidable problem facing the paving industry is the lack of laboratory conditioning protocols that reasonably simulate environmental effects and aging in a mixture during the service life of a pavement. Ideally, a mixture conditioning protocol and test method(s) would be available that could simulate WMA or HMA aging over time (in particular the first several years of service life). Reliable laboratory conditioning protocols and evaluation methods could provide the Mississippi Department of Transportation (MDOT) with a more reasonable means of predicting the long-term performance of asphalt pavements. To date, only limited laboratory mixture conditioning protocols have been available; protocols focusing on binder only have been more prevalent over the past few decades.

To investigate the performance of WMA compared to HMA, one HMA and three WMA mixes were designed by the US Army Corps of Engineers (USACE) Airfields and Pavements Branch (APB) at the Engineer Research and Development Center (ERDC). These four mixes were produced by APAC Mississippi, Inc. at their Vicksburg facility and used to pave test sections at ERDC for trafficking and other investigations as described in Doyle et al. (2013a and 2013b), Rushing et al. (2013a and 2013b), and Mejias-Santiago et al. (2014). Large plant produced samples of each mix were provided to the Mississippi State University (MSU) Construction Materials Research Center (CMRC) and used as described in the remainder of this document as the mixes studied have applicability to airfield and highway pavements.

1.2 Objectives and Scope

This report is part of a three volume series that investigated: 1) the effects field aging has on asphalt concrete produced at hot mix temperatures and hauled long distances; and 2) the effects field aging has on asphalt concrete produced at different mixing temperatures and hauled a moderate distance. This research effort utilized laboratory and field testing of asphalt mixtures and binders, literature review, and data analysis. The research program was funded by MDOT through Project 106526 101000, State Study 266 (SS266), and State Study 270 (SS270). The three report volumes do not coincide with MDOT funding mechanisms, rather are divided according to technical content. Collectively, these three reports contain all

deliverables for these three funded endeavors (1 through Materials Division, 2 through Research Division).

Volume 1 (FHWA/MS-DOT-RD-18-266/270-Volume 1) includes data and analysis of reference mixtures that are intended largely for benchmarking and interpretation of Volume 2 and Volume 3 data. Volume 2 (FHWA/MS-DOT-RD-18-266/270-Volume 2) focused most of its effort on the effects field aging has on asphalt concrete produced at hot mix temperatures and hauled long distances. Volume 3 (FHWA/MS-DOT-RD-18-266/270-Volume 3) focused most of its efforts on the effects field aging has on asphalt concrete produced at different mixing temperatures and hauled a moderate distance.

The main objective of this report (Volume 3) was to characterize asphalt containing warm mix technologies at various levels of field aging and laboratory conditioning in terms of mixture and binder properties encompassing the temperature range experienced in Mississippi. To accomplish this objective, field aging was performed to compare HMA to WMA over time, as was laboratory conditioning where individual and combined effects of oxidation, moisture, and freeze-thaw were incorporated. Another component of the characterization was to evaluate laboratory conditioning protocols and mixture test methods for their combined ability to reasonably simulate field aging of asphalt mixtures. Almost all of the data in Volume 3 was obtained from testing of plant-mixed and laboratory compacted (PMLC) specimens either through mechanical property testing of mixtures or through assessment of recovered binder.

Chapter 2 presents a literature review focusing on past work relative to WMA field aging and laboratory conditioning protocols. Chapter 3 describes the materials and test methods utilized herein. Chapter 4 presents all test data that is used in the remaining chapters for analysis and achievement of this report's two main objectives.

1.3 Summary of Asphalt Mixtures Considered

There were a total of 20 asphalt mixtures (M01 to M20) tested for this research program (Project 106526 101000, SS266, and SS270). This section is repeated in all three volumes for clarity, and an asphalt mixture is defined as a unique combination of ingredients at consistent proportions. A single mixture could be produced in different ways and at different points in time using the same aggregate and asphalt binder sources at consistent proportions. For example, one mixture could be plant-mixed and field compacted (PMFC), plant-mixed and laboratory compacted (PMLC), or laboratory-mixed and laboratory compacted (LMLC). M01 to M13 were the focus of Volume 1 as an investigation of single aggregate source (SAS) and Air Force Base (AFB) mixtures which were often field aged on the full-scale test section described in Chapter 3 of Volume 2. M14 to M16 were the focus of Volume 2 which considers the full-scale and non-trafficked test section described in Chapter 3 of Volume 2. This report (Volume 3) relies on results from M17 to M20 which were also field aged on the full-scale test section. Tables 1.1 to 1.3 provide mixture design volumetric information, ingredient source information, and gradations, respectively. All terms used in Tables 1.1 to 1.3 are provided in the list of symbols.

Table 1.2 describes constituent materials in M01 to M20 by type, source, and sample (where documented). M01 to M10 were lab mixed from constituent materials and M11 to M20 were plant mixed. Aggregate sources which were sampled in more than one paving season are differentiated by year, and sample number differentiates binder samples. Notice that a single sample of asphalt binder was used for M01 to M10 and M17 to M20.

Table 1.1. Mixture Volumetric Properties Utilized During Research Program

Mix ID	T^{design} (°C)	T^{production} (°C)	G_{mm}	G_{sb}	G_{se}	G_{sa}	P_b (%)	P_{be} (%)	P_{ba (mix)} (%)	VMA (%)	Design V_a (%)	V_{be} (%)	P₂₀₀ (%)	NMAS (mm)
M01	163	163	2.250	2.385	2.520	2.651	8.3	6.2	2.3	16.9	4	12.9	6.0	12.5
M02	163	163	2.250	2.385	2.520	2.651	8.3	6.2	2.3	16.9	4	12.9	6.0	12.5
M03	163	163	2.250	2.385	2.520	2.651	8.3	6.2	2.3	16.9	4	12.9	6.0	12.5
M04	129	129	2.248	2.385	2.505	2.651	8.0	6.1	2.1	16.8	4	12.8	6.0	12.5
M05	129	129	2.248	2.385	2.505	2.651	8.0	6.1	2.1	16.8	4	12.8	6.0	12.5
M06	129	129	2.248	2.385	2.505	2.651	8.0	6.1	2.1	16.8	4	12.8	6.0	12.5
M07	163	163	2.479	2.694	2.733	2.743	6.2	5.7	0.5	17.2	4	13.2	5.9	12.5
M08	129	129	2.481	2.694	2.735	2.743	6.2	5.7	0.5	17.0	4	13.0	5.9	12.5
M09	163	163	2.123	2.248	2.362	2.507	8.7	6.7	2.2	17.2	4	13.2	6.2	12.5
M10	129	129	2.125	2.248	2.351	2.507	8.3	6.5	2.0	16.8	4	12.8	6.2	12.5
M11	150	150	2.531	2.693	2.753	2.811	5.2	4.4	0.8	14.1	4	10.1	4.5	12.5
M12	166	160	2.370	2.484	2.560	2.653	6.0	4.8	1.2	14.3	4	10.3	4.0	12.5
M13	177	160	2.381	2.481	2.556	2.607	5.9	4.8	1.2	14.3	4	10.3	4.5	12.5
M14	160	164	2.378	2.515	2.567	2.663	5.4	4.6	0.8	14.1	4	10.1	5.9	12.5
M15	160	153	2.378	2.515	2.567	2.663	5.4	4.6	0.8	14.1	4	10.1	5.9	12.5
M16	160	148	2.378	2.515	2.567	2.663	5.4	4.6	0.8	14.1	4	10.1	5.9	12.5
M17	143	143	2.461	2.609	2.668	2.688	5.3	4.5	0.8	14.3	4	10.3	4.9	12.5
M18	129	132	2.461	2.609	2.668	2.688	5.3	4.5	0.8	14.3	4	10.3	4.9	12.5
M19	129	132	2.461	2.609	2.668	2.688	5.3	4.5	0.8	14.3	4	10.3	4.9	12.5
M20	129	132	2.461	2.609	2.668	2.688	5.3	4.5	0.8	14.3	4	10.3	4.9	12.5

Table 1.2. Mixture Components Information Utilized During Research Program

Mix ID	Aggregates						Asphalt Binder						
	Gravel		Limestone		Sand		RAP	HL	PG	Warm Mix		Sample	
Source	(%)	Source	(%)	Source	(%)	(%)	(%)	Grade	Source	Technology			
M01	Hamilton, MS ('13)	100	---	---	---	---	---	67-22	Vicksburg, MS	---	1		
M02	Hamilton, MS ('13)	100	---	---	---	---	---	67-22	Vicksburg, MS	0.5% Evo.	1		
M03	Hamilton, MS ('13)	100	---	---	---	---	---	67-22	Vicksburg, MS	1.5% Sasobit	1		
M04	Hamilton, MS ('13)	100	---	---	---	---	---	67-22	Vicksburg, MS	---	1		
M05	Hamilton, MS ('13)	100	---	---	---	---	---	67-22	Vicksburg, MS	0.5% Evo.	1		
M06	Hamilton, MS ('13)	100	---	---	---	---	---	67-22	Vicksburg, MS	1.5% Sasobit	1		
M07	---	---	Tuscaloosa, AL ('13)	100	---	---	---	67-22	Vicksburg, MS	---	1		
M08	---	---	Tuscaloosa, AL ('13)	100	---	---	---	67-22	Vicksburg, MS	---	1		
M09	Creede, CO	100	---	---	---	---	---	67-22	Vicksburg, MS	---	1		
M10	Creede, CO	100	---	---	---	---	---	67-22	Vicksburg, MS	---	1		
M11	---	---	California	100	---	---	---	70-10	California	---	1		
M12	Hamilton, MS ('13)	51	Tuscaloosa, AL ('13)	33	Hamilton, MS ('13)	15	---	1	76-22	Memphis, TN	---	1	
M13	Hamilton, MS ('13)	41	Tuscaloosa, AL ('13)	25	Hamilton, MS ('13)	13	20	1	70-22	Memphis, TN	---	1	
M14	Hamilton, MS ('11)	39	Tuscaloosa, AL ('11)	35	Hamilton, MS ('11)	10	15	1	67-22	Vicksburg, MS	---	2	
M15	Hamilton, MS ('11)	39	Tuscaloosa, AL ('11)	35	Hamilton, MS ('11)	10	15	1	67-22	Vicksburg, MS	Foamed	2	
M16	Hamilton, MS ('11)	39	Tuscaloosa, AL ('11)	35	Hamilton, MS ('11)	10	15	1	67-22	Vicksburg, MS	0.5% Evo.	2	
M17	Undocumented	25	Calera, AL	60	Undocumented	15	---	---	67-22	Vicksburg, MS	---	1	
M18	Undocumented	25	Calera, AL	60	Undocumented	15	---	---	67-22	Vicksburg, MS	Foamed	1	
M19	Undocumented	25	Calera, AL	60	Undocumented	15	---	---	67-22	Vicksburg, MS	0.5% Evo.	1	
M20	Undocumented	25	Calera, AL	60	Undocumented	15	---	---	67-22	Vicksburg, MS	1.5% Sasobit	1	

Hydrated Lime (HL); Reclaimed Asphalt Pavement (RAP); Evotherm 3G™ (Evo.)

Table 1.3. Mixture Gradations Utilized During Research Program

Mix ID	Percent Passing (%)										
	25 mm	19 mm	12.5 mm	9.5 mm	No. 4	No. 8	No. 16	No. 30	No. 50	No. 100	No. 200
M01	100	100	96	88	70	53	37	27	14	7.6	6.0
M02	100	100	96	88	70	53	37	27	14	7.6	6.0
M03	100	100	96	88	70	53	37	27	14	7.6	6.0
M04	100	100	96	88	70	53	37	27	14	7.6	6.0
M05	100	100	96	88	70	53	37	27	14	7.6	6.0
M06	100	100	96	88	70	53	37	27	14	7.6	6.0
M07	100	100	96	87	67	48	25	17	12	8.4	5.9
M08	100	100	96	87	67	48	25	17	12	8.4	5.9
M09	100	100	96	87	67	48	29	17	12	8.6	6.2
M10	100	100	96	87	67	48	29	17	12	8.6	6.2
M11	100	100	95	83	64	49	33	22	13	7.0	4.5
M12	100	100	96	88	61	44	31	22	11	6.0	4.0
M13	100	100	93	85	57	38	27	21	11	6.0	4.5
M14	100	100	95	85	54	36	25	19	11	7.5	5.9
M15	100	100	95	85	54	36	25	19	11	7.5	5.9
M16	100	100	95	85	54	36	25	19	11	7.5	5.9
M17	100	100	96	85	68	54	38	28	15	6.8	4.9
M18	100	100	96	85	68	54	38	28	15	6.8	4.9
M19	100	100	96	85	68	54	38	28	15	6.8	4.9
M20	100	100	96	85	68	54	38	28	15	6.8	4.9

CHAPTER 2 LITERATURE REVIEW

2.1 Overview of Literature Review

This literature review had two main objectives. First, to summarize literature concerning the behaviors, properties, and performance of WMA compared to HMA as a function of either laboratory conditioning or field aging, and second to describe studies which have attempted to simulate field aging via laboratory conditioning methods. Section 2.2 provides a brief introduction into warm-mix technologies (WMTs) in which a sample of literature is summarized concerning WMT usefulness, mechanisms of temperature reduction, categories into which they are divided, and production temperatures. Section 2.3 gives a brief overview of typical behaviors of different WMTs found throughout literature. Section 2.3.1 considers literature which investigated how field aging affected the difference in initial properties between WMA and HMA. Section 2.3.2 then addresses the effects of laboratory conditioning on WMA mixtures relative to HMA, as found in literature. Section 2.4 summarizes a number of studies which have attempted to simulate some length of field aging time with a method of laboratory conditioning. Lastly, Section 2.5 summarizes how test methods which are utilized to evaluate mixtures can affect conclusions relative to mixture performance.

2.2 Definition of Warm Mixed Asphalt

WMA has become an increasingly popular technology due to its potential environmental, economic, and safety benefits. Reduced production temperatures result in lower fuel usage for asphalt plants as well as lower emissions. Lower compaction temperatures increase the safety of asphalt paving crews by exposing the workers to lower ambient temperatures and reduced amounts of asphalt fumes. Additionally, WMA additives can allow for the increase of haul distances and extend the construction season into the cooler months (Vaitkus et al. 2016). WMAs are produced with additives or processes that are generally classified into three categories of WMTs: foamed asphalt, chemical additives, and organic waxes. Foamed asphalt is produced either by direct water injection into hot binder or through the use of an additive, such as a zeolite, which has a crystalline structure with entrapped water that is released when heated to temperatures above 80-90°C (Vaiana et al. 2013). Organic waxes have melting points below typically HMA production temperatures where they help to reduce binder viscosity; however, at typical service temperatures, organic waxes can have a stiffening effect. Chemical additives are usually proprietary blends which are blended into asphalt binder at a supply terminal or asphalt plant (Bonaquist 2011). The objective of a WMT is to lower binder viscosity so that acceptable aggregate coating, mixture workability, and compaction levels can be achieved at reduced production and construction temperatures.

The temperature, or temperature range, at which an asphalt concrete must be produced to be considered “warm mix” as opposed to “hot mix” is not clearly defined in literature. The Federal Highway Administration (FHWA) states that WMA is produced at 30 to 120°F lower than traditional HMA (<https://www.fhwa.dot.gov/innovation/everydaycounts/edc-1/wma.cfm>). The 3rd edition of the WMA Best Practices published by the National Asphalt Pavement Association (NAPA) (Prowell et al. 2012) defined WMA as being produced in the range of 212-280°F as opposed to HMA being produced at temperatures from 280°F to 320°F. National Cooperative Highway Research Program (NCHRP) Report 691: WMA Mix Design Practices (Bonaquist 2011) says that WMA is produced at temperature approximately 50°F (28°C) lower than traditional

HMA. This matches what is claimed in the SuperPave volumetric mix design standard (AASHTO R35) that states, “WMA refers to asphalt mixtures that are produced at temperatures approximately 50°F (28°C) or more lower than typically used in the production of HMA.”

Note that the use of WMT in an asphalt mixture is not what constitutes a WMA. It was found in some literature (i.e. Hurley and Prowell 2005a; Diefenderfer and Hearon 2008) where mixtures were evaluated with WMTs produced at both traditional HMA temperatures and reduced temperatures to investigate if mixture differences are due to temperature reduction, WMT, or a combination of the two factors. In the majority of cases evaluated herein, mixtures containing a WMT were produced at WMA temperatures, according to the authors of respective studies.

2.3 Performance and Behaviors of Warm Mixed Asphalt Technologies

Lower production and compaction temperatures are thought by some to decrease the short-term aging typically experienced during production and construction of HMA, and in turn, affect the short-term and long-term properties of pavements (Safaei et al. 2014). For example, initial laboratory studies performed at the National Center for Asphalt Technology (NCAT) recognized that lower production and compaction temperatures of WMA may lead to higher rutting, stripping, and moisture damage susceptibility to varying degrees dependent on the technology or additive implemented (Hurley and Prowell 2005a, 2005b, and 2006). However, it is expected that the reduced short-term aging may have a positive impact on the fatigue and cracking characteristics of pavements produced with WMA. Literature focusing on rutting, fatigue and thermal cracking, and moisture damage resistance of the three categories of WMT (i.e. foamed, chemical additives, and organic waxes) was consulted and summarized in Table 2.1 to investigate general trends of unaged properties of WMA mixtures.

Table 2.1. General Behaviors of Warm Mix Technologies

WMT Category	Performance Parameter	Typical Findings	References
Foam	Rutting	Foamed asphalt was typically found to either worsen or have no effect on rutting behavior of asphalt mixtures.	Bennert (2012a), Alhasan et al. (2014), Kavussi and Hashemian (2012), Ali et al. (2012), Bennert (2014)
	Fatigue Cracking	Foamed asphalt was mostly found to improve or have no effect on intermediate temperature fatigue performance. In an isolated case, foamed asphalt had worse fatigue performance than HMA.	Bennert (2012b), Gu et al. (2015a), Cucalon et al. (2017), Safaei et al. (2014), Goh and You (2011), Bennert (2014)
	Thermal Cracking	Foamed asphalt consistently exhibited decreased resistance to low temperature cracking relative to HMA.	Hill et al. (2012), Medeiros et al. (2012), Alhasan et al. (2014), Kim et al. (2015)
	Moisture Susceptibility	Foamed asphalt was found to have approximately the same or slightly more moisture susceptibility than HMA.	Martin et al. (2014), Bennert (2012a), Xiao et al. (2009), Cucalon et al. (2017), Medeiros et al. (2012), Kavussi and Hashemian (2012), Goh and You (2011), Ali et al. (2012), Bennert (2014)
Chemical	Rutting	With the exception of an isolated case where Evotherm improved rut resistance (i.e. Hurley and Prowell 2006) chemical additives typically have no effect on or decrease rut resistance relative to HMA.	Diefenderfer et al. (2007), Hurley and Prowell (2006), Prowell et al. (2007), Wu et al. (2017), Suleiman and Mandal (2013), Leng et al. (2013)
	Fatigue Cracking	Chemical additives mostly improve initial fatigue performance.	Safaei et al. (2014), Gu et al. (2015), Behl and Chandra (2017), Wu et al. (2017), Lee and Kim (2014)
	Thermal Cracking	Chemical additives usually improve low temperature cracking resistance.	Hill et al. (2012), Behl and Chandra (2017), Wu et al. (2017), Lee et al. (2013), Leng et al. (2013)
	Moisture Susceptibility	Chemical additives generally increase moisture damage potential relative to HMA or have similar behavior.	Diefenderfer et al. (2007), Hurley and Prowell (2006), Prowell et al. (2007), Lee and Kim (2014)
Wax	Rutting	WMAs produced with organic wax usually have similar or better rutting performance than HMA.	Diefenderfer et al. (2007), Behl and Chandra (2017), Diefenderfer and Hearon (2008), Zelelew et al. (2013), Malladi et al. (2015), Hurley and Prowell (2005b)
	Fatigue Cracking	Sasobit either caused no change in fatigue performance or had a detrimental effect.	Behl and Chandra (2017), Diefenderfer and Hearon (2008), Bonaquist (2011), Zelelew et al. (2013), Haggag et al. (2011)
	Thermal Cracking	Organic wax modification most always causes some level of decrease in low temperature performance.	Behl and Chandra (2017), Porras et al. (2012), Liu and Li (2012), Das et al. (2011), Hill et al. (2012), Medeiros et al. (2012)
	Moisture Susceptibility	Moisture damage resistance of organic wax WMAs appear to show varying trends across literature. Hurley and Prowell (2005b) determined that the effect of Sasobit on moisture damage resistance was dependent on binder and aggregate type.	Diefenderfer et al. (2007), Diefenderfer and Hearon (2008), Lee and Kim (2014), Malladi et al. (2015), Hurley and Prowell (2005b)

As seen in Table 2.1, WMA produced with foaming technologies and chemical additives have similar properties that are indicative of softer mixtures. In most cases, it was found that both technology types improved fatigue cracking and moisture damage resistance while decreasing rutting resistance. The two technologies diverged in thermal cracking characteristics with foaming typically reducing cracking resistance and chemical additives causing an improvement. Organic waxes were typically found to have the opposite effects of foaming technologies and chemical additives. Waxes usually improved rutting resistance while having a detrimental effect on thermal and fatigue cracking properties. This can be attributed to the temperature dependence of organic waxes. Above their melting temperatures, organic waxes can be mixed with asphalt binder to reduce viscosity, aiding in mixing and compaction. However, during typical in-service or testing temperatures, the waxes are below their melting point and increase the stiffness of the asphalt binder. There has been trouble throughout literature defining the moisture characteristics of organic wax produced WMAs.

As described in Table 2.1, moisture damage resistance of organic waxes was evaluated by several authors and resulted in conflicting findings among the different studies and even within individual studies. Hurley and Prowell (2005b) suggested that the moisture damage resistance of organic wax WMAs is dependent on aggregate type. WMT type is not the only factor that effects mixture performance. Other factors include but are not limited to production temperature, short term oven aging (STOA) time and temperature of laboratory mixed material, and inclusion of recycled materials such as reclaimed asphalt pavement (RAP) or recycled asphalt shingles (RAS).

Hurley and Prowell (2005a) and Diefenderfer and Hearon (2008) performed studies of asphalt mixtures produced with WMTs at reduced WMA temperatures as well as typical HMA temperatures. Hurley and Prowell (2005a) produced foamed LMLC asphalt specimens at temperatures ranging from 190-300°F. Data showed that WMA produced at 190°F had M_R values less than HMA produced at 300°F. However, as production temperature of WMA increased, resilient modulus (M_R) of WMA approached that of HMA, and when produced at 300°F exceeded the M_R of its HMA equivalent. Diefenderfer et al. (2007) found that increased production temperatures of WMA produced with Sasobit (organic wax) resulted in improved moisture resistance relative to HMA. There has also been research conducted to determine the effects of different STOA times (e.g. Hurley and Prowell 2005a, 2005b, and 2006, and Mogawer et al. 2011) and temperatures (Safaei et al. 2014, Yin et al. 2013 and Bonaquist 2011). It was found by the authors that as STOA time increased, the difference in stiffness and moisture damage resistance between WMA and HMA was reduced. In the same manner, decreases in STOA temperatures were found to decrease WMA stiffness compared to HMA.

When WMA was introduced in the US market, its compatibility with RAP was of considerable interest. The main interest was determining if RAP may be able to alleviate some of the initial rutting and moisture damage resistance issues which can result from some WMTs (Doyle and Howard 2013). Boggs (2008), Doyle et al. (2011), Hodo et al. (2009), Mallick et al. (2008), and Doyle and Howard (2013) all found that inclusion of RAP improved rutting resistance of WMA mixtures. Likewise, Mejias-Santiago et al. (2011), Middleton and Forfylyow (2009), Mogawer et al. (2011), and Doyle and Howard (2013) reported improved resistance to moisture damage of high RAP content WMAs.

2.3.1 Field Aging of Warm Mix Asphalt

From the 1950's to present, there has been considerable use of controlled field experiments to determine a relationship between laboratory mixture properties and field performance. Copas and Pennock (1979) summarized several studies about field aging from the 1950's to 1970's which were conducted to correlate asphalt properties to pavement performance by means of binder testing. The researchers defined pavement durability as function of asphalt binder properties. Hardness was considered a main property associated with pavement performance. It was found that hardness depends on asphalt grade, temperature, construction, aggregate type, mix design, and several other factors. Bell (1989) also summarized studies conducted in the field which aimed to correlate asphalt binder properties to overall field performance. Bell (1989) began to shift focus from consideration of binder properties only, to a combination of binder and total mixture properties through evaluation of field aged mixture or extracted and recovered (E/R) binder. The author recommended that more field data was needed to better understand field aging behaviors and performance of asphalt pavements.

Recently, many additives and modifications (i.e. WMT, RAP, RAS, polymer, hydrated lime, etc.) have become common in asphalt pavements, which result in complex mixtures which often have different properties than virgin mixtures. A review of state specifications found that hydrated lime is typically used at 1% of dry aggregate weight in the southeast US. Some states, such as Georgia, require a minimum of 1% by virgin aggregate mass and an additional 0.5% by RAP aggregate mass. Hansen et al. (2017) summarized a NAPA survey which showed that during the 2015 US construction season, the average RAP content was 20%. Additionally, Hansen et al. (2017) stated that of the 365 million tons of asphalt produced, 120 million of them (roughly 1/3rd of the total tonnage) utilized WMT, 72% of which was foamed asphalt. Some studies stated that addition of RAP can improve mixtures stiffness, which can be an early-life concern with WMA (Kim et al. 2012).

Doyle and Howard (2013) found that addition of high RAP content improved rutting resistance of WMA mixtures. However, other studies have shown that inclusion of RAP in WMA mixtures may result in inadequate blending between RAP and virgin binders due to lower production temperatures, especially when high RAP percentages are used (Bennert 2012b, Mogawer et al. 2012, Bonaquist 2011). With this increasing complexity of asphalt mixtures, monitoring of changes in asphalt properties during field aging is still widely used to observe the effects of such materials (i.e. Prowell et al. 2007, Martin et al. 2014, and others). Tables 2.2, 2.3, and 2.4 summarize several efforts which evaluated field performance of pavements constructed with WMA technologies. Table 2.2 includes studies which evaluated mixture properties obtained from field aged test sections. Table 2.3 summarizes field studies conducted on extracted and recovered binder. Table 2.4 summarizes field distress surveys of WMA pavements found throughout literature.

Table 2.2. Summary of Field Aging of WMA Pavements (Mixture Testing)

Reference	Description of Test Section(s)	Loc.	RAP (%)	Field Aging Time (yr)	Test methods	Findings
Bower et al. (2016)	1 HMA and 4 WMA sections with wax and foaming	WA	15-20	4.0	HLWT, M_R , FE_{+20} , and FE_{-10}	Wax and foam had stiffness similar to HMA. Wax showed better resistance to fatigue cracking while foam was comparable to HMA. Rutting results were inconsistent.
Gu et al. (2015b)	1 HMA and 2 WMA with foaming & chemical additive	TX	NS	1.3	OT	Evotherm slightly improved the cracking resistance while foaming was comparable to HMA.
Hurley et al. (2010)	1 HMA and 2 WMA sections with wax and chemical additive	WI	NS	0.3	IDT	Sasobit initially had slightly lower S_t than HMA, and Evotherm had much lower S_t . After 4 months in the field, S_t of both WMAs had increased significantly; however, Evotherm was still below initial S_t of HMA. 4-month cores could not be obtained for the HMA section.
Jones et al. (2011)	1 HMA and 1 WMA section with foaming	WA	20	3.3	IDT, TSR, HLWT, and M_R	WMA and HMA exhibited similar stiffness, moisture susceptibility and rutting performance.
Sargand et al. (2012)	1 HMA and 3 WMA sections with chemical additive, wax, and foaming	OH	15	3.8	LFWD, IDT, and TSR	LFWD showed significantly higher moduli for Aspha-min and Evotherm than for Sasobit and HMA after 46 months in the field. At 3 months in service, all mixtures had similar tensile strength. After 46 months, HMA had the highest tensile strength. TSR values of 46-month cores indicated improved moisture resistance for Evotherm and Sasobit relative to HMA. Aspha-min had lower TSR than HMA.
Shen et al. (2017)	28 sites each consisting of control HMA sections and WMA sections with wax, chemical additive, and foaming	*	0-30	10.0	LFWD, IDT, FE, and HLWT	WMA pavements produced with organic wax additives showed reduced cracking resistance in the long term, relative to chemical additive or foamed WMA pavements. Rutting and moisture damage resistance was not significantly different for the HMA and WMA pairs, nor among the different WMA technologies.
Yin et al. (2014)	2 HMA and 2 WMA with chemical additive and wax	IA TX	0-17	1.0	M_R , dry and wet IDT, and HLWT	HMA initially had higher M_R than WMA; however, after 6 months in IA and 8 months in TX, there was little difference. HMA initially had better resistance to moisture damage than WMA, but after one summer of field aging WMA had equivalent or better performance.

* MT, TN, IA, TX, LA, MD, MO, MN, OH, PA, VA, IL, SC, WA, CO, NE, NV, and CA.

Loc.= location; RAP= Reclaimed Asphalt Pavement; IDT= Indirect Tensile; FE= Fracture Energy; TSR= Tensile Strength Ratio; HLWT= Hamburg Load Wheel Tracking; M_R =Resilient Modulus; LFWD= Light Falling Weight Deflectometer; OT = Texas Overlay Tester.

Table 2.3. Summary of Field Aging of WMA Pavements (Binder Testing)

Reference	Description of Test Section(s)	Loc.	RAP (%)	Field Aging Time (yr)	Test methods	Findings
Bernier et al. (2017)	6 WMA sections with wax	MA	0-18	8.0	FTIR	FTIR results showed no discernable difference among the test sections after 8 years in service.
Bower et al (2016)	1 HMA and 4 WMA sections with wax and foaming	WA	15-20	4.0	PG tests, MSCR, frequency sweep, fatigue and thermal cracking testing	WMA binders exhibit lower complex shear modulus values and less resistance to fatigue cracking and rutting than HMA binders. Overall, WMAs were mostly comparable to corresponding HMA.
Diefenderfer and Hearon (2008)	2 HMA and 2 WMA sections with wax	VA	20	1.0	DSR and BBR	HMA high temperature grade increased one grade over 1 year, while WMA did not. WMA low temperature grade increased for one mix type over 1 year, while other mixtures did not change.
Diefenderfer and Hearon (2010)	3 HMA and 3 WMA sections with wax and chemical additive	VA	20-35	2.0	PG grading	PG grading showed that stiffness gain rate of Sasobit was reduced after construction. No difference in PG was appeared for Evothorn and HMA, except for an increase of one low temperature grad for Evothorn at 2 year.
Farshidi et al. (2013)	3 HMA and 10 WMA sections with foaming, wax, and chemical additives	CA	NS	4.3	DSR, MSCR, frequency sweep, and BBR	Frequency sweeps showed no difference in WMAs and their control HMAs at any aging level. Complex viscosity values typically showed that WMAs produced with organic waxes had higher rates of aging than HMA. Aging rates of mixtures produced with chemical additives and foaming appeared dependent on factors other than the WMT.
Jones et al. (2013)	2 HMA and 7 WMA with chemical additive, wax, and foaming	CA	NS	4.0	BBR and DSR	Binder tests showed early rutting susceptibility for WMA; however, WMA and HMA performed similarly with wax additive having slightly better rutting resistance for all test sections.

Loc.= Location; RAP= Reclaimed Asphalt Pavement; MSCR= Multiple Stress Creep Recovery; DSR= Dynamic Shear Rheometer; FTIR= Fourier Transform Infrared Spectroscopy; BBR= Bending Beam Rheometer; PG= Performance Grade

Table 2.4. Summary of Field Aging of WMA Pavements (Field Surveys)

Reference	Description of Test Section(s)	Loc.	RAP (%)	Field Aging Time (yr)	Test methods	Findings
Bernier et al. (2012)	1 HMA and 2 WMA sections with wax and foaming	CT	NS	1.0	Field distresses surveys	Rutting and cracking were significantly different for all three sections. Sasobit had the highest rut depth and foamed asphalt had the lowest. Sasobit had the most amount of cracking and HMA had the least.
Bernier et al. (2017)	6 WMA sections with wax	MA	0-18	8.0	PCI ASTM D5340	Visual inspection showed no discernable difference among the test sections after 8 years in service.
Bower et al. (2016)	1 HMA and 4 WMA sections with wax and foaming	WA	15-20	4.0	Field distresses survey.	WMA initial seemed to be more resistant to reflective transverse cracking than HMA. No moisture damage was observed in any section. Overall, WMA and HMA showed similar performance.
Hajj et al. (2011)	1 HMA and 2 WMA with foaming	NV	15	2.0	Field distresses surveys	Lab results showed WMA had lower rutting resistance, but no rutting was observed in field. Overall, WMA and HMA performed similar.
Diefenderfer and Hearon (2010)	3 HMA and 3 WMA sections with wax and chemical additives	VA	20-35	2.0	Field distresses surveys	Centerline cracking was present mainly in HMA section but some in WMA sections; otherwise, no significant difference was observed among the 4 test sections for the 2-year period.
Jones et al. (2011)	1 HMA and 1 WMA with foaming	WA	20	3.3	Sand patch testing ASTM E965	HMA and WMA sections exhibited similar field performance.
Jones et al. (2013)	2 HMA and 7 WMA with chemical additives, wax, and foaming	CA	NS	4.0	Field distresses surveys	Field evaluation showed that WMA performance was comparable to HMA; however, one test section showed early aging rutting compared with corresponding HMA.
Kim et al. (2012)	2 HMA and 2 WMA with foaming and chemical additive	NE	NS	3.0	IRI	WMA and HMA showed similar performance according to IRI. No cracking was observed, while rutting and roughness of WMA were similar to HMA.
Lavorato et al. (2011)	1 HMA and 1 WMA with chemical additive	Ontario	NS	0.7	Field distresses surveys	HMA and WMA field performance were similar and acceptable.
Sargand et al. (2012)	1 HMA and 3 WMA with chemical additive, wax, and foaming	OH	15	3.8	IRI	IRI values were not significantly different among the sections at any point in time; however, Evotherm initially had the lowest IRI but had the highest after 46 months. No measurable rutting was observed in any of the sections.
Shen et al. (2017)	28 sites HMA and WMA sections with wax, chemical additive, and foaming.	*	0-30	10.0	Field distresses survey.	HMA and WMA pavements showed comparable rutting performance. Chemical and foamed asphalts showed better long term resistance to longitudinal and transverse cracking than wax. Field transverse and longitudinal cracking was mostly seen in pavements 4 years or older.
Wielinski et al. (2009)	2 HMA and 2 WMA with foaming	CA	15	0.4	Field distresses surveys	Initial field performance of WMA and HMA were comparable.

* MT, TN, IA, TX, LA, MD, MO, MN, OH, PA, VA, IL, SC, WA, CO, NE, NV, and CA;

Loc.= Location; RAP= Reclaimed Asphalt Pavement; PCI= Pavement Conditions Index; IRI= International Roughness Index

In addition to WMT, inclusion of RAP, RAS, other materials, and mixing /compaction temperature can have effects on WMA performance. Test methods can also a factor when assessing performance. Bazuhair et al. (2018) showed that indirect tensile (IDT) results were affected differently by oxidation than moisture damage. Mixture test results from Bower et al. (2016) showed that foamed asphalt mixtures had more or similar rutting than HMA. This was found dependent on production temperature. For thermal cracking, foam and wax produced at temperatures lower than 130°C performed better than HMA while having comparable performance when produced above 130°C. Binder test results of Bower et al. (2016) showed that WMA binders exhibited less resistance to fatigue and rutting than the HMA binders. For thermal cracking, the authors found no difference between foamed WMA binders and their corresponding HMA binders, but that Sasobit binders had better resistance to thermal cracking than HMA binder. Bower et al. (2016) noted that binder test results may not successfully characterize performance of asphalt mixtures when produced with RAP. Complete blending of virgin and recycled binder during the extraction and recovery process may skew results as this full blending does not occur during plant production. Farshidi et al. (2013) also found that aging rates of mixtures produced with chemical and foaming additives appeared dependent on factors other than the WMT.

Tables 2.2 to 2.4 showed that field distress surveys found similar WMA and HMA performance. Most laboratory evaluations found that wax had low cracking resistance compared to chemical and foaming technologies, while mixtures with WMTs had similar field rutting performance. Note that most field aged studies used one of two evaluation methods. First, some obtained cores to investigate the initial properties of WMA and conducted field distress surveys to measure field performance. Others obtained cores from known pavement sections and compared them with those from corresponding HMA sections. There is still a lack in studies which have been conducted on test sections monitored continuously from the time of construction.

2.3.2 Laboratory Aging of Warm Mix Asphalt

As previously mentioned, WMA and HMA mixtures typically have several discrepancies in their properties at time of production; however, as discussed in Section 2.3.1, these differences in properties change as mixtures are exposed to environmental effects and/or traffic loading. To capture the effects of environmental exposure on asphalt mixtures and binders, field aging studies are of vital importance; however, field aging can be highly variable from location to location, and even from year to year within the same location. With laboratory conditioning, the effects of individual damage mechanisms that maybe experienced by asphalt mixtures in the field, such as oxidation, moisture, and freeze-thaw (FT) can be isolated, and applied at controlled levels. This type of evaluation allows for investigation into WMA behavior compared to HMA without corrections or assumptions for variations in field conditions.

Laboratory conditioning is typically applied in one of two manners: oxidative damage via long term oven aging (LTOA), and moisture damage via hot water conditioning and/or FT cycles. Bell (1989) recognized that there had been little work performed on the aging of asphalt mixtures. As such, there was a series of studies conducted (i.e. Bell 1989 and Bell et al. 1994a and 1994b) which resulted in the suggestion of LTOA protocols ranging from 2 to 8 days at 85°C. From this, the current prevailing aging protocol (AASHTO R30) was developed, which consists of 5 days LTOA at 85°C. This method, along with others (e.g. Cucalon et al. 2017, Diefenderfer and Hearon 2008, Yin et al. 2014, etc.) is commonly used to induce oxidative damage on asphalt specimens.

The current prevailing moisture conditioning methods are AASHTO T283 (developed from Lottman 1978) and ASTM D4867 (developed from Tunnicluff and Root 1984). T283 consists of vacuum saturating compacted specimens, subjecting them to one 16 hour FT cycle, then transferring them to a 60°C water bath for 24 ± 1 hour. D4867 consists of vacuum saturating compacted specimens, then soaking them in a 60°C water bath for 24 ± 1 hour. D4867 also has an option for a 15 hour FT cycle. While not all literature uses these exact methods (e.g. Diefenderfer and Hearon 2008 and Malladi et al. 2015), they are very common for determining moisture susceptibility. Others, such as Cucalon et al. (2017) and Xiao et al. (2011), have utilized more novel moisture conditioning methods (summarized in Table 2.6) to evaluate moisture susceptibility of asphalt mixtures.

Tables 2.5 and 2.6 summarize studies which evaluated changes in properties of mixtures produced with WMTs due to oxidative and moisture conditioning, respectively. In these tables, only conditioning which follows either STOA or plant production is considered. In cases where mixtures were laboratory produced, short-term aging protocols followed by the authors are not of interest, thus are not described in the table. Also, there is no Hamburg loaded wheel-tracker (HLWT) data in Tables 2.5 and 2.6, although it is a common method to evaluate moisture susceptibility. It is envisioned that HLWT literature will be included in companion works to be written at a future date.

Table 2.5. Effects of Laboratory Oxidative Conditioning on Warm Mix Technologies

Reference	WMT(s)	Conditioning	Testing	Summary of Findings
Abbas et al. (2016)	Foaming	R30	DSR, GPC, and FTIR on E/R binder	DSR showed similar or slightly reduced WMA binder stiffness vs. HMA. FTIR and GPC indicated WMA binders aged slightly less than HMA binders.
Alhasan et al. (2014)	Foaming	2h LTOA @ T _c + R30	TSRST	HMA mixtures had colder fracture temperatures than WMA prior to LTOA. Mixtures performed similarly after LTOA.
Bonaquist (2011)	Advera, Evotherm, and Sasobit	R30	CDT	CDT showed comparable fatigue performance between HMA and WMA after LTOA.
Cucalon et al. (2017)	Foaming, Sasobit, Evotherm, and Rediset	3 mo. LTOA @ 60°C	DMA	HMA had better fatigue cracking resistance than most WMA mixtures before LTOA. LTOA reduced performance differences between HMA and WMA; however, HMA still outperformed all WMAs except for the foam mixture.
Diefenderfer and Hearon (2008)	Sasobit	4 & 8 days LTOA @ 85°C	IDT	HMA initially had slightly better S _t than WMA. This difference decreased with 4 days of LTOA but increased with 8 days.
Ghandi et al. (2010)	Sasobit and Asphamin	R30	GPC on E/R binder	GPC indicated that binder in WMA mixtures aged differently than HMA.
Haggag et al. (2011)	Advera, Evotherm, and Sasobit	R30	CDT	No testing was performed before LTOA. After LTOA there was significant differences in dynamic modulus among HMA and WMA mixtures.
Hurley and Prowell (2005a)	Aspha-min	1, 3, & 5 days LTOA @ 85°C	IDT	S _t of all mixtures decreased due to LTOA, but there was little to no difference between HMA and WMA.
Hurley and Prowell (2005b)	Sasobit	1, 3, & 5 days LTOA @ 85°C	IDT	WMA had tensile strengths similar to or lower than HMA before LTOA. Increased LTOA caused WMA S _t to approach HMA.
Hurley and Prowell (2006)	Evotherm	1, 3, & 5 days LTOA @ 85°C	IDT	IDT was not adequate in characterizing this WMA relative to HMA after conditioning.
Kim et al. (2015)	Foaming	R30 on loose & compacted mix	TSRST	TSRST cracking temperature of WMA was worse than HMA prior to LTOA, with statistical significance. After LTOA there was no statistically significant difference.
Safaei et al. (2014)	Evotherm and Foaming	2 & 8 days LTOA @ 85°C	CX CDT and E*	E* was higher for HMA at all aging levels, but as aging increased E* of WMA approached HMA. CDT showed better fatigue performance for HMA before and after 2 days of LTOA; however, after 8 days of LTOA there was negligible difference.
Yin et al. (2014)	Evotherm, Sasobit, and Foaming	7, 14, 28, 56, & 112 days LTOA @ 60°C	M _R	M _R of HMA was initially greater than WMA. For one mix design, this difference remained approximately the same for all aging levels. For the second mix design, after 2 weeks of LTOA at 60°C, M _R values for all mixture were approximately the same.

LTOA= long term oven aging; R30= AASHTO R30; DSR= dynamic shear rheometer; GPC= gel permeation chromatography; FTIR= fourier transform infrared spectroscopy; E/R= extracted & recovered; IDT= indirect tensile; |E*|= dynamic modulus; M_R= resilient modulus; DMA= dynamic mechanical analysis; CDT= cyclic direct tension; CX= controlled crosshead; TSRST= thermal stress restrained specimen test.

Table 2.6. Effects of Laboratory Moisture Conditioning on Warm Mix Technologies

Reference	WMT(s)	Laboratory Conditioning	Testing	Summary of Findings
Ali et al. (2012)	Foaming	T283	IDT	TSR showed WMA was slightly more susceptible to moisture damage than HMA.
Bonaquist (2011)	Advera, Evotherm, and Sasobit	T283	IDT and CDT	WMA had lower wet S_t and TSR.
Cucalon et al. (2017)	Foaming, Sasobit, Evotherm, and Rediset	0 & 3 months LTOA of saturated specimens @ 60°C	DMA	HMA had better fatigue cracking resistance than most WMA mixtures before LTOA. LTOA reduced performance difference between HMA and WMA; however, HMA still outperformed all WMAs except for the foam mixture.
Diefenderfer and Hearon (2008)	Sasobit	Modified T283 (no 16h curing or 24h storage)	IDT	TSR for WMA was similar to or better than HMA.
Goh and You (2011)	Foaming	T283	IDT	T283 conditioning caused little to no decrease in WMA S_t , while S_t of HMA decreased considerably. However, WMA consistently had lower S_t than HMA.
Hurley and Prowell (2005a)	Aspha-min	D4867	IDT	D4867 conditioning significantly decreased WMA S_t more than HMA.
Hurley and Prowell (2005b)	Sasobit	D4867	IDT	Effects of D4867 conditioning appeared to be dependent on factors other than WMT.
Hurley and Prowell (2006)	Evotherm	D4867	IDT	S_t was not adequate in characterizing characteristics of this WMA relative to HMA after conditioning.
Kavussi and Hashemian (2012)	Foaming	T283	IDT	WMA had lower S_t . One mixture had TSR similar to HMA while another had significantly lower TSR.
Lee and Kim (2014)	Chemical, Foaming, and Wax	T283	CDT and IDT	CDT showed T283 conditioning caused similar reductions in fatigue life between HMA and Evotherm. The other chemical additive, foamed WMA, and waxes had much greater reductions in fatigue life. T283 conditioning had considerably greater detrimental effects on S_t of all WMA relative to HMA.
Malladi et al. (2015)	Sasobit, Advera, and Foaming	Modified (no FT) T283	IDT and APA	S_t of Sasobit mixtures were less effected by T283 conditioning than HMA. S_t of Advera and foamed mixtures were greatly reduced due to T283 conditioning. APA rut depth of Advera and foamed mixtures were not affected by moisture conditioning.
Porras et al. (2012)	Advera, Sasobit, and Evotherm	1 and 3 FT cycles	E* and IDT	FT cycles had little effect on HMA S_t . Increased cycles continued to reduce WMA S_t . At zero and one FT cycle, Sasobit had higher E* than HMA, Advera, and Evotherm (which were all similar). After three FT cycles, all mixtures had similar E* .
Prowell et al. (2007)	Evotherm	D4867 with 1 FT cycle	IDT	HMA and WMA had similar unconditioned S_t . Conditioning reduced WMA S_t much more than HMA. Authors stated this could be due to discrepancies in air void levels.
Xiao et al. (2011)	Aspha-min and Sasobit	1, 60, & 90 days in 60°C water	IDT	As moisture conditioning time increased, wet S_t of all mixtures decreased. HMA consistently had higher S_t than WMA.

LTOA= long term oven aging; T283= AASHTO T283; D4867= ASTM D4867; IDT= indirect tensile; |E*|= dynamic modulus; APA= asphalt pavement analyzer; DMA= dynamic mechanical analysis; CDT= cyclic direct tension.

Of particular interest in this literature review was the type of damage inflicted on compacted asphalt specimens. As seen from the two separate tables (2.5 and 2.6) oxidative and moisture conditioning are typically evaluated separately from each other. A majority of studies do not consider the effects of one on the other; mainly, how continued oxidation effects WMA resistance to moisture damage relative to HMA. However, there are several cases (i.e. Cucalon et al. 2016, Diefenderfer 2008, Xiao et al. 2011 and 2013, and Yin et al. 2014) where resistance to moisture damage was evaluated with a version of AASHTO T283 and/or HLWT testing as a function of oxidative aging times, usually induced via LTOA.

Cucalon et al. (2016) utilized a control HMA and four WMA mixtures, where two mixtures were produced with Evotherm and two with foaming. One Evotherm and one foam mixture was produced with a modified PG 70-22 binder and no recycled materials. The other Evotherm and foam mixtures were produced with an unmodified binder and included 15% RAP and 3% RAS. To determine the differences in moisture susceptibility as a function of LTOA, Cucalon et al. (2016) utilized dry and wet IDT testing per AASHTO T283 before and after performing R30 conditioning. The authors found that WMA mixtures were more susceptible to moisture damage than HMA before LTOA. After R30, wet tensile strengths and tensile strength ratio (TSR) showed that the WMA mixtures had moisture damage resistance similar to HMA.

Diefenderfer and Hearon (2008) evaluated WMA mixtures produced with the organic wax Sasobit, relative to a control HMA. The authors induced oxidative damage via LTOA for 4 and 8 days at 85°C, and moisture conditioning was performed following a modified version of AASHTO T283, where the stated 16 hour curing time and 24 hour storage time were not applied. IDT testing was performed by the authors on both dry and wet specimens before LTOA and after 4 and 8 days of LTOA to investigate how moisture susceptibility of WMA relative to HMA changes with increased oxidative damage. Diefenderfer and Hearon (2008) found that initial WMA TSR was similar to or better than HMA, and TSR increased more with increased LTOA times for WMA than it did for HMA. Considering tensile strength values, HMA initially had higher wet and dry tensile strength. The authors observed WMA dry tensile strength approached HMA after 4 days of LTOA, indicating a convergence of values; however, after 8 days, the difference between HMA and WMA had increased. Wet tensile strength data collected by Diefenderfer and Hearon (2008) showed a faster rate of increase for WMA than HMA in the aging time span considered by the authors. As such, wet tensile strength of WMA would be expected to reach that of HMA with prolonged LTOA.

Xiao et al. (2012) evaluated moisture susceptibility of WMAs produced with Aspha-min (a foaming zeolite additive), Sasobit, and Evotherm with the South Carolina standard denoted SC T 70 (24 hours in 60°C water). The authors determined wet and dry tensile strengths of specimens before and after LTOA via AASHTO R30. Before LTOA, the authors found that HMA and Sasobit had slightly higher wet tensile strengths than Evotherm, and that Aspha-min performed very poorly. Xiao et al. (2012) observed that LTOA improved moisture damage resistance of Sasobit and Evotherm-produced mixtures, relative to HMA; however, Aspha-min still had greatly reduced performance compared to all other mixture types. Additionally, the authors found that for all mixtures SC T 70 improved flow resistance.

Xiao et al. (2013) investigated the aged and unaged moisture susceptibility of five different WMA mixtures produced with Asphamin, Cecabase, Evotherm, Rediset, and Sasobit. LTOA and moisture conditioning were induced via AASHTO R30 and T283, respectively. Wet and dry tensile strength data for the mixtures considered by the authors is presented in Xiao et al. (2009) and showed that the only difference among the mixtures was a reduced moisture damage resistance for

Aspha-min. Xiao et al. (2013), which reports the dry and wet tensile strengths and TSR values of the mixtures after R30 aging, found that after LTOA there was little difference among most mixtures. However, TSR was still significantly lower for Aspha-min.

Yin et al. (2014) evaluated two mix designs produced with Evotherm, Sasobit, and foaming, each from different field projects located in Iowa (IA) and Texas (TX). Moisture conditioning was performed per AASHTO T283 before and after different lengths of LTOA. Laboratory mixed- laboratory compacted (LMLC) specimens of IA and TX mix designs were long term aged for 16 weeks at 60°C and evaluated using wet and dry IDT testing. LMLC specimens of just TX mix design specimens were aged for 2 weeks at 60°C and 5 days at 85°C and evaluated via HLWT testing as well as wet and dry IDT. Prior to LTOA, the authors observed higher moisture susceptibility for WMA mixtures than HMA; however, after 16 weeks at 60°C or 5 days at 85°C, Yin et al. (2014) reported similar moisture damage resistance for all mixtures.

2.4 Replicating Field Aging with Laboratory Conditioning

In the 1950 to 1980 time range, a series of controlled road tests were performed in order to link multiple laboratory tests to field measured data (see Copas and Pennock 1979). In this period, pavement aging was mainly evaluated with binder properties (Copas and Pennock 1979, and Bell 1989). In the late 1980's and into the 1990's, studies started to evaluate and recommend accelerated pavement aging methods based on mixture performance and aging (e.g. Bell 1989, Kim et al 1986, McHattie 1983). A series of laboratory conditioning methods was developed from Bell (1989), Bell et al. (1994a), and Bell et al. (1994b), which recommended LTOA for 2 to 8 days at 85 °C depending on the field aging time and climatic conditions that were to be simulated. From this, the current prevailing long term mixture conditioning method, AASHTO R30, was developed, which consists of two methods for STOA followed by LTOA. The first STOA method recommended by R30 is 2 hours at compaction temperature for volumetric design, and the second method is 4 hours at 135°C for mechanical property testing (all STOA recommendations are performed on loose mixture immediately prior to compaction). STOA is typically not performed on plant-mixed material prior to lab compaction since it has already experienced short-term aging during production. LTOA, according to R30, is performed for 5 days at 85°C following compaction. Standard methods for accelerated aging of asphalt binders (i.e. rolling thin film oven and pressure aging vessel) were also developed by another series of studies (e.g. Peterson et al. 1994a, Branthaver et al. 1993, Anderson et al. 1994, and Peterson et al. 1994b).

There are two schools of thought that exist with respect to conditioning asphalt mixtures for subsequent mechanical property testing. The first is to age loose mixed material well beyond STOA prior to compaction, and then test the compacted mix soon thereafter. The second is to compact mix immediately following STOA and then condition the compacted specimen prior to mechanical property testing. Aging of loose mixtures results in uniform aging throughout the final compacted specimen, while LTOA of compacted specimens or cores results in an aging gradient. Elwardany et al. (2016) claims that the uniform aging resulting from loose mix LTOA is an attribute to the process. The authors state that while aging gradients are present in field pavements, they are exclusively from the top down; whereas, gradients of lab-aged specimens originate from all exposed faces. Elwardany et al. (2016) presents this lack of aging gradient, increased speed of oxidation, and reduced issues with specimen integrity during aging as reasons to perform LTOA on loose mix in favor of compacted specimen aging. However, Reed (2010) determined that increasing LTOA time of loose mixture did not result in dynamic modulus trends similar to those

found with increasing field aging time, while increasing LTOA of compacted specimens did. While there is a significant amount of research related to LTOA of loose asphalt mixture for performance testing, this literature search suggests that the compacted aging method described in AASHTO R30 is currently the most widely used accelerated laboratory aging method; however, the validity of the method has recently been brought into question. As such there are a large number of studies using the basic concepts of R30 with altered mixture aging times and temperatures.

AASHTO R30 claims that it can replicate similar mixture properties as pavements which have been in service for 7-10 years. However, recent research has suggested that this claim may be an overestimation (e.g. Harrigan 2007, Howard and Doyle 2015, Martin et al. 2014, Cox et al. 2017, Isola et al. 2014, etc). This overestimation could be a result of the increasing complexity of asphalt mixtures which often incorporate a multitude of additives, modifiers, and recycled materials such as WMA technologies, polymer modifiers, RAS, ground tire rubber (GTR), and others. Another concern with R30 is that it only considers one damage mechanism (i.e. oxidation through heating) while pavements in service experience multiple types of climate-based mechanism, such as moisture and freeze-thaw. Thus, laboratory conditioning protocols which consider modern asphalt mixtures as well as multiple damage mechanisms are needed. Towards this effort, several recent studies have been conducted in the laboratory and field to capture performance and behaviors of asphalt mixtures and/or binders as a function of aging. Table 2.7 summarizes the findings of several such studies.

Table 2.7. Correlation of Field Aging and Laboratory Conditioning of Asphalt Mixtures

Reference	Conditioning/ Field Aging	Test Method(s)	Material Properties	Findings
Cox et al. (2017)	<ul style="list-style-type: none"> • R30 • Other methods were performed but not used in prediction of field aging times • 1-2 years in Starkville-Columbus, MS 	CML	Variety of mixtures which included RAP ranging 0-20%, some with polymer or GTR modified binders. Hydrated lime and varying WMTs were used in some mixtures.	CML testing indicated that R30 represented approximately 12-30 months of field aging depending on mix type.
Elwardany et al. (2016)	<ul style="list-style-type: none"> • Combinations of LTOA of loose and compacted mixture with and without pressure • LTOA times ranged 1-35 days • LTOA temperatures ranged 70-95°C • 8 years at FHWA ALF in McLean, VA 	E* and S-VECD on mixtures; DSR and FTIR on E/R binder	Compacted vs. loose mix LTOA study used all virgin lab produced mixture. Field validation used SBS modified mixture with 1% hydrated lime.	The authors suggest loose mix aging at 95°C. 21 days of aging at 95°C was required to match binder properties of the top half inch of an 8 year old field core. The required aging time decreases with increased pavement depth.
Elwardany et al. (2018)	<ul style="list-style-type: none"> • LTOA of loose mix @ 70, 85, and 95°C. 	DSR on E/R binder	One mixture with SBS modification. All others were unmodified. Presence and amounts of recycled materials or other modifiers/ additives were not specified.	Maps of the US were generated which specify the amount of loose mix LTOA that is required to represent binder properties after 4, 8, and 16 years at pavement depths of 6, 20, and 50 mm.
Houston et al. (2005)	<ul style="list-style-type: none"> • 5 days @ 80, 85, and 90°C • 12 years in Flagstaff, AZ • 9 years in Kingman, AZ • 9 years in MnRoad, MN • 7 years in WesTrack, NV 	E*	All mixtures used an AC-20 binder except that in Kingman, AZ which used an AC-30. No RAP or polymer modification was used.	Dynamic modulus of lab aged material was mostly similar to or greater than that of field aged. The authors compared LTOA of 4 inch diameter cores cut from laboratory compacted specimens to 4 inch diameter sub-cores cut horizontally from 6 inch field aged cores.
Howard and Doyle (2015)	<ul style="list-style-type: none"> • R30 • 28 days LTOA @ 60°C • 1 year in Starkville, MS 	CML	HMA with 15% RAP and hydrated lime.	R30 represented less than one year of field aging while 28 days @ 60°C represented approx. 1 year.
Isola et al. (2014)	<ul style="list-style-type: none"> • R30 • CPPC • R30 + CPPC • Field aging not specified 	Superpave IDT	Two granite mixtures, one with hydrated lime, and a third limestone mix. Unmodified PG 67-22 binder was used.	CPPC continued to reduce FE past what was observed for R30 alone. Reduction in FE from the combination of R30 and CPPC was similar to that of field aged pavements.

- Table continues on next page

Li et al. (2018)	<ul style="list-style-type: none"> • R30 of loose mixture • 0-3 years at FHWA ALF in McLean, VA 	DTMT	HMA and WMA produced with foaming and chemical additives. RAP and RAS contents ranged from 0-44% and 0-6%, respectively. One of the two binder types contained 5% REOB.	DTMT showed that R30 aging of loose mixture exceeded the aging observed in 3 year cores.
Yin et al. (2016)	<ul style="list-style-type: none"> • 14 days LTOA @ 60°C • 3 and 5 days LTOA @ 85°C • 8-22 months field aging in TX, NM, WY, SD, IA, IN, and FL. 	M _R and HLWT	HMA and WMAs produced with foaming and chemical additives. Mixtures included 0-25% RAP and 0-3% RAS. Some binders were polymer modified.	3 days @ 85°C and 14 days at 60°C resulted in mixture properties similar to cores aged for 7 months in warmer climates and 12 months in cooler climates. 5 days @ 85°C replicated 12 and 23 months of field aging in warmer and cooler climates, respectively.

R30= AASHTO R30; CML= Cantabro Mass Loss; RAP= Reclaimed Asphalt Pavement; GTR= Ground Tire Rubber; LTOA= Long Term Oven Aging; FHWA= Federal Highway Administration; ALF= Accelerated Loading Facility; |E*|= Dynamic Modulus; S-VECD= Simplified Visco-Elastic Continuum Damage; DSR= Dynamic Shear Rheometer; FTIR= Fourier Transform Infrared Spectroscopy; E/R= Extracted and Recovered; SBS= Styrene-Butadiene-Styrene; CPPC= Cyclic Pore Pressure Conditioning; IDT= Indirect Tensile; FE= Fracture Energy; DTMT= direct tension monotonic test; RAS= Recycled Asphalt Shingles; REOB= Re-refined Engine Oil Bottoms.

Note that with the exception of Isola et al. (2014), all sources in Table 2.7 utilized only oxidative damage via LTOA to replicate field aging. Moisture conditioning is extremely common in attempting to evaluate moisture damage resistance of an asphalt mixture (see Table 2.6); however, there has been very little literature found which has attempted to correlate laboratory induced moisture damage to field aging time. Shen et al. (2018) evaluated 28 full-scale pavement test sections across the US and found that cracking was more prevalent in high moisture areas. As such, excluding moisture damage from laboratory conditioning could be highly problematic in predicting future mixture properties. Companion efforts (i.e. related to the research presented in this document), such as Howard et al. (2018) and Smith and Howard (2018), have made strides in filling this gap in current research. Howard et al. (2018) utilized six of the seven laboratory conditioning protocols (CPs) described later in this report and found that to simulate long term field aging of asphalt mixtures in the Mississippi climate, more severe conditioning protocols than are currently being used are needed. The authors state that AASHTO R30 simulated, at most, less than 3 years of environmental damage. Smith and Howard (2018) implemented all of the same seven CPs used in this document and determined that AASHTO R30 does not adequately replicate a long time of field aging in the Southeast US (i.e. consistently less than 2 years' worth of environmental damage). Based on Cantabro mass loss (CML) results, the authors suggested using one of the more severe alternative CPs that were evaluated, which were found to simulate up to 5 years of field aging.

Although Isola et al. (2014) has also performed moisture conditioning as an accelerated laboratory aging method, there are still areas that the authors do not cover. Isola et al. (2014) only observed fracture properties utilizing Superpave IDT. Isola et al. (2014) sampled many field projects, but their laboratory mixed material did not exactly match all mixtures that were field aged. The authors do not provide estimated field aging times which their conditioning methods replicated, instead they state that the combination of R30 plus cyclic pore pressure conditioning (CPPC) resulted in cracking properties similar to what was observed in the field. While Isola et al. (2014) has made great strides by combining moisture and oxidation laboratory aging methods, there are areas which Howard et al. (2018) [volume 1 of this work], Smith et al. (2018) [volume 2 of this work], and the current document hope to expand when viewed collectively.

It was also observed in this literature review that, a majority of the studies summarized in Table 2.7 correlated field aging of asphalt cores to laboratory conditioning of laboratory compacted specimens, or to cores sampled immediately after construction and aged in the laboratory. Studies have shown that there are often differences in the performance of field compacted and laboratory compacted specimens due to factors such as discrepancies in short-term aging and compaction temperatures (e.g. Aschenbrenner 1995). There have been few studies prior to the work of MDOT SS266/270 which have compared laboratory compacted specimens that were conditioned in the lab and aged in the field (i.e. Kemp and Predoehl 1981, and Howard and Doyle 2015). Kemp and Predoehl (1981), conducted a study between 1974 and 1980 where laboratory produced specimens were aged at four test sites in California representing mountain (South Lake Tahoe), valley (Sacramento), coastal (Fort Bragg), and desert (Indio) climates for 1, 2 and 4 years. Extracted asphalt properties and resilient modulus of mixtures were used to compare the effects of environmental exposure to laboratory compacted specimens and virgin binders that were subjected to several different accelerated mixture and binder aging methods. Howard and Doyle (2015) aged laboratory compacted specimens for one year in Mississippi and compared the aged mixture properties with those of specimens subjected to either AASHTO R30 or LTOA for

28 days at 60 °C. This methodology removes the need for corrections or assumptions due to the differences in laboratory versus field compacted mixtures.

2.5 Test Methods to Detect Environmental Damage

A test method capable of characterizing the amount of damage performed due to field aging as represented by laboratory conditioning is needed. Ideally, a test method which can quantify oxidation and moisture related damages would be used. As discussed in Isola et al. (2014), some test methods can reliably detect oxidation but not moisture-induced damage. Other studies have demonstrated that there is no relationship between tensile strength and moisture-related pavement distresses (e.g. Kanitong and Bahia 2008, and Zaniewski and Viswanathan 2006). Cox et al. (2017) discusses several years worth of CML testing on dense graded asphalt to demonstrate the usefulness of mass loss (*ML*) values in detecting durability and brittleness. Therein, binder grade, binder type, binder content, aggregate type, recycled materials, air voids, dust-binder ratio, and aging were assessed in a favorable manner with CML data. One of the most useful attributes about CML testing is that distresses related to durability and brittleness all lead to increased *ML* values. Table 2.8 summarizes several other studies which evaluated varying test methods to detect different types of asphalt mixture and/or binder damage.

Table 2.8. Test Method Evaluations in Literature

Source	Materials Tested	Damage Mechanism	Testing	Major Findings
Bankowski et al. (2016)	SMA 8 & AC 16 P with 35/50 and 45/80-55: HMA & WMA.	STOA & LTOA @ 145°C for HMA & 125°C or 105°C for WMA.	IDT, fatigue, low-temp. cracking, G*, & SCB- LMLC & E/R binder.	ITSR changed less than 10% from unaged to STOA to LTOA mixes.
Harvey and Tsai (1997)	19mm NMAS granite with PG 58/64-10 & PG 58-28.	R30 STOA & LTOA @ 85°C for 3 or 6 days.	Fatigue- beams from LMLC slabs.	CSFB test detected aging, & changes in binder content & V _a .
Isola et al. (2014)	12.5mm NMAS with PG 67-22. Three mixes: granite, lime-treated granite, & limestone.	R30 STOA & LTOA with & without CPPC.	SIDT- LMLC	FE detected combined moisture & oxidation damage.
Kumbargeni and Biligiri (2016)	19mm NMAS with two virgin, one polymer, and one crumb rubber modified binder.	R30, RTFO, & PAV.	E* , Pen., softening point, η, & asphaltene extraction- PAV & E/R binder.	Asphaltene content is an accurate indicator of binder oxidation.
Safaei et al. (2014)	9.5mm NMAS with PG 70-22: Evotherm & foam.	R30 STOA for HMA & 117°C for WMA, LTOA @ 85°C for 2 or 8 days.	E* , CDT, DSR, & fatigue- LMLC & E/R binder.	All test methods detected increase in oxidation damage.
Yin et al. (2016)	Various aggregate sources with binders ranging PG 76-28 to PG 64-22.: HMA, foam, Sasobit, & Advera.	R30 & R30 STOA + 2 weeks @ 60°C or 3 days at 85°C. Field aging in 7 states with varying climates.	M _r and HLWT- LMLC & PMFC	M _r detected change in WMA type, aggregate absorption, and recycled materials, but not production temperature.

CPPC= Cyclic Pore Pressure Conditioning; SIDT= SuperPave Instrumented Indirect Tensile Test; M_R= Resilient Modulus; HLWT= Hamburg Loaded Wheel Tracking; |E*|= Dynamic Modulus; CDT= Cyclic Direct Tension; E/R= Extracted & Recovered; η= Viscosity; G*= Complex Modulus; SCB= Semi-Circular Bending; ITSr= Indirect Tensile Strength Ratio; FE= Fracture Energy, CSFB= Controlled Strain Flexural Beam; LMLC= Lab Mixed-Lab Compacted; PMFC= Plant Mixed-Field Compacted; IDT= Indirect Tensile; PAV= Pressure Aging Vessel; RTFO= Rolling Thin Film Oven; LTOA= Long Term Oven Aging; STOA= Short Term Oven Aging; PG= Performance Grade; NMAS= Nominal Maximum Aggregate Size; V_a= Air Voids.

CHAPTER 3-EXPERIMENTAL PROGRAM

3.1 Overview of Experimental Program

The experimental program evaluated HMA and WMA aging using different conditioning and testing methods. The program includes up to four years of field aging as well as eight laboratory conditioning protocols (CPs) that are later discussed. In evaluating aging, mixture and binder testing were employed. A summary of the specimens tested and specimen test plan are included in Section 3.2, Table 3.1, and Table 3.2. The asphalt mixtures evaluated are described in Section 3.3. Section 3.4 discusses specimen preparation. Section 3.5 describes asphalt mixture testing. Section 3.6 describe binder extraction, recovery, and testing. Overlap with other volumes of this report series (e.g. photographs, test descriptions) occurs since testing for all efforts occurred during the same time frame.

3.2 Specimens Tested and Test Matrices

A total of 1614 mixture specimens were tested for mixes M17 to M20. Of these 1614 specimens, 210 were tested for reasons outside the scope of this report. These specimens were largely tested for MDOT SS250 (Cox and Howard 2015) and include Marshall Stability, PURWheel, and IDT tests (both instrumented and non-instrumented). Table 3.1 summarizes the testing plan for the remaining 1404 mixture specimens of relevance to this report which were conditioned as follows: 192 specimens were tested without any laboratory conditioning or field aging, and are denoted 0-yr or CP0 specimens, 384 specimens were field aged for up to four years and are denoted 1-yr, 2-yr, 3-yr, or 4-yr, 816 specimens were laboratory conditioned and denoted CP1 to CP8, and 12 specimens were field aged for up to one year to test for the effects of PVC sleeve covering (6 with sleeves and 6 without sleeves). Each of the first seven lab CPs were treated identically in regards to number of specimens tested; therefore, the numbers displayed in Table 3.1 for CP1 to CP7 are an accumulation of specimens tested for all lab CPs. Table 3.1 summarize all mixture tests performed: Cantabro Mass Loss (CML), Indirect Tensile Testing (IDT), Fracture Energy (FE) at 20°C and -10°C, Asphalt Pavement Analyzer (APA), and Hamburg Loaded Wheel Tracking (HLWT). Some control specimens were tested within days of compaction. Those that were not tested immediately were stored away from sunlight at room temperature in laboratories at Mississippi State University (MSU).

Table 3.2 includes 56 binder samples that were evaluated via Penetration (*Pen.*), Dynamic Shear Rheometer at intermediate (DSR_{8mm}) and high (DSR_{25mm}) temperatures, Bending Beam Rheometer (BBR), and Fourier Transform Infrared (FTIR) spectroscopy testing. Binder was recovered from specimen slices as described later in Section 3.6.1. Either the top slices, bottom slices, or a combined sample of the top and bottom were used for binder testing. For 0-yr, one binder sample extracted and recovered from loose mixture was utilized for each mixture type. For field aging, binder was recovered from 2-yr and 4-yr specimens. For 4% air voids (V_a), one binder sample was recovered from the top specimen slices. For 7% V_a , two samples were recovered (one sample from the top specimen slices and one sample from the bottom specimen slices). For laboratory conditioning protocols, top and bottom slices of specimens were combined for each mixture type to make one sample since laboratory conditioning is essentially symmetrical.

1 **Table 3.1. Summary of Mixture Testing Plan**

Specimen Type	Target V _a (%)	Mix ID	Specimens Tested for Each Test Method					
			CML	IDT	HLWT	APA	FE ₊₂₀	FE ₋₁₀
0-yr	4	M17	3	3	6	6	3	3
		M18	3	3	6	6	3	3
		M19	3	3	6	6	3	3
		M20	3	3	6	6	3	3
	7	M17	3	3	6	6	3	3
		M18	3	3	6	6	3	3
		M19	3	3	6	6	3	3
		M20	3	3	6	6	3	3
1-yr	4	M17	3	3	2	2	---	---
		M18	3	3	2	2	---	---
		M19	3	3	2	2	---	---
		M20	3	3	2	2	---	---
	7	M17	3	3	2	2	---	---
		M18	3	3	2	2	---	---
		M19	3	3	2	2	---	---
		M20	3	3	2	2	---	---
2-yr	4	M17	3	3	---	6	3	3
		M18	3	3	---	6	3	3
		M19	3	3	---	6	3	3
		M20	3	3	---	6	3	3
	7	M17	3	3	---	6	3	3
		M18	3	3	---	6	3	3
		M19	3	3	---	6	3	3
		M20	3	3	---	6	3	3
3-yr	4	M17	3	3	---	---	---	---
		M18	3	3	---	---	---	---
		M19	3	3	---	---	---	---
		M20	3	3	---	---	---	---
	7	M17	3	3	---	---	---	---
		M18	3	3	---	---	---	---
		M19	3	3	---	---	---	---
		M20	3	3	---	---	---	---
4-yr	4	M17	3	3	---	2	3	3
		M18	3	3	---	2	3	3
		M19	3	3	---	2	3	3
		M20	3	3	---	2	3	3
	7	M17	3	3	---	2	3	3
		M18	3	3	---	2	3	3
		M19	3	3	---	2	3	3
		M20	3	3	---	2	3	3
CP1 to CP7*	4	M17	21	21	---	---	---	---
		M18	21	21	---	---	---	---
		M19	21	21	---	---	---	---
		M20	21	21	---	---	---	---
	7	M17	21	21	0	42	21	21
		M18	21	21	42	42	21	21
		M19	21	21	42	42	21	21
		M20	21	21	42	42	21	21
CP8**	7	M18-M20	9	9	---	---	---	
Sleeve	7	M17	12	---	---	---	---	
Total			309	297	190	296	156	156

2 * CP1 to CP7 is cumulative. Each protocol has 3 specimens per test for both CML and IDT, and 6 specimens for FE, HLWT, and APA.

3 **CP8 is cumulative for M18 to M20, each mixture type has 3 specimens.

Table 3.2. Summary of Binder Testing Plan

Specimen Type	Target V _a (%)	Mix ID	Total Samples	Specimens Tested for Each Test Method				
				Pen.	DSR _{8mm}	DSR _{25mm}	BBR	FTIR
0-yr	Loose Mix	M17	1	LM	LM	LM	LM	LM
		M18	1	LM	LM	LM	LM	LM
		M19	1	LM	LM	LM	LM	LM
		M20	1	LM	LM	LM	LM	LM
2-yr	4	M17	1	T	T	T	T	T
		M18	1	T	T	T	T	T
		M19	1	T	T	T	T	T
		M20	1	T	T	T	T	T
	7	M17	2	T & B	T & B	T & B	T & B	T & B
		M18	2	T & B	T & B	T & B	T & B	T & B
		M19	2	T & B	T & B	T & B	T & B	T & B
		M20	2	T & B	T & B	T & B	T & B	T & B
4-yr	4	M17	1	T	T	T	T	T
		M18	1	T	T	T	T	T
		M19	1	T	T	T	T	T
		M20	1	T	T	T	T	T
	7	M17	2	T & B	T & B	T & B	T & B	T & B
		M18	2	T & B	T & B	T & B	T & B	T & B
		M19	2	T & B	T & B	T & B	T & B	T & B
		M20	2	T & B	T & B	T & B	T & B	T & B
CP1 to CP7*	7	M17	7	T/B	T/B	T/B	T/B	T/B
		M18	7	T/B	T/B	T/B	T/B	T/B
		M19	7	T/B	T/B	T/B	T/B	T/B
		M20	7	T/B	T/B	T/B	T/B	T/B
Total			56					

LM= Binder taken from loose mixture; T= binder taken from top slices of specimens; B= binder taken from bottom slices of specimens; T/B= binder taken from combined slices of specimens' tops and bottoms; T&B= binder taken from both top and bottom slices of specimens but kept separate from each other

*CP1 to CP7 is cumulative. Each protocol has 1 sample that is (T/B).

A fairly large quantity of virgin binder and warm mix technologies were sampled during plant production that are envisioned to be used in companion works to assess binder conditioning in the laboratory relative to field aging. This effort is not presented in this report, but is envisioned to appear in a future document and be similar conceptually to the efforts of Volume 2 with regard to binder characterization. For example, estimating how long binder needs to be pressure aging vessel conditioned to replicate a given amount of field aging.

3.3 Asphalt Mixtures Tested

The four asphalt mixtures consisted of one HMA and three WMA's. They were produced at the APAC Mississippi, Inc. facility in Vicksburg and, for MSU purposes, are denoted M17-M20 (publications by ERDC referred to these as mixes 1-4). M17 is the only HMA considered and with a mixing temperature of 143°C it is on the lower end of allowable temperatures for an HMA definition. M18 through M20 were produced with the following WMA technologies: 2.0% foaming process (M18), 0.5% Evotherm™ 3G (M19), and 1.5% Sasobit® (M20), where the percent values are dosage rates as a percent of binder mass. These mixes were designed with 60% limestone, 25% crushed gravel, and 15% natural sand. Note that communication with ERDC engineers revealed that some of their reports incorrectly stated these mixes contained 40% limestone, 45% crushed gravel, and 15% natural sand. No reclaimed asphalt pavement (RAP), hydrated lime, or liquid anti-strip was present in any of

the mixes. All mixtures utilized the same unmodified PG 67-22 base binder, and were produced with the same aggregate blend. Mixture volumetric properties and aggregate gradation can be found in Tables 1.1 and 1.3, respectively. Any additional information regarding the aggregate and binder types or sources can be found in Table 1.2. Loose asphalt mixture was sampled in metal buckets from the paver (Figure 3.1a) during construction of the ERDC test section described in Doyle et al. (2013a and 2013b), Rushing et al. (2013a and 2013b), and Mejias-Santiago et al. (2014). The buckets were stacked on wooden pallets at the paving site (Figure 3.1c) and transported to MSU where they were kept in that state in an air conditioned building until needed, as shown in Figure 3.1b.



Figure 3.1. Stacked Asphalt Buckets Prior to Testing

Eight maximum mixture specific gravity (G_{mm}) measurements (two on each of the four mixes) were performed at both the MSU and the ERDC labs for a total of sixteen measurements, summarized in Table 3.3. Since the largest difference among the measured values was 0.018, and AASHTO T209 allows for a range of 0.024 for multilaboratory precision, G_{mm} was assumed to be the same for all mixtures at an average value of 2.460.

Table 3.3. G_{mm} Measurements for Mixtures M17 to M20

Laboratory	ERDC		MSU	
	Mix ID	G_{mm} Test 1	G_{mm} Test 2	G_{mm} Test 1
M17	2.464	2.459	2.456	2.449
M18	2.460	2.460	2.462	2.457
M19	2.459	2.461	2.462	2.461
M20	2.467	2.462	2.454	2.458

3.4 Specimen Preparation

3.4.1 Laboratory Compaction

Prior to compaction, the metal buckets of asphalt in Figure 3.1b were reheated one at a time to approximately 93°C (taking around 1 hour) and then the mixture was removed from the bucket and batched into metal pans with lids. The pans were typically cooled and then reheated immediately before compaction by setting the oven to approximate plant mixing temperatures of 146°C (295°F) for the HMA and 116°C (240°F) for the three WMAs for around three hours. All specimens were compacted with a Superpave Gyratory Compactor (SGC) exemplified in Figure 3.2. Specimens were compacted to a target V_a level in one of the following sizes: 150 mm diameter by 115 mm tall, 150 mm diameter by 75 mm tall, 150 mm diameter by 63 mm tall, or 100 mm diameter by 63 mm tall.



Figure 3.2. Pine AFGC 125X SGC

Two target V_a levels were selected to represent common cases evaluated in laboratory testing. For this project, 4% and 7% V_a based on AASHTO T166 were taken as equivalent to 4.5 and 8.0% V_a based on AASHTO T331; therefore, laboratory compacted specimens were produced at target bulk mixture specific gravity (G_{mb}) values equivalent to $4.5 \pm 0.5\%$ and $8.0 \pm 0.5\%$ V_a based on T331 density measurements using the average G_{mm} measured on loose mix from the paver (2.460). Reported V_a values are based on T331 measurements; however, for consistency among related works, target V_a levels are discussed at 4% and 7%.

3.4.2 Laboratory Conditioning

The eight laboratory conditioning protocols (CPs) used in this report are shown in Table 3.4. These laboratory CPs were utilized in an attempt to find a method that reasonably replicates field aging of a given duration. Combinations of three conditioning methods (oven, hot water, and freeze-thaw) were applied. CPs were always applied in the previous mentioned order when more than one method was employed in a protocol. More detail concerning the conditioning methods is provided in the following sub-sections.

Table 3.4. Laboratory Conditioning Protocols

Protocol ID	Oven	64°C Water	Freeze-Thaw
CP1	5 days @ 85°C	--	--
CP2	28 days @ 60°C	--	--
CP3	--	14 days	--
CP4	--	14 days	1 cycle
CP5	--	14 days	2 cycles
CP6	--	28 days	--
CP7	5 days @ 85°C	14 days	1 cycle
CP8	10 days @ 85°C	--	--

3.4.2.1 Oven Conditioning

All oven-conditioning was performed in a forced draft oven (Figure 3.3 is an example) with the specimens placed in direct contact with the oven shelves, which had some open spaces but were mostly solid. Oven-aged specimens were non-sleeved, allowing full movement of air around the sides and tops. Conditioning was performed for 120 ± 0.5 hr at 85°C or for 672 ± 3 hr at 60°C. Room temperature specimens were transferred to an oven preheated to the conditioning temperature at the beginning of conditioning. After conditioning was completed, specimens were cooled to room temperature inside the oven (with the oven turned off and the door opened) prior to being removed.



Figure 3.3. Example Oven Conditioning Photograph

3.4.2.2 Hot Water Conditioning

Specimens subjected to hot water conditioning were vacuum saturated to 70 to 80 % of T166 measured V_a volume. Note that four specimens exceeded this range with saturation reaching approximately 85% of T166 but this item was neglected in analysis. Specimens were then temporarily stored in water at room temperature for varying time before being transferred to a water bath pre-heated to 64°C (Figure 3.4). Note that adding room temperature specimens to the water bath reduced the temperature of the water. The time required for the water bath to

return to 64°C was recorded and is reported in Table 3.5 as $t_{\text{warm-up}}$. Conditioning time, which is also reported in Table 3.5, began when the water bath temperature had returned to 64°C. For specimens not undergoing FT conditioning, hot water was drained away from specimens as soon as conditioning ended, except in the cases of trials 11, 12, and 13 denoted in Table 3.5 where the water was cooled overnight before the specimens were removed.

Specimens subjected to FT conditioning were slowly cooled to near-room temperature while submerged in water. Fans circulated room temperature air over the water surface to facilitate cooling to room temperature overnight, then specimens were transferred directly to FT conditioning while at their submerged saturation level. At the end of hot water conditioning, most specimens prepared for testing were air dried for at least six weeks at room temperature (HLWT specimens were only dried for a minimum of one week before testing). There were thirteen water bath trials used to complete conditioning all specimens as shown in Table 3.5. Trials 1-10 included specimens used in this report and in Smith et al. (2018). Trials 11-13 included only specimens considered in this report. Fabrication, calibration, and setup of the water bath is described in further detail in Smith et al. (2018).



Figure 3.4. Example of Water Conditioning.

Table 3.5. Water Bath Conditioning Trials

Trial	Start Date	$t_{\text{warm-up}}$ (hours)	Conditioning Time (hours)	Conditioning Time (days)	Conditioning Temp		Followed by FT?
					Avg (°C)	St. Dev. (°C)	
1	11/25/2014	16.3	672.2	28.0	63.9	0.8	No
2	08/21/2015	4.3	335.2	14.0	64.1	0.8	No
3	09/25/2015	6.6	336.4	14.0	63.7	0.6	No
4	10/12/2015	8.4	335.4	14.0	64.1	0.4	Yes
5	10/28/2015	6.3	336.0	14.0	64.0	0.3	Yes
6	12/01/2015	6.3	336.2	14.0	64.2	0.3	Yes
7	01/04/2016	6.5	335.7	14.0	63.8	0.4	Yes
8	01/25/2016	10.0	335.9	14.0	63.6	0.3	Yes
9	02/15/2016	5.5	673.2	28.1	64.0	0.4	No
10	04/15/2016	3.5	335.3	14.0	64.2	0.6	Yes
11	05/11/2017	5.4	335.4	14.0	64.0	0.3	Yes/ No ^a
12	05/31/2017	5.0	335.8	14.0	64.1	0.2	Yes
13 ^b	06/21/2017	3.0	674.1	28.1	63.9	0.5	No

a: Trial had some specimens followed by FT and some that were not.

b: Five days of temperature data did not record in the middle of trial because of technical issue.

3.4.2.3 Freeze-Thaw Conditioning

In the cases where freeze-thaw (FT) conditioning was performed, it was always preceded by hot water conditioning. After specimens cooled to near-room temperature while submerged in water, they were transferred to a freezer (Figure 3.5) pre-chilled to freeze to -22°C (nominal temperature). The freezer doors were closed and freezers were kept on for 24 hours, after which, the freezers were turned off and specimens were thawed to approximately 5°C with the doors closed. If specimens were being subjected to a single FT cycle, the doors were then opened, and specimens returned to room temperature. If two FT cycles were performed, freezer doors were only opened for 30 minutes, then shut again. The freezers were turned back on for 24 hours, then the specimens were thawed to 5°C with the freezers off and doors closed, at which point the doors were opened and specimens returned to room temperature. All FT specimens were allowed to air dry for at least six weeks before testing, except HLWT specimens which dried for a minimum of one week.



Figure 3.5. Example Freeze-Thaw Conditioning Photograph

Two different sized thermal calibration specimens instrumented thermocouples were used to estimate internal specimen temperatures during the FT process. In the thermal calibration specimens measuring 63 mm tall and 100 mm diameter, a single thermocouple was installed in the specimen center. For 115 mm tall by 150 mm diameter specimen, one thermocouple was inserted in the specimen center and a second inserted half the distance between the specimen center and specimen edge (mid-radius). Smith et al (2018) provides more details and information about freezer calibration and setup.

In trial 13, temperature data of freezer 1 (F1) and freezer 2 (F2) was not recorded from 18 hr to 24 hr due to a technical issue. The temperature was checked at 24 hr and discovered to be -5°C and -22°C for F1 and F2, respectively. Upon investigation, it was found that F1 did not reach the -22°C setpoint, as seen in Figure 3.6, because the freezer door was not completely shut. The concept of FT conditioning is that the change in density of water as a function of temperature causes expansion and contraction which damages asphalt specimens. The maximum density of water occurs at 4°C where it is approximately 1000 kg/m^3 . At -5°C and -22°C , the density of ice is 917.5 kg/m^3 and 919.5 kg/m^3 , respectively, equating to a change in density of approximately 0.2% (<http://www.engineeringtoolbox.com/ice-thermal-properties->

d_576.html). Since the density of ice change between -5°C and -22°C is minimal, it was assumed that freezer 1 not reaching the setpoint of -22°C (but reaching -5°C instead) did not cause a meaningful difference in the amount of damage inflicted on the specimens and was neglected in analysis.

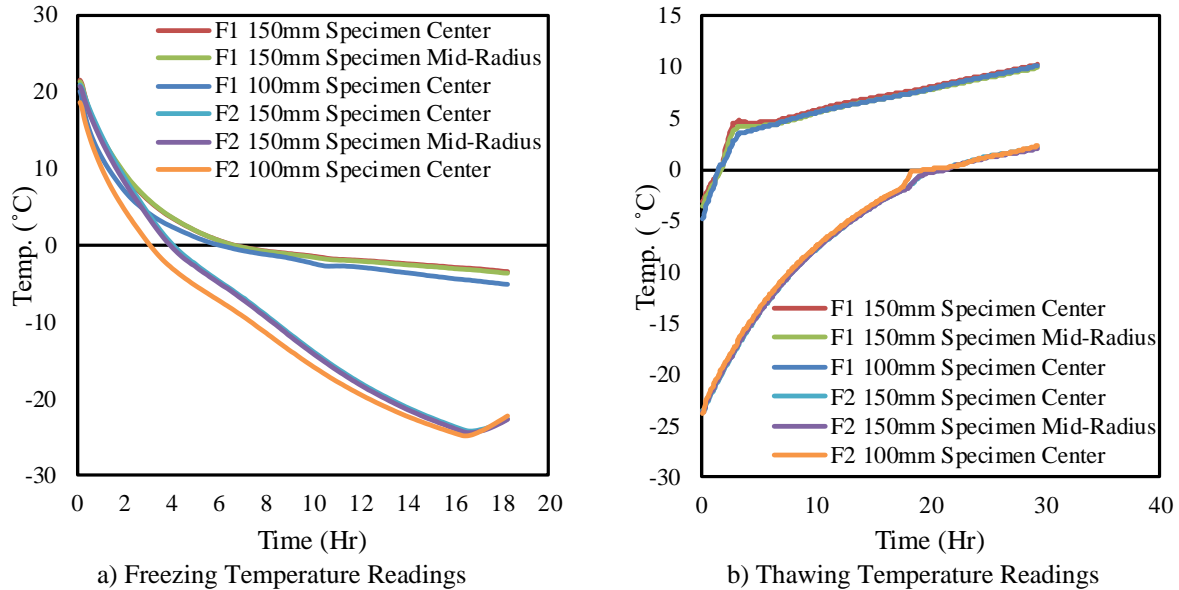


Figure 3.6. Freeze-thaw Temperature of Trial 13

3.4.3 Field Aging

Specimens were placed in the field on Nov. 1st and 2nd of 2012. Field aging was performed in PVC sleeves (Figure 3.7) so that only specimen tops were exposed to direct sunlight and weathering. Standard commercially available pipe was purchased and sliced to sleeve heights of 114.3 ± 1.6 mm or 63.5 ± 1.6 mm. Sleeve diameters were just larger than the specimens (101.6 mm and 152.4 mm diameters). A total of 480 specimens were field aged beginning in 2012. These specimens were organized into 48 blocks, each containing ten specimens (3 that were 150 mm diameter by 115 mm tall, 3 that were 100 mm diameter by 63 mm tall, and 4 that were 150 mm diameter by 63 mm tall). Of these 480 specimens, 384 are considered in this study, while 96 were utilized in SS250 (Cox and Howard 2015). A portion of the specimens were removed from the field and tested at 1-year intervals for a span of four years. Specimens were removed from the field on Oct. 30th of 2013, 2014, and 2015 for 1-yr, 2-yr, and 3-yr specimens respectively. 4-yr specimens were removed from the field on Oct. 31th of 2016. For 1-yr, 2-yr, 3-yr, and 4-yr, the number of specimens removed was 80, 144, 48, and 112, respectively.

Twelve specimens were also field aged for the purpose of studying the effects of sleeved versus non-sleeved aging. Six specimens were aged in PVC sleeves and six more were aged with no sleeves so that all faces were exposed to direct sunlight except for the bottom, which was in direct contact with the underlying asphalt pavement (Figure 3.7). The specimens were placed in the field on Oct. 30th 2015. Six specimens (three sleeved and three non-sleeved) were removed after six months of aging on Apr. 30th 2016, and the remaining six specimens were removed after one year on Oct. 31st 2016.

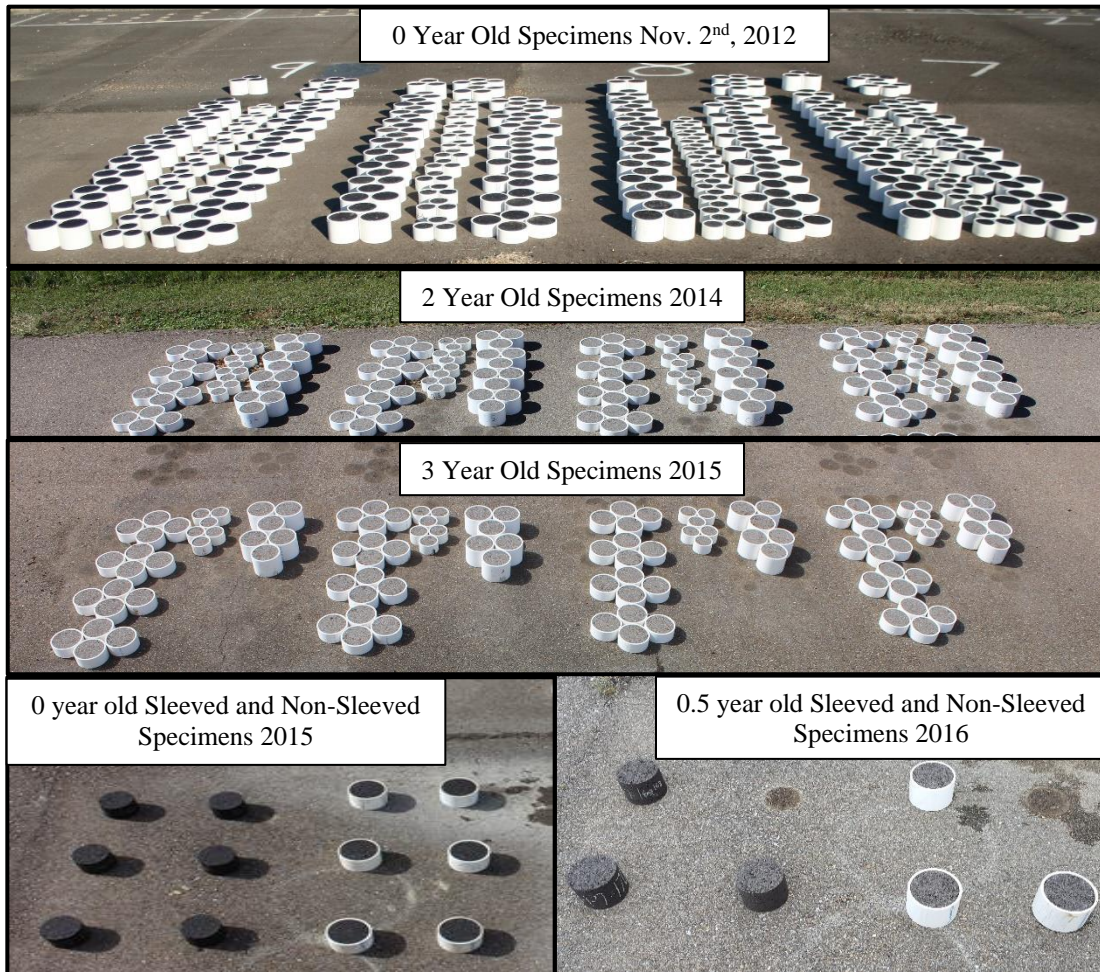


Figure 3.7. Compacted Specimens During Field Aging

Weather data reported at the Columbus Air Force Base (CAFB), which is approximately 19 km from the field aging site, was recorded throughout this study. As shown in Tables 3.6 to 3.9, the aging environment consisted of typically mild winters and hot summers.

Table 3.6. Year 1 Weather Summary (November 2012 to October 2013)

Month	Days	Avg. Daily Temp		High Daily Temp		Low Daily Temp		Rainfall		Relative Humidity	
		Mean	St. Dev	Mean	St. Dev	Mean	St. Dev	Total	Days of	Mean	St. Dev
		(°C)	(°C)	(°C)	(°C)	(°C)	(°C)	(cm)	1.25 cm+	(%)	(%)
Nov-12	30	9.5	3.4	17.8	4.2	1.3	3.4	4.8	2	77.6	10.7
Dec-12	31	9.6	5.5	15.3	5.6	3.8	6.2	15.3	3	82.5	13.2
Jan-13	31	8.3	5.8	13.2	6.1	3.3	6.4	19.7	6	80.3	12.8
Feb-13	28	7.7	3.4	13.4	3.8	1.8	4.2	13.0	3	75.2	13.6
Mar-13	31	9.2	4.7	15.8	6.1	2.6	4.4	18.3	3	66.8	15.8
Apr-13	30	16.3	4.2	22.9	5.0	9.8	4.5	14.9	4	76.5	11.2
May-13	31	19.9	4.5	26.1	4.6	13.9	5.2	9.0	3	76.9	11.7
Jun-13	30	25.5	1.7	31.1	2.1	19.9	1.9	11.4	3	78.0	6.7
Jul-13	31	25.6	1.5	30.5	2.0	20.8	1.7	22.0	5	81.1	7.1
Aug-13	31	26.1	1.9	31.5	2.3	20.8	2.1	6.3	1	81.8	5.7
Sep-13	30	23.9	2.9	30.3	3.7	17.6	3.1	12.1	3	75.6	9.3
Oct-13	31	17.7	4.6	23.7	4.4	11.7	5.6	4.3	2	84.6	9.8
All	365	16.7	8.1	22.7	8.2	10.7	8.7	151.1	39	78.1	11.7

Table 3.7. Year 2 Weather Summary (November 2013 to October 2014)

Month	Days	Avg. Daily Temp		High Daily Temp		Low Daily Temp		Rainfall		Relative Humidity	
		Mean	St. Dev	Mean	St. Dev	Mean	St. Dev	Total	Days of	Mean	St. Dev
		(°C)	(°C)	(°C)	(°C)	(°C)	(°C)	(cm)	1.25 cm+	(%)	(%)
Nov-13	30	9.3	5.3	15.3	5.5	3.1	6.2	8.2	3	74.2	12.7
Dec-13	31	6.8	5.9	12.2	6.8	1.3	6.2	15.8	7	81.6	10.0
Jan-14	31	1.8	5.3	9.2	6.5	-5.7	5.2	5.2	1	60.4	16.2
Feb-14	28	6.6	5.1	12.4	6.8	0.7	4.6	9.2	2	75.6	11.8
Mar-14	31	10.4	4.4	17.7	5.7	3.0	4.2	9.0	2	71.8	14.1
Apr-14	30	16.5	4.0	23.3	4.5	9.7	4.5	20.2	4	74.9	13.7
May-14	31	21.2	3.4	28.0	3.7	14.8	4.3	11.2	3	72.9	11.2
Jun-14	30	25.4	1.5	30.7	2.3	20.4	1.3	15.2	3	80.6	7.0
Jul-14	31	24.6	2.3	30.1	2.8	19.2	2.4	9.5	3	78.5	8.7
Aug-14	31	26.3	1.7	32.4	2.0	20.3	2.0	7.7	1	77.1	8.3
Sep-14	30	24.3	2.6	30.4	2.4	18.4	3.4	4.1	2	76.9	6.7
Oct-14	31	18.1	4.2	25.3	4.1	11.0	5.2	11.4	3	80.5	9.7
All	365	16.0	9.2	22.3	9.3	9.7	9.7	126.7	34	75.3	12.3

Table 3.8. Year 3 Weather Summary (November 2013 to October 2014)

Month	Days	Avg. Daily Temp		High Daily Temp		Low Daily Temp		Rainfall		Relative Humidity	
		Mean	St. Dev	Mean	St. Dev	Mean	St. Dev	Total	Days of	Mean	St. Dev
		(°C)	(°C)	(°C)	(°C)	(°C)	(°C)	(cm)	1.25 cm+	(%)	(%)
Nov-14	30	8.2	5.5	14.9	6.0	1.5	6.0	10.7	2	70.6	11.3
Dec-14	31	8.4	3.8	13.3	4.1	3.2	4.4	18.2	5	85.0	10.0
Jan-15	31	4.9	4.7	11.3	5.9	-1.5	4.8	12.2	4	72.0	16.5
Feb-15	29	3.6	4.6	9.1	6.2	-2.2	4.2	37.9	3	65.2	17.3
Mar-15	31	13.1	5.2	18.7	6.3	7.4	5.9	15.6	5	82.6	12.9
Apr-15	30	18.1	3.2	24.1	3.5	12.3	4.2	18.9	4	79.2	13.9
May-15	31	22.5	2.9	29.7	2.9	15.5	4.2	11.2	4	73.8	14.0
Jun-15	30	25.9	2.2	31.7	2.5	20.2	2.4	2.0	0	77.2	6.0
Jul-15	31	27.9	1.9	33.8	2.6	22.2	1.4	6.2	3	76.1	7.2
Aug-15	31	26.0	2.3	31.8	2.7	20.4	2.7	12.0	4	77.8	9.0
Sep-15	30	23.4	2.8	29.9	3.0	17.1	3.8	2.2	0	76.9	6.4
Oct-15	31	17.8	3.7	24.7	4.9	11.2	5.1	40.6	1	76.4	11.8
All	366	16.7	9.1	22.8	9.6	10.7	9.4	187.9	35	76.2	12.8

Table 3.9. Year 4 Weather Summary (November 2015 to October 2016)

Month	Days	Avg. Daily Temp		High Daily Temp		Low Daily Temp		Rainfall		Relative Humidity	
		Mean	St. Dev	Mean	St. Dev	Mean	St. Dev	Total	Days of	Mean	St. Dev
		(°C)	(°C)	(°C)	(°C)	(°C)	(°C)	(cm)	1.25 cm+	(%)	(%)
Nov-15	30	14.1	4.8	19.8	3.7	8.3	6.6	7.4	1	83.2	11.0
Dec-15	31	12.5	5.5	17.9	4.7	7.0	7.3	0.0	0	85.9	11.0
Jan-16	31	5.2	4.3	10.8	5.2	-0.7	4.4	18.5	3	74.0	10.6
Feb-16	28	9.4	5.1	15.4	5.3	3.1	6.2	21.4	4	68.7	15.8
Mar-16	31	14.7	4.4	21.1	5.0	8.3	5.0	27.3	5	74.9	12.8
Apr-16	30	17.3	3.2	23.6	3.6	11.1	4.0	15.2	2	72.9	12.4
May-16	31	20.9	3.4	27.3	3.5	14.6	4.1	3.0	1	74.2	8.5
Jun-16	30	26.6	1.7	32.5	1.7	20.9	2.6	19.3	3	77.8	6.9
Jul-16	31	27.9	1.3	33.6	1.6	22.3	1.6	10.9	3	82.7	7.3
Aug-16	30	28.1	0.9	33.7	1.9	22.8	0.9	8.7	3.0	85.8	6.6
Sep-16	31	26.0	2.6	33.4	2.8	18.9	3.3	0.5	0.0	69.7	8.0
Oct-16	30	20.1	3.1	29.1	2.8	11.4	4.0	2.5	1.0	68.2	8.7
All	365	18.6	8.2	24.8	8.4	12.3	8.6	134.7	26	76.6	11.9

Four parameters were used in this effort to describe cumulative weather patterns over time: 1) high temperature cumulative degree days (CDD_{high}); 2) cumulative freezing index (CFI); 3) cumulative days of temperature fluctuation ($CD_{fluctuation}$); and 4) cumulative precipitation. CDD_{high} is defined in Equation 3.1 and describes the accumulation of high temperature days over time (Figure 3.8a). CFI is defined in Equation 3.2 and describes the accumulation of °C-days below freezing based on daily low temperatures (Figure 3.8b). $CD_{fluctuation}$ reports the number of days where the maximum and minimum temperatures were different by more than a defined baseline. For example, the 18°C baseline in Figure 3.8c

reaches a maximum of 161 days with at least an 18°C temperature fluctuation within one day. Cumulative precipitation over the four year aging period is shown in Figure 3.8d.

$$CDD_{high} (\text{°C-days}) = \sum (T_{dmax} - \text{Baseline}) \text{ if } T_{dmax} > \text{Baseline} \quad (3.1)$$

$$CFI (\text{°C-days}) = \sum (T_{dlow}) \text{ if } T_{dlow} < 0\text{°C} \quad (3.2)$$

Where,

T_{dlow} = Minimum Daily Temperature (°C)

T_{dmax} = Maximum Daily Temperature (°C)

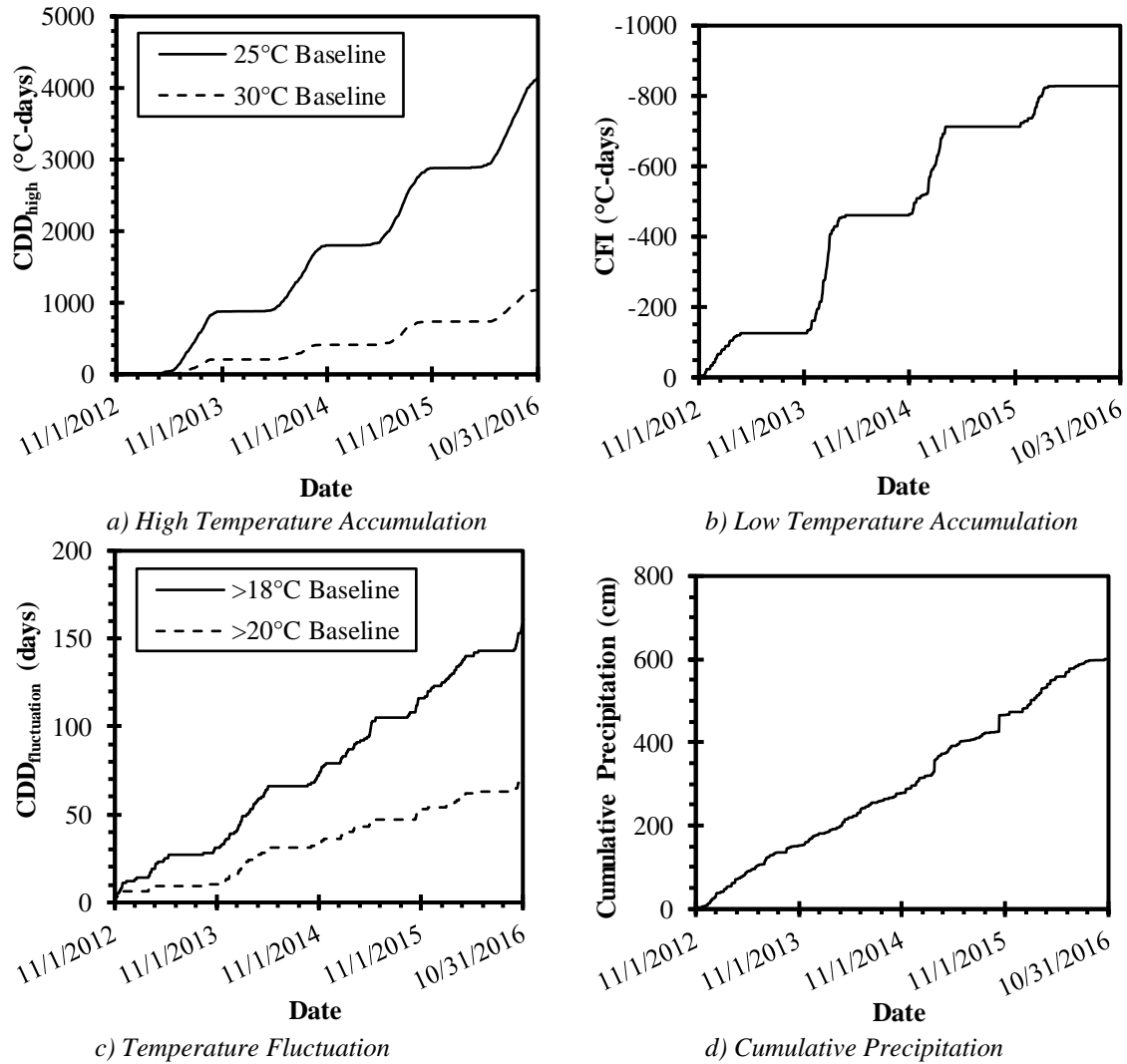


Figure 3.8. Cumulative Weather Summary

3.4.4 Specimen Slicing

Specimens compacted to 63 mm height and 150 mm diameter specimen were used for both binder extraction and recovery (E/R), and fracture energy (FE). Tops and bottoms were

sliced as shown in Figures 3.9a and 3.9b using the saw in Figure 3.9c. A 12.5 mm slice was sawn from the top of the 63 mm tall specimens, and then the FE test specimen was sliced from the center of the original specimen with a target thickness of 31 mm. After accounting for saw blade thickness, this left an approximately 12.5 mm slice at the bottom of the specimen.

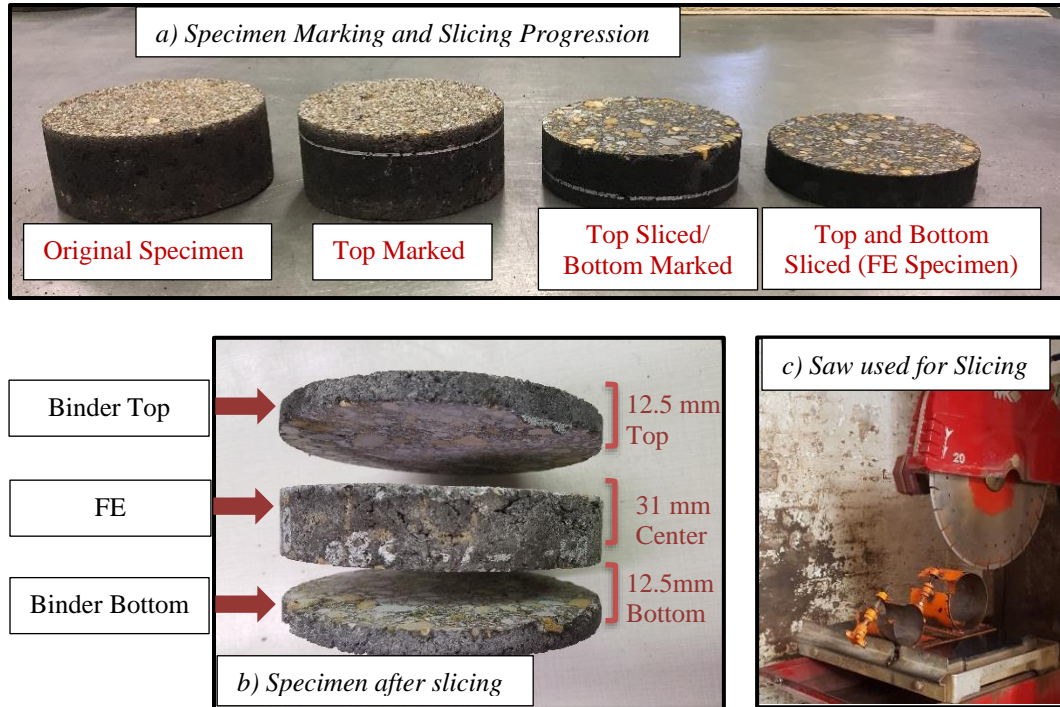


Figure 3.9. Specimen Slicing Process for Binder and Fracture Energy Specimens

3.5 Mixture Testing

3.5.1 Cantabro Testing

Cantabro testing was performed on 150 mm diameter by 115 mm tall specimens. Specimens were conditioned at 25°C in air overnight in an environmental chamber prior to testing, and removed from the chamber no longer than 30 minutes before the start of testing. Compacted specimens were tumbled one at a time in a Los Angeles (LA) abrasion drum (Figure 3.10a) without steel spheres for 300 revolutions at 25 ± 2 °C. Specimen mass was measured before testing (Figure 3.10b), dust was lightly brushed off the specimen after the 300 revolutions, and the specimen was weighed again (Figure 3.10c). Equation 3.3 was used to calculate the percent mass loss (*ML*). CML testing was performed on each specimen type and mix type at both target *V_a* levels. Three *ML* values were averaged to represent one test result.

$$ML = \frac{M_1 - M_2}{M_1} \times 100 \quad (3.3)$$

Where,

ML = percent mass loss

M₁ = specimen mass before testing

M₂ = specimen mass after testing

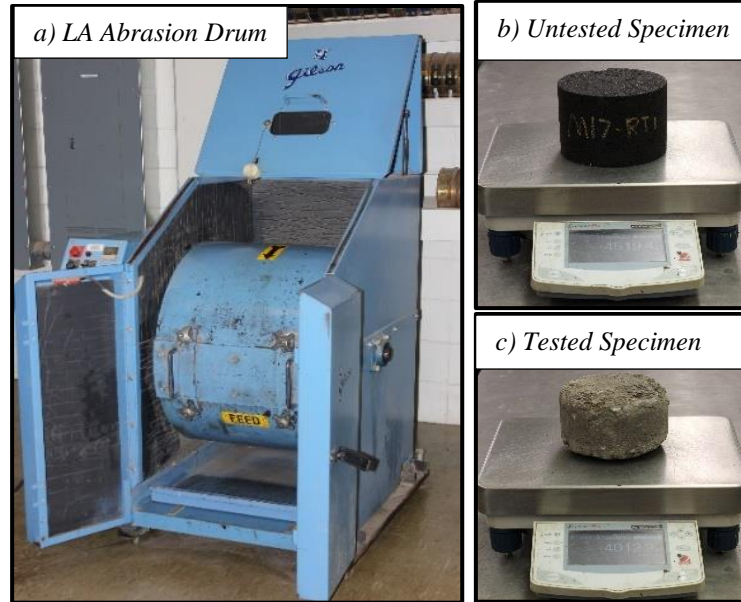


Figure 3.10. Cantabro Testing Examples

3.5.2 Indirect Tensile Testing

Indirect Tensile (IDT) testing refers to the non-instrumented method that was performed in a universal load frame as shown in Figure 3.11. IDT specimens were 100 mm diameter by 63 mm tall. Testing was conducted at 25°C, after conditioning at the same temperature in air. Specimens were loaded at a rate of 50 mm/min until failure (according to AASHTO T283), and Equation 3.4 was used to calculate the IDT strength (S_t). IDT testing was performed on each specimen type and mix type at both target V_a levels. Three S_t values were averaged to represent one test result.

$$S_t = \frac{2000 \times P_{\max}}{\pi \times t \times D} \quad (3.4)$$

Where,

P_{\max} = maximum load (N)

t = specimen thickness (mm)

D = specimen diameter (mm)

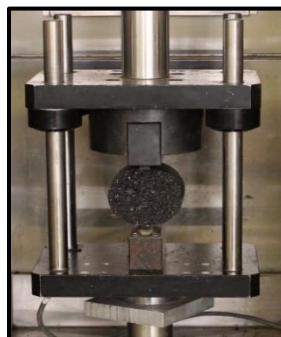


Figure 3.11. Non-Instrumented IDT Test

3.5.3 Fracture Energy Testing

Fracture Energy (FE) testing refers to the instrumented IDT testing performed in the same universal loading frame as the non-instrumented IDT testing (Figure 3.11) where only the FE values are considered herein (resilient modulus and creep compliance were also determined for 0-yr and 2-yr specimens for use in SS 250). A total of four test temperatures were included in the overall body of work: 20°C (FE₊₂₀) and -10°C (FE₋₁₀) were used in this report, while 0°C and -20°C were only considered in SS250 (Cox and Howard 2015). All specimens were initially 150 mm diameter by 63 mm tall. Before testing, specimen tops and bottoms were sliced off for use in binder testing as described in Section 3.4.4. After slicing, four gauge points were glued to each side of 31 mm specimen centers using the jig shown in Figure 3.12a. Specimens were conditioned at their testing temperature in the environmental chamber for 3 ± 1 hours prior to testing. Epsilon 3910 extensometers (LVDTs) were attached to the specimen to measure deformation and the specimens were tested as shown in Figure 3.12b. FE testing was performed at both target V_a levels for 0-yr, 2-yr, and 4-yr specimens (no FE testing was performed on 1-yr or 3-yr specimens). For lab conditioned specimens, FE testing was only performed on 7% V_a specimens.

For FE testing, three specimens were tested as a single group, yielding six values (one from each specimen face) to determine a representative FE. For each specimen group, probable outliers were removed, then the highest and lowest of the remaining values were trimmed so long as there would still be three values to average after trimming. As discussed in Smith et al. (2018), FE is defined as the area under the stress-strain curve until the point of fracture. The point of fracture is determined by plotting the vertical minus horizontal deformations on the deformation differential curve (DDC), and taking the peak as the fracture point. From there, there are four possible cases for each specimen face. Measurements in need of no correction were denoted case 1. Case 2 was taken to be when the point of fracture occurred after the peak load. In case 2, excessive FE values are reported, which require only the area under the stress-strain curve up to the peak load to be considered. Case 3 indicates that during testing LVDTs appeared to have shifted, resulting in only the area under the stress-strain curve prior to shifting being considered. In case 4, the DDC was never positive and the test was determined invalid.

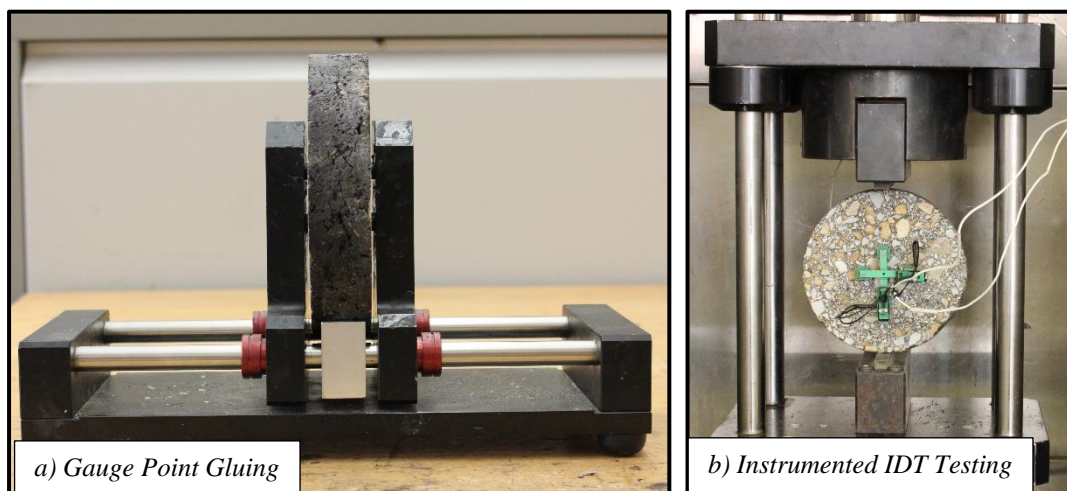


Figure 3.12. Instrumented IDT Testing Process

3.5.4 Asphalt Pavement Analyzer Testing

Asphalt Pavement Analyzer (APA) testing was conducted according to AASHTO T340, except for minor differences as described in this section. The APA equipment in Figures 3.13a and 3.13b was used to conduct tests to 8,000 cycles (16,000 passes) at 64°C. Rut depth (RD_{APA}) was recorded at 1000, 2000, 4000, and 8000 cycles while RD_{APA} at 8,000 cycles was the primary result reported in this study. Rubber hoses in contact with the specimens were pressurized to 690 kPa and a vertical load of 445 N was applied. To conduct a test, the average rut depth of two specimens (denoted as a set) was recorded. APA testing was conducted at both V_a levels for 0-yr, 1-yr, 2-yr, and 4-yr specimens, while all lab conditioned specimens that were tested had a target V_a level of 7%. Three sets (six specimens) of each mix type were tested for 0-yr, 2-yr, and lab conditioned specimens; however, only one set was tested for each mix type was tested at 1-yr and 4-yr. 0-yr specimens were compacted to the 75 mm height of the mold. 2-yr APA specimens were 115 mm tall, in which case, the bottoms of the specimens were trimmed using the saw in Figure 3.9c and disposed of leaving the top 75 mm for testing. 1-yr and 4-yr specimens were 63 mm tall and plastered to height using Plaster of Paris (Figure 3.13c). For laboratory conditioned APA specimens, all M18, M19, and M20 specimens were compacted to 75 mm. However, due to a shortage of material, all laboratory conditioned APA specimens for M17 were compacted to 63 mm tall and plastered to the height of the molds.

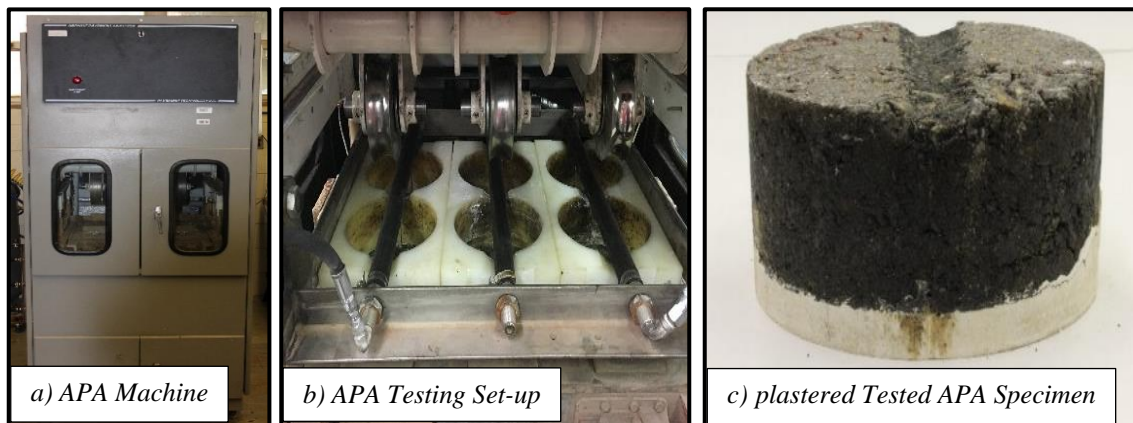


Figure 3.13. APA Testing Equipment and Specimen

3.5.5 Hamburg Loaded Wheel Tracking

Hamburg Loaded Wheel Tracking (HLWT) was performed according to AASHTO T324, using the same machine as APA testing. HLWT was conducted to 20,000 passes (or failure at 12.5 mm rut depth) with solid metal wheels (Figure 3.14a) contacting the asphalt surface with a 705 N vertical load. Rut depth (RD_{HLWT}) was recorded at 5000, 10000, 15000, and 20000 passes, while RD_{HLWT} at 20,000 passes or failure was the primary result reported in this study. Specimens were submerged in 50°C water for 30 ± 1 minutes prior to, and throughout testing. The cabin temperature was also maintained at 50°C. All specimens were 63 mm tall. Two specimens were used to conduct an HLWT test, as shown in Figure 3.14b, and the average rut depth of these specimens were recorded as a set. Both V_a levels were evaluated for 0-yr and 1-yr specimens, with three sets being tested at 0-yr and one set tested at

1-yr (see Table 3.1). Additionally, three sets of each mix type, except M17, were tested at 7% V_a for lab conditioned specimens. Lab conditioned M17 specimens were not tested due to a shortage of material.

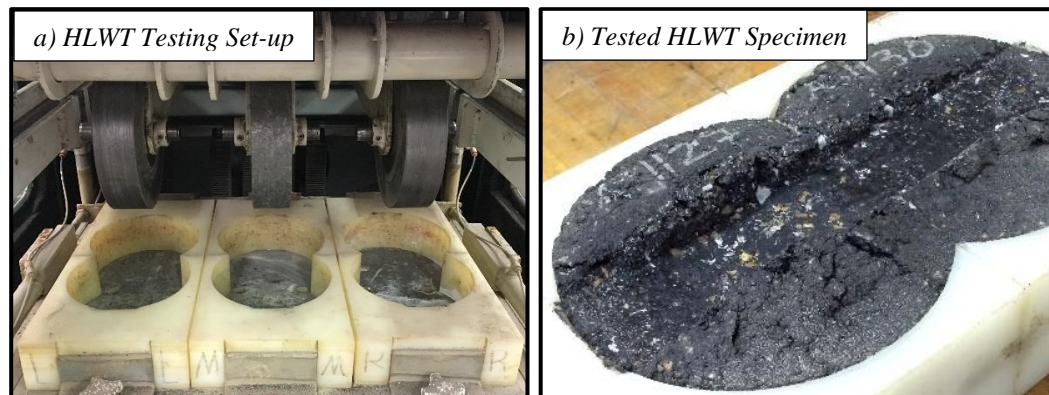


Figure 3.14. HLWT Testing Equipment and Specimens

3.6 Recovered Binder Testing

3.6.1 Binder Extraction and Recovery

Extraction and recovery was performed on one of the following sample types: loose-mix sampled from the paver during construction, sliced sections from laboratory compacted field aged specimens, or sliced sections from laboratory compacted laboratory conditioned specimens. For loose-mix, buckets were heated to approximately 93°C, mix was removed and cooled while keeping it loose. Once cooled, the mix was ready to begin the extraction process. For compacted specimens, top and bottom slices were sawn as described in Section 3.4.4. Top and bottom slices of field aged specimens were kept separate and never tested together; however, for lab conditioned specimens, top and bottom slices were combined since laboratory conditioning was symmetrical for practical purposes. Slices were heated in a forced draft oven at 149°C for 5 minute intervals and broken into loose-mix (Figure 3.15a) at which point, either the extraction process began or samples were placed in sealed bags for storage until needed for extraction.

Primary extraction was performed with a Humboldt H-1471 centrifuge (Figure 3.15b). Three solvent types were used in the following order: 1) recovered toluene from previous extractions, 2) virgin toluene, and 3) an 85% virgin toluene and 15% ethanol blend. Mix was first soaked in recovered toluene for 45-65 minutes, then the centrifuge was accelerated to 3,600 rpm and kept at that rate until drainage ceased. Secondary washes consisted of 5 minute soaks in 250 mL of virgin toluene followed by acceleration of the centrifuge, repeated until extract was no longer black. Extraction was finished with a minimum of 3 wash-centrifuge cycles using the toluene/ethanol blend. Extract containing ethanol was kept separate from non-ethanol containing extract.

After extraction, the filterless centrifuge in Figure 3.15c was used to remove particles smaller than 0.075 mm from the extract, producing filtrate. The centrifuge was primed with 350 mL of recovered toluene before processing extract. Extract without ethanol was processed

first, followed by the extract containing ethanol. Ethanol and non-ethanol containing streams were kept separated.

Binder recovery was performed using a BUCHI Rotavapor R-114 shown in Figure 3.15d. Ice-chilled water was circulated through the condensation coils, and the recovery flask was heated in Paratherm heat transfer fluid, initially heated to 60°C. Ethanol-containing filtrate was processed first to allow ethanol to cool for approximately 15 minutes before increasing the temperature to 110°C. An initial vacuum pressure of 600 mmHg was used, and decreased to approximately 525 mmHg once the filtrate was stable enough to avoid boiling. Once all filtrate was in the recovery flask, vacuum pressure was decreased by 25 mmHg each time the condensate flask was emptied, until the filtrate began to noticeably thicken. The vacuum pressure was then set to 200 mmHg and extraction continued until condensation slowed to approximately one to two drops from the condensation coils every 30 seconds. The recovery flask was then heated to 163°C and vacuum pressure decreased to 150 mmHg. Recovery continued for another 30 minutes, then the recovery flask was emptied into a small tin and transferred to the oven apparatus in Figure 3.15e at 163°C for 15 minutes to allow remaining binder to drain into the tin. A final recovered binder sample is shown in Figure 3.15f. Recovered binder samples were sealed and stored in ambient conditions.

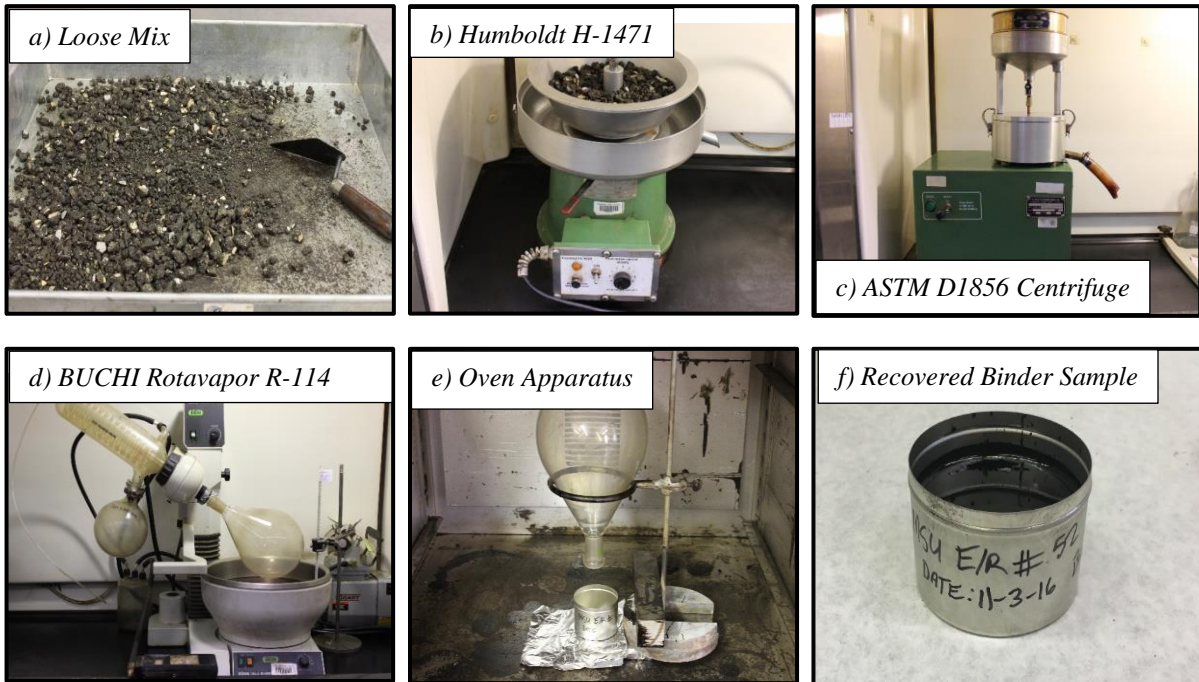


Figure 3.15. Binder Extraction and Recovery Equipment

3.6.2 Dynamic Shear Rheometer Testing

Dynamic shear rheometer (DSR) testing was performed at intermediate (DSR_{8mm}) and high (DSR_{25mm}) temperatures. Complex shear modulus (G^*) and phase angle (δ) were determined for each extracted and recovered binder sample. DSR_{8mm} was performed utilizing 8 mm plates with a 2 mm gap. DSR_{25mm} was performed with 25 mm plates and a 1 mm gap.

Testing was performed following AASHTO T315 to determine intermediate and high critical temperatures (T_c). T_c (calculated according to Equation 3.5) was defined as the temperature where $G^*/\sin\delta$ reached the 2.2 kPa minimum and $G^*\sin\delta$ exceeds the 5,000 kPa maximum as defined in AASHTO M320. The Anton Paar SmartPave 301 in Figure 3.16 was used for all DSR testing.

$$T_c = T_1 + \left(\frac{\log_{10}(P_s) - \log_{10}(P_1)}{\log_{10}(P_2) - \log_{10}(P_1)} \right) (T_2 - T_1) \quad (3.5)$$

Where:

T_c = Critical temperature, °C

T_1 = Lower of the two test temperatures, °C

T_2 = Higher of the two test temperatures, °C

P_s = Specification value for property

P_1 = Test result for the specification value for property at T_1

P_2 = Test result for the specification value for property at T_2

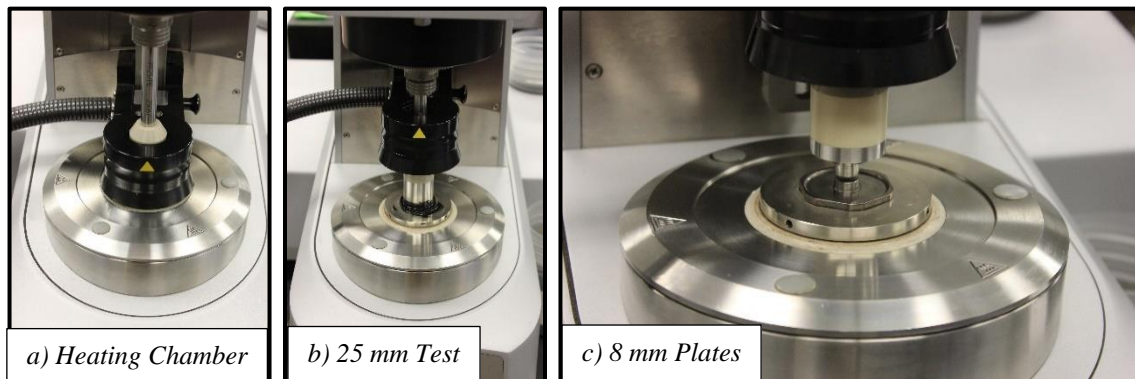


Figure 3.16. DSR Equipment

3.6.3 Bending Beam Rheometer Testing

Bending Beam Rheometer (BBR) testing was performed on samples of extracted and recovered binder to evaluate low temperature behavior per AASHTO T313. The critical temperatures from creep stiffness (T_{c-s}) and m-value (T_{c-m}) are based on the failure criteria stated in AASHTO M320 (maximum 300 mPa for stiffness (S), and minimum 0.300 for m-value). T_{c-m} and T_{c-s} were calculated using Equation 3.5 in the same manner as with DSR data. All BBR testing in this study utilized the Cannon TE-BBR Thermoelectric Bending Beam Rheometer in Figure 3.17.

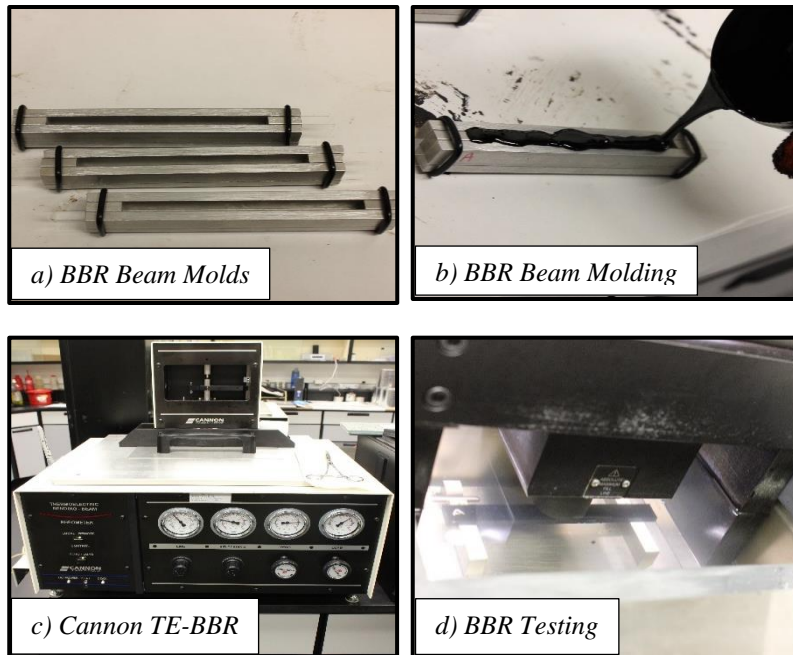


Figure 3.17. BBR Equipment

3.6.4 Penetration Testing

Penetration (*Pen.*) testing was performed at 25°C in accordance with ASTM D5, using the equipment and setup shown in Figure 3.18. Specimens were transferred to testing containers and conditioned in a 25°C water bath for a minimum of 1 hour prior to testing. Testing was performed on three different areas of the same sample. The three resulting values were averaged to determine the *pen.* value of the sample.

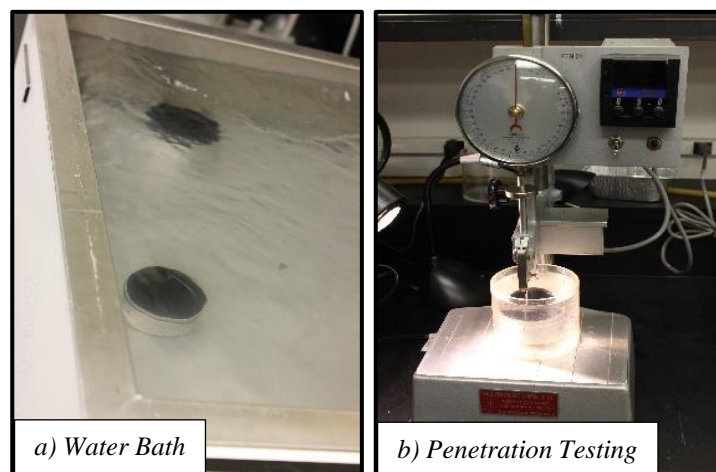


Figure 3.18. *Pen.* Testing Equipment

3.6.5 Fourier Transform Infrared Spectroscopy Testing

Fourier transform infrared (FTIR) spectroscopy was performed utilizing the Nicolet 380 FT-IR analyzer shown in Figure 3.19. Testing was conducted to determine notable changes

in the chemical characteristics of binder samples after conditioning compared to non-conditioned samples. FTIR samples were prepared at the same time as rheology samples by pouring material onto wax paper, cooling, and trimming smaller pieces of the binder sample using a heated spatula. Areas trimmed with the heated spatula were never placed over the FTIR spectrometer detector, and there was no control over film thickness in this investigation. Absorbance peak (Abs_P) spectra were used to determine the carbonyl index (CI) and sulfoxide index (SI) relative to asphalt aging. In analysis, the Abs_P peak heights at wave counts of 1700 cm^{-1} and 1031 cm^{-1} were divided by the Abs_P level at 1375 cm^{-1} to produce CI and SI indices, respectively.



Figure 3.19. Nicolet 380 FT-IR Analyzer

CHAPTER 4 - RESULTS

4.1 Overview of Results

This chapter summarizes all data that was collected from specimen testing relative to the scope of this document. Section 4.2 considers mixture properties via CML, IDT, FE₊₂₀, and FE₋₁₀ testing. Section 4.3 contains all wheel-tracking results (i.e. HLWT and APA results), and Section 4.4 contains results collected from testing of extracted and recovered binder samples which included *Pen.*, intermediate and high temperature DSR, BBR and FTIR testing. Within each section, there are subsections that analyze results from each individual test method. For example, within Section 4.2, Section 4.2.1 discusses CML test results only, Section 4.2.2 discusses IDT test results only, and so on. Correlations or comparisons to data from other test methods are not made in these subsections, nor are there references to literature. For example, in Section 4.2.1, which discusses CML test results, the only data considered is that in the 3rd and 4th columns from the left in Table 4.1. The purpose of these subsections is to make general observations based solely on the data from each individual test method.

4.2 Mixture Properties

This section summarizes all data collected from asphalt mixture property testing (i.e. CML, IDT, FE₊₂₀, and FE₋₁₀). Table 4.1 summarizes all test results from CML, IDT, FE₊₂₀, and FE₋₁₀ testing. All test results reported in Table 4.1 are averages of three test values obtained from testing of three separate but identical specimens. The following subsections analyze the results of each test method (i.e. CML, IDT, FE₊₂₀, and FE₋₁₀) individually, in the manner described in Section 4.1.

Table 4.1. CML, IDT, and FE Test Results for All Specimen Types

Specimen Type	Mix ID	ML (%)		St (kPa)		FE ₊₂₀ (kJ/m ³)		FE ₋₁₀ (kJ/m ³)	
		4% ^a	7% ^b	4% ^a	7% ^b	4% ^a	7% ^b	4% ^a	7% ^b
0-yr	M17	10.4	11.8	1712	1322	2.73	3.49	0.95	0.68
	M18	9.0	10.2	1451	1207	4.64	3.83	0.86	0.86
	M19	8.9	10.1	1718	1219	4.61	4.11	0.96	0.69
	M20	10.8	11.0	1549	1166	2.76	1.78	0.68	0.47
1-yr	M17	11.9	11.8	1826	1460	---	---	---	---
	M18	11.0	15.5	1825	1435	---	---	---	---
	M19	10.4	11.0	1965	1575	---	---	---	---
	M20	12.1	11.6	1836	1390	---	---	---	---
2-yr	M17	12.8	13.6	1950	1522	0.88	3.62	0.62	0.65
	M18	12.3	12.9	1931	1565	1.17	2.42	0.83	0.99
	M19	11.9	12.8	2024	1717	1.92	2.13	0.54	0.60
	M20	11.4	14.4	1977	1494	0.35	1.34	0.70	0.68
3-yr	M17	14.1	15.2	2094	1723	---	---	---	---
	M18	13.0	13.3	2219	1802	---	---	---	---
	M19	12.2	12.9	2364	2008	---	---	---	---
	M20	13.6	16.8	2151	1614	---	---	---	---
4-yr	M17	13.3	14.4	2156	1730	1.03	2.05	0.78	0.55
	M18	14.6	15.5	2149	1778	2.32	1.46	0.61	0.78
	M19	12.5	16.0	2251	1943	2.46	2.17	0.64	0.50
	M20	14.4	17.1	2072	1587	1.74	1.35	0.66	0.61
CP1	M17	11.6	12.1	1760	1375	---	1.74	---	0.70
	M18	11.2	12.8	1739	1385	---	2.32	---	0.64
	M19	10.7	12.2	1773	1478	---	1.86	---	0.72
	M20	12.4	14.5	1724	1390	---	1.53	---	0.47
CP2	M17	10.5	12.3	1720	1561	---	2.26	---	0.55
	M18	10.8	10.8	1833	1357	---	2.12	---	0.58
	M19	11.6	11.2	1967	1451	---	2.79	---	0.64
	M20	12.7	13.0	1665	1267	---	0.91	---	0.33
CP3	M17	14.2	15.6	1889	1391	---	2.65	---	0.67
	M18	13.9	13.5	1611	1069	---	2.31	---	0.59
	M19	12.7	14.5	1864	1350	---	2.92	---	0.83
	M20	14.7	16.5	1690	1199	---	2.54	---	0.49
CP4	M17	13.0	12.0	1794	1286	---	3.20	---	0.56
	M18	11.9	13.6	1645	1213	---	2.17	---	0.70
	M19	11.4	13.3	1910	1328	---	2.79	---	0.55
	M20	13.9	14.8	1725	1156	---	1.76	---	0.45
CP5	M17	11.9	14.0	1980	1387	---	2.13	---	0.48
	M18	13.1	12.8	1846	1180	---	4.22	---	0.76
	M19	11.7	14.7	1931	1413	---	3.49	---	0.81
	M20	14.5	14.6	1814	1295	---	3.77	---	0.67
CP6	M17	12.0	13.5	1975	1194	---	2.27	---	0.73
	M18	11.7	12.6	1700	1212	---	2.43	---	0.70
	M19	10.9	11.7	1887	1360	---	3.66	---	0.69
	M20	13.0	13.3	1643	1285	---	3.18	---	0.56
CP7	M17	15.4	16.2	1946	1388	---	2.01	---	0.61
	M18	14.9	15.1	1711	1285	---	1.98	---	0.56
	M19	12.6	16.8	1957	1426	---	2.52	---	0.62
	M20	16.9	17.9	1690	1238	---	1.36	---	0.52
CP8	M18	---	15.9	---	1606	---	---	---	---
	M19	---	15.4	---	1756	---	---	---	---
	M20	---	18.6	---	1594	---	---	---	---
Sleeved 0.5-yr	M17	---	12.8	---	---	---	---	---	
Sleeved 1-yr	M17	---	12.1	---	---	---	---	---	
Non-Sleeved 0.5-yr	M17	---	13.6	---	---	---	---	---	
Non-Sleeved 1-yr	M17	---	13.6	---	---	---	---	---	

a= 4% V_a ; b=7% V_a

4.2.1 Cantabro Mass Loss (CML) Results

Figures 4.1a and 4.1b display CML results for field aged specimens for 4% and 7% target V_a levels, respectively. The trendline displayed in each figure is based on all ML data for each year. Average ML for each year is also displayed. It can be observed from the trendline slopes, that ML of 7% V_a specimens increased at a faster rate than for 4% V_a specimens. Also, average ML for each year was higher for 7% V_a specimens, and trendline equations for each individual mix type (which are also shown in Figures 4.1a and 4.1b) indicate that at both air void levels the WMA mixtures (M18-M20), had lower ML than the HMA (M17) except for 0-yr M20 specimens at 4% V_a which had approximately the same ML as M17 at 0-yr. Additionally, ML of M18, M19, and M20 increased at a faster rate than the M17 (except for M18 at 7% V_a which increased at a slightly reduced rate). For the sleeved vs non-sleeved experiments, ML results indicated that there were no major effects between sleeved specimens and non-sleeved specimens for this modest experiment.

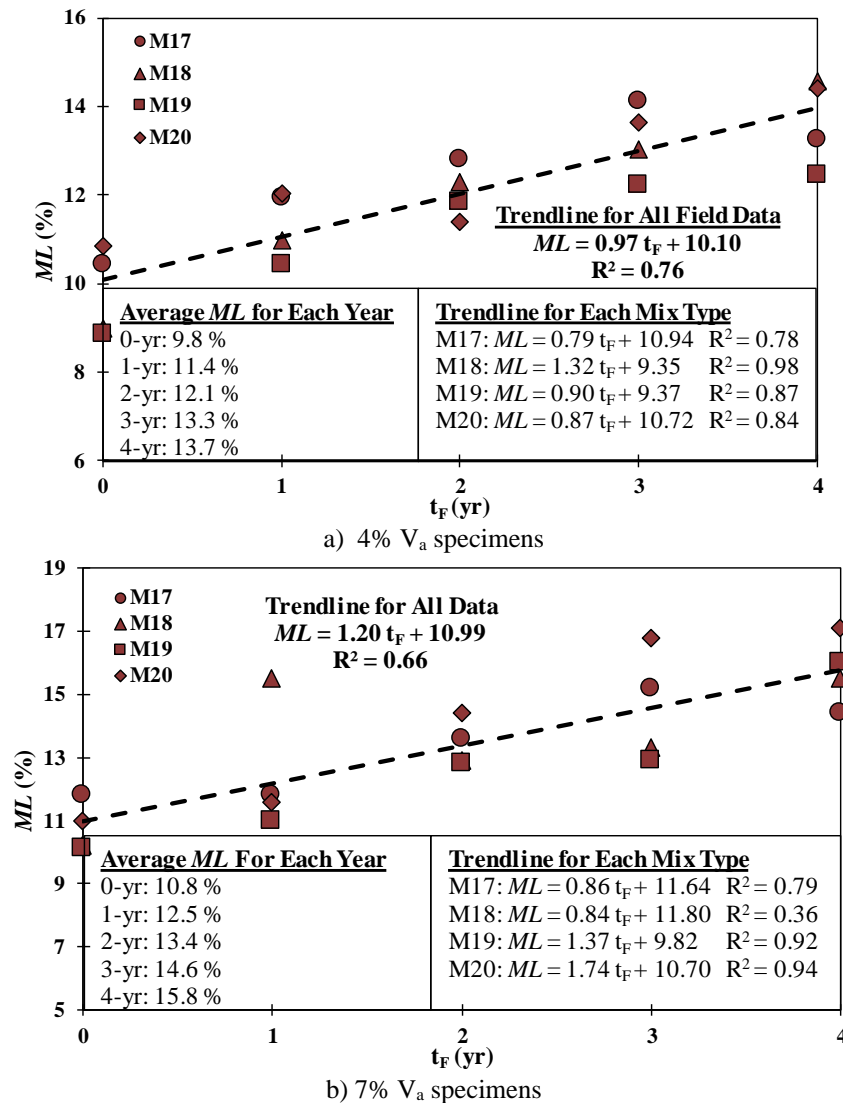


Figure 4.1. CML Field Aged Results

Figure 4.2 summarizes CML results of 4% and 7% V_a of laboratory conditioned specimens via equality plots comparing each lab CP to unconditioned specimens. Equality plots were made using individual test values instead of the averaged results summarized in Table 4.1 (i.e. the 3 individual test values that were averaged to yield results displayed in Table 4.1 were plotted). Each data point in the equality plots represents a pair of test values, where the y-value represents the *ML* of a conditioned specimen, and the x-value represents the *ML* of an otherwise identical unconditioned specimen. Any point above the equality line indicates that the CP increased *ML*. If a point is below the equality line, conditioning decreased *ML*, and if a point is on the equality line, conditioning had no effect on *ML*. Trendlines are shown to indicate how much a given protocol effected *ML*, on average. Trendlines are color coded according to the damage mechanism utilized by the represented CP. Equality plots with red trendlines indicate that oxidative damage only was used, those with blue lines utilized moisture and/or FT damage, and green trendlines represent CP7 which used a combination of oxidation, moisture, and FT induced damaged. Note that for CP8, only 7% target V_a specimens were tested, and due to a shortage of material, no M17 (HMA) specimens were subjected to CP8.

Figure 4.2 shows that as the severity of CPs increased, *ML* values also increased. For example, CP7 is simply CP1 followed by CP4; therefore, should result in a greater amount of damage than either CP1 or CP4 individually. This was observed at both V_a levels with higher *ML* for CP7 than for CP1 or CP4 individually. CP1 and CP2 resulted in the lowest trendline slopes with a range of 1.08 to 1.19 as seen in Figures 4.2a, 4.2b, 4.2h, and 4.2i, while CP3, CP4, CP5, and CP6 resulted in higher slopes ranging from 1.18 to 1.41 as displayed in Figures 4.2c, 4.2d, 4.2e, 4.2f, 4.2j, 4.2k, 4.2l, and 4.2m. CP7, which utilized a combination of oxidation and moisture damage, had the highest trendline slopes of 1.51 and 1.52 for 4% and 7% target V_a specimens, respectively. Additionally, there was little difference in trendline slopes of the same CPs at different V_a levels. For example, CP2 had the greatest difference with slopes of 1.08 and 1.16 for 4% and 7% V_a , respectively. As previously mentioned, M17 was not included in CP8 conditioning; therefore, for comparison, an equality plot for CP7 was also produced without M17 and resulted in a trendline slope of 1.58. CP8 had a trendline slope of 1.59, indicating that, on average, CP7 and CP8 increased *ML* of M18, M19, and M20 by approximately the same amount.

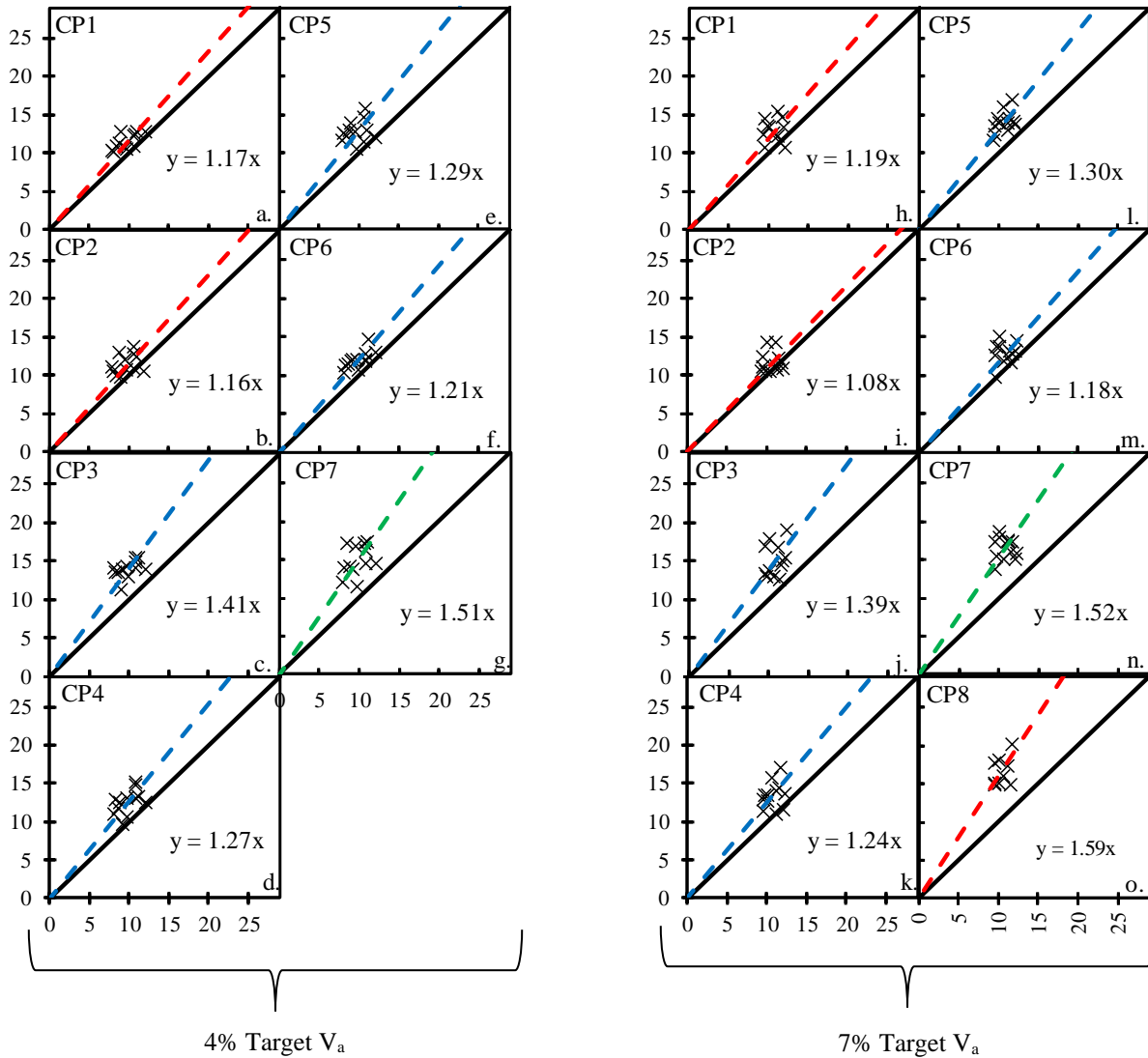
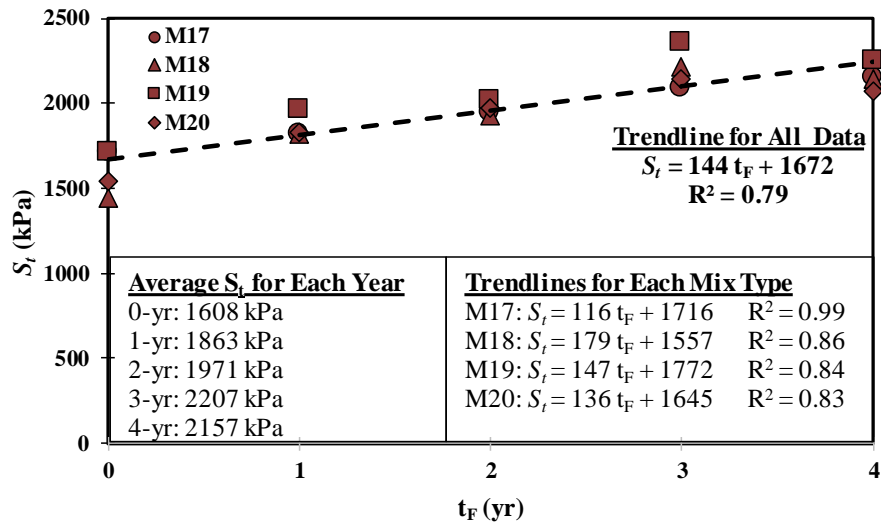


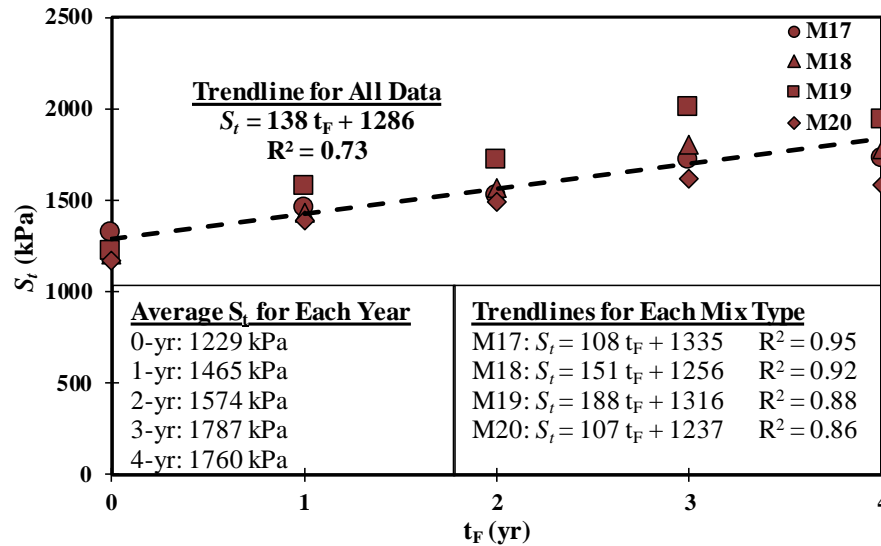
Figure 4.2. CML Laboratory Conditioned Equality Plots

4.2.2 Indirect Tensile Strength (IDT) Results

Figures 4.3a and 4.3b display IDT results from field aged specimens for 4% and 7% target V_a levels, respectively. The trendline displayed in each figure is based on all S_t data for each year. Average S_t for each year is also displayed. It was observed from the trendline slopes, that S_t of the 4% and 7% V_a specimens increased at approximately equivalent rates; however, S_t was consistently lower for the 7% specimens. Additionally, at both V_a levels, the average tensile strengths increased steadily from 0 years to 3 years in the field but decreased slightly from 3 to 4 years. Trendline equations for each mix type, which are also displayed in Figures 4.3a and 4.3b, show that WMA (i.e. M18-M20) initially had similar or lower S_t than the HMA (M17); however, S_t of M18, M19, and M20 increased at a faster rate than HMA, except for M20 at 7% V_a which increased at approximately the same rate as M17.



a) 4% Target V_a Specimens



b) 7% Target V_a Specimens

Figure 4.3. IDT Field Aged Results

Figure 4.4 summarizes IDT results of 4% and 7% V_a laboratory conditioned specimens via equality plots comparing each lab CP to unconditioned specimens. Equality plots were made using individual test values instead of the averaged results summarized in Table 4.1 (i.e. the 3 individual test values that were averaged to yield results displayed in Table 4.1 were plotted). Each data point in the equality plots represents a pair of test values, where the y-value represents the S_t of a conditioned specimen, and the x-value represents the S_t of an otherwise identical unconditioned specimen. Any point above the equality line indicates that the CP increased S_t . If a point is below the equality line, conditioning decreased S_t , and if a point is on the equality line, conditioning had no effect on S_t . Trendlines are shown to indicate how much a given protocol effected S_t , on average. Trendlines are color coded according to the damage mechanism utilized by the represented CP. Equality plots with red trendlines indicate that oxidative damage only was used, those with blue

lines utilized moisture and/or FT damage, and green trendlines represent CP7 which used a combination of oxidation, moisture, and FT induced damaged. Note that for CP8, only 7% target V_a specimens were tested, and due to a shortage of material, no M17 (HMA) specimens were subjected to CP8.

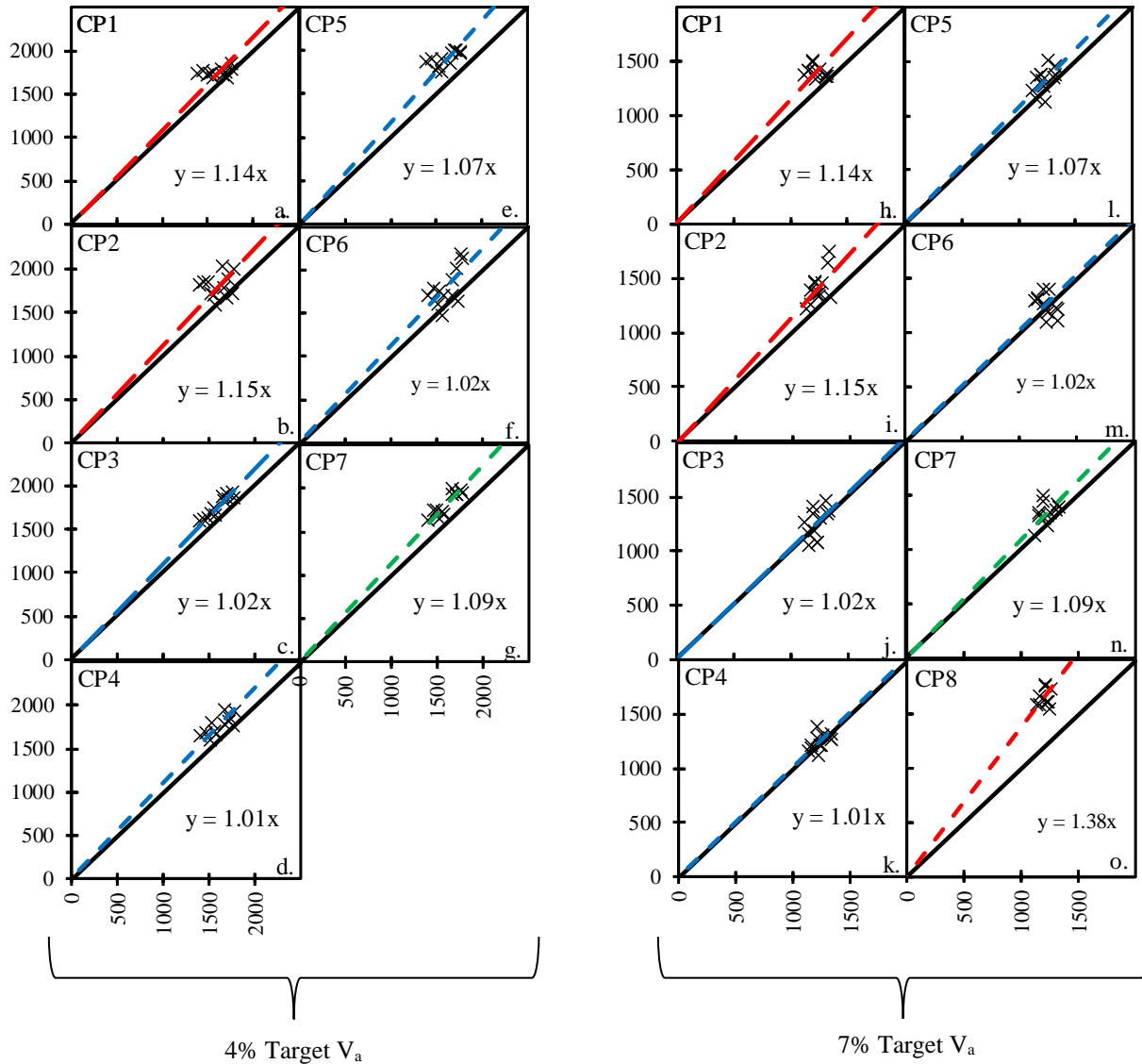


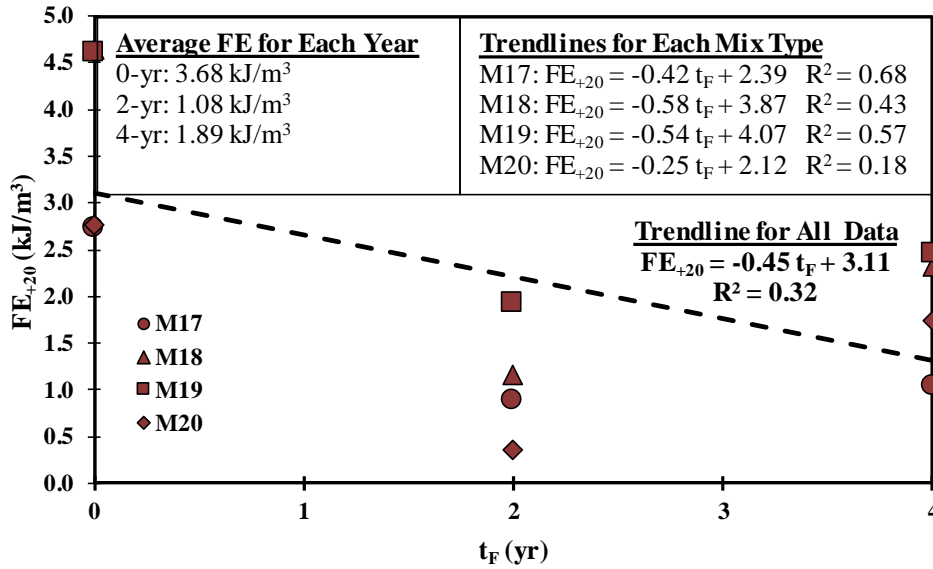
Figure 4.4. IDT Laboratory Conditioned Equality Plots

An observation made from Figure 4.4 was how the different V_a levels influenced the effects of the different damage mechanisms. For example, trendline slopes in Figure 4.4 show that CP1 and CP2 (CPs utilizing oxidation only) had two of the lowest trendline slopes for 4% target V_a level specimens, yet had two of the highest slopes when used on 7% target V_a specimens. On the other hand, CP3-CP7, all of which included moisture and/or FT conditioning, had a meaningful effect on S_f of 4% V_a specimens, but not as much on 7% V_a specimens. As previously mentioned, CP8 was not performed on M17 specimens. For comparison, an equality plot of CP7 without M17

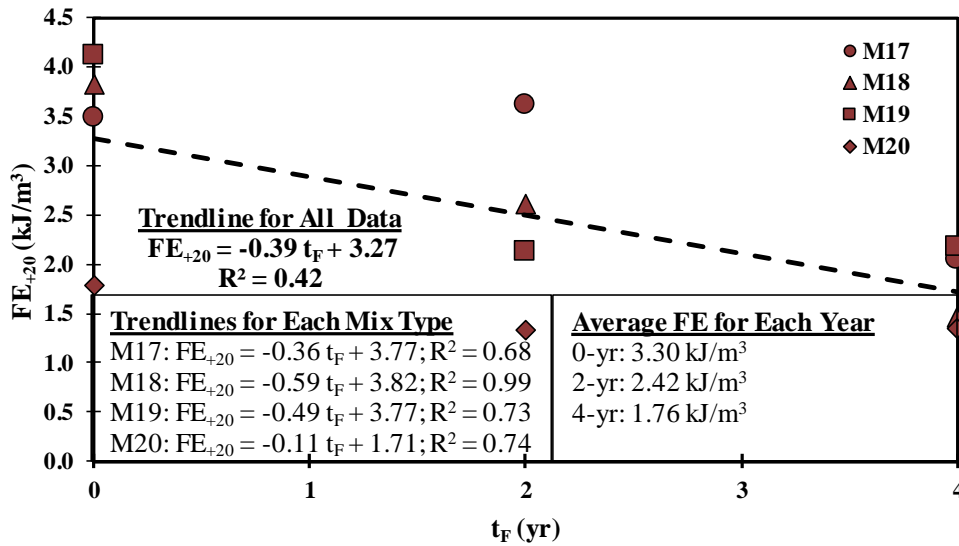
was created, which yielded a trendline slope of 1.10. This is meaningfully less than the 1.38 slope of the CP8 trendline, indicating that CP8 had a much greater effect on tensile strength than CP7.

4.2.3 20°C Fracture Energy (FE_{+20}) Results

Figures 4.5a and 4.5b display FE_{+20} results from field aged specimens for 4% and 7% target V_a levels, respectively. The trendline displayed in each figure is based on all FE_{+20} data for each year. Average FE_{+20} for each year is also displayed. Figure 4.5 shows that on average FE_{+20} of specimens at both target V_a levels decreased from 0 to 4 years of field aging; however, as seen in Figure 4.5a, FE_{+20} for 4% V_a specimens decreased from 0 to 2 years, then increased from 2 to 4 years. This was observed for the average FE_{+20} value for each year, as well as for the individual results of all four mix types. Results of 7% V_a specimens showed varying trends. The average values for each year indicated a steady decrease in FE_{+20} as a function of t_F ; however, when considering each mix type individually, different behaviors were observed. M17 (HMA) slightly increased in FE_{+20} from 0 to 2 years, then decreased from 2 to 4 years. M18 steadily decreased in FE_{+20} , and M19 and M20 decreased from 0 to 2 years, then increased from 2 to 4 years. Trendline equations for each mix type, which are also displayed in Figure 4.5, showed that for both 4% and 7% V_a specimens, M18 and M19 decreased in FE_{+20} at a faster rate than M17, while M20 decreased at slower rate than any other mix type.



a) 4% Target V_a Specimens



b) 7% Target V_a Specimens

Figure 4.5. FE_{+20} Field Aged Results

Figure 4.6 summarizes the results obtained from FE_{+20} testing of laboratory conditioned specimens compacted to a target V_a level of 7% (no FE_{+20} testing was performed on laboratory conditioned 4% target V_a specimens). Also displayed in Figure 4.6 are the results of 0-yr specimens for comparison. The average FE_{+20} of each CP indicates that all protocols reduced FE_{+20} except CP5 which resulted in a slight increase. FE_{+20} was reduced more by CPs which utilized oxidative damage only (i.e. CP1 and CP2) compared to those which used moisture and/or FT induced damage (i.e. CP3-CP6). CP7, which used a combination of oxidation, moisture, and FT conditioning, lowered average FE_{+20} to approximately the same level as CP1 and CP2. Figure 4.6 also shows that M17 (HMA) initially had a lower FE_{+20} than M18 or M19 (two of the three WMAs), while M20 (the third WMA) had the lowest initial FE_{+20} . After conditioning, mix types

did not show consistent trends. For example, CP5 caused minimal change in FE₊₂₀ for M18 and M19, but meaningfully decreased M17 and increased M20.

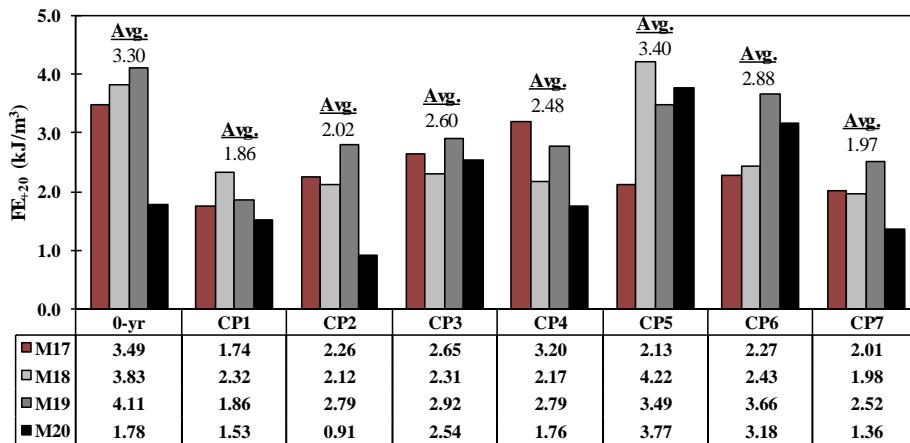
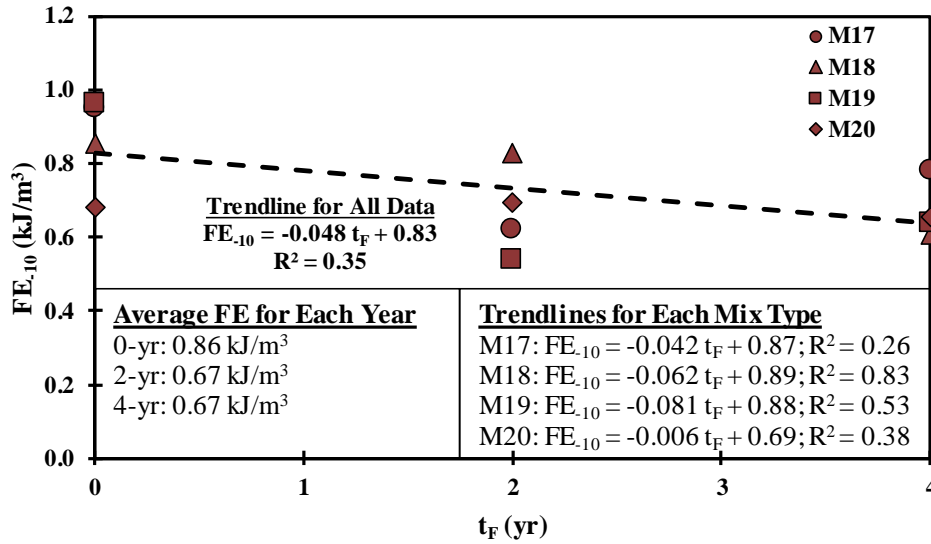


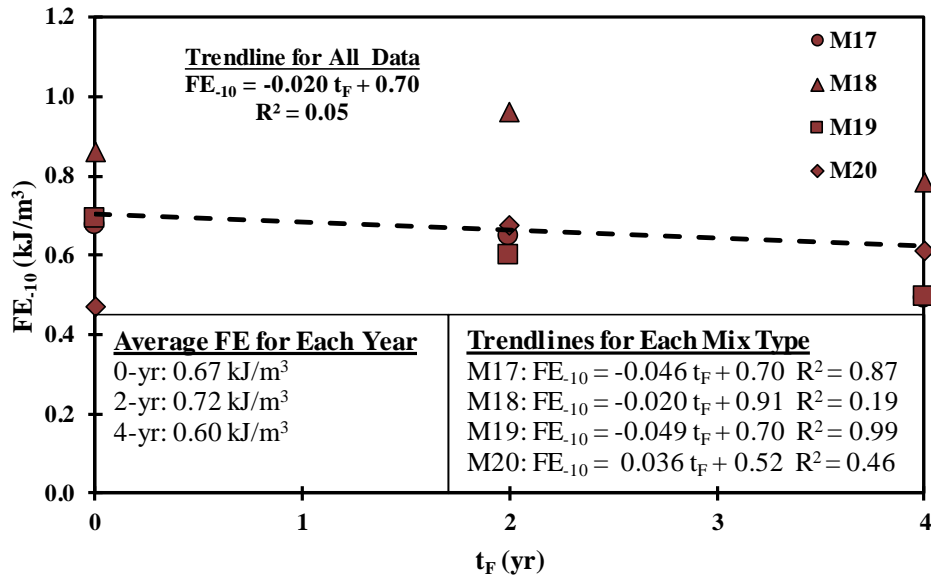
Figure 4.6. FE₊₂₀ Laboratory Conditioned Results

4.2.4 -10°C Fracture Energy (FE₋₁₀) Results

Figures 4.7a and 4.7b display FE₋₁₀ results from field aged specimens for 4% and 7% target V_a levels, respectively. The trendline displayed in each figure is based on all FE₋₁₀ data for each year. Average FE₋₁₀ for each year is also displayed. Trendline slopes indicate that the 4% V_a specimens decreased in FE₋₁₀ at a faster rate than the 7% V_a as a function of field aging. For 4% target V_a level specimens, trendline equations for each mix type displayed in Figure 4.7a show that FE₋₁₀ of M18 and M19 (both of which are WMAs) decreased at a faster rate than M17 (HMA); however, trendline equations in Figure 4.7b show that at a target V_a level of 7%, M18 had a slower rate of change than M17, and M19 had approximately the same rate. M20 (also a WMA) had almost no change in FE₋₁₀ at 4% V_a, and increased in 7% target V_a specimens.



a) 4% Target V_a Specimens



b) 7% Target V_a Specimens

Figure 4.7. FE_{-10} Field Aged Results

Figure 4.8 summarizes the results obtained from FE_{-10} testing of laboratory conditioned specimens compacted to a target V_a level of 7% (no FE_{-10} testing was performed on laboratory conditioned 4% target V_a specimens). Also displayed in Figure 4.8 are the results of 0-yr specimens for comparison. Average FE_{-10} results show CP2 had the greatest effect on FE_{-10} results, followed by CP4, then CP7. CP1, CP3, CP5, and CP6 all had little to no effect on average; however, it is important to note that when each mix is considered individually, there were meaningful changes observed. M20 had the lowest FE_{-10} of any mixture before and after conditioning, except after CP5 where M17 FE_{-10} was lower than that of M20. Overall, FE_{-10} results of laboratory conditioned specimens were highly variable.

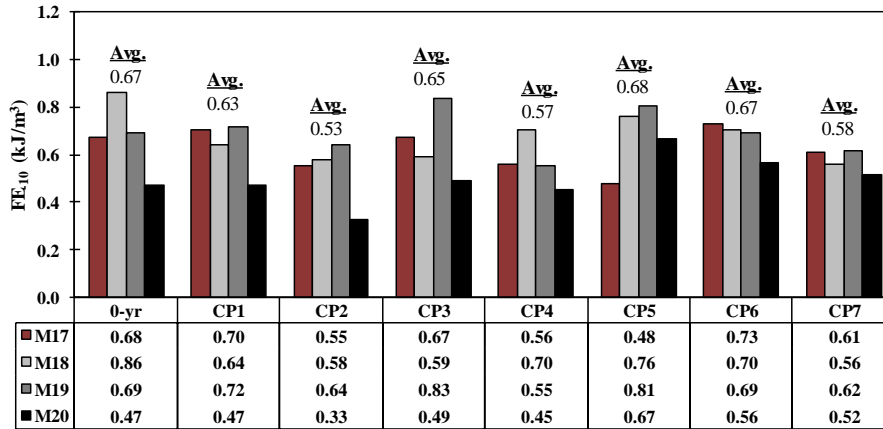


Figure 4.8. FE-10 Lab Conditioned Results

4.3 Wheel-Tracking Tests

This section summarizes all test results from HLWT and APA testing. Tables 4.2 and 4.3 display HLWT results for 0-yr and field aged, and laboratory conditioned specimens, respectively. As described in Chapter 3, one test value is produced from the testing of two specimens denoted as a specimen set (i.e. data reported in Tables 4.2 and 4.3 were obtained from testing two identical specimens). Note that three sets (i.e. six specimens) of each mix type were HLWT tested for 0-yr and laboratory conditioned specimens while just one set of each mix type was tested for 1-yr. If a test reached failure (i.e. RD_{HLWT} of 12.5mm), the pass number at which failure was reached is reported. Also, average RD_{HLWT} for each mix type at 5K (i.e. 5,000), 10K, 15K, and 20K passes are reported in Tables 4.2 and 4.3. In the same manner, Tables 4.4 and 4.5 display APA results for 0-yr and field aged, and laboratory conditioned specimens, respectively. As with HLWT testing, two specimens comprise a set for APA testing. Three sets of each mix type were tested for 0-yr, 2-yr, and laboratory conditioned specimens, while only one set was tested for 1-yr and 4-yr specimens. RD_{APA} at 1K, 2K, 4K, and 8K passes is reported in Tables 4.4 and 4.5 for each specimen set as well as an average of the three sets to represent each mix type.

Sections 4.3.1 and 4.3.2 interpret HLWT and APA data, respectively. In the same manner as described in Section 4.1, these sections utilize only the data presented in the tables in this section relative to each separate method. For example, any analysis performed, or observations made in Section 4.3.1 (i.e. the section where HLWT results are discussed) used only data presented in Tables 4.2 and 4.3. No comparisons were made to other test methods used in this study, nor are there references to related literature, as these are incorporated later in this report.

Table 4.2. HLWT Results for 0-yr Control and 1-yr Field Aged Specimens

Age	Mix	RD _{HLWT} (mm) at Pass No.									
		4% V _a					7% V _a				
		5K	10K	15K	20K	P _{12.5}	5K	10K	15K	20K	P _{12.5}
0-yr	M17	4.0	5.1	6.0	7.1	---	3.9	4.9	5.6	6.3	---
		4.9	6.0	7.0	8.3	---	5.0	6.3	7.3	8.4	---
		5.3	6.1	6.9	7.6	---				8.2 ^a	---
	Avg.	4.7	5.8	6.6	7.7	---	4.5	5.6	6.5	7.7	---
	M18	5.0	6.8	9.9	---	17594	4.6	6.1	7.6	10.0	---
		5.8	7.4	9.3	---	17858	6.9	9.8	---	---	12988
		4.5	6.5	9.8	---	17572	6.5	9.2	---	---	13570
	Avg.	5.1	6.9	9.7		17675	6.0	8.3	7.6	10.0	13279
	M19	2.7	4.0	4.8	5.6	---	5.7	7.8	10.2	---	18190
		3.0	4.8	6.1	7.4	---	7.0	10.1	---	---	13072
		3.0	4.3	5.5	9.0	---	7.2	9.4	11.8	---	16238
	Avg.	2.9	4.4	5.5	7.3	---	6.6	9.1	11.0	---	15833
M20	2.2	4.6	6.5	9.8	---	4.8	6.0	7.4	9.9	---	
	2.3	4.1	5.6	9.6	---	6.1	7.3	8.3	10.3	---	
	2.3	3.7	4.6	5.9	---	4.7	5.9	6.8	8.6	---	
Avg.	2.3	4.1	5.5	8.4	---	5.2	6.4	7.5	9.6	---	
1-yr	M17	2.1	2.4	3.0	3.4	---	4.5	5.6	6.3	7.2	---
	Avg.	2.1	2.4	3.0	3.4	---	4.5	5.6	6.3	7.2	---
	M18	3.8	5.0	5.7	6.4	---	5.1	6.5	7.8	9.5	---
	Avg.	3.8	5.0	5.7	6.4	---	5.1	6.5	7.8	9.5	---
	M19	2.3	2.9	3.4	3.9	---	4.8	6.2	7.5	8.9	---
	Avg.	2.3	2.9	3.4	3.9	---	4.8	6.2	7.5	8.9	---
	M20	2.9	3.8	4.2	4.4	---	2.7	3.5	4.0	4.7	---
	Avg.	2.9	3.8	4.2	4.4	---	2.7	3.5	4.0	4.7	---

^aFinal RD recorded manually

Table 4.3. HLWT Results for Laboratory Conditioned Specimens

Age	Mix	RD _{HLWT} (mm) at Pass No.					Mix	RD _{HLWT} (mm) at Pass No.				
		5K	10K	15K	20K	P _{12.5}		5K	10K	15K	20K	P _{12.5}
CP1	M17	---	---	---	---	---	M19	4.7	6.0	6.9	7.9	---
		---	---	---	---	---		4.3	5.4	5.9	6.6	---
		---	---	---	---	---		4.4	5.7	6.6	7.5	---
	Avg.	---	---	---	---	---	Avg.	4.5	5.7	6.5	7.3	---
	M18	5.7	6.8	7.6	8.4	---	M20	3.9	4.9	5.7	6.3	---
CP2	M17	---	---	---	---	---	M19	4.3	5.4	5.9	6.6	---
		---	---	---	---	---		4.4	5.7	6.6	7.5	---
	Avg.	---	---	---	---	---	Avg.	4.5	5.7	6.5	7.3	---
	M18	4.1	5.2	6.1	6.9	---	M20	3.8	4.5	5.0	5.6	---
		3.9	4.8	5.4	6.0	---		4.0	4.9	5.4	5.9	---
CP3	M17	---	---	---	---	---	M19	5.7	7.4	8.6	9.8	---
		---	---	---	---	---		4.5	5.7	6.5	7.4	---
	Avg.	---	---	---	---	---	Avg.	4.9	6.2	7.2	8.1	---
	M18	4.5	5.5	6.4	7.1	---	M20	3.9	4.9	5.6	6.2	---
		5.0	6.3	7.1	8.0	---		3.4	4.4	5.2	5.8	---
CP4	M17	---	---	---	---	---	M19	4.5	5.7	6.5	7.4	---
		---	---	---	---	---		4.4	5.6	6.4	7.1	---
	Avg.	---	---	---	---	---	Avg.	4.9	6.2	7.2	8.1	---
	M18	5.0	6.3	7.1	8.0	---	M20	3.4	4.4	5.2	5.8	---
		4.7	5.8	6.7	7.7	---		3.5	4.5	5.3	5.8	---
CP5	M17	---	---	---	---	---	M19	6.8	12.2	---	---	10286
		---	---	---	---	---		5.4	8.4	---	---	14284
	Avg.	---	---	---	---	---	Avg.	6.0	9.8	---	---	13097
	M18	6.0*	---	---	---	9142	M20	5.4	7.9	---	---	14234
		5.0	6.9	---	---	14720		4.0	5.0	5.8	6.9	---
CP6	M17	---	---	---	---	---	M19	5.8	8.6	---	---	14722
		---	---	---	---	---		5.8	8.6	---	---	14722
	Avg.	---	---	---	---	---	Avg.	6.0	9.8	---	---	13097
	M18	5.2	7.4	11.1	---	16104	M20	5.4	7.9	---	---	14234
		5.4	7.1	11.1	---	13322		4.0	5.0	5.8	6.9	---
CP7	M17	---	---	---	---	---	M19	4.3	5.6	7.2	---	19874
		---	---	---	---	---		4.3	5.6	7.2	---	19874
	Avg.	---	---	---	---	---	Avg.	4.6	6.2	6.5	6.9	17054
	M18	6.2	9.1	---	---	13152	M20	4.7	6.1	7.5	9.8	---
		5.5	7.6	11.6	---	15572		5.5	7.0	8.6	10.4	---
CP8	M17	---	---	---	---	---	M19	5.9	7.7	10.0	---	18502
		---	---	---	---	---		5.9	7.7	10.0	---	18502
	Avg.	---	---	---	---	---	Avg.	5.3	6.9	8.7	10.1	18502
	M18	6.0	7.8	11.0	---	15162	M20	5.2	6.7	8.3	---	19658
		5.9	8.2	11.3	---	14629		4.2	5.5	6.9	11.1	---
CP9	M17	---	---	---	---	---	M19	4.7	6.0	7.4	10.1	---
		---	---	---	---	---		4.7	6.0	7.4	10.1	---
	Avg.	---	---	---	---	---	Avg.	4.7	6.0	7.5	10.6	19658
	M18	6.4	9.2	---	---	13616	M20	6.1	9.9	---	---	12394
		6.5	10.5	---	---	10989		6.1	8.8	---	---	13840
CP10	M17	---	---	---	---	---	M19	5.8	8.9	---	---	13038
		---	---	---	---	---		5.8	8.9	---	---	13038
	Avg.	---	---	---	---	---	Avg.	6.0	9.2	---	---	13091
	M18	6.5	11.7**	---	---	10326	M20	5.2	7.2	---	---	14464
		6.6	---	---	---	9024		5.0	7.6	---	---	13366
CP11	M17	---	---	---	---	---	M19	6.4	9.2	---	---	13616
		---	---	---	---	---		5.1	6.6	8.9	---	17558
	Avg.	---	---	---	---	---	Avg.	5.1	7.1	8.9	---	15129
	M18	6.7	8.6	11.1	---	16702	M20	6.6	8.2	10.3	---	19504
		6.4	8.4	12.1	---	15386		6.9	9.2	12.1	---	15568
CP12	M17	---	---	---	---	---	M19	5.6	7.4	9.8	---	18952
		---	---	---	---	---		5.6	7.4	9.8	---	18952
	Avg.	---	---	---	---	---	Avg.	6.3	8.3	10.7	---	18008
	M18	6.7	8.4	11.0	---	16746	M20	5.5	6.9	8.6	---	19866
		6.6	8.4	11.4	---	16278		6.0	7.3	9.2	---	18786
CP13	M17	---	---	---	---	---	M19	5.7	7.4	10.4	---	16234
		---	---	---	---	---		5.7	7.4	10.4	---	16234
	Avg.	---	---	---	---	---	Avg.	5.8	7.2	9.4	---	18295
	M18	4.1	5.1	5.9	6.8	---	M20	5.1	6.3	7.1	7.7	---
		4.5	5.5	6.4	7.5	---		4.4	5.0	5.0	5.4	---
CP14	M17	---	---	---	---	---	M19	5.2	5.7	5.8	6.1	---
		---	---	---	---	---		5.2	5.7	5.8	6.1	---
	Avg.	---	---	---	---	---	Avg.	4.9	5.7	6.0	6.4	---
	M18	4.7	5.5	5.9	6.4	---	M20	4.0	4.8	5.4	5.7	---
		4.7	5.5	5.9	6.4	---		3.4	4.4	5.1	5.9	---
CP15	M17	---	---	---	---	---	M19	3.8	4.6	5.0	5.4	---
		---	---	---	---	---		3.8	4.6	5.0	5.4	---
	Avg.	---	---	---	---	---	Avg.	3.7	4.6	5.2	5.7	---
	M18	4.4	5.1	5.9	6.8	---	M20	3.4	4.4	5.1	5.9	---
		4.4	5.3	6.1	6.9	---		3.8	4.6	5.0	5.4	---

*Stripping inflection point (SIP) observed at pass no. 69851; **SIP observed at pass no. 8468

Table 4.4. APA Results for 0-yr and Field Aged Specimens

Age	Mix	RD _{APA} (mm) at Pass No.							
		4% V _a				7% V _a			
		1K	2K	4K	8K	1K	2K	4K	8K
0-yr	M17	1.8	3.0	4.1	5.1	2.2	3.2	3.7	4.6
		1.7	2.7	4.1	5.1	3.0	3.8	4.3	5.4
		2.6	3.7	5.0	5.9	2.0	2.9	3.8	4.7
		Avg.	2.0	3.2	4.4	5.3	2.4	3.3	3.9
	M18	1.5	2.2	2.9	3.6	3.2	4.0	4.9	6.0
		1.4	1.8	2.4	2.8	3.0	3.6	4.4	5.2
		1.4	1.8	2.3	2.8	3.0	3.8	4.7	5.8
		Avg.	1.4	2.0	2.5	3.0	3.1	3.8	4.7
	M19	2.0	3.4	4.6	5.6	4.3	5.4	6.7	8.2
		2.4	3.6	4.8	5.8	4.1	5.4	7.1	9.0
		3.1	4.6	5.9	6.9	4.9	6.1	7.6	9.2
		Avg.	2.5	3.9	5.1	6.1	4.4	5.6	7.1
M20	2.3	3.0	3.7	4.3	2.4	3.2	4.0	4.9	
	2.2	2.9	3.4	3.9	2.3	2.9	3.6	4.3	
	1.9	2.4	2.8	3.4	2.4	3.0	3.7	4.6	
	Avg.	2.1	2.7	3.3	3.9	2.4	3.0	3.7	4.6
1-yr	M17	1.3	1.8	2.4	3.1	2.0	2.7	3.7	4.7
		Avg.	1.3	1.8	2.4	3.1	2.0	2.7	3.7
	M18	1.3	1.8	2.4	3.1	3.9	4.6	5.5	6.6
		Avg.	1.3	1.8	2.4	3.1	3.9	4.6	5.5
	M19	4.2	5.4	6.4	6.7	2.8	4.3	5.4	6.6
		Avg.	4.2	5.4	6.4	6.7	2.8	4.3	5.4
	M20	1.0	1.3	1.6	1.9	2.0	2.7	3.5	4.2
		Avg.	1.0	1.3	1.6	1.9	2.0	2.7	3.5
2-yr	M17	3.4	4.4	5.0	5.7	4.8	5.9	6.8	7.8
		3.2	4.3	5.2	6.1	4.4	5.7	6.9	8.2
		3.7	4.7	5.6	6.5	5.1	6.4	7.8	9.2
		Avg.	3.4	4.5	5.3	6.1	4.8	6.0	7.2
	M18	2.4	3.4	4.4	5.5	2.9	3.8	4.8	5.8
		1.9	2.7	3.5	4.4	2.6	3.4	4.2	5.2
		2.0	2.7	3.4	4.1	3.7	4.6	5.6	6.8
		Avg.	2.1	2.9	3.8	4.7	3.1	3.9	4.9
	M19	2.8	4.1	5.3	6.3	3.5	4.9	6.2	7.5
		3.6	4.6	5.8	6.8	4.3	5.6	7.0	8.6
		4.2	5.1	6.3	7.4	5.6	7.1	8.5	10.2
		Avg.	3.5	4.6	5.8	6.8	4.5	5.8	7.2
M20	1.7	2.2	2.9	3.5	2.9	3.5	4.2	4.8	
	1.5	2.0	2.5	3.1	2.5	3.1	3.6	4.2	
	1.5	1.9	2.4	2.9	3.0	3.7	4.3	5.0	
	Avg.	1.5	2.1	2.6	3.2	2.8	3.4	4.0	4.7
4-yr	M17	0.8	1.2	1.6	2.1	1.2	1.7	2.5	3.5
		Avg.	0.8	1.2	1.6	2.1	1.2	1.7	2.5
	M18	0.8	1.0	1.4	1.7	1.5	2.1	2.7	3.5
		Avg.	0.8	1.0	1.4	1.7	1.5	2.1	2.7
	M19	0.9	1.3	1.7	2.4	1.4	2.2	2.9	4.2
		Avg.	0.9	1.3	1.7	2.4	1.4	2.2	2.9
	M20	0.9	1.1	1.4	1.8	1.5	2.2	2.8	3.6
		Avg.	0.9	1.1	1.4	1.8	1.5	2.2	2.8

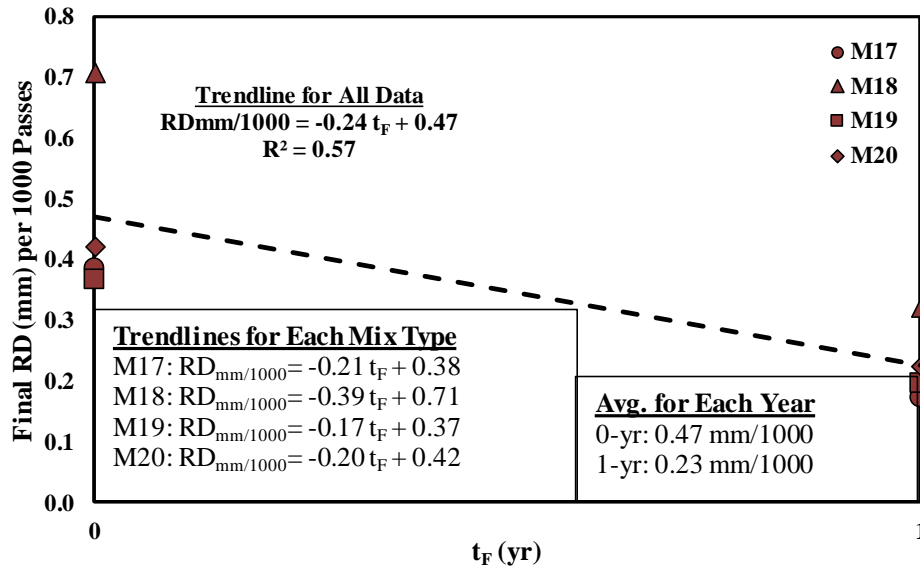
Table 4.5. APA Results for 7% V_a Laboratory Conditioned Specimens

Age	Mix	RD _{APA} (mm) at Pass No.				Mix	RD _{APA} (mm) at Pass No.			
		1K	2K	4K	8K		1K	2K	4K	8K
CP1	M17	2.6	3.9	5.5	7.1	M19	4.0	4.5	5.2	6.2
		2.3	3.2	4.3	5.4		3.9	5.1	6.4	7.8
		2.3	3.4	4.9	6.9		3.8	4.9	6.3	7.7
	Avg.	2.4	3.5	4.9	6.5	Avg.	3.9	4.8	6.0	7.2
	M18	2.8	3.4	4.2	5.2	M20	2.7	3.4	4.0	4.5
		2.5	3.2	4.0	5.0		2.4	3.0	3.8	4.6
3.3		4.3	5.3	6.7	2.7		3.4	4.2	5.0	
Avg.	2.9	3.7	4.5	5.6	Avg.	2.6	3.3	4.0	4.7	
CP2	M17	2.2	3.0	4.0	5.3	M19	4.7	5.9	7.1	8.6
		2.0	2.8	3.8	5.1		3.1	4.2	5.4	6.7
		2.6	3.7	5.3	7.0		2.7	3.7	4.9	6.2
	Avg.	2.2	3.1	4.4	5.8	Avg.	3.5	4.6	5.8	7.2
	M18	3.8	5.0	6.3	7.9	M20	4.3	5.3	6.2	7.2
		3.7	5.0	6.6	8.5		3.9	4.9	5.7	6.5
5.4		6.6	7.7	8.8	3.0		3.9	4.7	5.6	
Avg.	4.3	5.5	6.9	8.4	Avg.	3.7	4.7	5.6	6.4	
CP3	M17	2.8	3.8	5.0	6.3	M19	5.1	6.2	7.4	8.6
		2.6	3.6	5.0	6.5		3.1	4.0	4.8	5.7
		2.0	2.7	3.6	4.5		4.8	6.0	7.1	8.3
	Avg.	2.5	3.4	4.5	5.8	Avg.	4.3	5.4	6.5	7.5
	M18	3.4	4.1	4.8	5.9	M20	2.8	3.7	4.6	5.4
		2.6	3.3	4.1	4.9		2.3	3.0	3.7	4.4
4.2		5.2	6.0	6.9	3.1		3.7	4.4	5.3	
Avg.	3.4	4.2	5.0	5.9	Avg.	2.7	3.5	4.2	5.0	
CP4	M17	2.0	2.7	3.5	4.4	M19	4.7	5.8	7.0	8.3
		1.9	2.7	3.6	4.7		3.4	4.1	5.0	6.0
		3.5	4.9	6.0	7.2		5.1	6.2	7.2	8.5
	Avg.	2.5	3.4	4.4	5.4	Avg.	4.4	5.4	6.4	7.6
	M18	3.6	4.6	5.5	6.5	M20	3.2	3.9	4.6	5.2
		2.9	3.7	4.6	5.7		2.4	3.1	3.8	4.4
4.8		5.9	6.8	7.9	4.1		5.0	5.8	6.6	
Avg.	3.8	4.7	5.6	6.7	Avg.	3.2	4.0	4.7	5.4	
CP5	M17	3.1	4.5	6.1	7.7	M19	3.5	4.6	6.0	7.4
		1.6	2.1	3.0	4.0		4.6	5.7	6.8	8.2
		1.7	2.4	3.3	4.3		5.1	6.2	7.3	8.7
	Avg.	2.1	3.0	4.1	5.3	Avg.	4.4	5.5	6.7	8.1
	M18	3.2	4.1	5.1	6.1	M20	3.1	3.7	4.3	4.9
		4.4	5.4	6.6	7.6		3.9	4.8	5.6	6.5
5.5		6.6	7.7	8.9	4.5		5.5	6.4	7.4	
Avg.	4.4	5.4	6.4	7.6	Avg.	3.9	4.7	5.5	6.2	
CP6	M17	2.1	2.7	3.4	4.2	M19	3.0	3.8	4.7	5.7
		2.0	2.8	3.7	4.8		3.8	4.8	6.0	7.5
		2.7	3.4	4.2	5.1		5.6	6.8	8.1	9.2
	Avg.	2.3	2.9	3.8	4.7	Avg.	4.1	5.1	6.2	7.5
	M18	4.7	5.8	6.9	7.9	M20	3.8	4.8	5.8	6.8
		2.8	3.4	4.0	4.8		2.7	3.4	4.0	4.6
4.8		6.0	7.1	8.2	3.8		4.9	6.1	7.2	
Avg.	4.1	5.1	6.0	6.9	Avg.	3.5	4.4	5.3	6.2	
CP7	M17	1.7	2.5	3.4	4.6	M19	3.4	4.5	5.6	6.8
		1.7	2.2	2.7	3.4		2.8	3.7	4.7	5.8
		2.0	2.8	3.9	4.8		4.9	5.9	7.0	8.1
	Avg.	1.8	2.5	3.3	4.3	Avg.	3.7	4.7	5.8	6.9
	M18	3.7	4.8	5.9	6.9	M20	2.7	3.6	4.6	5.5
		2.7	3.4	4.2	5.1		2.2	2.9	3.4	4.0
3.8		5.0	6.2	7.1	3.4		4.5	5.5	6.4	
Avg.	3.4	4.4	5.4	6.4	Avg.	2.8	3.6	4.5	5.3	

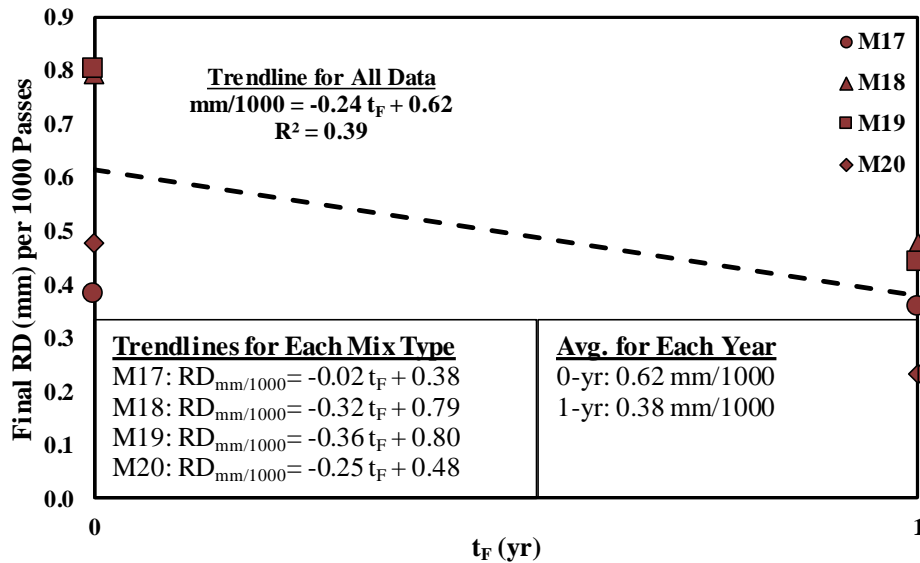
4.3.1 Hamburg Loaded Wheel Tracker (HLWT) Results

As described in Section 3.5.5, HLWT testing was performed to 20,000 passes, unless RD_{HLWT} reached 12.5mm, at which point the test was terminated and the number of passes to reach 12.5mm was recorded. Because some specimens sets completed 20,000 passes while others reached 12.5 mm RD_{HLWT} prior to completing the test, final rut-depth could not be used solely for comparison; therefore, a parameter denoted mm/1000 was used. This parameter was calculated by dividing the final rut depth of a set of HLWT specimens (mm units) by the number of passes (in thousands) at which RD_{HLWT} of 12.5 mm was reached. For example, Table 4.2 shows that M18 0-yr at 7% target V_a level had one set of specimens that completed all 20,000 passes at a final rut depth of 10 mm. For the other two sets of M18 0-yr specimens, the maximum rut depth of 12.5 mm was reached at 12988 and 13570 passes. To calculate mm/1000 for the first set, 10 mm was divided by 20 to yield a mm/1000 value of 0.5. For the two sets that reached failure, 12.5mm was divided by 12.988 and 13.570 to yield mm/1000 values of 0.96 and 0.92, respectively. The three mm/1000 values were then averaged to yield 0.79 mm/1000. In cases where there was only one set of specimens tested, the mm/1000 value calculated from the one test was used for comparison.

Figures 4.9a and 4.9b display mm/1000 values from field aged specimens for 4% and 7% target V_a levels, respectively. The trendline displayed in each figure is based on all mm/1000 values for each year. Average mm/1000 for each year is also displayed. The trendline slopes in Figures 4.9a and 4.9b indicate that both air voids levels aged at the same rate (i.e. the slope for both trendlines are the same). However, the averages for each year show that the mm/1000 was greater for the 7% target V_a specimens. The trendline equations for each mix type that were provided in Figure 4.9a show that for the 4% V_a specimens, M19 had a decreased rate of aging (as indicated by a more negative trendline slope) compared to M17 (HMA), while M18 had an increased rate, and M20 was approximately the same as M17. The trendline equations for each mix type that were provided in Figure 4.9b show that for the 7% target V_a specimens, M17 (HMA) showed the slowest rate of aging, and all three WMAs (M18, M19, and M20) showed aging characteristics similar to one another.



a) 4% Target V_a Specimens



b) 7% Target V_a Specimens

Figure 4.9. HLWT Field Aged Results

Figure 4.10 summarizes the mm/1000 values calculated from HLWT testing of laboratory conditioned specimens compacted to a target V_a level of 7% (no HLWT testing was performed on laboratory conditioned 4% target V_a specimens). Also displayed in Figure 4.10 are the results of 0-yr specimens for comparison. Note that HLWT testing on laboratory conditioned M17 specimens was not conducted due to a shortage of the material. Figure 4.10 indicates that CPs which utilized oxidative conditioning only (i.e. CP1 and CP2) meaningfully decreased rutting, as represented by the average mm/1000. However, for CP3-CP6 (i.e. those using moisture and/or FT damage only), mm/1000 either decreased very little or increased. CP7, which utilized a combination of oxidation, moisture, and FT conditioning, resulted in the lowest average mm/1000

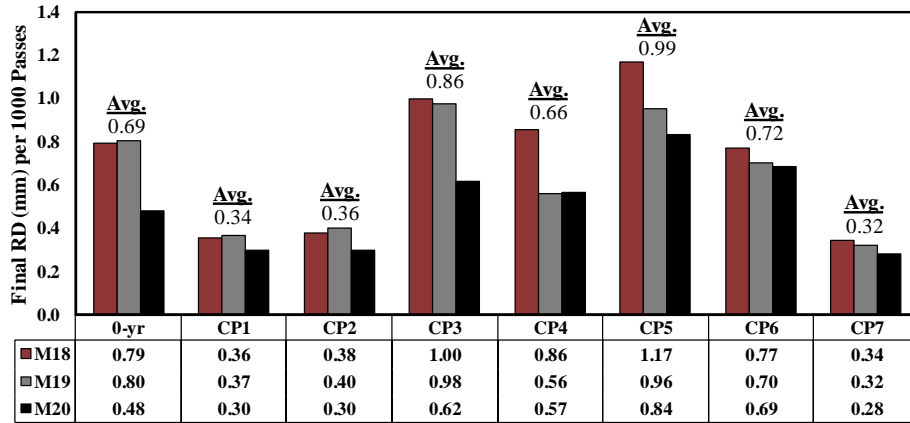
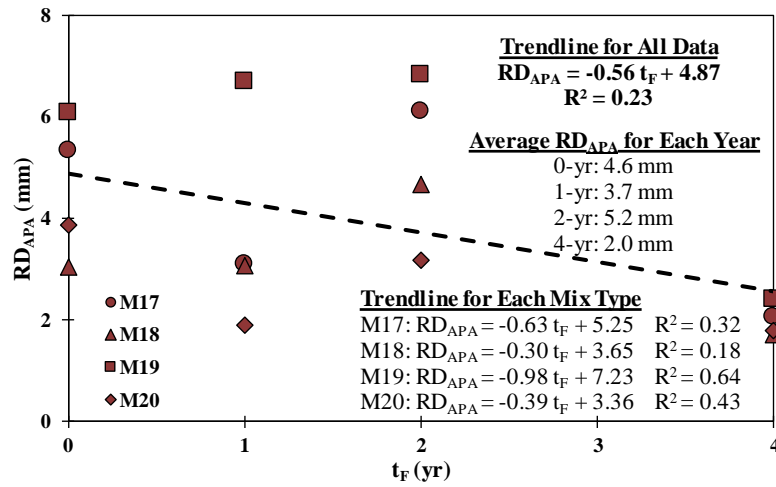


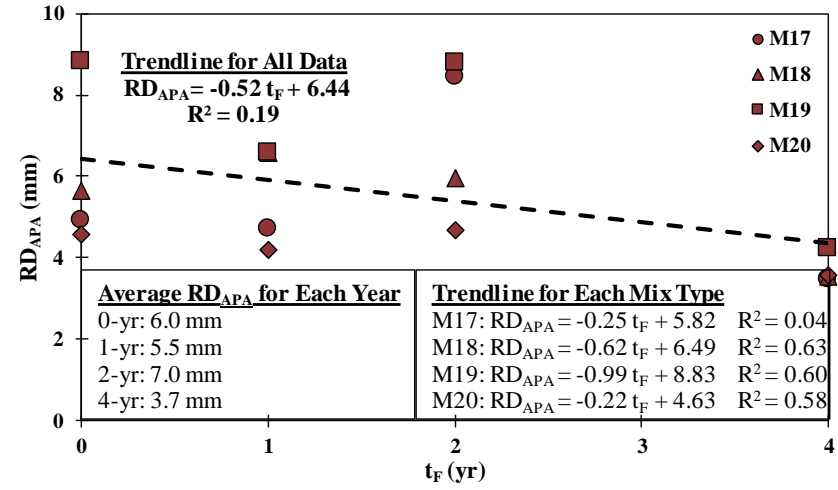
Figure 4.10. HLWT Laboratory Conditioned Results

4.3.2 Asphalt Pavement Analyzer (APA) Results

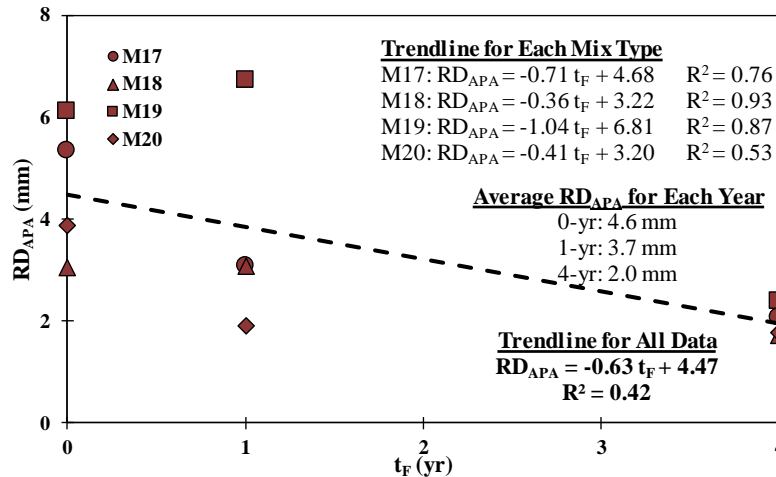
Figures 4.11a and 4.11b display RD_{APA} results from field aged specimens for 4% and 7% target V_a levels, respectively. The trendline displayed in each figure is based on all RD_{APA} results for each year. Average RD_{APA} results for each year were also displayed. The average RD_{APA} for each year shows that at both V_a levels, RD_{APA} was highest for 2-yr specimens, even compared to 0-yr specimens. This was inconsistent with the steady decrease in rut depth that was observed at every other year of field aging. This was likely the result of larger specimens being used for 2-yr APA testing relative. 115 mm specimens were cut to the 75 mm height of the mold for 2-yr specimens, while 0-yr specimens were 75 mm tall, and 1-yr and 4-yr specimens were 63 mm tall. Because of this discrepancy with the 2-yr data, Figures 4.11c and 4.11d summarize the same data as Figures 4.11a and 4.11b with 2-yr data eliminated. The R^2 of the trendlines for all data increased when 2-yr data was removed. Overall, 7% V_a specimens had higher rut depths than 4% V_a . Trendline equations for each mix type, which were also displayed in each part of Figure 4.11, show that differences in WMA and HMA aging rates (i.e. rate of decrease in final RD_{APA} as indicated by trendline slopes) were variable. For example, Figure 4.11c shows that final average RD_{APA} M18 and M20 at 4% V_a decreased at faster rate compared to M17 (HMA), while M20 decreased at a slower rate. Figure 4.11d shows the same trend for 7% V_a specimens.



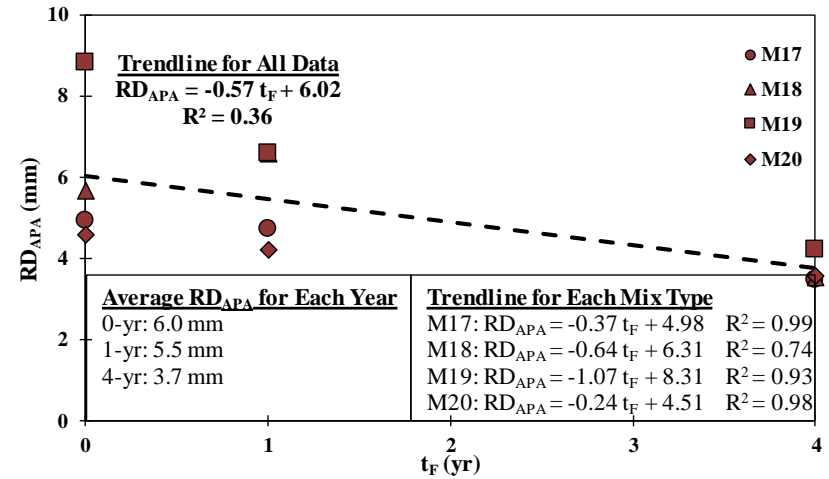
a) 4% V_a Results



b) 7% V_a Results



c) 4% V_a Results (without 2-yr Results)



d) 7% V_a Results (without 2-yr Results)

Figure 4.11. APA Field Aged Results

Figure 4.12 summarizes the final RD_{APA} results obtained from APA testing of laboratory conditioned specimens compacted to a target V_a level of 7% (no APA testing was performed on lab conditioned 4% target V_a specimens). Also displayed in Figure 4.12 are the results of 0-yr specimens for comparison. On average, CP1 resulted in no change of RD_{APA} relative to 0-yr specimens, and CP2 specimens increased in average final RD_{APA}. All CPs utilizing moisture and/or FT conditioning only (i.e. CP3-CP6) caused an increase in final rut depth. CP7, which consisted of a combination of oxidation, moisture, and FT conditioning, had the lowest average final RD_{APA}. When considering the different mix types, M17 (HMA) and M20 typically had the lowest rut depths, and M19 had the highest rut depth after all CPs except CP2, in which case M18 had the highest.

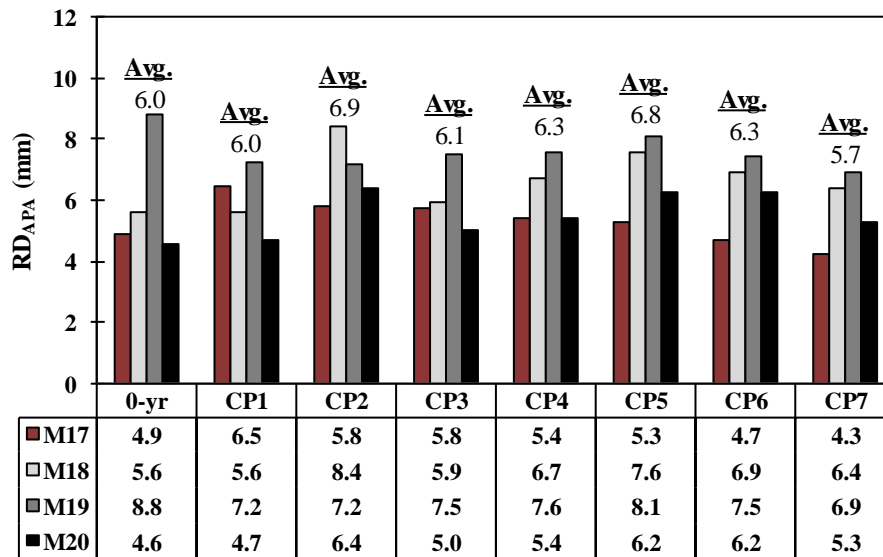


Figure 4.12. APA Laboratory Conditioned Results

4.4 Binder Properties

Tables 4.6 and 4.7 display results from testing of binder samples extracted and recovered from field aged and laboratory conditioned specimens, respectively. As described in Section 3.2, 0-yr binder samples were recovered from loose mix (LM) that was sampled at the time of paving the test section, 4% V_a binder samples were recovered only from the top (T) 12.5 mm of mixture specimens, and 7% V_a binder samples were recovered from 12.5 mm thick slices from both the top (T) and bottom (B) of specimens. Top and bottom slices of field aged specimens were kept separate from each other, while top and bottom slices of laboratory conditioned specimens were combined prior to the extraction and recovery process. The slicing procedure and binder extraction and recovery process are described in Sections 3.4.4 and 3.6.1, respectively. Binder tests were conducted at low temperature (BBR test), intermediate temperature (*Pen.*, and DSR_{8mm} tests), and high temperature (DSR_{25mm} test). Critical Temperature (T_c) was determined for DSR_{8mm}, DSR_{25mm}, and BBR (T_c was calculated based on stiffness and m-value for BBR testing) using Equation 3.5 defined in Section 3.6.2. In addition, carbonyl and sulfoxide indices were calculated using FTIR results as described in Section 3.6.5 and were reported in Tables 4.6 and 4.7.

Table 4.6. Binder Results for 0-yr and Field Aged Specimens

Specimen Type	Mix ID	Loc.	V _a (%)	Pen. (dmm)	Int. Temp. DSR (8mm)			High Temp DSR (25mm)			BBR Testing					FTIR		CI + SI	
					Passing	Failing	T _c (°C)	Passing	Failing	T _c (°C)	Passing		Failing		T _{c-s*} (°C)	T _{c-m**} (°C)	CI		SI
					G* <i>sin</i> δ (kPa)(°C)	G* <i>sin</i> δ (kPa)(°C)		G* <i>sin</i> δ (kPa)(°C)	G* <i>sin</i> δ (kPa)(°C)		Stiffness (MPa)(°C)	m-value	Stiffness (MPa)(°C)	m-value					
0-yr	M17	LM	-	28.3	3930 (22)	5670 (19)	20.0	4.73 (64)	2.12 (70)	69.8	203.5 (-18)	0.320	449.0 (-24)	0.257	-20.9	-19.9	0.12	0.37	0.49
	M18	LM	-	31.3	4650 (19)	6860 (16)	18.4	2.45 (70)	1.17 (76)	70.9	175.5 (-18)	0.329	421.0 (-24)	0.262	-21.7	-20.6	0.09	0.47	0.56
	M19	LM	-	34.7	3420 (22)	5040 (19)	19.1	4.59 (64)	2.06 (70)	69.5	181.0 (-18)	0.334	477.5 (-24)	0.257	-21.1	-20.6	0.12	0.40	0.52
	M20	LM	-	37.0	4490 (19)	6720 (16)	18.2	4.42 (64)	2.03 (70)	69.4	188.0 (-18)	0.333	384.0 (-24)	0.275	-21.9	-21.4	0.08	0.37	0.45
2-yr	M17	T	4	20.7	4810 (22)	6670 (19)	21.6	2.79 (76)	1.34 (82)	77.9	118.0 (-12)	0.334	210.5 (-18)	0.295	-21.7	-17.2	0.10	0.44	0.54
		T	7	26.0	3850 (25)	5430 (22)	22.7	2.99 (76)	1.43 (82)	78.5	107.0 (-12)	0.352	232.5 (-18)	0.295	-20.0	-17.4	0.13	0.38	0.51
		B	7	25.7	4940 (22)	7120 (19)	21.9	2.26 (76)	1.10 (82)	76.2	208.5 (-18)	0.312	395.5 (-24)	0.266	-21.4	-19.5	0.11	0.41	0.52
	M18	T	4	24.5	3680 (25)	5210 (22)	22.4	2.41 (76)	1.12 (82)	76.7	218.0 (-18)	0.309	423.0 (-24)	0.259	-20.9	-19.0	0.13	0.39	0.52
		T	7	27.0	4410 (22)	6450 (19)	21.0	4.51 (70)	2.05 (76)	75.5	196.5 (-18)	0.308	375.0 (-24)	0.270	-21.9	-19.2	0.13	0.43	0.56
		B	7	29.0	3960 (22)	5850 (19)	20.2	3.37 (70)	1.54 (76)	73.3	194.5 (-18)	0.312	381.5 (-24)	0.276	-21.9	-20.0	0.12	0.51	0.63
	M19	T	4	28.3	4040 (22)	5980 (19)	20.4	3.76 (70)	1.72 (76)	74.1	191.5 (-18)	0.330	392.0 (-24)	0.274	-21.8	-21.2	0.11	0.39	0.50
		T	7	26.7	4310 (22)	6350 (19)	20.8	4.04 (70)	1.84 (76)	74.6	212.5 (-18)	0.312	386.5 (-24)	0.272	-21.5	-19.8	0.11	0.44	0.55
		B	7	26.7	4910 (22)	7290 (19)	21.9	3.53 (70)	1.63 (76)	73.7	232.5 (-18)	0.326	419.0 (-24)	0.247	-20.6	-19.9	0.13	0.44	0.57
	M20	T	4	20.3	4090 (25)	5730 (22)	23.2	2.78 (76)	1.31 (82)	77.9	120.5 (-12)	0.338	252.0 (-18)	0.277	-19.4	-15.7	0.09	0.40	0.49
		T	7	22.3	3710 (25)	5230 (22)	22.4	2.57 (76)	1.22 (82)	77.2	107.0 (-12)	0.342	244.0 (-18)	0.279	-19.5	-16.0	0.13	0.42	0.55
		B	7	25.7	4310 (22)	6270 (19)	20.8	4.05 (70)	1.88 (76)	74.8	106.0 (-12)	0.358	221.5 (-18)	0.297	-20.5	-17.7	0.14	0.44	0.58
4-yr	M17	T	4	21.7	3710 (25)	5280 (22)	22.5	3.46 (73)	1.68 (82)	79.8	115.0 (-12)	0.332	223.0 (-18)	0.278	-20.7	-15.6	0.10	0.40	0.50
		T	7	19.3	4300 (25)	6070 (22)	23.7	4.14 (76)	1.97 (82)	81.1	131.0 (-12)	0.321	254.0 (-18)	0.271	-19.5	-14.5	0.15	0.45	0.60
		B	7	20.7	3940 (25)	5670 (23)	23.0	3.22 (76)	1.56 (82)	79.2	141.0 (-12)	0.333	281.0 (-18)	0.283	-18.6	-16.0	0.14	0.43	0.57
	M18	T	4	20.7	3980 (25)	5680 (22)	23.1	3.35 (76)	1.62 (82)	79.5	129.0 (-12)	0.323	247.0 (-18)	0.291	-19.8	-16.3	0.16	0.52	0.68
		T	7	21.3	3800 (25)	5450 (22)	22.7	3.24 (76)	1.55 (82)	79.1	126.0 (-12)	0.326	238.0 (-18)	0.294	-20.2	-16.9	0.15	0.49	0.64
		B	7	21.3	4210 (25)	6080 (22)	23.6	2.91 (76)	1.38 (82)	78.2	146.0 (-12)	0.322	258.0 (-18)	0.290	-18.5	-16.1	0.16	0.47	0.63
	M19	T	4	23.0	3610 (25)	5280 (22)	22.4	2.79 (76)	1.35 (82)	78.0	130.0 (-12)	0.333	250.0 (-18)	0.294	-19.7	-17.1	0.18	0.48	0.66
		T	7	22.3	4220 (25)	6070 (22)	23.6	3.28 (76)	1.58 (82)	79.3	142.0 (-12)	0.324	271.0 (-18)	0.291	-18.9	-16.4	0.15	0.46	0.61
		B	7	22.8	4040 (25)	5930 (22)	23.3	2.57 (76)	1.23 (82)	77.3	146.0 (-12)	0.334	279.0 (-18)	0.295	-18.7	-17.2	0.16	0.53	0.69
	M20	T	4	20.0	4230 (25)	5990 (22)	23.6	3.62 (76)	1.72 (82)	80.0	139.0 (-12)	0.312	253.0 (-18)	0.283	-19.7	-14.5	0.14	0.43	0.57
		T	7	19.3	4500 (25)	6390 (22)	24.1	4.03 (76)	1.89 (82)	80.8	144.0 (-12)	0.321	280.0 (-18)	0.269	-18.6	-14.4	0.18	0.38	0.56
		B	7	20.7	4560 (25)	6510 (22)	24.2	3.06 (76)	1.44 (82)	78.6	158.0 (-12)	0.307	289.0 (-18)	0.277	-18.4	-13.4	0.15	0.45	0.60

*T_{c-s} refers to the critical temperature (°C) for the stiffness criteria as determined in the BBR test.

**T_{c-m} refers to the critical temperature (°C) for the m-value criteria as determined in the BBR test.

Table 4.7. Binder Results for Laboratory Conditioned Specimens

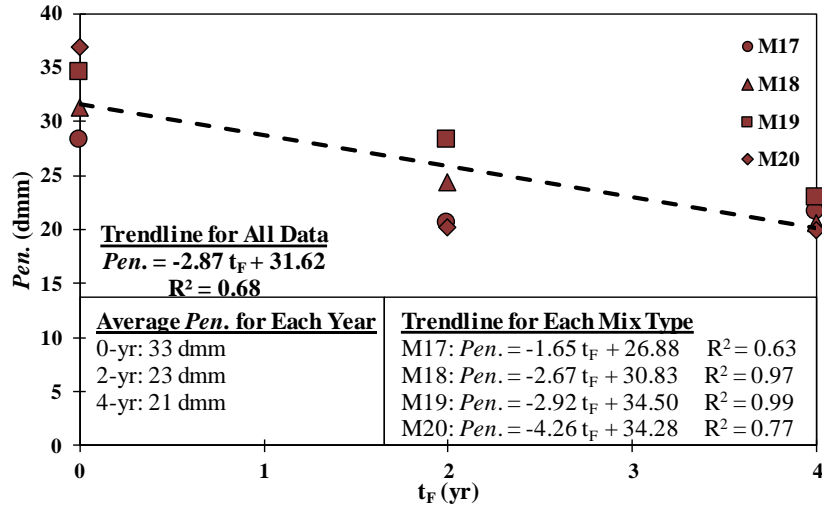
Specimen Type	Mix ID	V _a (%)	Pen. (dmm)	Int. Temp. DSR (8mm)			High Temp DSR (25mm)			BBR Testing				FTIR					
				Passing		Failing	T _c (°C)	Passing		Failing	Passing		Failing		T _{c-s} (°C)	T _{c-m} (°C)	CI	SI	CI + SI
				G* $\sin\delta$ (kPa)(°C)	G* $\sin\delta$ (kPa)(°C)	G* $\sin\delta$ (kPa)(°C)		G* $\sin\delta$ (kPa)(°C)	T _c (°C)	Stiffness (MPa)(°C)	m-value	Stiffness (MPa)(°C)	m-value						
CP1	M17	7	28.0	4750 (19)	6680 (16)	18.5	2.62 (76)	1.26 (82)	77.4	185.0 (-18)	0.305	358.5 (-24)	0.275	-22.4	-18.9	0.12	0.47	0.59	
	M18	7	33.0	4960 (19)	6710 (16)	18.4	3.70 (70)	1.69 (76)	74.0	183.5 (-18)	0.315	343.5 (-24)	0.277	-22.7	-20.4	0.13	0.43	0.56	
	M19	7	34.0	4960 (19)	7260 (16)	18.9	3.10 (70)	1.46 (76)	72.7	184.5 (-18)	0.318	349.5 (-24)	0.282	-22.6	-20.9	0.14	0.47	0.61	
	M20	7	27.0	3780 (22)	5410 (19)	19.7	4.38 (70)	2.08 (76)	75.5	91.1 (-12)	0.357	194.0 (-18)	0.297	-21.5	-17.7	0.15	0.43	0.58	
CP2	M17	7	25.7	3770 (22)	5420 (19)	19.7	2.44 (76)	1.18 (82)	76.9	201.0 (-18)	0.312	416.0 (-24)	0.249	-21.3	-19.1	0.14	0.45	0.59	
	M18	7	32.0	4450 (19)	6450 (16)	18.1	2.78 (70)	1.30 (76)	71.8	181.0 (-18)	0.328	342.0 (-24)	0.271	-22.8	-20.9	0.11	0.42	0.53	
	M19	7	31.3	4810 (19)	7030 (16)	18.7	2.75 (70)	1.34 (76)	71.9	193.0 (-18)	0.332	387.0 (-24)	0.274	-21.8	-21.3	0.11	0.46	0.57	
	M20	7	29.7	4600 (19)	6650 (16)	18.3	3.11 (70)	1.44 (76)	72.7	180.0 (-18)	0.320	375.0 (-24)	0.265	-22.2	-20.1	0.13	0.41	0.54	
CP3	M17	7	25.3	4820 (19)	6890 (16)	18.7	4.53 (70)	2.08 (76)	75.6	180.7 (-18)	0.322	358.5 (-24)	0.273	-22.4	-20.7	0.14	0.41	0.55	
	M18	7	31.3	4430 (19)	6440 (16)	18.0	2.95 (70)	1.39 (76)	72.3	177.0 (-18)	0.328	370.0 (-24)	0.280	-22.3	-21.5	0.15	0.43	0.58	
	M19	7	37.0	4210 (19)	6220 (16)	17.7	4.91 (64)	2.19 (70)	70.0	168.0 (-18)	0.342	329.5 (-24)	0.281	-23.2	-22.1	0.11	0.39	0.50	
	M20	7	27.7	3570 (22)	5060 (19)	19.1	3.18 (70)	1.50 (76)	72.9	200.3 (-18)	0.310	403.7 (-24)	0.269	-21.5	-19.5	0.13	0.40	0.53	
CP4	M17	7	33.0	3780 (19)	5500 (16)	16.8	2.79 (76)	0.69 (82)	70.0	145.5 (-18)	0.341	305.0 (-24)	0.290	-23.9	-22.8	0.13	0.41	0.54	
	M18	7	34.3	3860 (19)	5400 (16)	16.7	2.86 (70)	1.37 (76)	72.1	145.0 (-18)	0.341	302.0 (-24)	0.287	-23.9	-22.5	0.10	0.43	0.53	
	M19	7	40.3	4730 (16)	6880 (13)	15.6	4.70 (64)	2.09 (70)	69.6	122.5 (-18)	0.354	249.5 (-24)	0.288	-25.6	-22.9	0.10	0.43	0.53	
	M20	7	49.7	4420 (13)	6280 (10)	11.9	3.52 (64)	1.61 (70)	67.2	151.0 (-24)	0.318	358.5 (-30)	0.274	-28.8	-26.5	0.09	0.42	0.51	
CP5	M17	7	29.7	4600 (19)	6650 (16)	18.3	3.11 (70)	1.44 (76)	72.7	180.0 (-18)	0.320	375.0 (-24)	0.265	-22.2	-20.1	0.16	0.43	0.59	
	M18	7	38.0	3410 (19)	5080 (16)	16.1	4.59 (64)	2.05 (70)	69.5	143.5 (-18)	0.347	293.0 (-24)	0.291	-24.2	-23.0	0.12	0.37	0.49	
	M19	7	30.3	3530 (22)	5120 (19)	19.2	2.56 (76)	1.27 (82)	77.3	210.5 (-18)	0.322	434.0 (-24)	0.264	-20.9	-20.3	0.11	0.42	0.53	
	M20	7	28.7	4530 (19)	6560 (16)	18.2	2.83 (70)	1.33 (76)	72.0	174.5 (-18)	0.318	365.5 (-24)	0.272	-22.4	-20.3	0.14	0.37	0.51	
CP6	M17	7	19.0	4600 (22)	6370 (19)	21.2	2.72 (82)	1.37 (88)	83.8	106.5 (-12)	0.340	210.0 (-18)	0.287	-21.2	-16.5	0.15	0.40	0.55	
	M18	7	28.0	4690 (19)	6830 (16)	18.5	2.97 (70)	1.37 (76)	72.3	195.5 (-18)	0.331	370.5 (-24)	0.273	-22.0	-21.2	0.12	0.40	0.52	
	M19	7	37.0	4030 (19)	6010 (16)	17.4	2.24 (70)	1.09 (76)	70.2	164.0 (-18)	0.345	337.0 (-24)	0.285	-23.0	-22.5	0.09	0.43	0.52	
	M20	7	28.7	4790 (19)	6870 (16)	18.6	3.49 (70)	1.61 (76)	73.6	194.5 (-18)	0.320	387.0 (-24)	0.268	-21.8	-20.3	0.12	0.39	0.51	
CP7	M17	7	18.3	4920 (22)	6580 (19)	21.8	2.81 (82)	1.39 (88)	84.1	110.5 (-12)	0.331	211.0 (-18)	0.289	-21.3	-16.4	0.19	0.42	0.61	
	M18	7	22.0	3650 (22)	5260 (19)	19.4	2.49 (76)	1.21 (82)	19.4	194.5 (-18)	0.308	374.0 (-24)	0.264	-22.0	-19.1	0.16	0.46	0.62	
	M19	7	23.7	4350 (22)	6310 (19)	20.9	2.33 (76)	1.11 (82)	76.5	223.5 (-18)	0.307	435.0 (-24)	0.257	-20.7	-18.8	0.10	0.47	0.57	
	M20	7	21.7	3900 (22)	5420 (19)	19.7	2.65 (76)	1.26 (82)	77.5	99.9 (-12)	0.345	197.0 (-18)	0.299	-21.7	-17.8	0.12	0.43	0.55	

*T_{c-s} refers to the critical temperature (°C) for the stiffness criteria as determined in the BBR test.

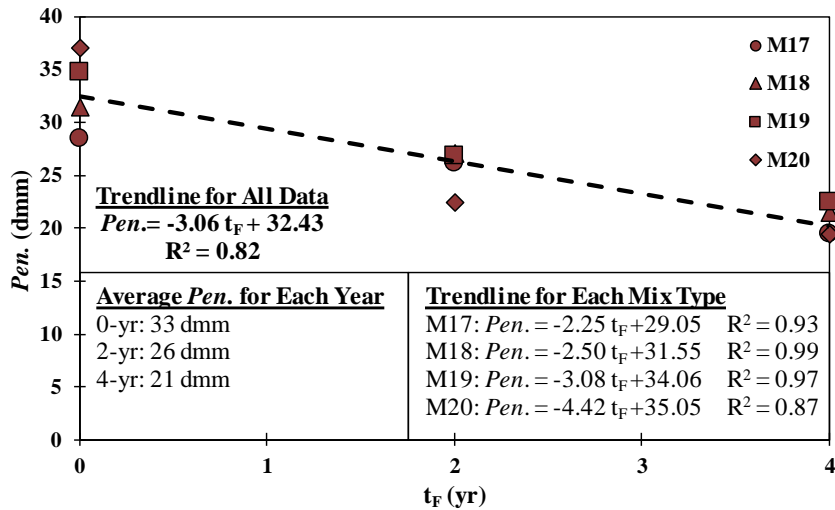
**T_{c-m} refers to the critical temperature (°C) for the m-value criteria as determined in the BBR test.

4.4.1 Penetration (*Pen.*) Results

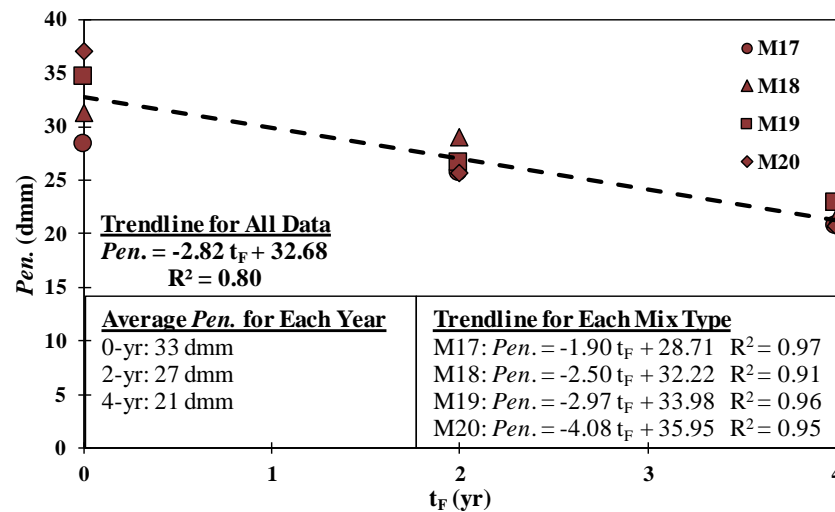
Figures 4.13a, 4.13b, and 4.13c display field aged *Pen.* results from 4% V_a specimen tops, 7% V_a specimen tops, and 7% V_a specimen bottoms, respectively. The trendline displayed in each figure is based on all *Pen.* data for each year. Average *Pen.* for each year is also displayed. Trendline slopes show that *Pen.* of 4% V_a tops, 7% V_a tops and 7% V_a bottoms specimens decreased at approximately equivalent rates, indicating little difference in the level of change based on the location of the binder sample. For all three cases (i.e. 4% V_a tops, 7% V_a tops, and 7% V_a bottoms), 2-yr *Pen.* was no more than 10dmm different than 0-yr, which is within the d2s limit defined in ASTM D5. 4-yr *Pen.* was also within the ds2 limit of 2-yr specimens; however, the 4-yr values are meaningfully different than 0-yr values. Trendline equations for each mix type, which are also displayed in Figures 4.13a, 4.13b, and 4.13c, indicate that at both target V_a levels and locations, binder samples from all WMA specimens (M18-M20) decreased in *Pen.* at a faster rate than the HMA (M17).



a) 4% Target V_a Specimens Top



b) 7% Target V_a Specimens Top



c) 7% Target V_a Specimens Bottoms

Figure 4.13. Pen. Field Aged Results

Figure 4.14 summarizes *Pen.* results from binder samples extracted and recovered from laboratory conditioned specimens compacted to a target V_a level of 7% (no *Pen.* testing was performed on lab conditioned 4% target V_a specimens). Also displayed in Figure 4.14 are the results of 0-yr specimens for comparison. According to the ds_2 limit of 10dmm defined in ASTM D5, CP7 was the only protocol that meaningfully changed *Pen.* values relative to 0-yr samples. CP1-CP6 all slightly decreased *Pen.*, except CP4 where average *Pen.* increased. M17 (HMA) had the lowest *Pen.* before conditioning, and after every CP, except for CP1 and CP5 where M20 was slightly lower.

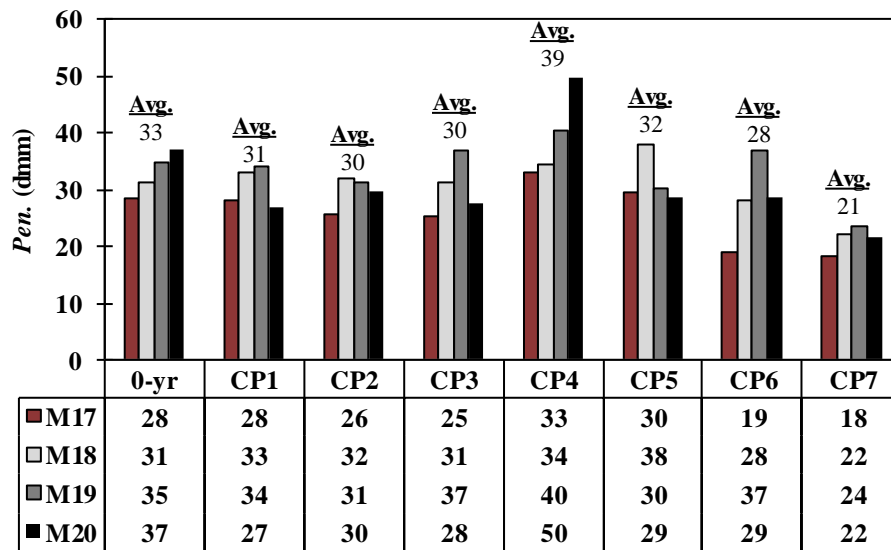
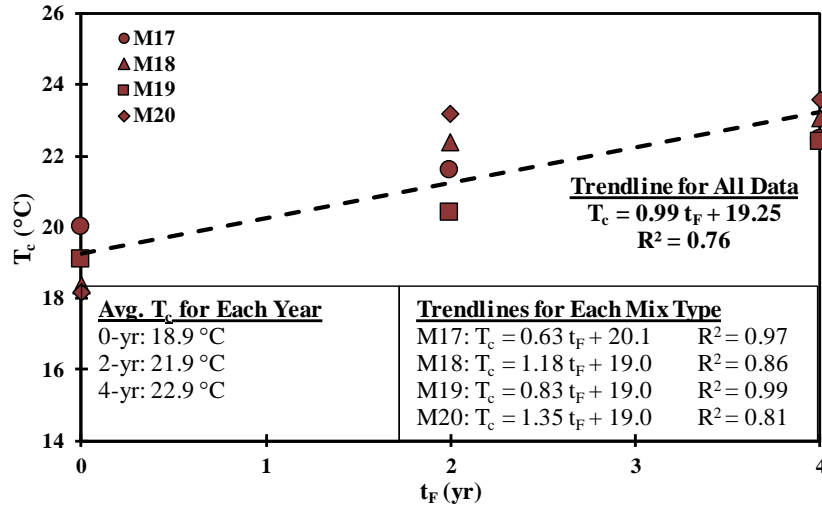


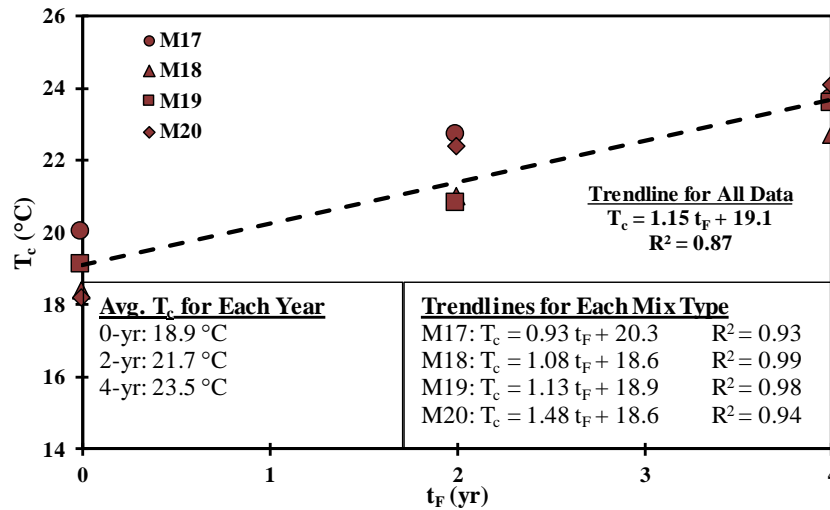
Figure 4.14. *Pen.* Laboratory Conditioned Results

4.4.2 Intermediate Temperature Dynamic Shear Rheometer (DSR_{8mm}) Results

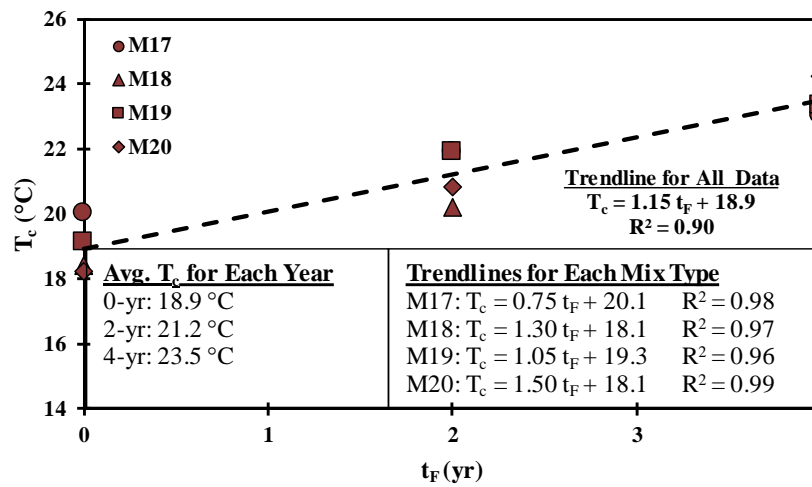
Figures 4.15a, 4.15b, and 4.15c display field aged T_c results obtained from DSR_{8mm} testing of 4% V_a specimen tops, 7% V_a specimen tops, and 4% V_a specimen bottoms, respectively. The trendline displayed in each figure is based on all T_c results for each year. Average T_c for each year was also displayed. Trendline slopes in Figure 4.15a and 4.15b indicate that the increase in air voids from 4% to 7% accelerated binder property changes in the top slice of the specimens. Additionally, trendlines for the top and bottom slices of 7% target V_a specimens (Figures 4.15b and 4.15c, respectively) are very similar, indicating minimal difference in binder properties of the top and bottom slices. The similarities between the two locations were also observed from average T_c values for each year. Although 2-yr averages differed slightly (21.7°C for top slices and 21.2°C for bottom slices), 4-yr averages for the tops and bottoms were equivalent at 23.5°C . At both target V_a levels and sample locations, the trendline equations for each mix type, which are also displayed in Figures 4.15a, 4.15b, and 4.15c, indicate that all three of the WMA mix types (i.e. M18, M19, and M20) increased in T_c at an accelerated rate compared to the HMA. Furthermore, the trendline for M20 consistently had the steepest slope, indicating an increased susceptibility to stiffening as function of t_F .



a) 4% Target V_a Specimens Top



b) 7% Target V_a Specimens Top



c) 7% Target V_a Specimens Bottoms

Figure 4.15. DSR_{8mm} Field Aged Results

Figure 4.16 summarizes T_c results obtained from DSR_{8mm} testing of binder samples extracted and recovered from laboratory conditioned specimens compacted to a target V_a level of 7% (no DSR_{8mm} testing was performed on laboratory conditioned 4% target V_a specimens). Also displayed in Figure 4.16 are the results of 0-yr specimens for comparison. Figure 4.16, shows average T_c was affected very little by conditioning, except in the case of CP4 where T_c was decreased considerably. However, effects on individual mix types varied. T_c for M17 increased after CP6 and CP7, but decreased as a result of CP1-CP5. Considering M18, T_c significantly decreases after CP4 and CP5, increased for CP7, and changed very little due to the remaining CPs. T_c for M19 increased after CP5 and CP7, while decreasing from all other CPs. M20 stayed the same or increased as a result of all CPs except for CP4. Overall, the consistent increase in T_c for every mix type that was observed after field aging, was only replicated with CP7.

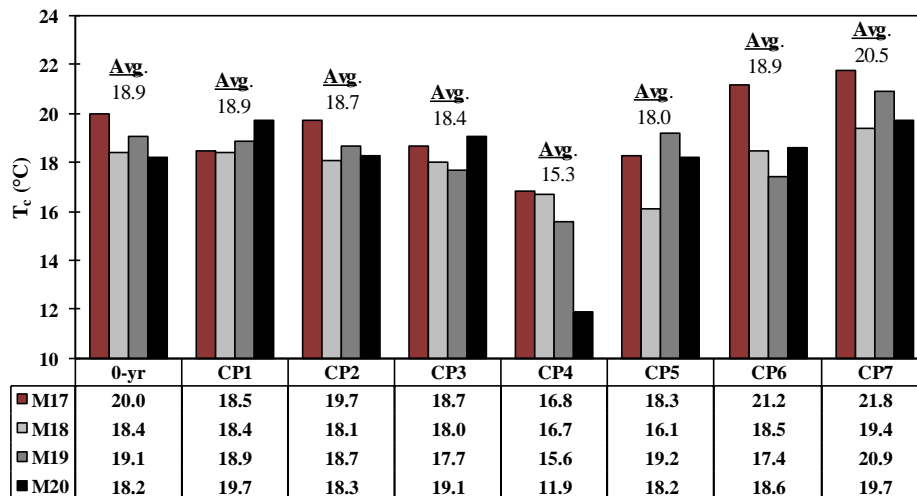
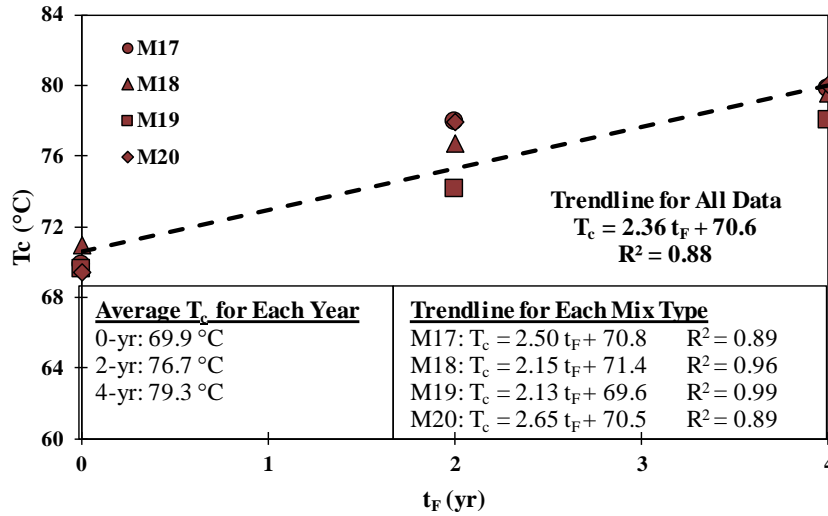


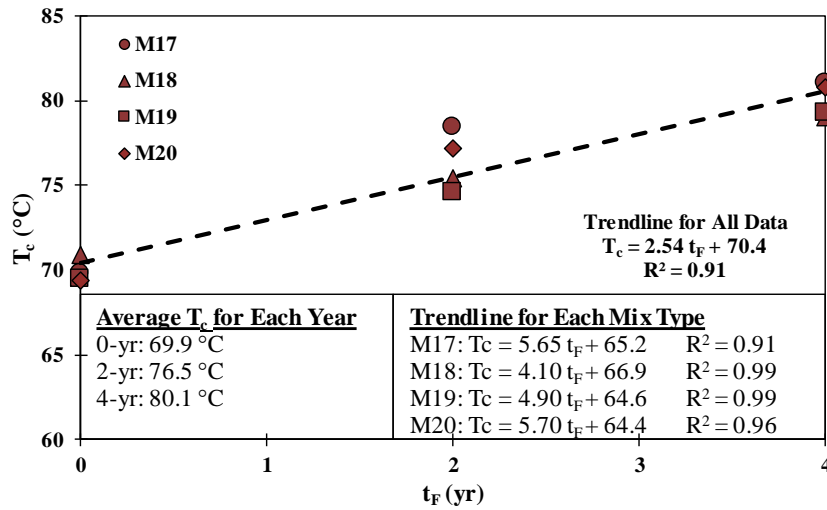
Figure 4.16. DSR_{8mm} Laboratory Conditioned Results

4.4.3 High Temperature Dynamic Shear Rheometer (DSR_{25mm}) Results

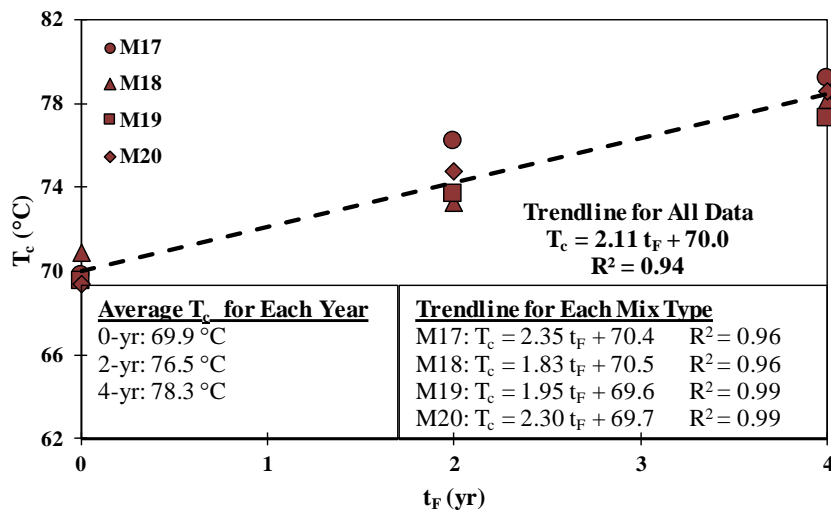
Figures 4.17a, 4.17b, and 4.17c display field aged T_c results obtained from DSR_{25mm} testing of 4% V_a specimen tops, 7% V_a specimen tops, and 4% V_a specimen bottoms, respectively. The trendline displayed in each figure is based on all T_c results for each year. Average T_c for each year is also displayed. There was minimal difference in average T_c for each year between top slices of 4% and 7% V_a specimens; however, T_c for 7% V_a specimen tops at a slightly faster rate than 4% V_a specimens. Also, there were slight differences between top and bottom slices of 7% V_a specimens, but T_c of bottom slices did increase at a slightly slower rate than specimen tops. Trendline equations for each mix type, which are also displayed in Figures 4.17a, 4.17b, and 4.17c, show this behavior in all cases, T_c for two of the WMA binders (i.e. M18 and M19) increased at a slower rate than M17 (HMA), while the third WMA binder (M20) increased at a similar or higher rate relative to M17.



a) 4% Target V_a Specimens Top



b) 7% Target V_a Specimens Top



c) 7% Target V_a Specimens Bottoms

Figure 4.17. DSR_{25mm} Field Aged Results

Figure 4.18 summarizes T_c results obtained from DSR_{25mm} testing of binder samples extracted and recovered from laboratory conditioned specimens compacted to a target V_a level of 7% (no DSR_{25mm} testing was performed on laboratory conditioned 4% target V_a specimens). Also displayed in Figure 4.18 are the results of 0-yr specimens for comparison. Average T_c shown in Figure 4.18 indicates that CPs which used oxidative conditioning only (i.e. CP1 and CP2) increased average T_c relative to 0-yr specimens, while moisture conditioning protocols (i.e. CP3, CP4, CP5, and CP6) had no effect or increased T_c . CP7, which included oxidation, moisture, and FT conditioning, resulted in the highest average T_c . M17 had the highest T_c after conditioning except in the cases of CP4 and CP5. T_c of WMA binders (i.e. M18, M19, and M20) were typically similar to one another.

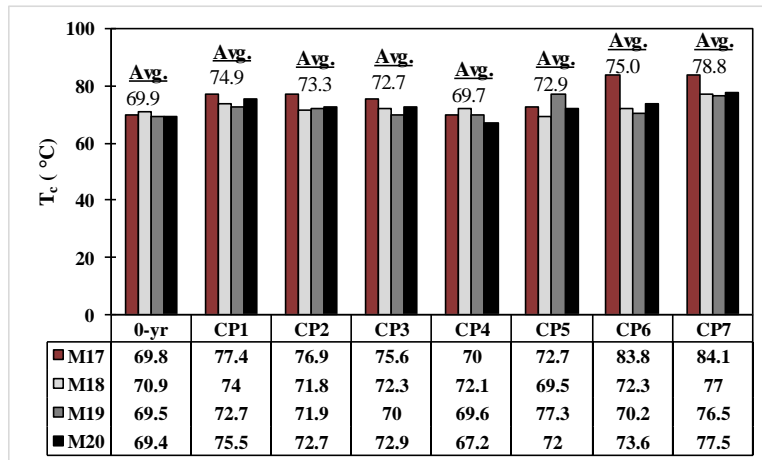
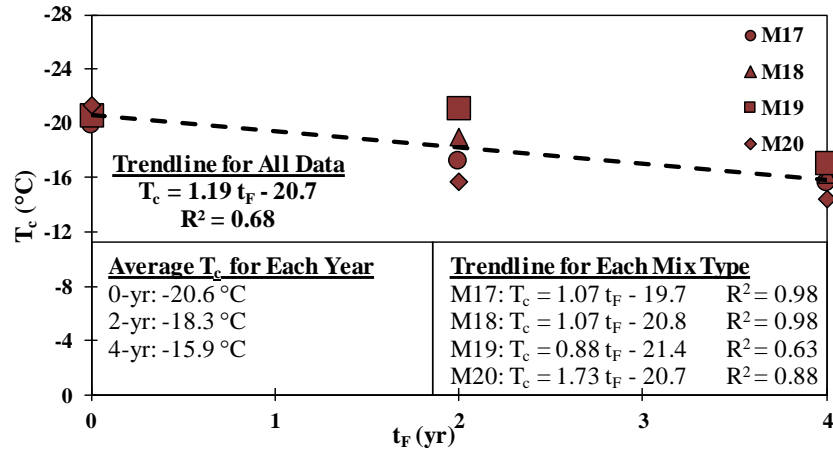


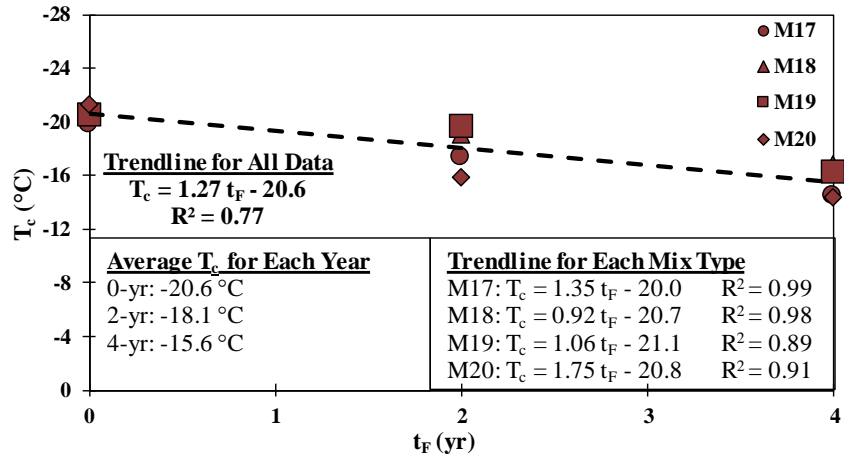
Figure 4.18. DSR_{25mm} Laboratory Conditioned Results

4.4.4 Bending Beam Rheometer (BBR) Results

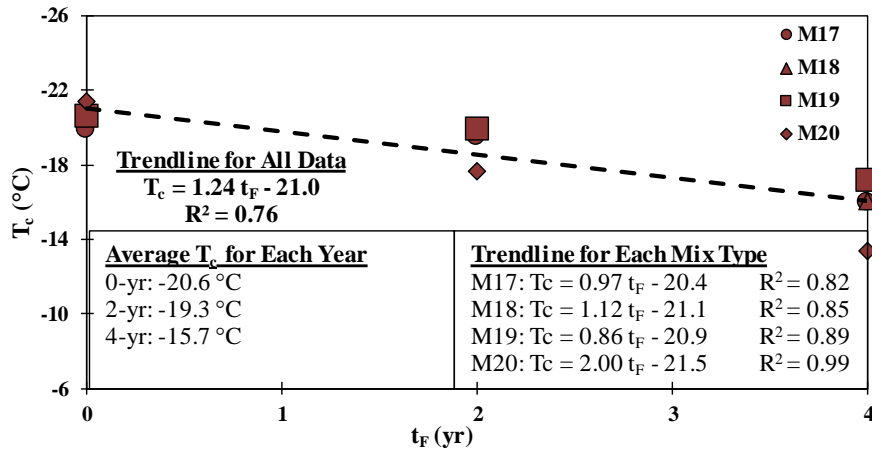
Figures 4.19a, 4.19b, and 4.19c display field aged T_{c-m} results obtained from BBR testing of 4% V_a specimen tops, 7% V_a specimen tops, and 7% V_a specimen bottoms, respectively. The trendline displayed in each figure is based on all T_{c-m} results for each year. Average T_{c-m} for each year is also displayed. Trendline slopes indicate that there was no major difference in the rate of increase of T_{c-m} among the 4% and 7% target V_a level tops and bottoms. Also, average T_{c-m} for each year shows there was minimal difference in 4-yr results among different V_a levels and binder sample locations. Trendline equations for each mix type, which are also displayed in each figure, show that in each case T_{c-m} of M19 increased at a slower rate than M17 (HMA), while the rate of increase for M20 was consistently higher than M17. M18 did not show consistent behavior in this regard.



a) 4% Target V_a Specimens Top



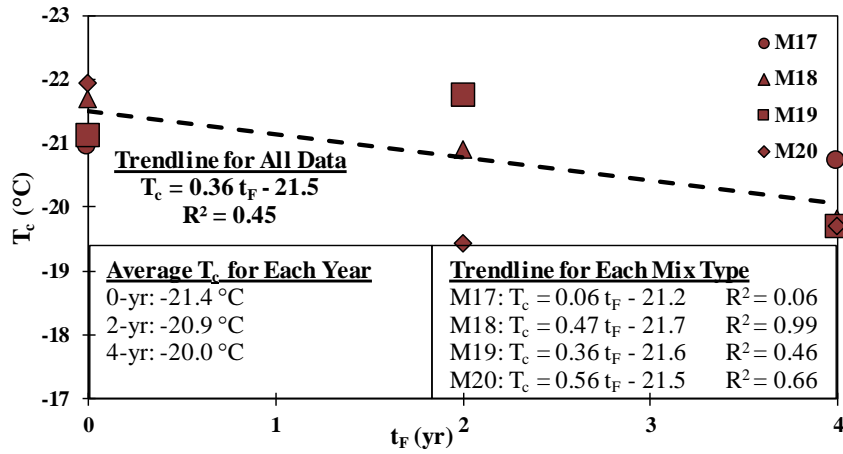
b) 7% Target V_a Specimens Top



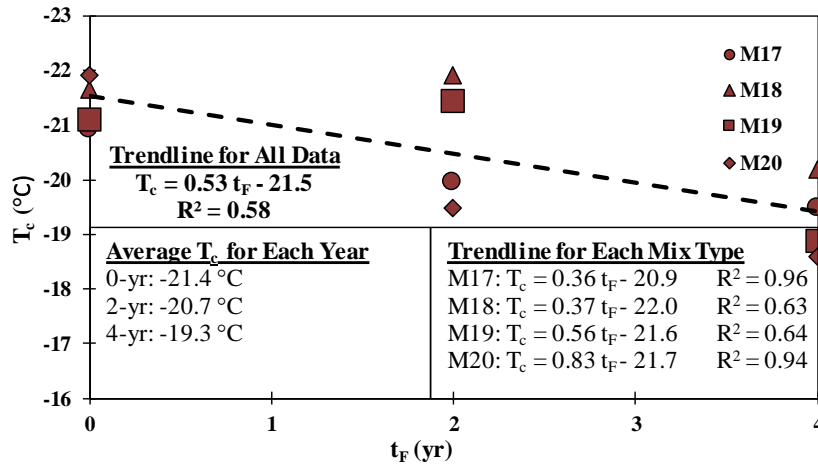
c) 7% Target V_a Specimens Bottoms

Figure 4.19. BBR m-value Field Aged Results

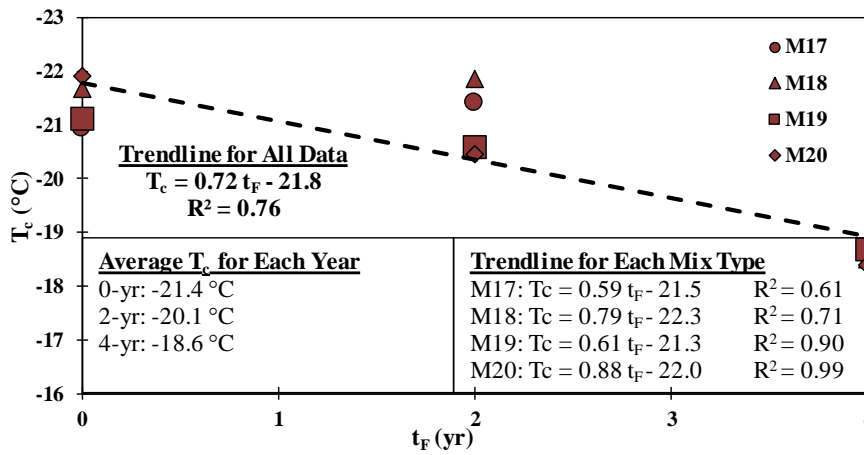
Figures 4.20a, 4.20b, and 4.20c display field aged T_{c-s} results obtained from BBR testing of 4% V_a specimen tops, 7% V_a specimen tops, and 4% V_a specimen bottoms, respectively. The trendline displayed in each figure is based on all T_{c-s} results for each year. Average T_{c-s} for each year are also displayed. Trendline slopes for all data indicate that 7% V_a specimen tops increased in T_{c-s} at a faster rate than 4% V_a specimen tops. Additionally, trendline slopes for all data in Figures 4.20b and 4.20c show that T_{c-s} increased at a faster rate for bottom slices of 7% V_a specimens, relative to top slices. Trendline equations for each mix type, which are also displayed in Figures 4.20a, 4.20b, and 4.20c, indicate that all WMA binders (i.e. M18, M19, and M20) increased in T_{c-s} faster than M17.



a) 4% Target V_a Specimens Top



b) 7% Target V_a Specimens Top



c) 7% Target V_a Specimens Bottoms

Figure 4.20. BBR Stiffness Field Aged Results

Figure 4.21 summarizes T_{c-m} results obtained from BBR testing of binder samples extracted and recovered from laboratory conditioned specimens compacted to a target V_a level of 7% (no BBR testing was performed on laboratory conditioned 4% target V_a specimens). Also displayed in Figure 4.21 are the results of 0-yr specimens for comparison. Average T_{c-m} provided in Figure 4.21 shows there was little difference in the effects of oxidative only CPs (i.e. CP1 and CP2) compared to the moisture only conditioning methods (i.e. CP3, CP4, CP5, and CP6). With the exception of CP4 and CP7, conditioning had little effect on T_{c-m} . CP7 was the only CP to cause a considerable increase in T_{c-m} , and CP4 caused a considerable decrease in average T_{c-m} . In most cases, WMA binders (i.e. M18, M19, and M20) had lower T_{c-m} than HMA binder (M17).

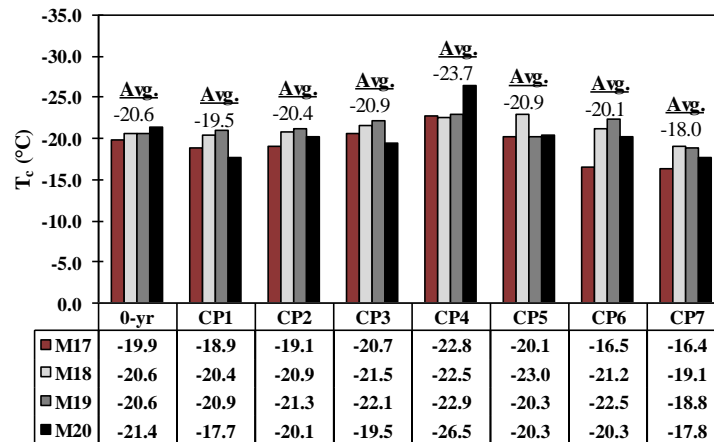


Figure 4.21. BBR m-value Laboratory Conditioned Results

Figure 4.22 summarizes T_{c-s} results obtained from BBR testing of binder samples extracted and recovered from laboratory conditioned specimens compacted to a target V_a level of 7% (no BBR testing was performed on laboratory conditioned 4% target V_a specimens). Also displayed in Figure 4.22 are the results of 0-yr specimens for comparison. On average, none of the CPs had a considerable effect on T_{c-s} , except CP4 which decreased T_{c-s} more any other CP. There was no noticeable difference in the effects of oxidative conditioning methods compared to moisture conditioning methods; however, it was observed that CP7 was the only CP that did not result in a decrease or increase in T_{c-s} . WMA binders typically had similar or lower T_{c-s} values relative to HMA (M17). These observations are mostly consistent with those made considering T_{c-m} .

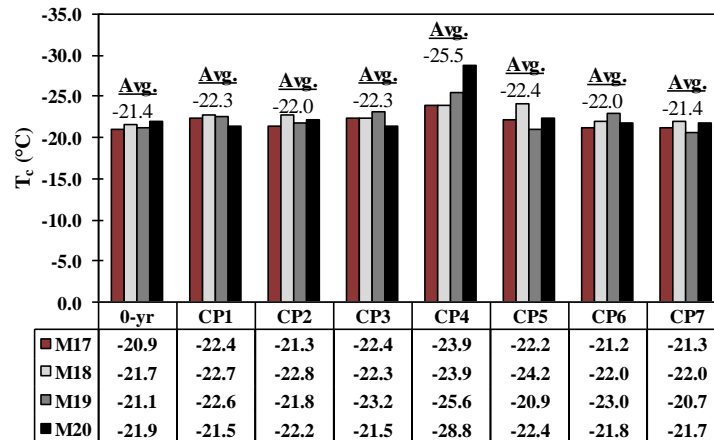
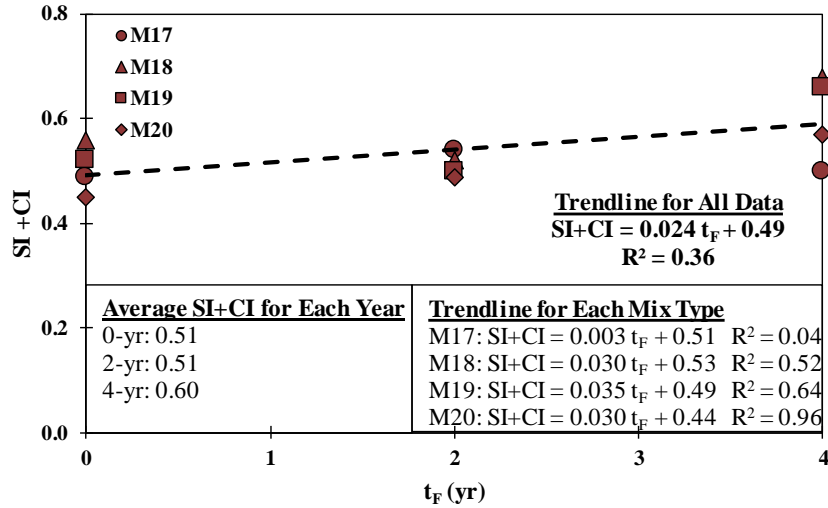


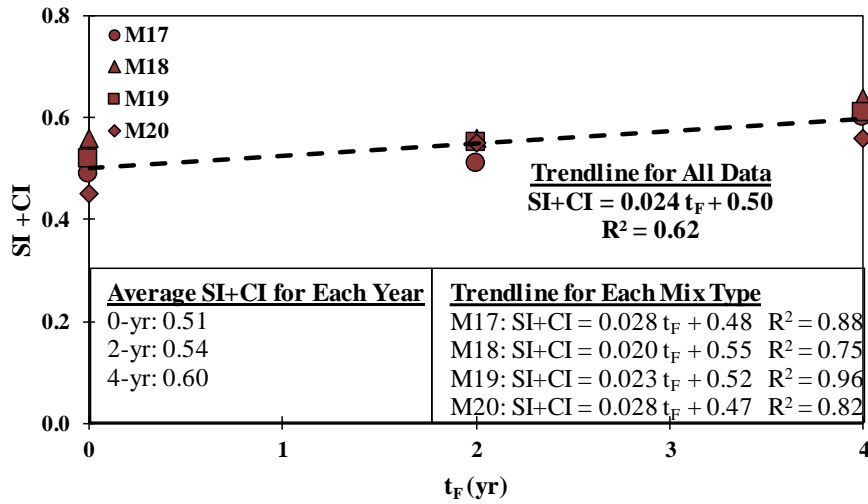
Figure 4.22. BBR Stiffness Laboratory Conditioned Results

4.4.5 Fourier Transform Infrared Spectroscopy (FTIR) Results

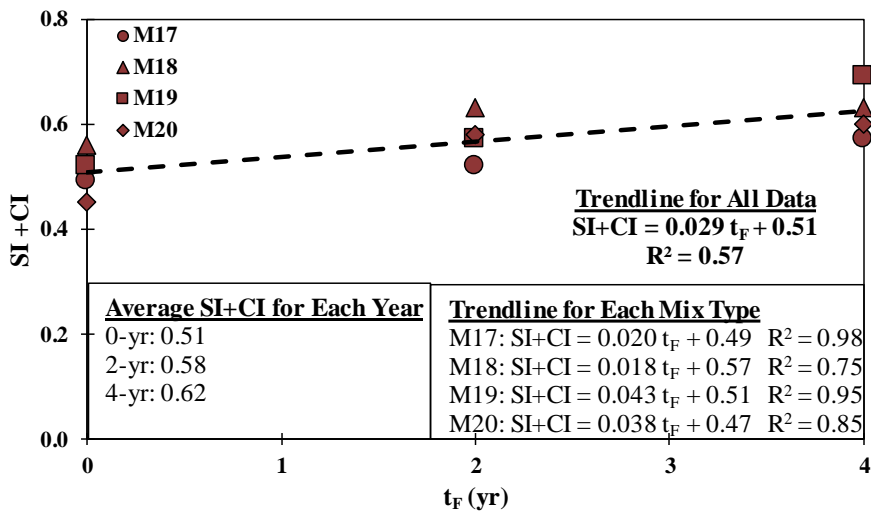
Figures 4.23a, 4.23b, and 4.23c display field aged SI+CI results obtained from FTIR testing of 4% V_a specimen tops, 7% V_a specimen tops, and 4% V_a specimen bottoms, respectively. The trendline displayed in each figure is based on all SI+CI results for each year. Average SI+CI for each year is also displayed. Trendline slopes for all data indicate that 4% and 7% V_a specimen tops increased in SI+CI at a similar rate, while 7% V_a specimen bottoms increased in slower rate compared to two levels V_a specimens top. Trendline equations for each mix type, which are also displayed in Figures 4.23a, 4.23b, and 4.23c, indicate that at 7% V_a , SI+CI of M18 increased at a slower rate than any other mix type, while at 4% M17 had the slowest rate of increase.



a) 4% Target V_a Specimens Top



b) 7% Target V_a Specimens Top



c) 7% Target V_a Specimens Bottoms

Figure 4.23. FTIR Field Aged Results

Figure 4.24 summarizes SI+CI results obtained from BBR testing of binder samples extracted and recovered from laboratory conditioned specimens compacted to a target V_a level of 7% (no BBR testing was performed on laboratory conditioned 4% target V_a specimens). Also displayed in Figure 4.22 are the results of 0-yr specimens for comparison. Oxidative conditioning (CP1 and CP2) increase SI+CI and Moisture condition (CP3, CP4, CP5, and CP6) increase SI+CI; however, the oxidative damage effect SI+CI more. CP7, the combined of oxidation and moisture, effects SI+CI as CP1. WMA binders typically had similar or lower SI+CI values relative to HMA (M17).

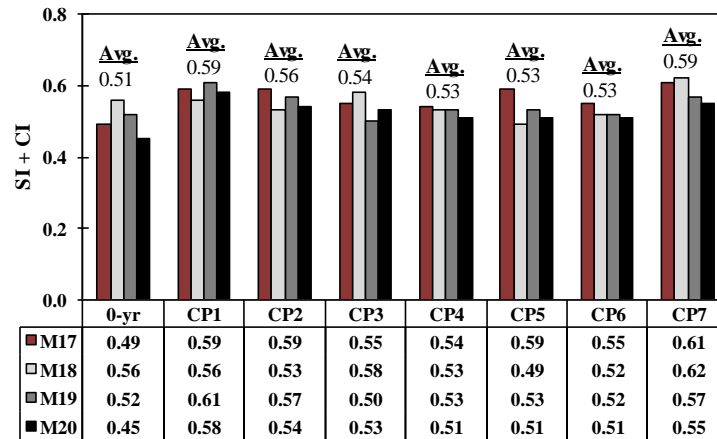


Figure 4.24. FTIR Laboratory Conditioned Results

CHAPTER 5-CONDITIONING PROTOCOL AND TEST METHOD COMBINATIONS TO DETECT MIXTURE DAMAGE

5.1 Overview

As presented in Chapter 2, several groups are pursuing conditioning and testing protocols to predict longer term mixture performance; however, most are not considering damage from multiple environmental effects simultaneously, which can lead to confounding results from binder and mixture properties. For example, oxidation of bitumen from aging leads to stiffening and brittleness while moisture damage may or may not lead to these same states. Conditioning of a mixture for a relatively brief period in warm to hot water can affect binder adhesion to aggregates, but the binder may not be aged considerably. Performing both aforementioned protocols on a single asphalt mixture specimen could lead to, for example, little to no change in S_t . Thus, this chapter aims to evaluate how a given test can simultaneously assess multiple types of damage (i.e. oxidation, moisture damage, and free-thaw damage). Oxidation (aging), moisture damage (adhesive or cohesive), and FT effects were evaluated individually and in combination using the CPs described in Chapter 3. After conditioning, intermediate temperature non-load associated properties were assessed with binder, IDT, and CML testing.

Data from Volumes 1 and 2 was used to form the hypothesis described in Figure 5.1. In Figure 5.1, “Day 1 Properties” represent some arbitrary initial S_t and ML for an asphalt mixture designed according to an acceptable method, properly produced, and placed into a pavement. At time of construction, this mixture could have properties anywhere in the spectrum of stiffness and durability. The hypothesis investigated in this chapter is what happens in the zone of Environmental Effects in Figure 5.1. In one extreme, if the mixture is placed in an environment dominated by oxidation (i.e. very hot with little to no moisture), ML and S_t are expected to increase; however, the Damage Envelope represents a limit to how much S_t would be able to increase relative to ML . On the other extreme, a moisture dominated environment is expected to increase ML , but S_t would be prone to decrease. Between the two extremes, where there is some meaningful level of both oxidation and moisture, ML is still expected to increase while the opposing effects of oxidation and moisture on S_t would likely cause little change in S_t relative to that which is expected at either extreme. This hypothesis is based on observations from Volumes 1 and 2 and if supported by the analysis performed here, the case for Cantabro testing is solidified relative to tensile strength. Note that the technical content from this chapter is also contained in Bazuhair et al. (2018).

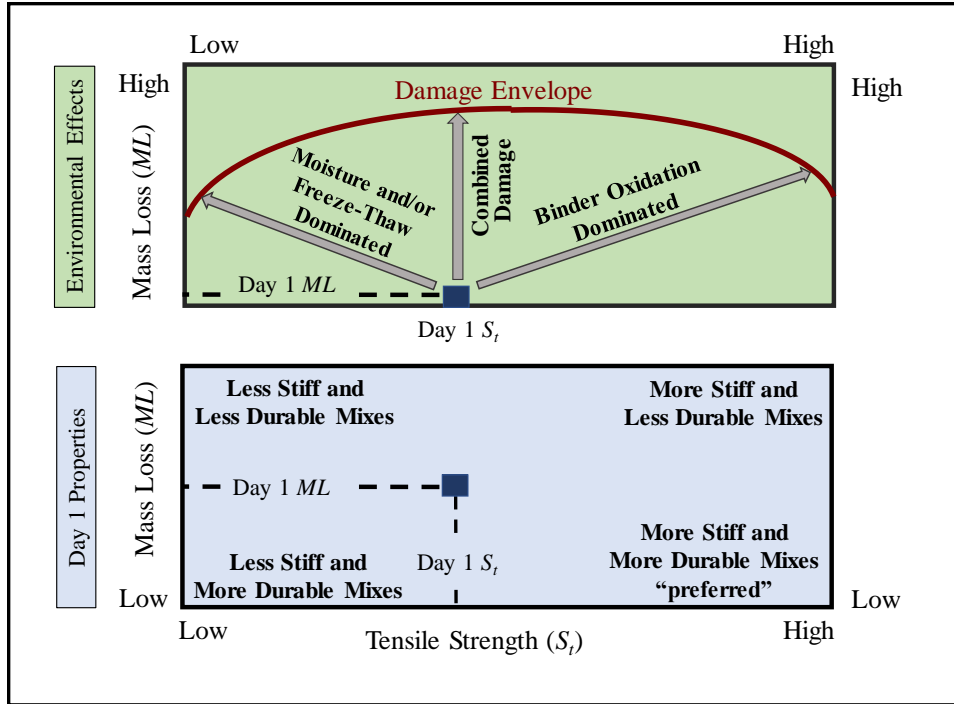


Figure 5.1. Mixture-Environmental Effects Hypothesis Diagram

5.2 Results and Discussion

Table 5.1 summarizes all data relative to the analysis performed in this chapter which is an excerpt from chapter 4. Since there is no field aging data considered here, unconditioned specimens referred to as 0-yr in Chapter 4 and elsewhere, are denoted CP0 for the purpose of this analysis. For example, 0-yr ML for 7% V_a specimens of 11.8% displayed in Table 4.1, is referred to as CP0 ML in this chapter, as seen in Table 5.1.

Figure 5.2 plots property values for each mix with linear regressions displayed to identify significant relationships (i.e. greater than 95% confidence) between each property. For example, Figure 5.2a displays S_t values from Table 5.1 on the y-axis and ML values from Table 5.1 on the x-axis. Based on p -values in Figures 5.2a, 5.2b, and 5.2c, ML did not correlate with S_t but did correlate with $Pen.$ and DSR_{8mm} with scatter (R^2 of 0.32 for $Pen.$ and 0.13 for DSR_{8mm}). S_t did not correlate either with $Pen.$ nor DSR_{8mm} (Figures 5.2d and 5.2e). $Pen.$ versus DSR_{8mm} (Figure 5.2f) showed the strongest correlation of all comparisons with a p -value of less than 0.01 and R^2 of 0.71. Thus, further mixture to binder comparisons rely only on $Pen.$

Figure 5.3 displays equality plots comparing CP0 mixture property values to each of the eight CPs based on the individual test results (mixture values in Table 5.1 are averages of three specimens). For example, each point in Figure 5.3a represents two CML tested specimens where one specimen was tested without conditioning (CP0) and one was tested after CP1. Colored dashed lines in Figure 5.3 are linear regression lines, which when running above equality line indicate higher values measured after conditioning, and when below the equality line indicate lower values measured after conditioning. Points on the equality line indicate no property change due to conditioning.

Table 5.2 presents statistical assessments to consider the effects of conditioning, represented by $\Delta(CP_i-CP_0)$ on ML and S_t . CP_i represents a value from any of the eight protocols

(i.e. CP1-CP8). Arrows are used to indicate an increase or decrease in the relevant mixture property. Comparison of mean $\Delta(\text{CPi-CP0})$ for each combination of mix, mixture property, and CP by t -tests is summarized in rows with no shading. For example, the value of 0.3 in column three and row one indicates a 0.3% ML increase in M17 specimens after CP1. Multiple comparison t -groupings based on average $\Delta(\text{CPi-CP0})$ for each CP are displayed in shaded rows. All CPs assigned to the same t -group letter are statistically similar. For example, the average $\Delta(\text{CPi-CP0})$ for ML due to CP7 and CP8 were statistically comparable since both CPs were assigned to t -group “E”.

Table 5.1. Relative Mixture and Binder Data

CP	Mix ID	Pen. (dmm)	DSR _{8mm} T _c (°C)	S _t (kPa)	ML (%)
CP0	M17	28	20.0	1322	11.8
	M18	31	18.4	1207	10.2
	M19	35	19.1	1219	10.1
	M20	37	18.2	1166	11.0
CP1	M17	28	18.5	1375	12.1
	M18	33	18.4	1385	12.8
	M19	34	18.9	1478	12.2
	M20	27	19.7	1390	14.5
CP2	M17	26	19.7	1561	12.3
	M18	32	18.1	1357	10.8
	M19	31	18.7	1451	11.2
	M20	30	18.3	1267	13.0
CP3	M17	25	18.7	1391	15.6
	M18	31	18.0	1069	13.5
	M19	37	17.7	1350	14.5
	M20	28	19.1	1199	16.5
CP4	M17	33	16.8	1286	12.0
	M18	34	16.7	1213	13.6
	M19	40	15.6	1328	13.3
	M20	50 ^a	11.9 ^a	1156	14.8
CP5	M17	30	18.3	1387	14.0
	M18	38	16.1	1180	12.8
	M19	30	19.2	1413	14.7
	M20	29	18.2	1295	14.6
CP6	M17	19	21.2	1194	13.5
	M18	28	18.5	1212	12.6
	M19	37	17.4	1360	11.7
	M20	29	18.6	1285	13.3
CP7	M17	18	21.8	1388	16.2
	M18	22	19.4	1285	15.1
	M19	24	20.9	1426	16.8
	M20	22	19.7	1238	17.9
CP8	M17	---	---	---	---
	M18	---	---	1606	15.9
	M19	---	---	1315	15.4
	M20	---	---	1594	18.6

a: Values believed to be outliers, thus not included in analysis.

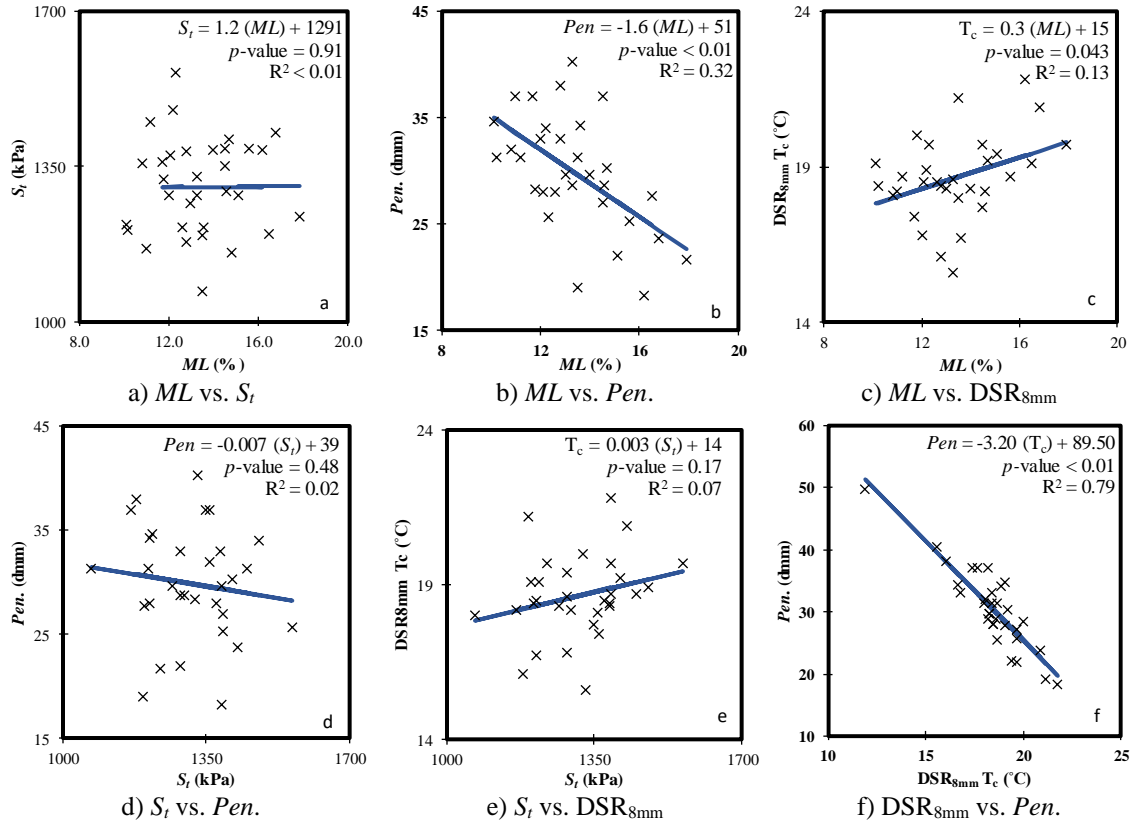


Figure 5.2. Test Property Correlations

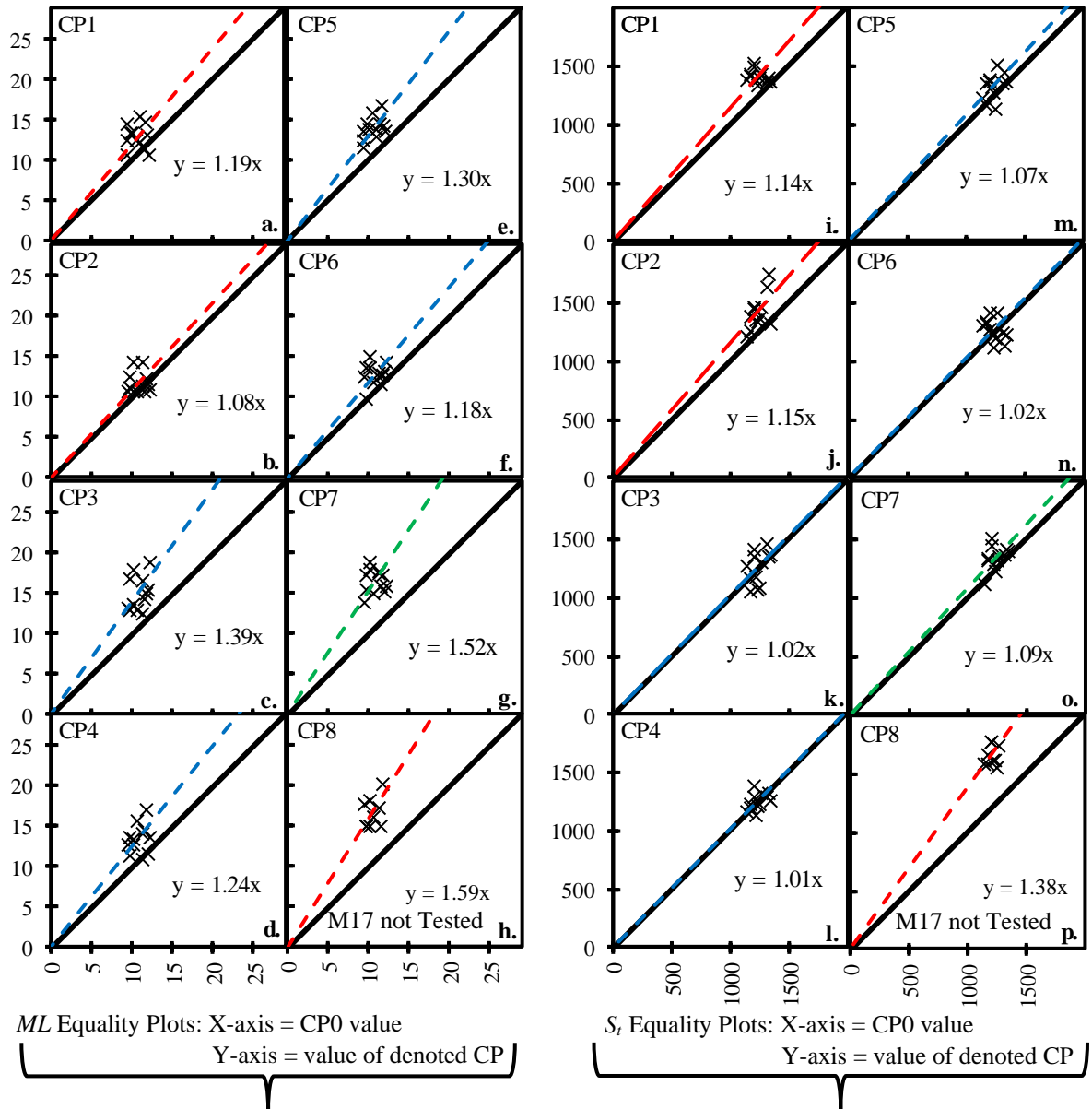


Figure 5.3. ML (%) and S_t (kPa) Equality Plots

Table 5.2. Statistical Assessment of Mixture Test Results

CP	Mix ID	ML (%)			All data <i>t</i> -grouping	S _r (kPa)			All data <i>t</i> -grouping
		Δ(CPi-CP0)	<i>p</i> -value	Sig?		Δ(CPi-CP0)	<i>p</i> -value	Sig?	
CP1	M17	0.3↑	0.77	No	---	53↑	<0.01	Yes	---
	M18	2.6↑	0.07	No	---	178↑	<0.01	Yes	---
	M19	2.1↑	0.07	No	---	259↑	<0.01	Yes	---
	M20	3.5↑	0.01	Yes	---	224↑	<0.01	Yes	---
	All Data	2.1↑	---	---	AB	179↑	---	---	A
CP2	M17	0.5↑	0.67	No	---	239↑	0.14	No	---
	M18	0.6↑	0.42	No	---	150↑	<0.01	Yes	---
	M19	1.1↑	0.16	No	---	232↑	<0.01	Yes	---
	M20	2.0↑	0.17	No	---	101↑	0.09	No	---
	All Data	1.1↑	---	---	A	181↑	---	---	A
CP3	M17	3.8↑	0.12	No	---	69↑	0.13	No	---
	M18	3.3↑	0.01	Yes	---	-138↓	<0.01	Yes	---
	M19	4.4↑	0.02	Yes	---	131↑	0.02	Yes	---
	M20	5.5↑	<0.01	Yes	---	33↑	0.47	No	---
	All Data	4.3↑	---	---	D	24↑	---	---	B
CP4	M17	0.2↑	0.81	No	---	-36↓	0.10	No	---
	M18	3.4↑	0.01	Yes	---	6↑	0.81	No	---
	M19	3.2↑	0.06	Yes	---	109↑	0.04	Yes	---
	M20	3.8↑	0.03	Yes	---	-10↓	0.75	No	---
	All Data	2.7↑	---	---	BC	17↑	---	---	B
CP5	M17	2.2↑	<0.01	Yes	---	65↑	0.10	No	---
	M18	2.6↑	0.07	Yes	---	-27↓	0.63	No	---
	M19	4.6↑	<0.01	Yes	---	194↑	0.01	Yes	---
	M20	3.6↑	0.04	Yes	---	129↑	0.04	Yes	---
	All Data	3.3↑	---	---	DC	90↑	---	---	AB
CP6	M17	1.7↑	0.03	Yes	---	-128↓	0.03	Yes	---
	M18	2.4↑	0.05	No	---	5↑	0.95	No	---
	M19	1.6↑	0.23	No	---	141↑	0.04	Yes	---
	M20	2.3↑	0.06	Yes	---	119↑	0.03	Yes	---
	All Data	2.0↑	---	---	AB	34↑	---	---	B
CP7	M17	4.4↑	<0.01	Yes	---	66↑	0.01	Yes	---
	M18	4.9↑	<0.01	Yes	---	78↑	0.15	No	---
	M19	6.7↑	<0.01	Yes	---	207↑	0.01	Yes	---
	M20	6.9↑	<0.01	Yes	---	72↑	0.34	No	---
	All Data	5.7↑	---	---	E	106↑	---	---	AB
CP8	M17	---	---	---	---	---	---	---	---
	M18	5.7↑	<0.01	Yes	---	399↑	<0.01	Yes	---
	M19	5.3↑	<0.01	Yes	---	96↑	<0.01	Yes	---
	M20	7.6↑	<0.01	Yes	---	428↑	<0.01	Yes	---
	All Data ^a	6.2↑	---	---	E	308↑	---	---	A

^a Δ(CPi-CP0) does not consider M17 from CP0

5.2.1 Oxidation Effects

Figure 5.1 displays the hypothesis that damage dominated by binder oxidation is expected to increase *ML* and *S_r*. Figure 5.3 and Table 5.2 show the oxidative conditioning protocols (i.e. CP1 and CP2) consistently increased *ML* and *S_r* at magnitudes statistically equivalent to each other. Additionally, coefficients from Figure 5.3 and average *ML* increases in Table 5.2 indicate that CP1

is slightly more damaging than CP2; however, Table 5.2 *t*-groups show the effects are not statistically different. This observation is similar to those in Volumes 1 and 2 where there were little to no differences detected between *ML* for CP1 and CP2. Penetration results indicated a slight increase in oxidation due to CP1 and CP2. These observations support the oxidation conditioning hypothesis in Figure 5.1 and indicate that *ML* and S_t were practically the same when considering this isolated damage type.

5.2.2 Moisture Effects

As hypothesized in Figure 5.1 moisture induced damage is expected to increase *ML* but decrease or have no effect on S_t . An increased number of FT cycles would increase mixture damage, thus CP3, CP4, and CP5 would be expected to rank from least to most severe. CP6 would also be expected to be more damaging than CP3 in all cases, since it is twice the length of water exposure time. Volume 1 ranked the moisture conditioning protocols from least to greatest as CP6, CP4, CP5, and Volume 2 ranked as CP3, CP4, CP5, CP6, and in all cases, *ML* results showed moisture conditioning to be more severe than oxidative-only conditioning. *ML* results in Figure 5.3 and Table 5.2 indicate that CP6, CP4, CP5, and CP3 produce sequentially more damage, while corresponding S_t values remained practically the same with no statistical difference. Although the order of severity was not as expected, chaining across *t*-groups in Table 5.2 for *ML* shows that these protocols produced comparable damage in some senses. Moisture dominated CPs were ranked from least to most severe as CP4, CP5, CP3, and CP6, according to penetration results. The moisture damage dominated hypothesis in Figure 5.1 is supported with these observations. Some evidence was also provided that shows *ML* has more potential than S_t in detecting moisture-related damage.

5.2.3 Combined Effects of Oxidation and Moisture

Relative to S_t , Figure 5.1 hypothesizes that combined damage could result in values anywhere within the interior portion of the damage envelope, where two or more damage mechanisms may even cancel each other out to produce no change in S_t . Considering *ML*, Figure 5.1 hypothesizes that multiple damage mechanisms would have a cumulative effect on results, thus causing a greater *ML* than either of the isolated damage cases. CP7 would be expected to be more severe than CP1, CP3, and CP4 as it is the combination of CP1 and CP4, where CP4 is equivalent to CP3 with the addition of a FT cycle. Such a trend in *ML* was observed in Volumes 1 and 2 and supported here as seen in Table 5.2 and Figure 5.3. S_t , on the other hand, shows a practically negligible increase from the combined conditioning mechanisms, as was hypothesized in Figure 5.1 (see S_t data in Table 5.2 and Figure 5.3). This raises concern in the ability of tensile strength to detect combined environmental effects.

To further investigate the differences observed between responses of *ML* and S_t , CP8 was performed, expecting to produce increased damage relative to CP1 for both mixture properties. This expectation was validated, as seen in Table 5.2 and Figure 5.3. *ML* and S_t data of CP7 and CP8 confirms that *ML* is more suitable than S_t for detecting combined environmental effects. *ML* observed high levels of damage for either heavily oxidized or combined oxidation, moisture, and freeze-thaw conditioning, while S_t did not. Logically, CP7 induces more damage than CP1, which S_t was unable to detect. Observations of the effects of combined damage types strongly supported the Figure 5.1 hypothesis.

CHAPTER 6 – INFLUENCE OF WMT TYPE ON MIXTURE AND BINDER RESPONSE TO LABORATORY INDUCED DAMAGE

6.1 Overview of Results

This chapter summarizes changes in mixture and binder properties due to different laboratory damage mechanisms, in an effort to display the differences in mixture and binder responses that can be attributed to WMT type. These changes were analyzed in four different sections corresponding to four different types of damage or damage combinations that were applied to asphalt mixture specimens. Section 6.2 evaluates the change in mixture and binder properties due to isolated oxidation while Section 6.3 evaluates changes due to isolated moisture. The effects of moisture conditioning followed by freeze-thaw cycles on mixture and binder properties are investigated in Section 6.4. The combined effects of oxidation, moisture, and freeze-thaw are described in Section 6.5. In each section, relative data is first displayed in figures, and general observations in trends and changes in mixture and binder properties are made. These observations are then related back to findings from related literature that was summarized in Chapter 2.

Asphalt mixture test methods include APA and HLWT for evaluation of high temperature properties (rutting resistance), CML and FE₊₂₀ for intermediate temperature properties (fatigue and durability), and FE₋₁₀ for low temperature fracture resistance. Due to a shortage of material, HLWT data for M17 was only obtained for CP0 specimens. E/R binder was also evaluated and is analyzed alongside mixture data. Binder properties considered here are high T_c (via DSR_{25mm} testing), intermediate temperature *Pen.*, and low T_c from BBR results. DSR testing was also performed at intermediate temperatures with an 8mm plate (DSR_{8mm}); however, as shown in Chapter 5, *Pen.* and DSR_{8mm} have statistically significant correlation with an R² value of 0.71. As such, *Pen.* is the only intermediate temperature binder property considered in this analysis. Additionally, the low T_c considered here is based on m-value (T_{c-m}), since m-value governed in all cases (i.e. T_c based on m-value was always warmer than that based on stiffness). For each mixture property, three replicate test values were obtained. Table 6.1 summarizes the average of these values as well as the standard deviation (*s*) and coefficient of variation (COV). Binder testing was not performed in triplicate; therefore, only the individual test values for each mix type and CP are summarized in Table 6.2. Tables 6.1 and 6.2 are excerpts of the data in Chapter 4.

Table 6.1. Asphalt Mixture Testing Data

CP	Mix ID	APA Testing			HLWT Testing			CML Testing			FE ₊₂₀ Testing			FE ₋₁₀ Testing		
		RD _{APA} (mm)	s	COV (%)	RD _{HLWT} (mm)	s	COV (%)	ML (%)	s	COV (%)	FE ₊₂₀ (kJ/m ³)	s	COV (%)	FE ₋₁₀ (kJ/m ³)	s	COV (%)
CP0	M17	4.9	0.4	7.5	7.7	1.0	13.7	11.8	0.5	4.3	3.49	0.7	19.2	0.68	0.10	14.4
	M18	5.6	0.4	6.5	NR	---	---	10.2	1.1	11.0	3.83	0.9	24.4	0.86	0.25	28.5
	M19	8.8	0.5	5.3	15833**	---	---	10.1	0.5	5.2	4.11	0.7	17.7	0.69	0.12	17.1
	M20	4.6	0.3	5.9	9.6	0.8	8.5	11.0	0.8	7.4	1.78	1.1	62.8	0.47	0.16	33.1
CP1	M17	6.5	0.8	13.0	NR	---	---	12.1	1.3	10.8	1.74	0.4	22.8	0.70	0.10	14.6
	M18	5.6	0.9	15.4	7.1	1.1	14.9	12.8	1.5	11.6	2.32	0.5	22.8	0.57	0.17	29.8
	M19	7.2	0.8	11.7	7.3	0.6	8.5	12.2	1.5	11.9	1.86	0.4	23.7	0.70	0.06	9.1
	M20	4.7	0.2	4.7	5.9	0.3	5.7	14.5	1.1	7.6	1.53	0.3	18.1	0.53	0.08	15.5
CP2	M17	5.8	0.9	15.9	NR	---	---	12.3	1.8	14.8	2.26	0.9	41.4	0.53	0.13	23.8
	M18	8.4	0.4	5.0	7.6	0.4	5.1	10.8	0.2	2.3	2.12	0.6	29.0	0.58	0.14	23.7
	M19	7.2	1.1	15.2	8.1	1.3	16.1	11.2	1.0	9.2	2.79	0.6	21.5	0.64	0.10	15.2
	M20	6.4	0.7	11.2	6.0	0.2	3.1	12.7	1.6	12.4	0.91	0.3	28.2	0.46	0.17	37.3
CP3	M17	5.8	1.0	16.7	NR	---	---	15.6	3.3	20.9	2.65	0.6	22.3	0.67	0.26	38.0
	M18	5.9	0.9	15.2	NR	---	---	13.5	0.8	5.7	2.31	0.9	39.4	0.59	0.03	5.5
	M19	7.5	1.4	18.8	NR	---	---	14.5	2.1	14.3	2.92	0.9	30.0	0.86	0.20	23.5
	M20	5.0	0.5	9.1	NR	---	---	16.5	1.5	8.9	2.54	0.3	11.2	0.61	0.14	22.3
CP4	M17	5.4	1.4	24.9	NR	---	---	12.0	1.4	11.4	3.20	0.8	25.6	0.58	0.05	8.8
	M18	6.7	1.0	15.2	14629**	---	---	13.6	0.9	6.2	2.17	0.7	32.4	0.70	0.15	21.6
	M19	7.6	1.3	16.7	NR	---	---	13.3	2.2	16.4	2.79	0.3	12.0	0.55	0.19	34.6
	M20	5.4	1.0	18.2	NR	---	---	14.8	1.9	12.9	1.76	0.5	27.6	0.49	0.08	16.3
CP5	M17	5.3	1.9	35.1	NR	---	---	14.0	0.3	1.9	2.13	1.1	52.4	0.51	0.06	11.9
	M18	7.6	1.3	16.7	NR	---	---	12.8	1.5	11.6	4.22	1.0	23.2	0.76	0.11	14.2
	M19	8.1	0.6	7.0	NR	---	---	14.7	1.2	8.3	3.49	1.3	37.6	0.81	0.03	3.2
	M20	6.2	1.1	17.8	NR	---	---	14.6	2.0	14.0	3.77	1.3	33.3	0.67	0.19	28.8
CP6	M17	4.7	0.4	9.2	NR	---	---	13.5	0.7	5.2	2.27	0.8	36.9	0.70	0.02	2.3
	M18	6.9	1.7	24.4	NR	---	---	12.6	1.1	8.4	2.43	0.6	24.5	0.70	0.10	13.8
	M19	7.5	1.6	20.9	NR	---	---	11.7	2.0	16.8	3.66	0.7	20.1	0.67	0.06	9.1
	M20	6.2	1.2	20.0	NR	---	---	13.3	1.4	10.4	3.18	1.0	32.6	0.63	0.04	6.3
CP7	M17	4.3	0.7	16.7	NR			16.2	1.3	8.0	2.01	0.4	19.6	0.58	0.06	10.0
	M18	6.4	1.0	16.1	6.9	0.5	7.0	15.1	1.1	7.6	1.98	0.7	36.5	0.56	0.06	11.5
	M19	6.9	1.0	14.9	6.4	1.1	16.9	16.8	1.5	8.9	2.52	0.7	29.3	0.62	0.14	23.3
	M20	5.3	1.1	20.8	5.7	0.2	3.4	17.9	0.8	4.6	1.36	0.5	34.8	0.50	0.06	11.2

* Values believed to be outlier; ** Number of passes when test reached max rut depth of 12.5mm.

NR: Three tests were performed for each mix-CP combination; however, in cases where one or two of the three tests reached failure RD of 12.5mm prior to reaching 20,000 passes the test data is not reported. Full HLWT data can be found in Chapter 4.

Table 6.2. Asphalt Binder Testing Data

CP Mix	ID	DSR _{25mm} T _c (°C)	Pen. (dmm)	BBR T _{c-m} (°C)
CP0	M17	69.8	28	-19.9
	M18	70.9	31	-20.6
	M19	69.5	35	-20.6
	M20	69.4	37	-21.4
CP1	M17	77.4	28	-18.9
	M18	74.0	33	-20.4
	M19	72.7	34	-20.9
	M20	75.5	27	-17.7
CP2	M17	76.9	26	-19.1
	M18	71.8	32	-20.9
	M19	71.9	31	-21.3
	M20	72.7	30	-20.1
CP3	M17	75.6	25	-20.7
	M18	72.3	31	-21.5
	M19	70.0	37	-22.1
	M20	72.9	28	-19.5
CP4	M17	70.0	33	-22.8
	M18	72.1	34	-22.5
	M19	69.6	40	-22.9
	M20	67.2	50*	-26.5
CP5	M17	72.7	30	-20.1
	M18	69.5	38	-23.0
	M19	77.3	30	-20.3
	M20	72.0	29	-20.3
CP6	M17	83.8	19	-16.5
	M18	72.3	28	-21.2
	M19	70.2	37	-22.5
	M20	73.6	29	-20.3
CP7	M17	84.1	18	-16.4
	M18	77.0	22	-19.1
	M19	76.5	24	-18.8
	M20	77.5	22	-17.8

In the early stages of analysis, a blocked analysis of variance (ANOVA) was performed on certain mixture properties (APA, CML, and FE₋₁₀), and the results are shown in Table 6.3. Within each CP, t-groups assigned to the same letter are statistically similar considering an observed significance level of 0.05. CPs which had no statistical differences among the different mixture types are denoted with the abbreviation “NSD” in the “t-group” column. As seen in Table 6.3, there were very few instances where there were statistically significant differences among the different mixture types. As such, the remainder of this chapter does not consider statistically significant differences and only discusses general trends and comparisons among the mixture as a function of laboratory damage and WMT type.

Table 6.3. Initial ANOVA of Certain Mixture Properties

CP	Mix ID	APA		CML		FE-10	
		RD (mm)	<i>t</i> -group	ML (%)	<i>t</i> -group	FE (kJ/m ³)	<i>t</i> -group
CP0	M17	4.9	BC	11.8	NSD	0.68	AB
	M18	5.6	B	10.2	NSD	0.86	A
	M19	8.8	A	10.1	NSD	0.69	AB
	M20	4.6	C	11.0	NSD	0.47	B
CP1	M17	6.5	AB	12.1	NSD	0.70	NSD
	M18	5.6	BC	12.8	NSD	0.57	NSD
	M19	7.2	A	12.2	NSD	0.70	NSD
	M20	4.7	C	14.5	NSD	0.53	NSD
CP2	M17	5.8	B	12.3	NSD	0.53	NSD
	M18	8.4	A	10.8	NSD	0.58	NSD
	M19	7.2	AB	11.2	NSD	0.64	NSD
	M20	6.4	B	12.7	NSD	0.46	NSD
CP3	M17	5.8	NSD	15.6	NSD	0.67	NSD
	M18	5.9	NSD	13.5	NSD	0.59	NSD
	M19	7.5	NSD	14.5	NSD	0.86	NSD
	M20	5.0	NSD	16.5	NSD	0.61	NSD
CP4	M17	5.4	NSD	12.0	NSD	0.58	NSD
	M18	6.7	NSD	13.6	NSD	0.70	NSD
	M19	7.6	NSD	13.3	NSD	0.55	NSD
	M20	5.4	NSD	14.8	NSD	0.49	NSD
CP5	M17	5.3	NSD	14.0	NSD	0.51	NSD
	M18	7.6	NSD	12.8	NSD	0.76	NSD
	M19	8.1	NSD	14.7	NSD	0.81	NSD
	M20	6.2	NSD	14.6	NSD	0.67	NSD
CP6	M17	4.7	NSD	13.5	NSD	0.70	NSD
	M18	6.9	NSD	12.6	NSD	0.70	NSD
	M19	7.5	NSD	11.7	NSD	0.67	NSD
	M20	6.2	NSD	13.3	NSD	0.63	NSD
CP7	M17	4.3	NSD	16.2	NSD	0.58	NSD
	M18	6.4	NSD	15.1	NSD	0.56	NSD
	M19	6.9	NSD	16.8	NSD	0.62	NSD
	M20	5.3	NSD	17.9	NSD	0.50	NSD

NDS= Not Significantly different

It is recognized that changes in mixture and binder properties can have varying affects at different temperatures. For example, a decrease in *Pen.* may result in an improvement in rutting resistance but may increase brittleness tendencies (reduce cracking resistance); however, this chapter does not explore these behavioral implications. With all test methods, there is inherent variability which can cause changes in test values that are not necessarily reflective of meaningful changes that may have an impact on mixture performance or behavior. Implications and the extent to which differences and changes in behavioral properties are meaningful are not discussed in this chapter. Standard deviation and COV are presented in Table 4.1 for basic comparisons between

changes in test values due to damage and inherent test method variability, but this point is not discussed in any detail in this chapter.

Note that in instances where results presented here are compared to available literature, other authors may have determined statistically significant differences among WMTs. When it is stated that results originating from data in this report agree or disagree with these sources, this should not be taken to mean that statistically significant difference were or were not found using these results. Instead, it means that the general trends observed here (increase or decrease in similar mixture or binder properties) agrees with those found in literature, absent statistical analysis.

6.2 Oxidation Effects

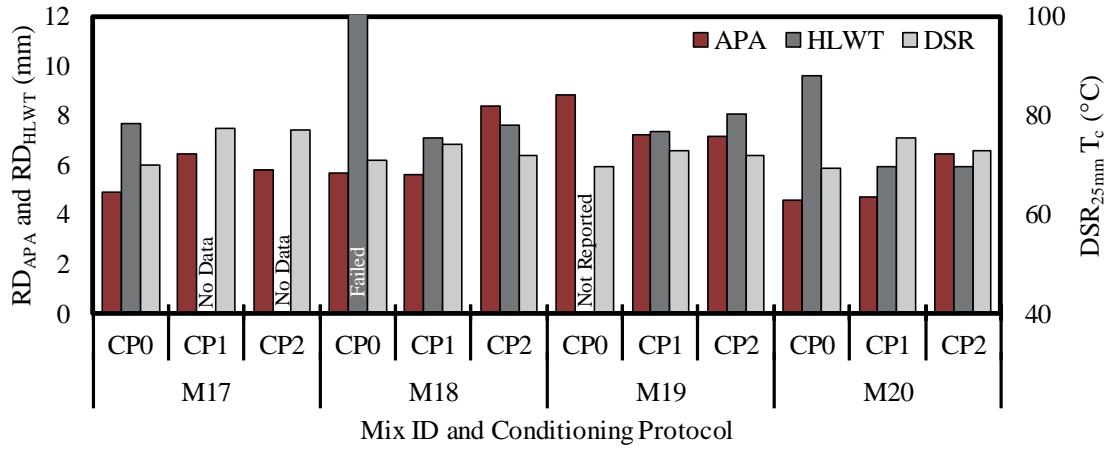
For M17, Figure 6.1a shows RD_{APA} increased for CP1 and CP2 specimens, relative to CP0; however, the average high T_c of M17 binder increased due to both CPs. At intermediate temperatures, Figure 6.1b shows an increase in ML and decreases in FE_{+20} and $Pen.$ CML and penetration testing were affected more by CP2 than CP1, while FE_{+20} showed the opposite. Data presented in Figure 6.1c shows CP1 resulted in an increase in FE_{-10} , while CP2 decreased FE_{-10} by a greater magnitude. T_{c-m} increased due to both CPs.

M18 high temperature data displayed in Figure 6.1a shows CP1 caused no change in final RD_{APA} while CP2 caused an increase of approximately 2-mm. Considering HLWT results, CP0 specimens for M18 reached the maximum RD_{HLWT} of 12.5-mm for two of the three replicates, while CP1 and CP2 both prevented failure during testing in all cases. DSR_{25mm} showed an increase in T_c ranging from 1-3°C. At intermediate temperatures, CML and FE_{+20} , showed increased brittleness due to both CPs for M18 (Figure 6.1b) and $Pen.$ values increased relative to CP0. FE_{-10} was decreased due to both CPs and BBR testing showed a change in T_{c-m} of less than 0.5°C.

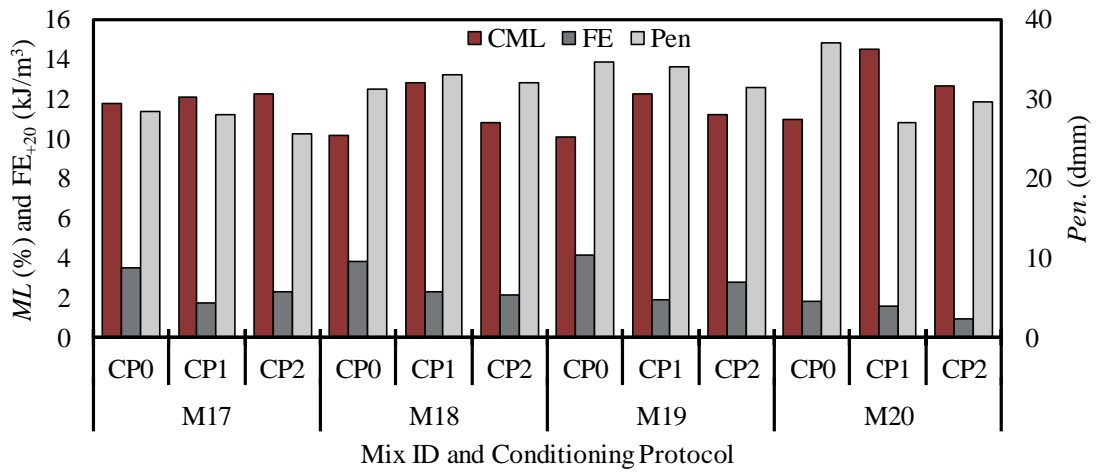
As seen in Figure 6.1a, CP1 and CP2 resulted in reduced RD_{APA} and RD_{HLWT} for M19 and caused an increase in high T_c . Intermediate temperature results in Figure 6.1b show an increase in ML , decrease in $Pen.$, and decrease in FE_{+20} . FE_{-10} and T_{c-m} (Figure 6.1c) for M19 changed by 0.004 and -0.054 kJ/m³ and -0.3 and -0.7°C for CP1 and CP2, respectively.

APA results for M20, as shown in Figure 6.1a, showed an increase in RD_{APA} ranging from 0.1 to 1.8-mm while RD_{HLWT} decreased by over 3.5-mm and T_c increased by over 6°C. Intermediate temperature test results in Figure 6.1b showed an increase in ML , decrease in $Pen.$, and decrease in FE_{+20} . Considering low temperature behavior (Figure 6.1c), M20 FE_{-10} increased from CP0 to CP1, but CP2 caused a decrease of 0.010 kJ/m³. BBR testing showed a 3.8°C increase in T_{c-m} (less negative) due to CP1 and a 1.3°C increase from CP2.

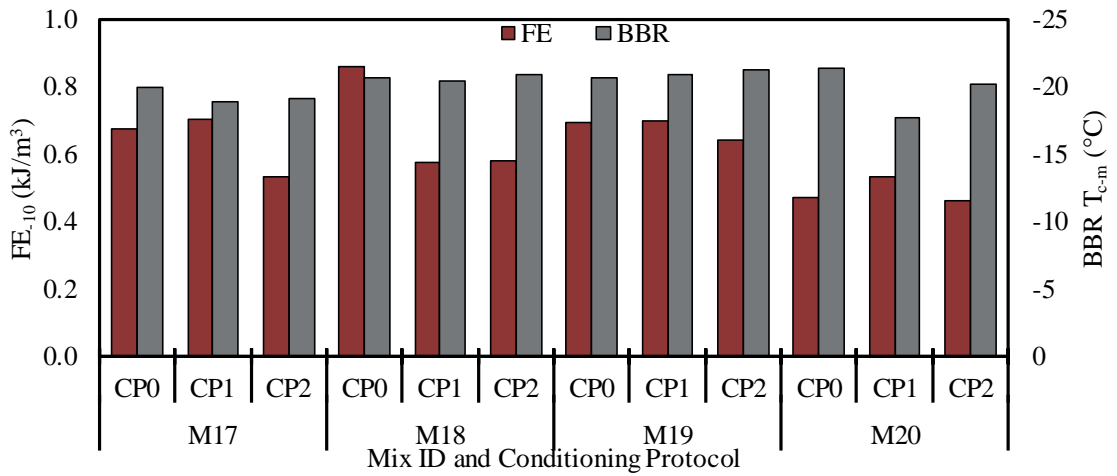
Table 6.4 summarizes the observations made herein relative to high, intermediate, and low temperature testing of mixture and recovered binder for each mix type.



a) High Temperature Data



b) Intermediate Temperature Data



c) Low Temperature Data

Figure 6.1. Effects of Oxidative Conditioning on Asphalt Mixture and Binder Properties

Table 6.4. Summary of Isolated Oxidation Observations

Mix ID (WMT)	Testing Temperature Range		
	High	Intermediate	Low
M17 (HMA)	RD _{APA} : Increased T _c : Increased	ML: Increased FE ₊₂₀ : Decreased Pen.: Decreased	FE ₋₁₀ : Increased or decreased T _{c-m} : Increased
M18 (Foam)	RD _{APA} : No change or increased RD _{HLWT} : Decreased T _c : Increased	ML: Increased FE ₊₂₀ : Decreased Pen.: Increased	FE ₋₁₀ : Decreased T _{c-m} : Increased or decreased
M19 (Evotherm)	RD _{APA} : Decreased RD _{HLWT} : Decreased T _c : Increased	ML: Increased FE ₊₂₀ : Decreased Pen.: Increased or decreased	FE ₋₁₀ : Increased or decreased T _{c-m} : Decreased
M20 (Sasobit)	RD _{APA} : Increased RD _{HLWT} : Decreased T _c : Increased	ML: Increased FE ₊₂₀ : Decreased Pen.: Decreased	FE ₋₁₀ : Increased or decreased T _{c-m} : Increased

Abbas et al. (2016) found that foamed asphalt aged at a slower rate than HMA according to high and intermediate temperature DSR testing of recovered binder. This agrees with high temperature trends observed here. Safaei et al. (2014) observed intermediate temperature trends similar to those in this analysis which indicated fatigue performance was reduced at a faster rate for foam (M18). At low temperatures, findings from Alhasan et al. (2014) and Kim et al. (2015) concerning change in mixture fracture resistance agreed with those in this analysis where there was little difference in the effects of LTOA on foamed asphalts compared to traditional HMA; however, both studies found that foamed mixtures initially had worse low temperature cracking resistance than HMA, which was not observed from data collected for this investigation. At intermediate temperatures, Yin et al. (2014), Hurley and Prowell (2005a), and Haggag et al. (2011) found increased rates of aging for WMAs produced with chemical additive and Hurley and Prowell (2005b) and Bonaquist (2011) made the same observations for organic wax mixtures, all of which support trends in Figure 6.1. These relations to literature are summarized in Table 6.5.

Table 6.5. Relation of Oxidation Observations to Literature

Reference(s)	Finding	Agrees with Data Previously Discussed?
Abbas et al. (2016)	Foamed asphalt high T _c increased at slower rate than HMA	No
Abbas et al. (2016)	Foamed asphalt int. T _c increased at slower rate than HMA	Yes
Safaei et al. (2014)	Int. temp. performance reduced at faster rate for foam	Mostly
Alhasan et al. (2014) & Kim et al. (2015)	Effect on low temp. fracture resistance of foamed asphalt was not significantly different than HMA	Mostly
Alhasan et al. (2014) & Kim et al. (2015)	Foam initially had worse low temperature fracture resistance	No
Yin et al. (2014), Hurley and Prowell (2005a), & Haggag et al. (2011)	WMAs with chemical additives aged at a faster rate than HMA according to int. temp. properties	Yes
Hurley and Prowell (2005b) & Bonaquist (2011)	WMAs with organic waxes aged at a faster rate than HMA, according to int. temp. properties	Yes

6.3 Moisture Effects

Figures 6.2a, 6.2b, and 6.2c summarize data from isolated moisture protocols (i.e. CP3 and CP6) compared to CP0. Figure 6.2a considers high temperature tests (HLWT results for isolated moisture CPs are not considered). Figure 6.2b displays intermediate temperature behaviors, and Figure 6.2c considers low temperature behaviors.

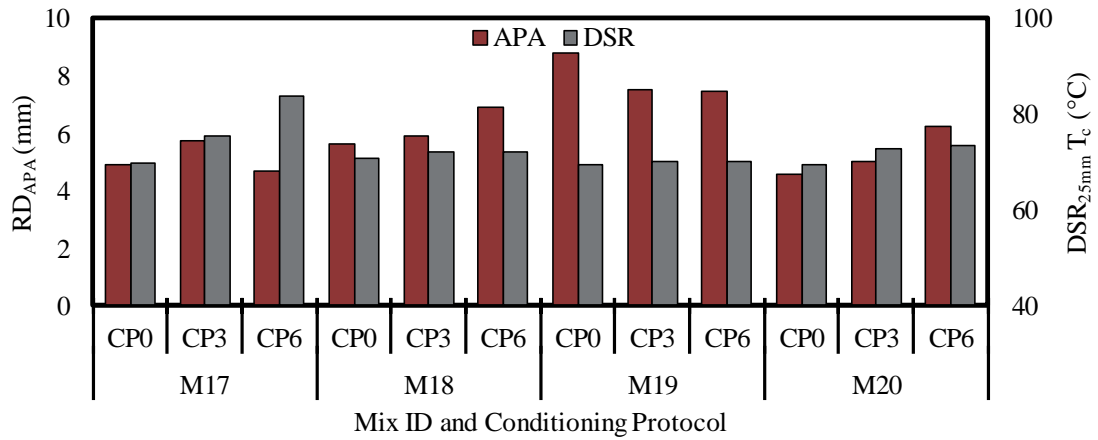
APA data for M17 (Figure 6.2a) showed CP3 increased RD_{APA} by less than 1-mm, but CP6 caused a decrease of 0.2-mm RD_{APA} . High T_c consistently increased from CP0 to CP3 to CP6. At intermediate temperatures, Figure 6.2b shows an increase in ML , decrease in FE_{+20} , and decrease in $Pen.$ values as moisture conditioning time increased. Low temperature results in Figure 6.2c indicated a change in FE_{-10} of -0.002 kJ/m^3 and 0.021 kJ/m^3 for CP3 and CP6, respectively. BBR testing indicated a decrease in T_{c-m} of less than 1°C due to CP3, but an increase of 3.4°C due to CP6.

Figure 6.2a shows a consistent increase in RD_{APA} of M18 but an increase in high T_c of 1.4°C for both CP3 and CP6. Intermediate temperature results in Figure 6.2b show decreased $Pen.$, increased ML , and decreased FE_{+20} . Figure 6.2c shows that FE_{-10} of M18 was reduced by 0.270 and 0.157 kJ/m^3 due to CP3 and CP6, respectively, with a decrease in T_{c-m} of less than 1°C for both protocols.

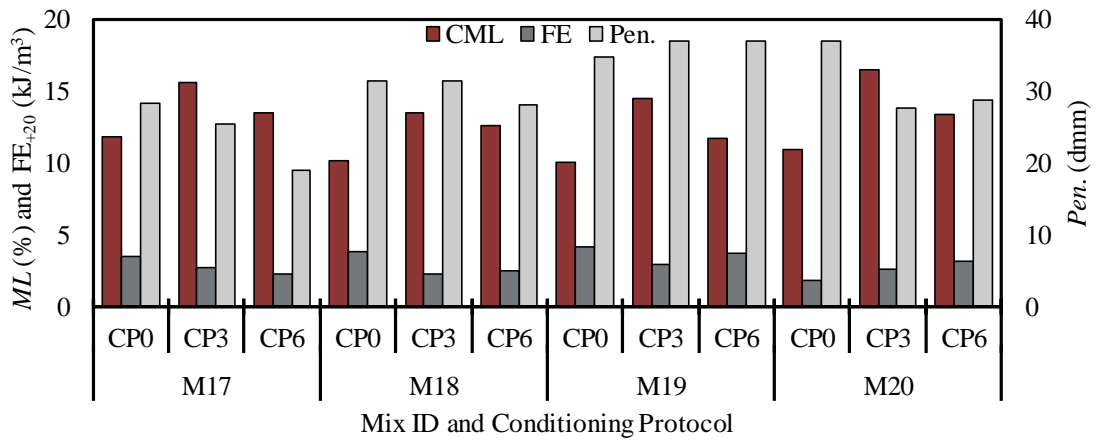
M19 had a decrease in RD_{APA} due to moisture conditioning (over 1-mm), as seen in Figure 6.2a, and an increase in high T_c of less than 1°C . Intermediate temperature testing showed an increase in $Pen.$ but still had an increase in ML and decrease in FE_{+20} (Figure 6.2b). Figure 6.2c shows M19 FE_{-10} increased by 0.168 kJ/m^3 due to CP3 but CP6 caused a decrease of 0.023 kJ/m^3 . This was accompanied by a consistent decrease in T_{c-m} as moisture conditioning time increased (-20.6 to -22.1 to -22.5°C for CP0, CP3, and CP6, respectively).

According to data displayed in Figure 6.2a, M20 RD_{APA} increased with increase in moisture conditioning time, but high T_c consistently increased. At intermediate temperatures, Figure 6.2b shows a decrease in $Pen.$ and increase in ML greater than all other mixture types; however, FE_{+20} consistently increased. At low temperatures (Figure 6.2c), FE_{-10} increased due to moisture conditioning while T_{c-m} increased.

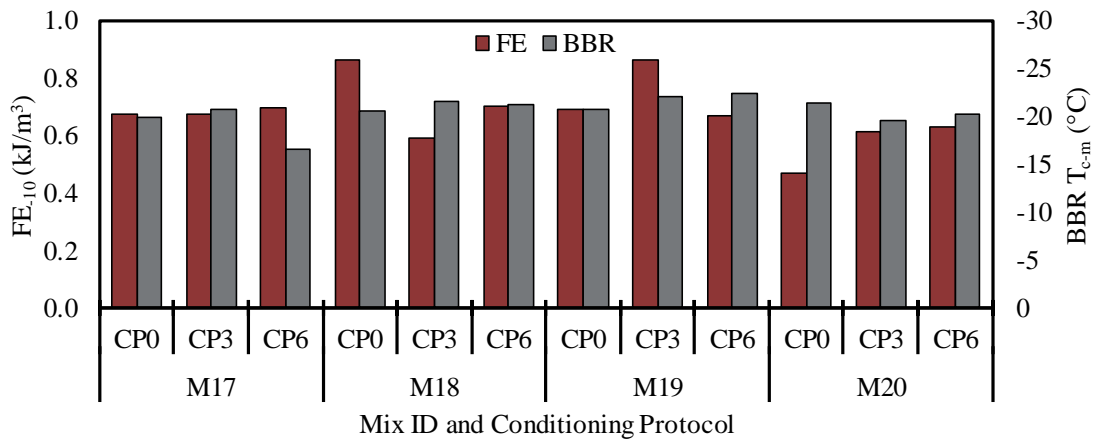
Table 6.6 summarizes the effects of moisture conditioning considering mixture and binder high, intermediate, and low temperature behavioral properties for each mix type.



a) High Temperature Data



b) Intermediate Temperature Data



c) Low Temperature Data

Figure 6.2. Effects of Moisture Conditioning on Asphalt Mixture and Binder Properties

Table 6.6. Summary of Isolated Moisture Observations

Mix ID (WMT)	Testing Temperature Range		
	High	Intermediate	Low
M17 (HMA)	RD _{APA} : Increased or decreased T _c : Increased	ML: Increased FE ₊₂₀ : Decreased Pen.: Decreased	FE ₋₁₀ : Decreased or increased T _{c-m} : Decreased or increased
M18 (Foam)	RD _{APA} : Increased T _c : Increased	ML: Increased FE ₊₂₀ : Decreased Pen.: No change or decreased	FE ₋₁₀ : Decreased T _{c-m} : Decreased
M19 (Evotherm)	RD _{APA} : Decreased T _c : Increased	ML: Increased FE ₊₂₀ : Decreased Pen.: Increased	FE ₋₁₀ : Increased or decreased T _{c-m} : Decreased
M20 (Sasobit)	RD _{APA} : Increased T _c : Increased	ML: Increased FE ₊₂₀ : Increased Pen.: Decreased	FE ₋₁₀ : Increased T _{c-m} : Increased

Malladi et al. (2014) found RD_{APA} was not meaningfully affected for WMAs produced with foaming; however, trends described in Table 6.6 show that foamed asphalt (M18) rut resistance was adversely affected by moisture damage. Hurley and Prowell (2005a) and Malladi et al. (2014) found foamed mixtures were more susceptible to moisture damage than HMA at intermediate temperatures, which contradicts findings presented in this analysis; however, observations in Xiao et al. (2011) supported those made here considering *ML* where foamed asphalt had similar changes in tensile strength as were seen in HMA, but HMA still had higher strengths. These relations to literature are summarized in Table 6.7.

Table 6.7. Relation of Moisture Observations to Literature

Reference(s)	Finding	Agrees with Data Previously Discussed?
Malladi et al. (2014)	APA results were not significantly affected for foaming	No
Hurley and Prowell (2005a) & Malladi et al. (2014)	Foamed asphalt was more susceptible to moisture damage than HMA at int. temp	No
Xiao et al. (2011)	Foamed asphalt had similar changed in int. temp. properties as HMA	Yes
Goh and You (2011)	Foamed asphalt int. temp. properties were less affected by moisture than HMA	No

6.4 Moisture and Freeze-Thaw Effects

Figure 6.3 investigates the effects of additional FT cycles on mixture and binder properties. All CPs considered in Figure 6.3, except CP0 (unconditioned), included the same level of moisture conditioning (i.e. 14 days in 64°C water); however, CP3 had no FT cycles following moisture conditioning, CP4 had one, and CP5 had two. Figures 6.3a, 6.3b, and 6.3c summarize data from high, intermediate, and low temperature testing, respectively. As with isolated moisture conditioning, no HLWT data is considered in these figures.

For M17, Figure 6.3a shows that final RD_{APA} increased in the range of 0.4 to 0.8-mm for all three CPs, relative to CP0. This was accompanied with increases in high T_c in the range of 0.2 to 5.8°C. As seen in Figure 6.3b, CP4 caused changes in *ML* and FE₊₂₀ of 0.2% and -0.3 kJ/m³,

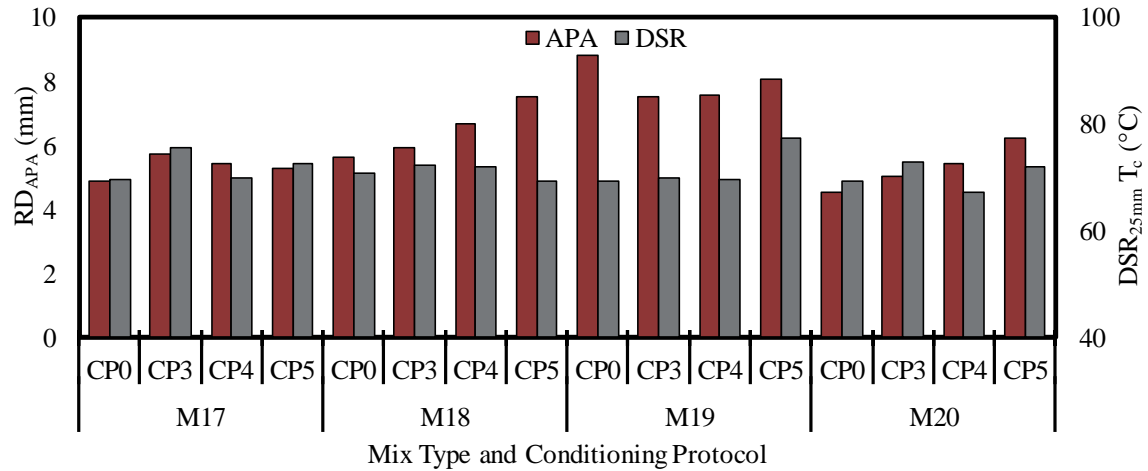
respectively while CP3 and CP5 increased ML by 3.8 and 2.1% and decreased FE_{+20} by 0.8 and 1.4 kJ/m^3 , respectively. $Pen.$ results did not follow any observable trend. Figure 6.3c shows that at low temperatures, FE_{-10} consistently decreased with the increasing severity of CPs; however, T_{c-m} decreased by nearly 3°C for CP4, but by less than 1°C due to either CP3 or CP5.

Figure 6.3a shows that RD_{APA} for M18 increased consistently due to the progressive addition of FT cycles, from 5.6-mm at CP0 to 7.6-mm after CP5. $DSR_{25\text{mm}}$ results showed changes in high T_c ranging from -1.4 to 1.4°C . Intermediate temperature properties displayed in Figure 6.3b showed an increase in M18 ML of 3.3% due to isolated moisture conditioning (i.e. CP3), but the additional FT cycles had either no further effect or decreased ML relative to CP3. CP5 increased FE_{+20} but both CP3 and CP4 caused a reduction. $Pen.$ did not change due to isolated-moisture conditioning (CP3), but CP4 and CP5 caused increases of 3.0 and 6.7 dmm, respectively. Low temperature testing (Figure 6.3c) showed a decrease in FE_{-10} , but colder T_{c-m} .

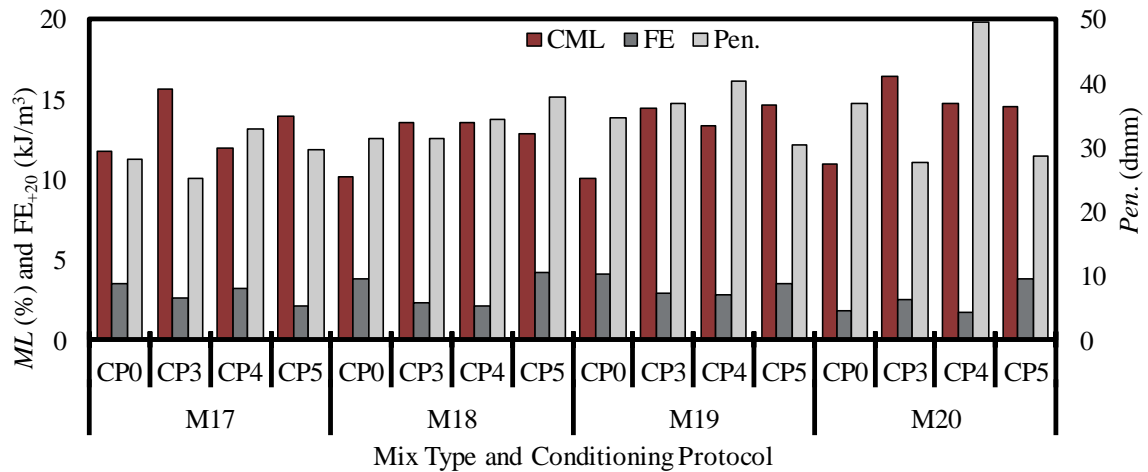
APA data summarized in Figure 6.3a for M19 shows CP3, CP4, and CP5 caused a decrease in RD_{APA} of 1.3-mm or less. High T_c increased almost 8°C due to CP5 but increased only by 0.5 and 0.1°C for CP3 and CP4, respectively. Figure 6.3b shows that at intermediate temperatures, ML increased and FE_{+20} decreased; however, $Pen.$ increased from CP0 to CP3 to CP4. CP5 though, resulted in a decrease in $Pen.$ relative to CP0. Low temperature M19 mixture results, seen in Figure 6.3c, are sporadic and inconclusive and binder results showed decrease in T_{c-m} due to CP3 and CP4 (1.5 and 2.3°C , respectively) with a 0.4°C increase due to CP5.

For M20, Figure 6.3a shows increasing RD_{APA} with the progression of CPs (4.6-mm for CP0 to 6.2-mm for CP5). High T_c increased due to CP3 and CP5 but decreased as a result of CP4. Figure 6.3b shows increase in ML for M20 yet an increased FE_{+20} . $Pen.$ was reduced by 9.3 and 8.3-dmm due to CP3 and CP5, respectively, but CP4 caused an increase of 12.7-dmm. Figure 6.3c displays an increase in FE_{-10} as well as in T_{c-m} for CP3 and CP5 specimens; however, T_{c-m} for CP4 was decreased.

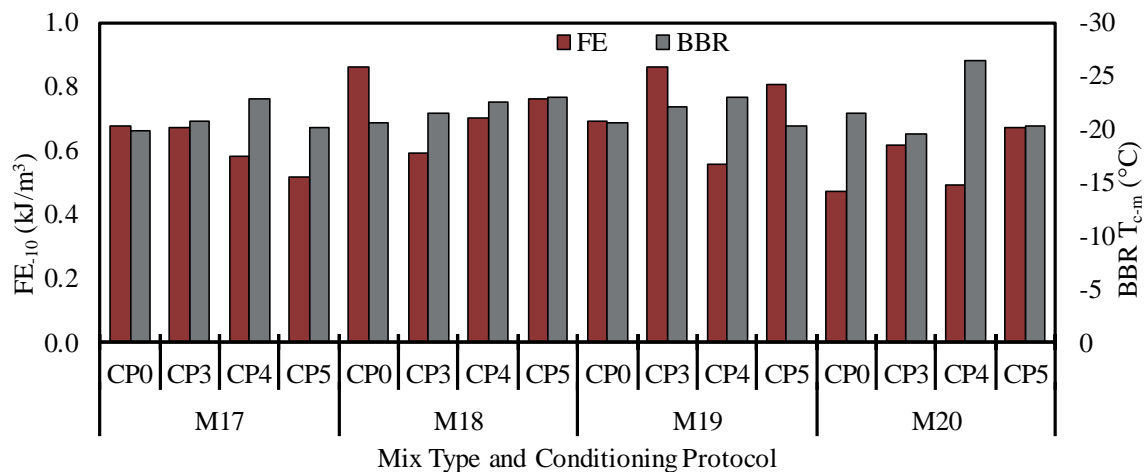
Table 6.8 summarizes the observations made here relative to mixture and binder high, intermediate, and low temperature testing for each mix type.



a) High Temperature Data



b) Intermediate Temperature Data



c) Low Temperature Data

Figure 6.3. Effects of Moisture with FT Conditioning on Asphalt Mixture and Binder Properties

Table 6.8. Summary of Moisture with FT Observations

Mix ID (WMT)	Testing Temperature Range		
	High	Intermediate	Low
M17 (HMA)	RD _{APA} : Increased T _c : Increased	ML: Increased FE ₊₂₀ : Decreased <i>Pen.</i> : Decreased or increased	FE ₋₁₀ : Decreased T _{c-m} : Decreased
M18 (Foam)	RD _{APA} : Increased T _c : Increased or decreased	ML: Increased FE ₊₂₀ : Decreased or increased <i>Pen.</i> : No change or increased	FE ₋₁₀ : Decreased T _{c-m} : Decreased
M19 (Evotherm)	RD _{APA} : Decreased T _c : Increased	ML: Increased FE ₊₂₀ : Decreased <i>Pen.</i> : Increased or decreased	FE ₋₁₀ : Increased or decreased T _{c-m} : Decreased or increased
M20 (Sasobit)	RD _{APA} : Increased T _c : Increased or decreased	ML: Increased FE ₊₂₀ : Increased or no change <i>Pen.</i> : Increased or decreased	FE ₋₁₀ : Increased T _{c-m} : Increased or decreased

In most cases found in literature, it was observed that WMAs sustained increased damage from the moisture conditioning with FT cycles than HMA (i.e. Ali et al. 2012, Diefenderfer et al. 2007, Lee and Kim 2014, Kavussi and Hashemain 2012, Prowell et al. 2007, Bonaquist 2011), which did not always agree with trends in mixture properties described here. Porras et al. (2012) subjected specimens to either 1 or 3 FT cycles and found that WMA was more susceptible to damage than HMA, which was the opposite trend observed in this analysis. As with isolated moisture conditioning, there appears to be a lack of literature concerning high and low temperature mixture property changes due to moisture conditioning with FT cycles, as well as a lack of binder data at all testing temperatures. These relations to literature are summarized in Table 6.9.

Table 6.9. Relation of Moisture with FT Observations to Literature

Reference(s)	Finding	Agrees with Data Previously Discussed?
Ali et al. (2012)	Foamed asphalt was slightly more affected than HMA at int. temperatures	No
Diefenderfer et al. (2007)	Int. temp. properties of WMA with Sasobit was less affected by moisture than HMA	No
Diefenderfer et al. (2007), Prowell et al. (2007), Bonaquist (2011), & Porras et al. (2012)	Int. temp. properties of WMA with Evotherm was more affected by moisture than HMA	Yes
Lee and Kim (2014)	Chemical additives caused similar or increased reduction in int. temp. performance	Yes
Lee and Kim (2014), Bonaquist (2011), & Porras et al. (2012)	Foamed WMA was significantly more affected than HMA at int. temp.	No
Lee and Kim (2014)	Wax WMA was significantly more affected than HMA at int. temp.	Yes
Kavussi and Hashemain (2012), Bonaquist (2011), & Porras et al. (2012)	Foamed asphalt int. temperature performance was affected at levels similar to HMA	Yes

6.5 Combined Oxidation, Moisture, and Freeze-Thaw Effects

Figure 6.4 displays results comparing individual and coupled oxidation and moisture with FT damage where Figure 6.4a summarizes high temperature properties, Figure 6.4b displays intermediate temperature properties, and Figure 6.4c shows low temperature properties. CP0 results are displayed for comparison with CP1, CP4, and CP7 results. CP1 and CP4 are displayed since the conditioning process followed for CP7 is the same as performing CP1 followed by CP4.

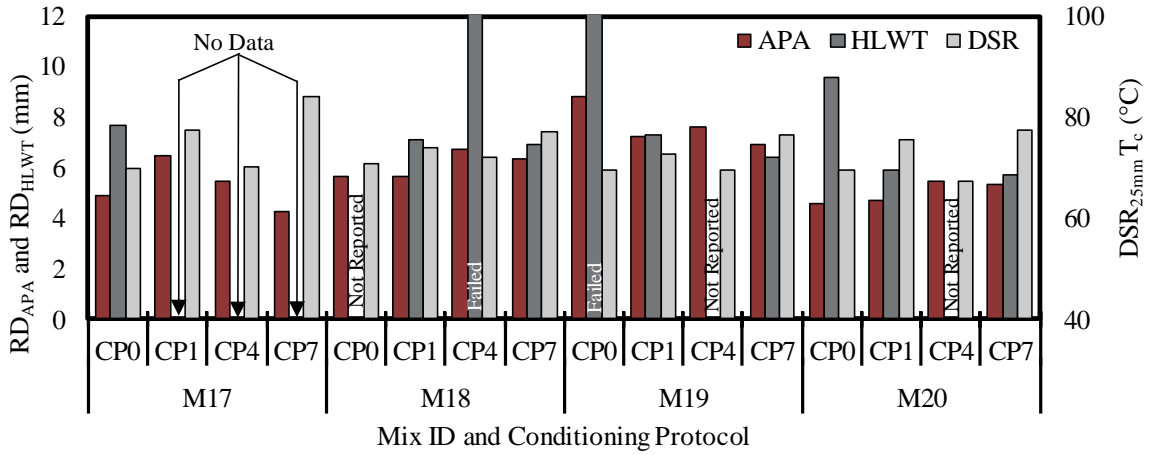
Figure 6.4a shows that CP1 and CP4 both increased RD_{APA} for M17, while CP7 reduced RD_{APA} . CP1 and CP4, when performed separately, increased high T_c by 7.6 and 0.2°C, respectively, but when applied together (i.e. CP7) T_c increased by 14.3°C. At intermediate temperatures, Figure 6.4b shows ML was increased due to CP1 and CP4 individually, but the combination caused a greater increase (i.e. 0.2% for both CPs individually and 4.4% for CP7); however, FE_{+20} values for CP7 fell between those of CP1 and CP4. $Pen.$ was much more heavily affected by CP7 than the other protocols. Low temperature M17 data summarized in Figure 6.4c shows CP7 caused a greater reduction in FE_{-10} than CP4 or CP1. T_{c-m} also increased more due to CP7 than CP1 or CP4 alone.

APA results for M18 displayed in Figure 6.4a show that CP1 had no effect on RD_{APA} , CP4 increased RD_{APA} , and CP7 caused a RD_{APA} between the two. HLWT showed CP0 and CP4 specimens reached maximum RD_{HLWT} prior to test completion (CP0 only reached maximum RD for two of the three test replicates) while CP1 and CP7 never reached maximum RD. CP7 had an increase in T_c of 6.9°C compared to 3.1°C for CP1 and 1.2°C for CP4. At intermediate temperatures, Figure 6.4b shows that for M18 CP7 increased ML , decreased FE_{+20} , and decreased $Pen.$ more than CP1 or CP4. For low temperature testing, Figure 6.4c shows CP7 reduced FE_{-10} approximately the same amount as CP1 (slightly more than CP4).

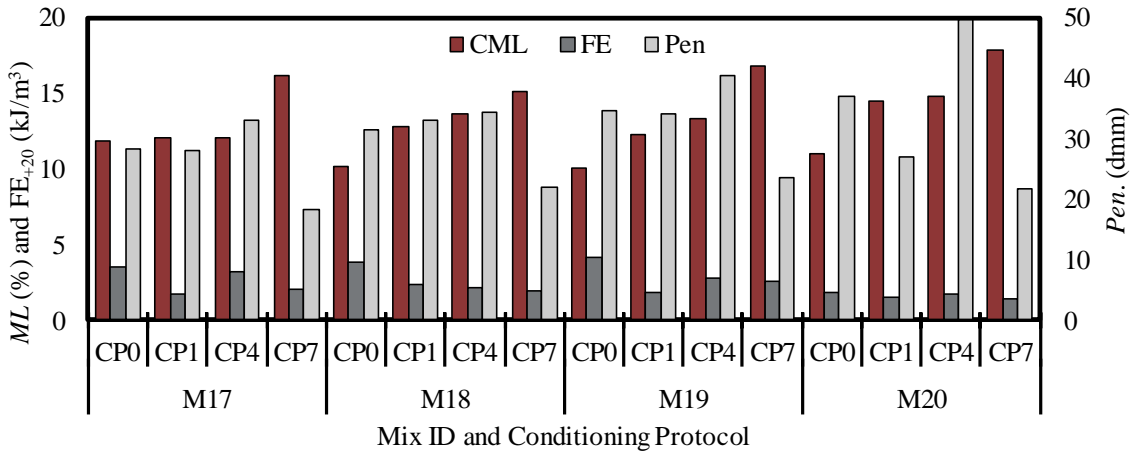
For M19, Figure 6.4a shows that all CPs considered (i.e. CP1, CP4, and CP7) decreased RD_{APA} and RD_{HLWT} (RD_{HLWT} reached max value for one of the replicates) and increased high T_c , with CP7 having the greatest effect. ML increased and $Pen.$ decreased more due to CP7 than CP1 or CP4, as seen for M19 in Figure 6.4b; however, average FE_{+20} for CP7 fell between values observed for CP1 and CP4 specimens. Note that for $Pen.$ testing, CP1 caused a decrease, CP4 caused an increase, and CP7 caused a decrease greater than CP1 (-0.7-dmm for CP1 compared to -11.0 for CP7). At low temperatures (Figure 6.4c), FE_{-10} showed the greatest reduction for M19 due to CP4 (-0.138 kJ/m³), and an increase from CP1 (0.004 kJ/m³), with CP7 falling between the two; however, binder test results showed CP7 caused the greatest increase in M19 T_{c-m} .

As seen for M20 in Figure 6.4a, all CPs increased RD_{APA} less than 1-mm. For HLWT, CP1 and CP7 decreased RD_{HLWT} to approximately the same level (a decrease from CP0 of just under 4-mm for both protocols). Figure 6.4b shows M20 ML increased consistently due to increasing damage, while FE_{+20} either did not change (as seen for CP4) or decreased by less than 0.5 kJ/m³. $Pen.$ was decreased due to CP1 and increased due to CP4; however, CP7 caused the greatest decrease (-15.3 dmm). At low temperatures (Figure 6.4c), M20 FE_{-10} increased due to each CP and T_{c-m} increased due to CP1 and CP7 but decreased due to CP4.

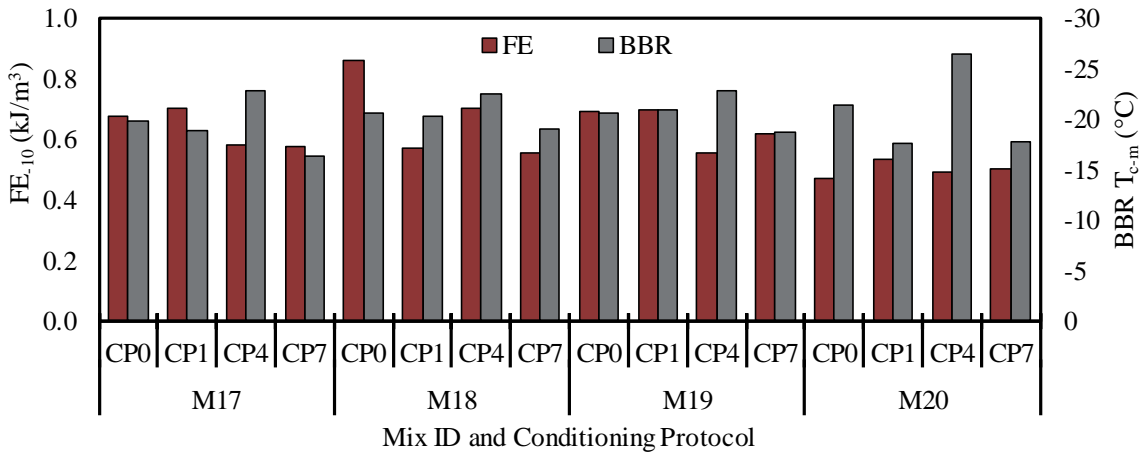
Table 6.10 summarizes these observations relative to mixture and binder high, intermediate, and low temperature testing for each mix type.



a) High Temperature Data



b) Intermediate Temperature Data



c) Low Temperature Data

Figure 6.4. Effects of Combined Oxidation and Moisture with FT Conditioning on Asphalt Mixture and Binder Properties

Table 6.10. Summary of Combined Oxidation and Moisture with FT Observations

Mix ID (WMT)	Testing Temperature Range		
	High	Intermediate	Low
M17 (HMA)	RD _{APA} : Decreased T _c : Increased	ML: Increased FE ₊₂₀ : Decreased Pen.: Decreased	FE ₋₁₀ : Decreased T _{c-m} : Increased
M18 (Foam)	RD _{APA} : Increased RD _{HLWT} : Decreased T _c : Increased	ML: Increased FE ₊₂₀ : Decreased Pen.: Decreased	FE ₋₁₀ : Decreased T _{c-m} : Increased
M19 (Evotherm)	RD _{APA} : Decreased RD _{HLWT} : Decreased T _c : Increased	ML: Increased FE ₊₂₀ : Decreased Pen.: Decreased	FE ₋₁₀ : Decreased T _{c-m} : Increased
M20 (Sasobit)	RD _{APA} : Increased RD _{HLWT} : Decreased T _c : Increased	ML: Increased FE ₊₂₀ : Decreased Pen.: Decreased	FE ₋₁₀ : Increased T _{c-m} : Increased

The only investigations found in literature which evaluated WMA mixtures with combined oxidation, moisture, and FT damages were those that performed AASHTO T283 conditioning and subsequent IDT testing following varying periods of LTOA. Of those, Cucalon et al. (2015) determined no distinguishable difference in wet IDT strengths after LTOA for WMAs produced with foaming or chemical additives compared to HMA. This supports intermediate temperature observations made in this analysis which indicate that M18 and M19 *ML* values began to approach the initially much larger *ML* of M17. Similar trends were observed in Xiao et al. (2013) for foamed asphalt and Yin et al. (2014) for Evotherm. Considering Sasobit mixtures, all relevant literature found (i.e. Xiao et al. 2013, Yin et al. 2014, and Diefenderfer and Hearon 2008) indicated that IDT strength was much less affected than HMA. This opposes *ML* and *Pen.* findings from this analysis which showed M20 properties changed more than any other mixture type considered due to the combination of oxidation, moisture, and FT damage. These relations to literature are summarized in Table 6.11.

Table 6.11. Relation of Oxidation and Moisture with FT Observations to Literature

Reference(s)	Finding	Agree with Data
Cucalon et al. (2016) & Xiao et al. (2013)	Foamed asphalt int. temp. properties approached those of HMA	Yes
Cucalon et al. (2016) & Yin et al. (2013)	Evotherm asphalt int. temp. properties approached those of HMA	Yes
Xiao et al. (2013), Yin et al. (2014), & Diefenderfer and Hearon 2008)	Sasobit was affected less than HMA at int. temp.	No

CHAPTER 7- FIELD AGING TEST RESULTS

7.1 Overview of Field Aging Results

This chapter summarizes all field aging data, considering mixture and E/R binder properties, which are displayed in Tables 7.1 and 7.2, respectively and are excerpts from chapter 4. Section 7.2 evaluates the change in mixture properties with time and which test methods were able to detect aging.

Section 7.3 analyzes the average response of each mixture type to field aging via testing of asphalt mixtures and E/R binder. Sections 7.4 and 7.5 describe how mixture and binder properties of individual mixture types changed with field aging time. In Section 7.6, linear trendline information for field aging was used to project if and when mixture and binder properties converge for the different WMTs evaluated.

Table 7.1. Mixture Test Results

Specimen Type	Mix ID	ML (%)		S _t (kPa)		FE ₊₂₀ (kJ/m ³)		FE ₋₁₀ (kJ/m ³)		RD _{APA} (mm)	
		4% ^a	7% ^b	4% ^a	7% ^b	4% ^a	7% ^b	4% ^a	7% ^b	4% ^a	7% ^b
0-yr	M17	10.4	11.8	1712	1322	2.73	3.49	0.95	0.68	5.3	4.9
	M18	9.0	10.2	1451	1207	4.64	3.83	0.86	0.86	3.0	5.6
	M19	8.9	10.1	1718	1219	4.61	4.11	0.96	0.69	6.1	8.8
	M20	10.8	11.0	1549	1166	2.76	1.78	0.68	0.47	3.9	4.6
	M17	11.9	11.8	1826	1460	---	---	---	---	3.1	4.7
1-yr	M18	11.0	15.5	1825	1435	---	---	---	---	3.1	6.6
	M19	10.4	11.0	1965	1575	---	---	---	---	6.7	6.6
	M20	12.1	11.6	1836	1390	---	---	---	---	1.9	4.2
	M17	12.8	13.6	1950	1522	0.88	3.62	0.62	0.65	---	---
2-yr	M18	12.3	12.9	1931	1565	1.17	2.42	0.83	0.99	---	---
	M19	11.9	12.8	2024	1717	1.92	2.13	0.54	0.60	---	---
	M20	11.4	14.4	1977	1494	0.35	1.34	0.70	0.68	---	---
	M17	14.1	15.2	2094	1723	---	---	---	---	---	---
3-yr	M18	13.0	13.3	2219	1802	---	---	---	---	---	---
	M19	12.2	12.9	2364	2008	---	---	---	---	---	---
	M20	13.6	16.8	2151	1614	---	---	---	---	---	---
	M17	13.3	14.4	2156	1730	1.03	2.05	0.78	0.55	2.1	3.5
4-yr	M18	14.6	15.5	2149	1778	2.32	1.46	0.61	0.78	1.7	3.5
	M19	12.5	16.0	2251	1943	2.46	2.17	0.64	0.50	2.4	4.2
	M20	14.4	17.1	2072	1587	1.74	1.35	0.66	0.61	1.8	3.6

a= 4% V_a ; b=7% V_a

Table 7.2. Binder Test Results

Specimen Type	Mix ID	Loc.	V _a (%)	Pen. (dmm)	DSR _{8mm} T _c (°C)	DSR _{25mm} T _c (°C)	BBR T _{c-s} (°C)	BBR T _{c-m} (°C)	CI + SI
0-yr	M17	LM	-	28.3	20.0	69.8	-30.9	-29.9	0.49
	M18	LM	-	31.3	18.4	70.9	-31.7	-30.6	0.56
	M19	LM	-	34.7	19.1	69.5	-31.1	-30.6	0.52
	M20	LM	-	37.0	18.2	69.4	-31.9	-31.4	0.45
2-yr	M17	T	4	20.7	21.6	77.9	-31.7	-27.2	0.54
		T	7	26.0	22.7	78.5	-30.0	-27.4	0.51
		B	7	25.7	21.9	76.2	-31.4	-29.5	0.52
	M18	T	4	24.5	22.4	76.7	-30.9	-29.0	0.52
		T	7	27.0	21.0	75.5	-31.9	-29.2	0.56
		B	7	29.0	20.2	73.3	-31.9	-30.0	0.63
	M19	T	4	28.3	20.4	74.1	-31.8	-31.2	0.50
		T	7	26.7	20.8	74.6	-31.5	-29.8	0.55
		B	7	26.7	21.9	73.7	-30.6	-29.9	0.57
	M20	T	4	20.3	23.2	77.9	-29.4	-25.7	0.49
		T	7	22.3	22.4	77.2	-29.5	-26.0	0.55
		B	7	25.7	20.8	74.8	-30.5	-27.7	0.58
4-yr	M17	T	4	21.7	22.5	79.8	-20.7	-15.6	0.50
		T	7	19.3	23.7	81.1	-19.5	-14.5	0.60
		B	7	20.7	23.0	79.2	-18.6	-16.0	0.57
	M18	T	4	20.7	23.1	79.5	-19.8	-16.3	0.68
		T	7	21.3	22.7	79.1	-20.2	-16.9	0.64
		B	7	21.3	23.6	78.2	-19.7	-16.1	0.63
	M19	T	4	23.0	22.4	78.0	-19.7	-17.1	0.66
		T	7	22.3	23.6	79.3	-18.9	-16.4	0.61
		B	7	22.8	23.3	77.3	-18.7	-17.2	0.69
	M20	T	4	20.0	23.6	80.0	-19.7	-14.5	0.57
		T	7	19.3	24.1	80.8	-18.6	-14.4	0.56
		B	7	20.7	24.2	78.6	-18.4	-13.4	0.60

7.2 Tests Methods Evaluation for Field Aged Data

Statistical analysis was conducted to demonstrate capabilities of mixture test methods to detect asphalt pavement damage. Table 7.3 provides results of multiple comparison *t*-grouping produced following an analysis of variance for average mixture property values of each year. Values displayed in Table 7.3 are the average values of all mixture types for each year of aging. All years assigned to identical letters from *t*-grouping are statistically similar; for example, 1-yr and 2-yr *ML* values at 4% V_a were assigned to letter “B” as they were statistically comparable. A year can be assigned to multiple *t*-groups if the mean was statically similar to means from multiple years. For example, 1-yr at 7% V_a for CML test was assigned to letters “B” and “C” which means that 1-yr statistically similar to 0-yr and 2-yr; however, 0-yr and 2-yr were statistically significantly different.

Figure 7.1 shows normalized values of all mixture tests with respect to time. All mixture test values were normalized to range between zero and one using Equation 7.1. Ideally 0-yr results should be represented by values of “0” and 4-yr should be represented by “1”, indicating that 0-yr specimens were the least aged and 4-yr specimens were the most aged. As an example of Eq 7.1, the averaged *ML* value of 2-yr at 7% V_a (13.4) is considered X_i. The highest value for *ML* at 7% (15.8) is considered X_{max} while the lowest value (10.8) is considered X_{min}. Thus, Y_i is equal to 0.5.

$$Y_i = \frac{X_i - X_{max}}{X_{max} - X_{min}} \quad (7.1)$$

Where:

Y_i : Normalized value of X_i

X_i : Test value of a given test

X_{max} : Higher test value of a given test

X_{min} : Lower test value of a given test.

Figure 7.1a and 7.1e show that both V_a levels of CML and APA captured field aging in a progressive manner, with field aging time consistently increasing ML and decreasing RD_{APA} . This observation is supported in Table 7.3, mean ML and RD_{APA} indicated statistically significant increases damage/aging with field aging time. IDT for both V_a levels increased with field aging from 0-yr to 3-yr; however, 4-yr values were lower than 3-yr values as shown in Figure 7.1b. Table 7.3; however, indicates there was no significant difference between the two tensile strengths. FE_{+20} at 4% V_a had scattered results, where 2-yr specimens had the greatest relative response while FE_{+20} at 7% V_a progressively increased with aging (Figure 7.1c) Table 7.3 shows statistical differences among FE_{+20} means at 4% and 7% V_a . At both V_a levels, FE_{-10} showed scattered results. Specimens at 4% V_a had similar aging rates for 2-yr and 4-yr while 7% V_a had the lowest aging rate at 2-yr as shown in Figure 7.1d. Table 7.3 showed that there is no statistical different between means of FE_{-10} at 4% or 7% V_a . It should be noted for 7% V_a specimens, the 2-yr mean was higher than at 0-yr.

Table 7.3. t -grouping Test for Mixture Properties with Respect to Field Aging Time

V_a (%)	yr	ML (%)		S_t (kPa)		FE_{+20} (kJ/m ³)		FE_{-10} (kJ/m ³)		RD_{APA} (mm)	
		t -grouping	Mean	t -grouping	Mean	t -grouping	Mean	t -grouping	Mean	t -grouping	Mean
4	0	C	9.8	D	1608	C	3.69	A	0.86	B	4.58
	1	B	11.4	C	1863	---	---	---	---	AB	3.70
	2	B	12.1	B	1971	A	1.08	A	0.67	---	---
	3	A	13.2	A	2207	---	---	---	---	---	---
	4	A	13.7	A	2157	B	1.89	A	0.67	A	2.00
7	0	C	10.8	C	1229	B	3.30	A	0.68	B	5.98
	1	CB	12.5	B	1465	---	---	---	---	B	5.53
	2	B	13.4	B	1575	AB	2.43	A	0.72	---	---
	3	BA	14.6	A	1787	---	---	---	---	---	---
	4	A	15.8	A	1760	A	1.76	A	0.60	A	3.70

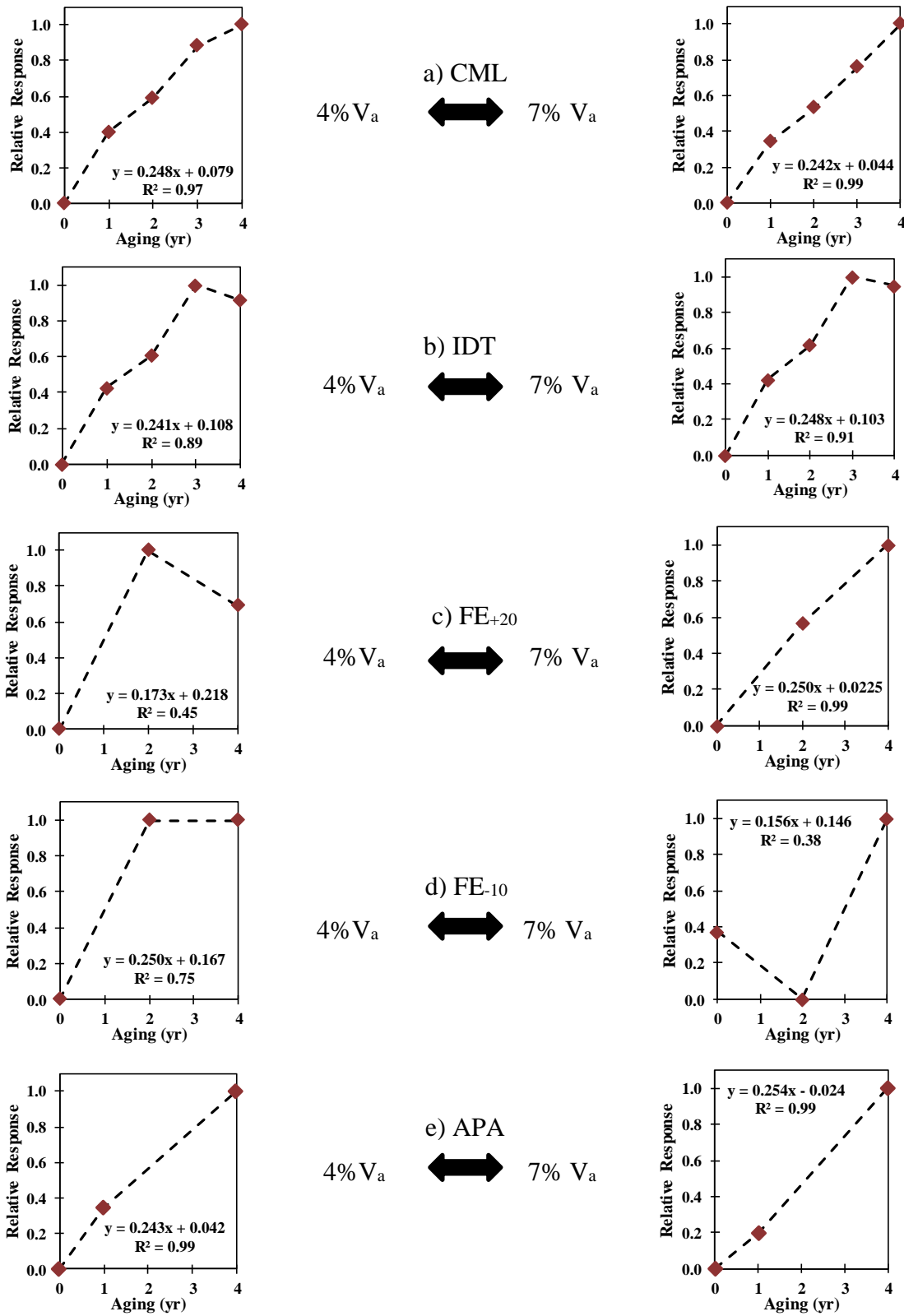


Figure 7.1. Relative Responses Based on Mixture Test Results

7.3 Statistical Comparison of Mixture Types

Tables 7.4 and 7.5 provide results of multiple comparison *t*-groupings produced following an analysis of variance for mixture and binder properties based on the average values of each mixture type considering the different mixture and binder properties. Assignment of *t*-group letters was performed in the same manner as described in Section 7.2. Values in Tables 7.4 and 7.5 were obtained by averaging all values for each property within each mixture type, across all aging levels.

As shown in Table 7.4, at 4% V_a *ML* indicated that M20, and M17 had statistically similar durability (based on CML) while M19 was statistically more durable. M18 had similar durability to both M19 and M17. S_t was statistically similar for M18, M20, and M17 had statistically similar S_t while M19 was statistically higher. FE_{+20} showed that M18 and M19 had statistically better cracking resistance than M17 while M20 was statistically similar to M17. FE_{-10} and APA indicated no difference between HMA and WMA in thermal cracking resistance or rutting susceptibility, respectively. *ML*, FE_{+20} , and APA showed no statistical difference among all mixture types for 7% V_a specimens. S_t showed that M20 was statistically softer (i.e. lowest S_t) than all other mixtures and M19 was significantly stiffer. M18 and M17 were statistically similar with values falling between those of M20 and M19. FE_{-10} showed that M18 had the best thermal cracking resistance at 7% V_a , while M19, M20, and M17 were statistically similar.

Table 7.5 showed there was no statistical difference between HMA and WMA according to DSR_{8mm} , T_{c-s} , T_{c-m} , or FTIR results for top slices of 4% V_a specimens. *Pen.* showed that M18, M20, and M17 had statistically similar stiffness. M19 was statistically softer than M17 but was statistically similar to M20 and M18. DSR_{25mm} indicated similar rutting performance for M18, M20, and M17. M19 was statistically more susceptible to rutting than M17 and was not statistically different than M18. For top slices of 7% V_a specimens, *Pen.*, DSR_{25mm} , and BBR stiffness and *m*-value showed statistically similar performance between WMA and HMA. DSR_{8mm} and FTIR results were statistically similar for M19, M20, and M17 while M18 was statistically more oxidized according to FTIR results but still more resistant to fatigue cracking based on DSR_{8mm} . For 7% V_a bottom slices, all binder tests methods showed statistically similar binder properties for all mixtures, except FTIR which showed that M18 was statistically more oxidized than M17.

Table 7.4. *t*-grouping Test for Mixture Properties Based on Mixture Type

V_a (%)	Mix ID	<i>ML</i> (%)		S_t (kPa)		FE_{+20} (kJ/m ³)		FE_{-10} (kJ/m ³)		RD_{APA} (mm)	
		<i>t</i> -groups	Mean	<i>t</i> -groups	Mean	<i>t</i> -groups	Mean	<i>t</i> -groups	Mean	<i>t</i> -groups	Mean
4	M17	A	12.5	B	1948	B	1.55	A	0.78	A	3.50
	M18	AB	12.0	B	1915	A	2.71	A	0.77	A	2.60
	M19	B	11.2	A	2064	A	3.00	A	0.71	A	5.07
	M20	A	12.5	B	1917	B	1.62	A	0.68	A	2.53
7	M17	A	13.4	B	1551	A	3.05	B	0.61	A	4.37
	M18	A	13.5	B	1557	A	2.63	A	0.87	A	5.23
	M19	A	12.6	A	1692	A	2.80	B	0.60	A	6.53
	M20	A	14.2	C	1450	A	1.49	B	0.59	A	4.13

Table 7.5. *t*-grouping Test for Binder Properties Based on Mixture Type

V _a (%)	Mix ID	Pen. (dmm)		DSR _{8mm} T _c (°C)		DSR _{25mm} T _c (°C)		BBR T _{c-s} (°C)		BBR T _{c-m} (°C)		FTIR	
		<i>t</i> -groups	Mean	<i>t</i> -groups	Mean	<i>t</i> -groups	Mean	<i>t</i> -groups	Mean	<i>t</i> -groups	Mean	<i>t</i> -groups	Mean
4 ^a	M17	B	23.7	A	21.4	A	75.8	A	-21.1	A	-17.6	A	0.51
	M18	AB	25.7	A	21.3	AB	75.7	A	-20.8	A	-18.6	A	0.59
	M19	A	28.7	A	20.6	B	73.9	A	-20.9	A	-19.6	A	0.56
	M20	AB	28.3	A	21.7	A	75.8	A	-20.3	A	-17.2	A	0.50
7 ^a	M17	A	24.3	A	22.1	A	76.5	A	-20.1	A	-17.3	B	0.53
	M18	A	26.3	B	20.7	A	75.2	A	-21.3	A	-18.9	A	0.59
	M19	A	28.0	AB	21.2	A	74.5	A	-20.5	A	-18.9	AB	0.56
	M20	A	26.0	AB	21.6	A	75.8	A	-20.0	A	-17.3	B	0.52
7 ^c	M17	A	25.0	A	21.6	A	75.1	A	-20.3	A	-18.5	B	0.53
	M18	A	27.0	A	20.7	A	74.1	A	-20.7	A	-18.9	A	0.61
	M19	A	28.3	A	21.4	A	73.5	A	-20.1	A	-19.2	AB	0.59
	M20	A	28.0	A	21.1	A	74.3	A	-20.3	A	-17.5	AB	0.54

a: top slices of specimens; b: bottom slices of specimens

7.4 Mixture Properties

While there were not always statistically significant differences among average mixture values, there are general observations that can be made concerning how mixture and binder properties of individual mixtures changed. At low temperature, FE₋₁₀ was used to evaluate thermal cracking for WMTs compared to HMA. CML, IDT, and FE₊₂₀ were utilized at intermediate temperature to evaluate mixture durability and cracking resistance. APA was used to evaluate rutting potential at high temperature.

7.4.1 Low Temperature properties

FE₋₁₀ was used to evaluate thermal cracking resistance of mixtures as shown in Figure 7.2. FE₋₁₀ values should reduce with aging; however, FE₋₁₀ for 4% V_a results showed that M17, M19, and M20 increased at some levels of aging and 7% V_a results of M18 and M20 also increased. Initially, M20 were shown by FE to have lower thermal cracking resistance for both V_a levels compared to M17, M19, and M18. M19 and M17 were comparable and had the highest resistance at 4% V_a while M18 had the highest resistance at 7% V_a. After aging, 4% V_a WMA specimens all had comparable low temperature cracking resistance, which was lower than M17. At 7% V_a, M19 and M17 had the lowest thermal cracking resistance while M18 showed slightly better thermal cracking resistance than all other mixtures.

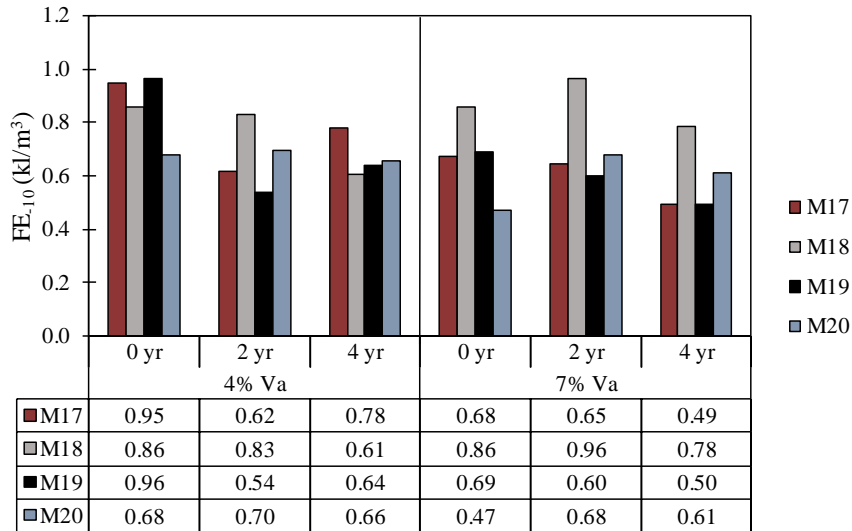


Figure 7.2. FE₋₁₀ Field Aged Results

7.4.2 Intermediate Temperature Properties

CML, IDT, and FE₊₂₀ were used to capture changes in intermediate temperature properties of mixtures due to field aging. Figure 7.3 shows *ML* results for HMA and WMA at 4% and 7% V_a indicated initially similar or better durability for WMA compared to HMA. M20 and M17 were comparable and had the lowest durability while M18 and M19 were similar to each other and showed better durability. After field aging, 4% V_a M19 specimens were most durable while M18 and M20 had the lowest durability. For 7% V_a, M17 was slightly more durable than WMA. For WMA, M20 seemed to be less durable than M18 and M19 while M18 was similar to or slightly less durable than M17.

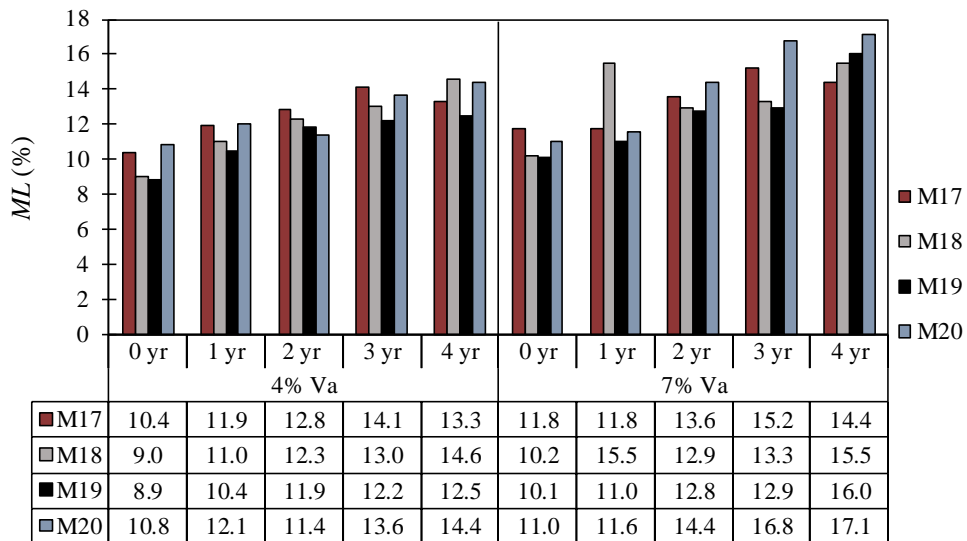


Figure 7.3. CML Field Aged Results

Figure 7.4 shows IDT test results from field aged specimens at 4% and 7% V_a . Initially, for 4% V_a specimens, M18 was the softest mixture followed by M20, with M17 and M19 having larger tensile strengths which were similar. Considering specimens at 7% V_a , HMA was initially the stiffest mixture with all WMA mixtures having similar S_t . After aging, for both V_a levels, M19 was the softest mixture, M20 was the stiffest. M17 and M18 had similar tensile strength which were between M19 and M20. It should be noted that for all WMAs S_t continuously increased from 0 to 3 years but slightly decreased from 3 to 4 years.

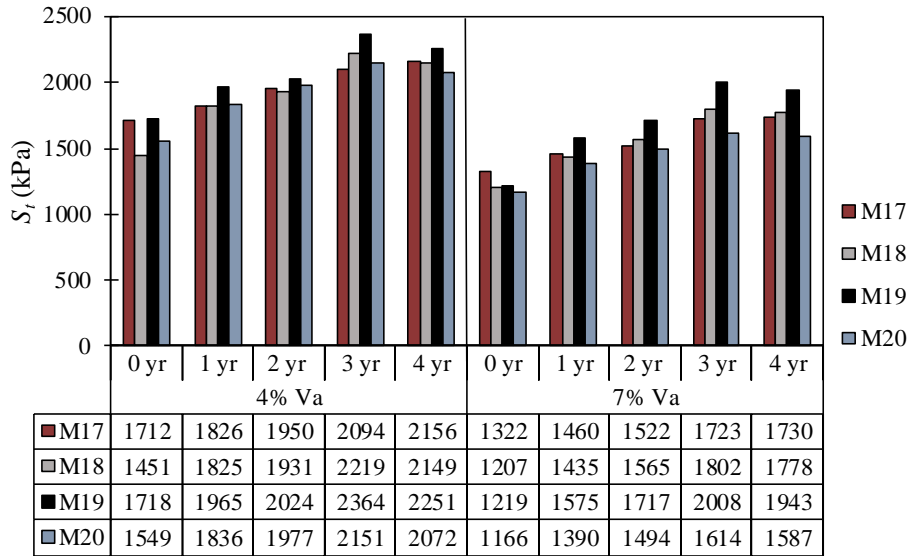


Figure 7.4. IDT Field Aged Results

FE_{+20} test results of field aging are shown in Figure 7.5 for 4% and 7% V_a levels. FE_{+20} values should decrease with aging time; however, at 4% V_a FE_{+20} was lower after 2 years than 4. For 7% V_a specimens, 2-yr FE_{+20} values were similar to 4-yr values for M19 and M20. For 4% V_a specimens, M18 and M19 were comparable and had higher cracking resistance than M17 and M20, before and after aging with M17 having the lowest cracking resistance after 4 years of field aging. For 7% V_a specimens, M19 initially had the highest cracking resistance followed by M18 then M17 with M20 having the lowest resistance. After field aging, M19 and M17 were comparable and had higher cracking resistance than M18 and M20, which were also comparable.

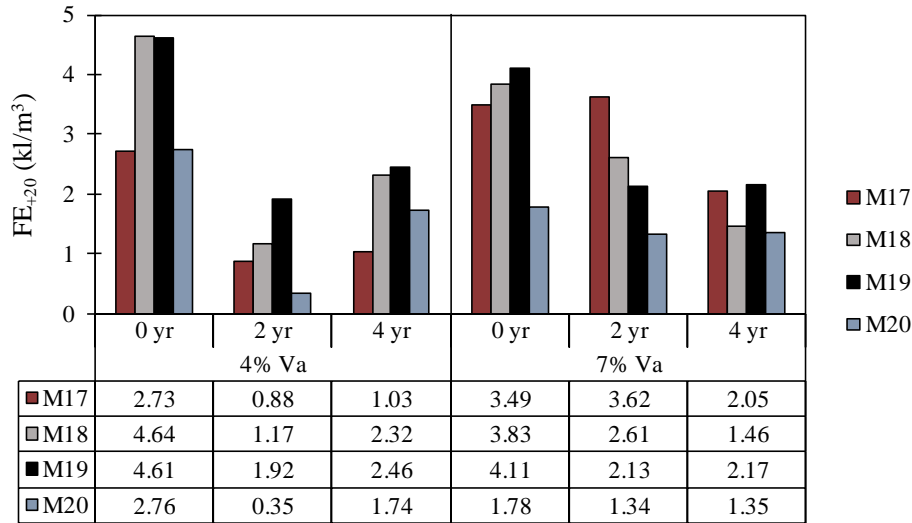


Figure 7.5. FE₊₂₀ Field Aged Results

7.4.3 High Temperature Properties

Rutting behavior of WMA and HMA is displayed in Figure 7.6. For 4% V_a specimens, M18 and M20 had lower rutting susceptibility than M17 while M19 initially had the highest amount of rutting. After aging, M19 was comparable to M17 while M18 and M20 had slightly lower RD_{APA}. Initially at 7% V_a, M20 had the lowest rutting and was comparable to M17 while M19, had the highest rutting and M18 slightly more rut prone than M17. After aging both M18 and M20 had rutting results similar to M17 while M19 still had slightly higher rutting than M17.

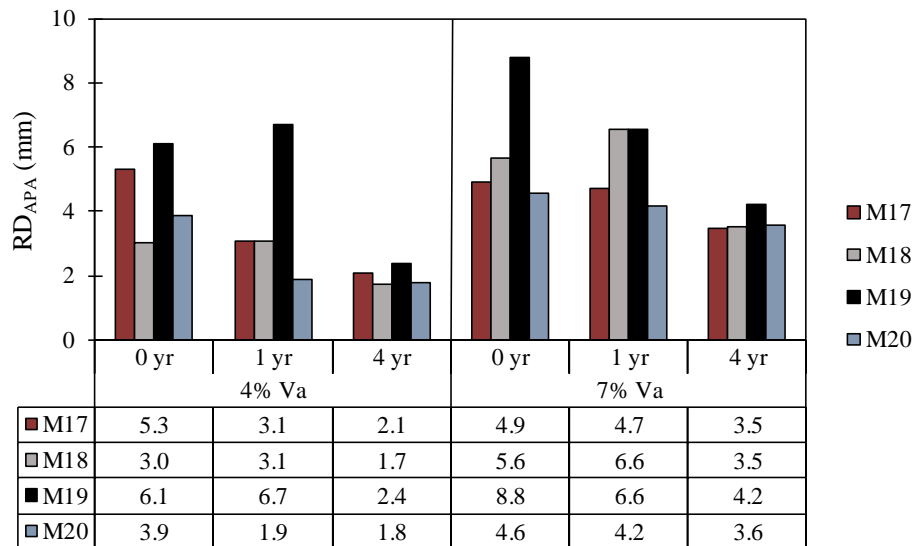


Figure 7.6. APA Field Aged Results

7.5 Binder Properties

Binder properties were evaluated at low temperatures with BBR stiffness and m-values. At intermediate temperatures, *Pen.* and DSR_{8mm} were used to measure stiffness and fatigue cracking properties. DSR_{25mm} was utilized to measure high temperature binder properties, and FTIR was used to investigate changes in binder chemical properties due to field aging.

Figure 7.7 shows aging rates for 4% and 7% V_a specimens considering E/R binder from top and bottom slices of specimens separately. Figure 7.7 shows that for all high and intermediate temperature binder properties (i.e. DSR_{25mm} , DSR_{8mm} , and *Pen.* results) top slices of both 4% and 7% V_a specimens aged a faster rate from 0-yr to 2-yr than from 2-yr to 4-yr; however, binder from bottom slices aged at a mostly constant rate for the entire 4 years. Low temperature testing resulted in mixed trends. Constant aging rates for the entire 4 years were observed for T_{c-s} for 7% V_a specimen bottoms, and T_{c-m} for 4% and 7% V_a specimen tops. T_{c-s} for 4% and 7% V_a tops, T_{c-m} for 7% V_a bottoms indicated a decreased rate of aging for the first two years of field aging compared to the second two. For chemical properties, CI+SI for 4% and 7% specimen tops showed a decreased rate of aging in the first two years relative to the second two years. 7% V_a specimen bottoms showed the opposite trend, where the first two years experienced faster aging than the second two years.

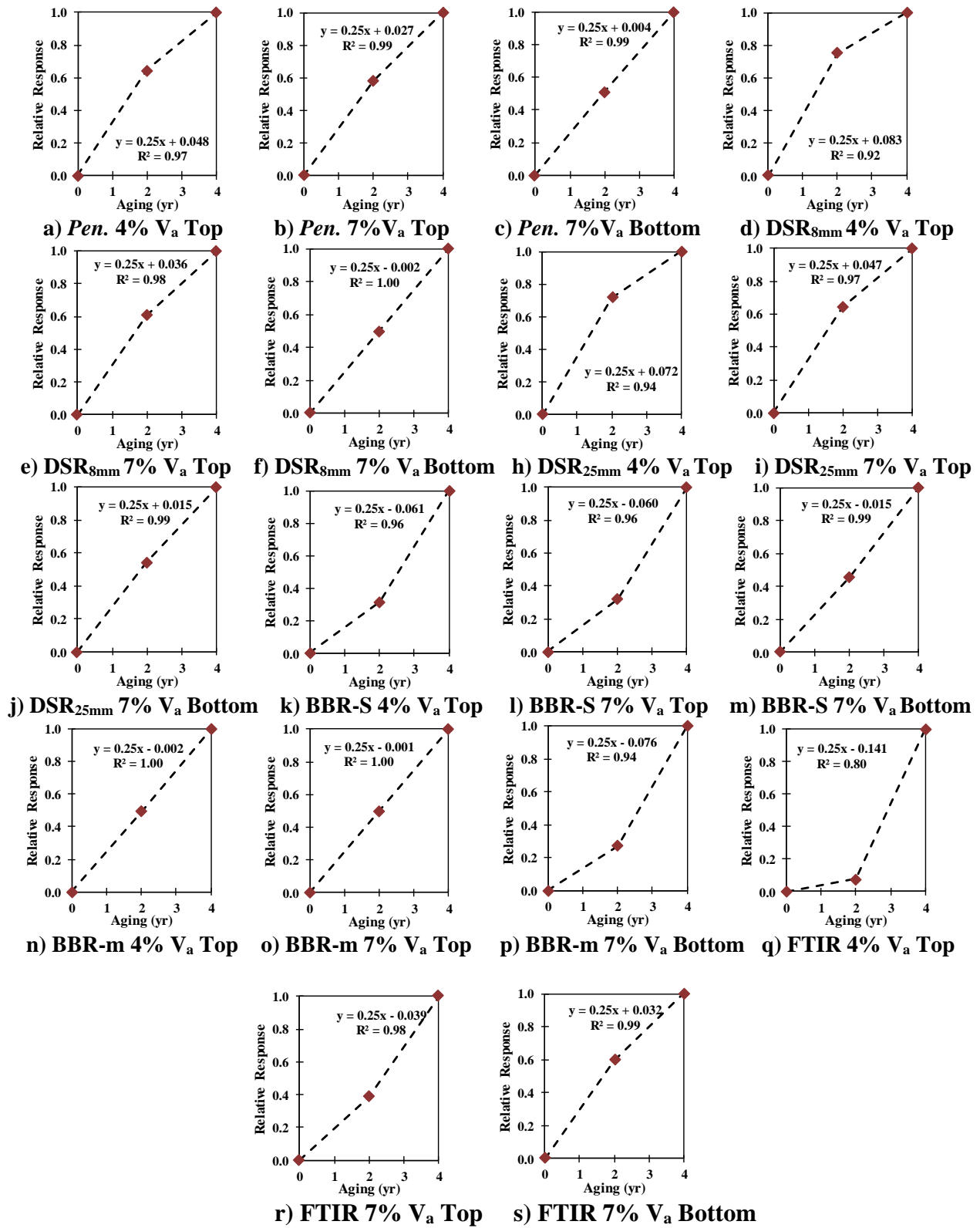


FIGURE 7.7. Relative Binder Responses

7.5.1 Low Temperature properties

Figure 7.8 shows T_{c-m} for all mixtures and V_a levels. Initially, all mixtures had mostly comparable thermal cracking resistance, with WMA having slightly greater resistance. After 4 year of aging, 4% V_a tops of specimens showed that M19 was most resistant to thermal cracking while M20 was least resistant and M18 had slightly better resistance than M17. 7% V_a specimen tops showed that M17 and M20 had approximately similar thermal cracking resistance while M18 and M19 had comparable resistance which was better than M17. After 4 years, 7% V_a bottoms of specimens showed that M20 had lowest cracking resistance while M19 had the highest and M18 was comparable to M17.

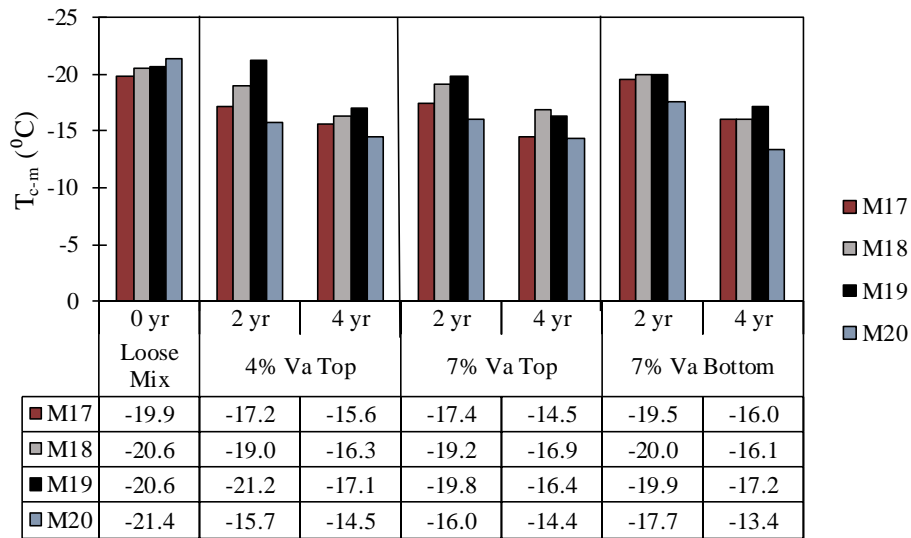


Figure 7.8. BBR m-value Field Aged Results

Figure 7.9 displays T_{c-s} values. Initially, WMA and HMA had comparable thermal cracking resistance with WMA being slightly softer than HMA in some cases. Tops of specimens at 4% V_a results showed that after 4 years, WMA had slightly reduced thermal cracking resistance compared to HMA. For 7% V_a specimens tops, 2 years of aging resulted in M18 and M19 having much greater cracking resistance than M17 or M20; however, after 4 years M19 and M20 were slightly more susceptible to thermal cracking than M17 while M18 showed slightly better properties. 7% V_a bottoms showed that HMA and WMA had comparable thermal cracking resistance after 4 years of aging.

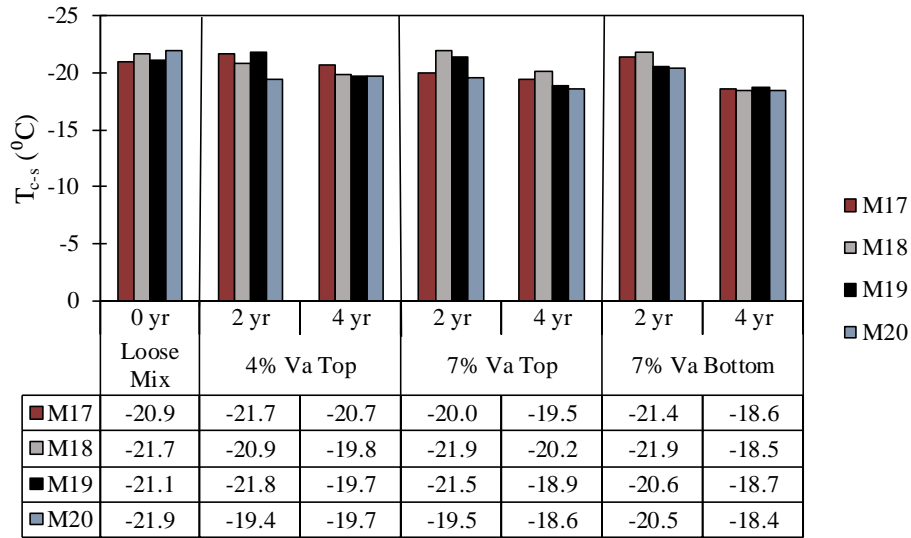


Figure 7.9. BBR Stiffness Field Aged Results

7.5.2 Intermediate Temperature Properties

Pen. and DSR_{8mm} were used to measure intermediate temperature binder properties. Figure 7.10 and 7.11 display *Pen.* and DSR_{8mm} test results, respectively. Initially, for HMA, *Pen.* indicated stiffer binder than WMA as shown by the lower *Pen.* value in Figure 7.10. Of the WMA mixtures, M20 had the softest binder, followed by M19 then M18. For top slices of 4% V_a specimens, 4 years of field aging resulted in mostly similar stiffness among all mixtures. For both tops and bottoms of 7% V_a specimens, M17 and M20 had comparable *Pen.* values after aging and were both slightly stiffer than M18 and M19, which were also comparable.

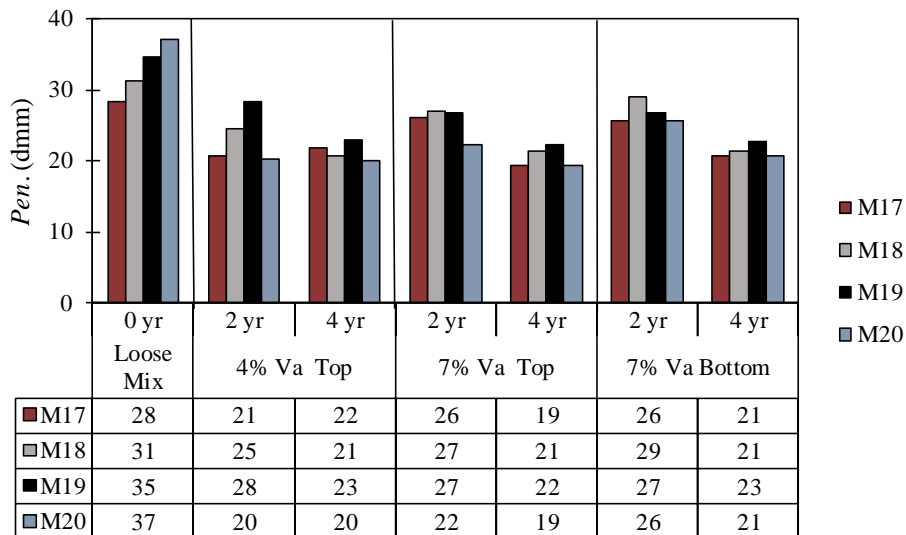


Figure 7.10. Pen. Field Aged Results

Figure 7.11 shows that at 0-yr, M17 had the greatest intermediate T_c followed by M19, M18, then M20 with a range of 1.8°C, and in all cases field aging resulted in increases in intermediate T_c . For all specimen types (i.e. 4% V_a tops and 7% V_a tops and bottoms) 2 years of field aging either slightly increased or had negligible effect on the range of intermediate T_c values among the different mixture types, relative to that observed for CP0. After 4 years of field aging, the range of intermediate T_c values had decreased slightly from 1.8°C for loose mix at 0-yr to 1.2°C for 4% V_a tops, 1.4°C for 7% V_a tops, and 1.2°C for 7% V_a bottoms.

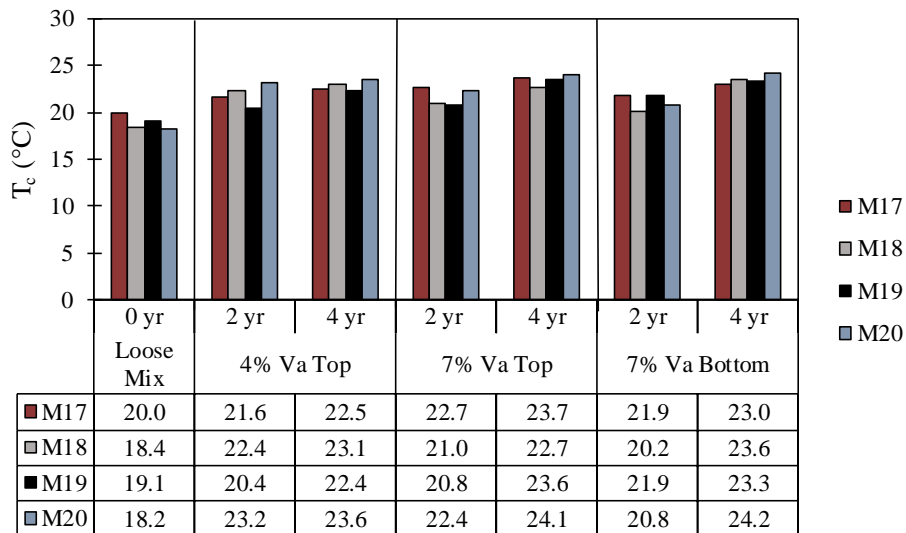


Figure 7.11. DSR_{8mm} Field Aged Results

7.5.3 High Temperature Properties

High temperature binder properties according to DSR_{25mm} (i.e. T_c) are displayed in Figure 7.12. Initially, HMA and WMA had comparable rutting resistance with T_c for M18 being slightly higher than other mixture types. After aging, 4% V_a specimen tops showed that M19 was slightly more susceptible to rutting while M18, M20, and M17 were all comparable. For 7% V_a tops, M17 was slightly more rut resistant than M18 and M19 but was very similar to M20. After 4 years, 7% V_a bottoms for HMA were slightly better than WMA in terms rutting resistance where M18 and M20 had similar resistance (just below that of M17) and M19 binder had the lowest grade. Properties were similar for all binder at any given aging level.

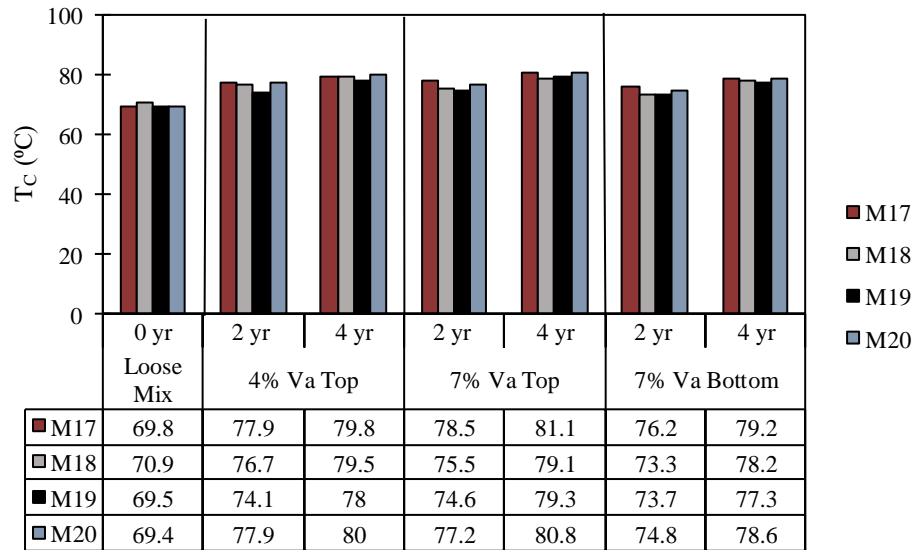


Figure 7.12. DSR_{25mm} Field Aged Results

7.5.4 Binder Chemical Properties

Figure 7.13 summarizes FTIR results of control and field aged specimens and shows that initially, M18 asphalt was the most oxidized (i.e. highest CI+SI) followed by M19, M17, then M20. The effects of field aging on CI+SI values varied depending on V_a level and binder sample location (top or bottom of specimen). For 4% V_a specimen tops, aging had little effect on HMA but meaningfully oxidized WMA binders, with M18 and M19 still having noticeably higher CI+SI values than M17 and M20. For 7% V_a specimen tops, 4 years of field aging results in similar increases in CI+SI for all mixtures. Considering 7% V_a bottoms, M19 appeared to be more heavily oxidized than other mixture types. Also, it can be observed among the 7% V_a data that the binder samples recovered from specimen bottoms appear to have been oxidized more after 4 years than specimen tops. This opposes observations made for most other binder properties that were evaluated in this analysis.

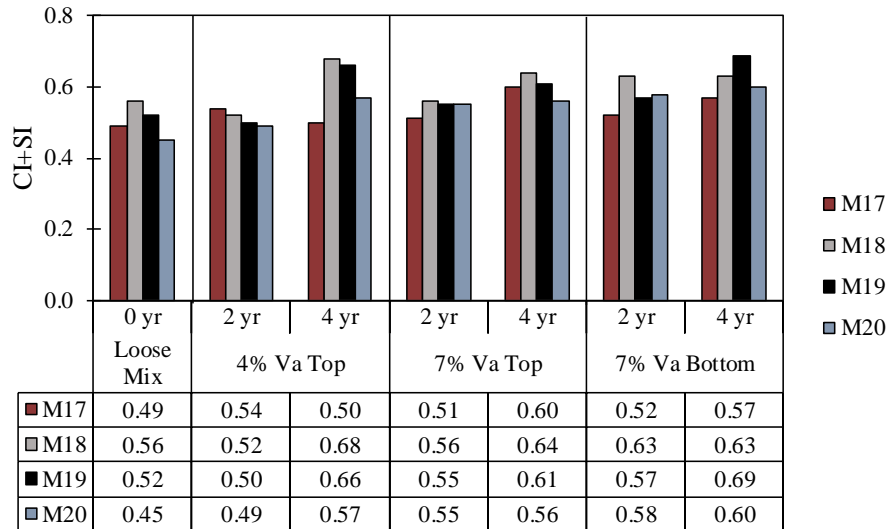


Figure 7.13. FTIR Field Aged Results

7.6 Convergence of WMA and HMA Properties with Field Aging

As described throughout previous sections, HMA and WMA mixtures and binders have different initial properties, mostly indicative of stiffer behavior for HMA compared to WMA. In such cases where WMA ages at a faster rate than HMA, these properties converge. To determine such conversion points in time, linear field aging trendlines from Chapter 4 were used, by setting y-values (i.e. input for a mixture or binder test result) of two mixtures equal to each other and solving for the required time of field aging (t_F). For example, Equations 7.2 and 7.3 represent linear trendlines for ML of 4% V_a M17 and M18 specimens, respectively (from Figure 4.1a in Chapter 4). As seen in Equation 7.4, when ML values for M17 and M18 are set equal to each other and rearranged to solve for t_F , the result is a convergence time of 3.0 years. Tables 7.6 and 7.7 describe these convergence times based on mixture and binder properties, respectively. Note that an “X” denotes a scenario where properties did not converge in positive time. For example, at 4% V_a , S_t of M19 was initially greater than that of M17; however, trendlines from Figure 4.3a in Chapter 4 indicate that M19 still aged at a faster rate than M17 (i.e. greater slope). Thus, convergence time for S_t , if calculated, would be a negative value.

$$ML_{M17} = 0.79t_F + 10.94 \quad (\text{Eq 7.2})$$

$$ML_{M18} = 1.32t_F + 9.35 \quad (\text{Eq 7.3})$$

$$t_F = \frac{10.94-9.35}{1.32-0.79} = \frac{1.59}{0.53} = 3.0 \quad (\text{Eq 7.4})$$

Where:

ML_{M17} = Mass Loss of M17 (%)

ML_{M18} = Mass Loss of M18 (%)

t_F = time in field (year)

Note that in almost all cases, WMA mixture properties converged with HMA indicating that overall, they age at an increased rate. When comparing the different WMTs to each other, the

results are mixed. It appears dependent not only the mixture type but also on test method and V_a level. Values in Table 7.6 that are bold are those where the WMA of interest had a property indicative of a stiffer behavior compared to HMA. In such cases, mixture properties still converged due to the WMA aging at a slower rate. It can be observed that the majority of these occurred with fracture properties and rutting resistance of M20. Considering binder properties in Table 7.7, convergence is not consistent. There are more cases where WMA and HMA properties did not converge compared to mixture properties; however, it can be noted that the majority of these points that did not converge were for M19 and M17. When comparing the different WMTs to each other, there were more cases where properties did not converge than when comparing them to HMA, indicating similar results to mixture properties. These convergence times, or lack thereof, also appear to be dependent on variables other than just WMT.

Table 7.6. Time in Years for Mixtures to Converge (Mixture Properties)

Comparison	Mix type	ML		S_r		FE ₊₂₀		FE ₋₁₀		RD _{APA}	
		4% ^a	7% ^b	4% ^a	7% ^b	4% ^a	7% ^b	4% ^a	7% ^b	4% ^a	7% ^b
HMA vs WMA	M17 vs M18	3.0	3.8	2.5	1.9	9.3	0.2	1.0	X	4.2	4.9
	M17 vs M19	14.3	3.6	X	0.2	14.0	0.0	0.3	0.0	6.5	4.8
WMA vs WMA	M17 vs M20	2.8	1.1	3.5	X	1.6	8.2	5.0	2.2	4.9	3.6
	M18 vs M19	0.0	2.9	6.6	X	X	0.5	X	X	5.3	4.7
WMA vs WMA	M18 vs M20	3.0	X	2.0	X	5.3	4.4	3.6	7.0	X	4.5
	M19 vs M20	45.0	X	X	X	6.7	5.4	2.5	2.1	5.7	4.6

a: 4% V_a ; b: 7% V_a ; X: mixes do not converge.

Table 7.7. Time in Years for Mixtures to Converge (Binder Properties)

Comp.	Mix Type	V_a (%) and Location	Pen.	DSR _{8mm}	DSR _{25mm}	BBR-S	BBR-m	FTIR
WMA vs. HMA	M17 vs M18	4% ^T	3.9	2.0	1.7	1.2	X	X
		7% ^T	10.0	11.3	1.1	110.0	X	8.8
		7% ^B	5.9	3.6	0.2	4.0	4.7	40.0
	M17 vs M19	4% ^T	6.0	5.5	X	1.3	X	0.6
		7% ^T	6.0	7.0	X	3.5	X	8.0
		7% ^B	4.9	2.7	X	X	X	X
M17 vs M20	4% ^T	2.8	1.5	2.0	0.6	1.5	2.6	
	7% ^T	2.8	3.1	16.0	1.7	2.0	X	
	7% ^B	3.3	2.7	X	1.7	1.1	1.1	
M18 vs M19	4% ^T	14.7	0.0	X	0.9	X	8.0	
	7% ^T	4.3	X	2.9	X	2.9	10.0	
	7% ^B	3.7	4.8	7.5	5.6	0.8	2.4	
WMA vs. WMA	M18 vs M20	4% ^T	2.2	0.0	1.8	X	X	X
		7% ^T	1.8	0.0	1.6	X	0.1	10.0
		7% ^B	2.4	0.0	1.7	X	0.5	5.0
M19 vs M20	4% ^T	X	0.0	X	X	X	X	
	7% ^T	0.7	0.9	0.2	0.4	X	10.0	
	7% ^B	1.8	2.7	X	2.6	0.5	X	

Comp.= Comparison; 4%^T= 4% V_a top specimens slices; 7%^T= 7% V_a top specimens slices; 7%^B= 7% V_a bottom specimens slices

CHAPTER 8 - SIMULATION OF FIELD AGING WITH LABORATORY CONDITIONING PROTOCOLS

8.1 Overview

This chapter examines the correlation between results from field aged asphalt specimens to those from laboratory conditioned specimens to produce reasonable ranges of simulated field aging time for the CPs discussed in previous chapters. All field aged data excerpted from chapter 4 and used in this analysis is displayed in Table 8.1, and all relative laboratory conditioned data is displayed in Table 8.2. Section 8.2 uses linear trendlines from Chapter 4 and average lab conditioned data summarized in Table 8.2 (i.e. individual mixture values are not considered) to estimate simulated field aging times for each CP. CML, IDT, FE₊₂₀, FE₋₁₀, and APA were utilized to evaluate mixture properties at a range of test temperatures. CML and IDT evaluated specimens compacted to 4% and 7% V_a while FE₊₂₀, FE₋₁₀, and APA evaluated only those at 7% V_a. Section 8.3 summarizes these simulated field aging times.

Table 8.1. Field Aged Mixture Test Results

Specimen Type	Mix ID	ML (%)		S _t (kPa)		FE ₊₂₀ (kJ/m ³)	FE ₋₁₀ (kJ/m ³)	RD _{APA} (mm)
		4% ^a	7% ^b	4% ^a	7% ^b	7% ^b	7% ^b	7% ^b
0-yr	M17	10.4	11.8	1712	1322	3.49	0.68	4.9
	M18	9.0	10.2	1451	1207	3.83	0.86	5.6
	M19	8.9	10.1	1718	1219	4.11	0.69	8.8
	M20	10.8	11.0	1549	1166	1.78	0.47*	4.6
	Avg.	9.8	10.8	1608	1229	3.30	0.68	6.0
1-yr	M17	11.9	11.8	1826	1460	---	---	4.7
	M18	11.0	15.5	1825	1435	---	---	6.6
	M19	10.4	11.0	1965	1575	---	---	6.6
	M20	12.1	11.6	1836	1390	---	---	4.2
	Avg.	11.4	12.5	1863	1465	---	---	5.5
2-yr	M17	12.8	13.6	1950	1522	3.62	0.65	---
	M18	12.3	12.9	1931	1565	2.42	0.99*	---
	M19	11.9	12.8	2024	1717	2.13	0.60	---
	M20	11.4	14.4	1977	1494	1.34	0.68	---
	Avg.	12.1	13.4	1971	1574	2.38	0.73	---
3-yr	M17	14.1	15.2	2094	1723	---	---	---
	M18	13.0	13.3	2219	1802	---	---	---
	M19	12.2	12.9	2364	2008	---	---	---
	M20	13.6	16.8	2151	1614	---	---	---
	Avg.	13.3	14.6	2207	1787	---	---	---
4-yr	M17	13.3	14.4	2156	1730	2.05	0.55	3.5
	M18	14.6	15.5	2149	1778	1.46	0.78	3.5
	M19	12.5	16.0	2251	1943	2.17	0.50	4.2
	M20	14.4	17.1	2072	1587	1.35	0.61	3.6
	Avg.	13.7	15.8	2157	1760	1.76	0.61	3.7

a= 4% V_a ; b=7% V_a; *= value believed to be outlier

Table 8.2. Laboratory Conditioned Mixture Test Results

Specimen Type	Mix ID	ML (%)		S _t (kPa)		FE ₊₂₀	FE ₋₁₀	RD _{APA}
		4% ^a	7% ^b	4% ^a	7% ^b	(kJ/m ³)	(kJ/m ³)	(mm)
CP1	M17	11.6	12.1	1760	1375	1.74	0.70	6.5
	M18	11.2	12.8	1739	1385	2.32	0.64	5.6
	M19	10.7	12.2	1773	1478	1.86	0.72	7.2
	M20	12.4	14.5	1724	1390	1.53	0.47	4.7
	Avg.	11.5	12.9	1749	1408	1.86	0.63	6.0
CP2	M17	10.5	12.3	1720	1561	2.26	0.55	5.8
	M18	10.8	10.8	1833	1357	2.12	0.58	8.4
	M19	11.6	11.2	1967	1451	2.79	0.64	7.1
	M20	12.7	13.0	1665	1267	0.91	0.33	6.4
	Avg.	11.5	11.7	1797	1409	2.02	0.55	6.9
CP3	M17	14.2	15.6	1889	1391	2.65	0.67	5.8
	M18	13.9	13.5	1611	1069	2.31	0.59	5.9
	M19	12.7	14.5	1864	1350	2.92	0.83	7.5
	M20	14.7	16.5	1690	1199	2.54	0.49	5.0
	Avg.	13.9	15.0	1764	1253	2.60	0.68	6.1
CP4	M17	13.0	12.0	1794	1286	3.20	0.56	5.4
	M18	11.9	13.6	1645	1213	2.17	0.70	6.7
	M19	11.4	13.3	1910	1328	2.79	0.55	7.6
	M20	13.9	14.8	1725	1156	1.76	0.45	5.4
	Avg.	12.6	13.4	1769	1246	2.48	0.58	6.3
CP5	M17	11.9	14.0	1980	1387	2.13	0.48	5.3
	M18	13.1	12.8	1846	1180	4.22	0.76	7.6
	M19	11.7	14.7	1931	1413	3.49	0.81	8.1
	M20	14.5	14.6	1814	1295	3.77	0.67	6.2
	Avg.	12.8	14.0	1893	1319	3.40	0.69	6.8
CP6	M17	12.0	13.5	1975	1194	2.27	0.73	4.7
	M18	11.7	12.6	1700	1212	2.43	0.70	6.9
	M19	10.9	11.7	1887	1360	3.66	0.69	7.5
	M20	13.0	13.3	1643	1285	3.18	0.56	6.2
	Avg.	11.9	12.8	1802	1263	2.89	0.67	6.3
CP7	M17	15.4	16.2	1946	1388	2.01	0.61	4.3
	M18	14.9	15.1	1711	1285	1.98	0.56	6.4
	M19	12.6	16.8	1957	1426	2.52	0.62	6.9
	M20	16.9	17.9	1690	1238	1.36	0.52	5.3
	Avg.	15.0	16.5	1826	1335	1.97	0.56	5.7
CP8	M17	---	---	---	---	---	---	---
	M18	---	15.9	---	1606	---	---	---
	M19	---	15.4	---	1756	---	---	---
	M20	---	18.6	---	1594	---	---	---
	Avg.	---	16.6	---	1652	---	---	---

a= 4% V_a ; b=7% V_a

8.2 Replicating Field Aging of Asphalt Mixture

This section analyzes the field aging times that were simulated by each CP, considering CML, IDT, FE₊₂₀, FE₋₁₀, and APA test results average across mixture types. Overall trendlines (i.e. not considering individual mixture types but collectively assessing all data) were used in conjunction with Equation 8.1 to estimate simulated field aging times.

$$t_{SF} = \frac{V_i - Y_t}{M_t} \quad (8.1)$$

Where:

t_{SF} = Simulated field aging time

V_i = Average test method value for CPs

M_t = Slope of field aging trendline for specific test method

Y_t = Y intercept of field aging trendline for specific test method

For example, Figure 4.1a shows an overall field aging trendline for 4% V_a CML specimens as “ $ML = 0.97 t_f + 10.10$ ”. Thus, for use in Equation 8.1, M_t is equal to 0.97, and Y_t is equal to 10.10, as shown in Equation 8.2.

$$t_{SF} = \frac{V_i - 10.10}{0.97} \quad (8.2)$$

Then, using the average 4% ML value for CP1 from Table 8.2 (11.5%), the simulated field aging time for CP1 based of CML testing of 4% V_a specimens is calculated as 1.4 years, as shown in Equation 8.3

$$t_{SF} = \frac{11.5 - 10.10}{0.97} = 1.4 \text{ years} \quad (8.3)$$

The following subsections apply this methodology to CML, IDT, FE, and APA test results for specimens at 4% and 7% target V_a levels (4% V_a only considered for CML and IDT results). For each test method and V_a level, a figure is displayed which summarizes all lab conditioned and field aged data, which was averaged for each aging level across mixture types. Aging levels (0-yr to 4-yr and CP1 to CP7) are denoted on the x-axis of each figure ranked from “least aged” to “most aged”. It should be noted that the analysis presented here is only one method to interpret the data. There are likely others that could be used which might result in slightly altered simulated field aging times from what are presented in the remainder of this chapter; however, it is believed that the following analysis provides reasonable estimates of simulated field aging times.

8.2.1 Conditioning Protocols in Conjunction with Cantabro Mass Loss

Figure 8.1 summarizes all CML data for 4% V_a specimens. Oxidative CPs (i.e. CP1 and CP2) were the least severe protocols according to CML simulating 1.0 to 2.0 years of field aging. Moisture related protocols ranked from least to most severe CP6, CP4, CP5, and CP3 with CP6 simulated approximately 2 years, CP4 and CP5 simulating between 2 and 3 years, and CP3 simulating about 4 years. It should be noted that CP6 is twice the conditioning time as CP3 at the same temperature, thus, should result in more aging. However, CP3 was observed to induce greater aging than CP6. Additionally, CP3 resulted in slightly higher ML than 4-year specimens, but according to trendline equations, simulated 3.9 years of aging. This modest discrepancy is caused by scatter in the trendline. CP7 was found to induce the greatest amount of aging representing predicted ML after up to 5.0 years in the field.

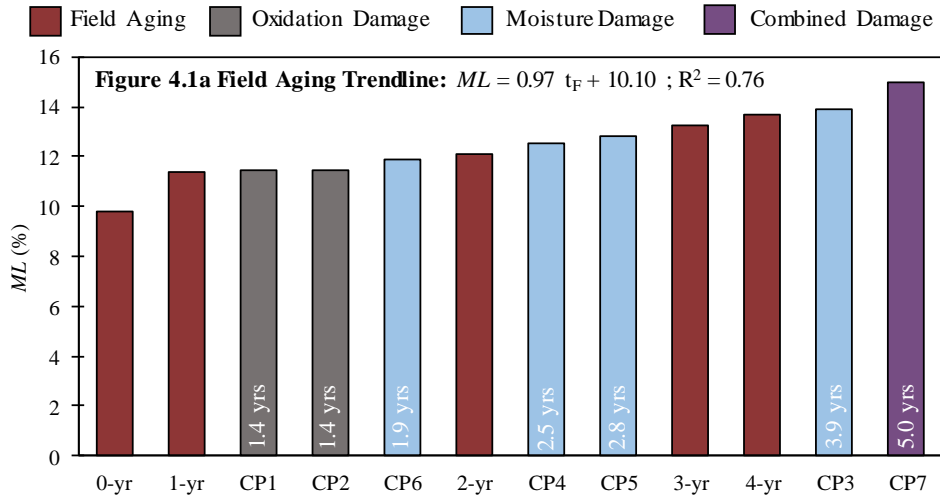


Figure 8.1. Correlating Field Aging and Laboratory Conditioning for CML at 4% V_a

Figure 8.2 presents all 7% V_a data from CML testing. CP1 and CP2 resulted in relatively low simulated aging at 1.6 and 0.6 years, respectively. Moisture damaging CPs ranked from least to most aging as CP6, CP4, CP5, and CP3 (same as at 4% V_a). Ranging in simulated aging times from about 1.5 years to almost 3.5 years. Again, CP6 resulted in less aging than CP3 although it is twice the amount of moisture conditioning. CP7 and CP8 were both found to replicate just over 4.5 years of aging.

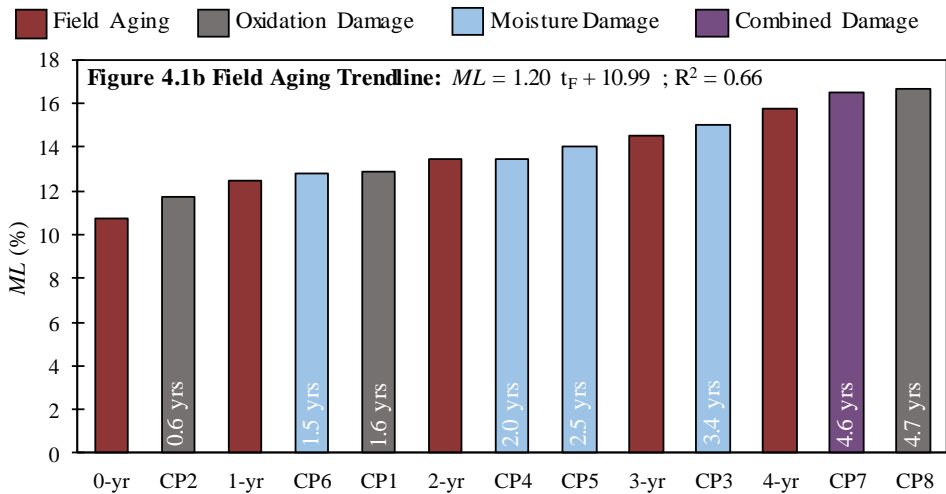


Figure 8.2. Correlating Field Aging and Laboratory Conditioning for CML at 7% V_a

8.2.2 Conditioning Protocols in Conjunction with Indirect Tensile Strength

Field aged and laboratory conditioned IDT data for 4% V_a specimens is summarized in Figure 8.3. CP1 and CP2 replicated approximately 0.5 years and 1.0 years of aging, respectively. Moisture damage protocols ranked from least to most aging as CP3, CP4, CP6, and CP5 with all protocols simulating about 0.5 years to 1.0 years of aging, except CP5 replicated the greatest amount of field aging at 1.5 years. CP7, which should be the most severe CP, replicated about one

year. Note that trendline scatter resulted in a simulated aging time of 1.1 years for CP7 although it resulted in a slightly lower tensile strength than 1.0 year of field aging.

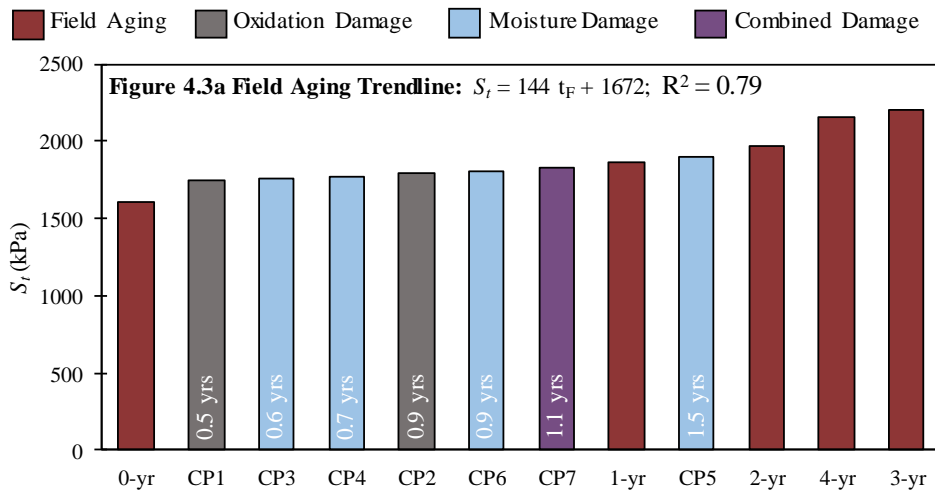


Figure 8.3. Correlating Field Aging and Laboratory Conditioning for IDT at 4% V_a

IDT results of all 7% V_a specimens are shown in Figure 8.4. Multiple moisture protocols (i.e. CP3, CP4, and CP6) had simulated aging times which were negative. Additionally, CP5 resulted in aging equivalent to 0.2 years of field aging. As such, CP3, CP4, CP5, and CP6 caused practically no change in tensile strengths for 7% V_a specimens. CP7 replicated almost 0.5 years, but still less than CP1 and CP2 which replicated almost 1.0 years of aging and CP8 which had a simulated aging time of 2.6 years. It should be noted that this is contrary to the observations made for 4% V_a specimens where oxidative CPs, CP1 and CP2, had simulated aging times which were similar or shorter than many moisture-related protocols.

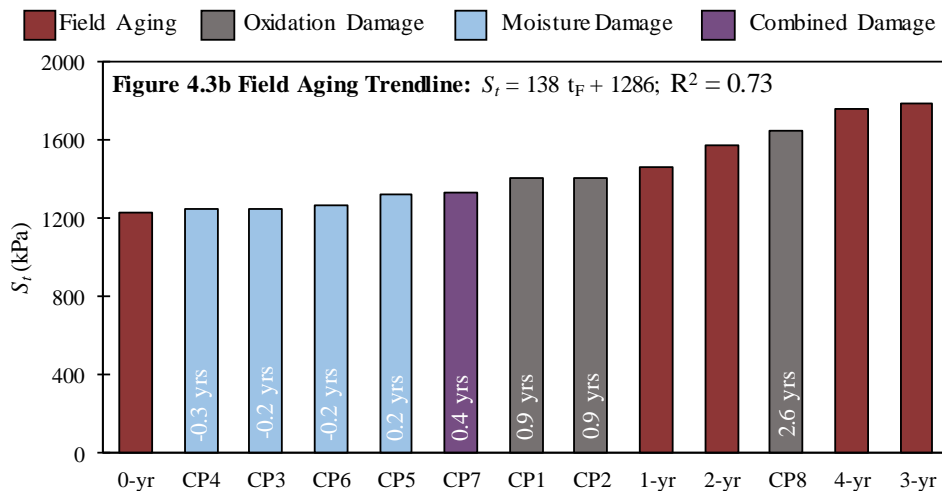


Figure 8.4. Correlating Field Aging and Laboratory Conditioning for IDT at 7% V_a

8.2.3 Conditioning Protocols in Conjunction with Fracture Energy

Figures 8.5 and 8.6 show fracture energy test results at 20°C and -10°C, respectively. Trendline scatter resulted in a simulated aging time of -0.3 years for CP5, indicating there was no practical change in FE_{+20} . CP6, CP3, and CP4 FE_{+20} values were all between those for 0-yr and 2-yr specimens, with simulated aging times of 1.0 years for CP6, 1.7 years for CP3, and 2.0 years for CP4. The order of these four moisture CPs is unintuitive, as CP5 has a greater number of FT cycles than CP3 or CP4, and CP6 was twice the conditioning time of CP3; however, FE_{+20} did not capture these increases in conditioning severity. According to FE_{+20} data in Figure 8.5, CP1 and CP2 replicated a meaningful amount of aging relative to other protocols at 3.6 to 3.2 years of field aging, respectively. CP7 FE_{+20} values fell between the two oxidative CPs with a simulated aging time of 3.3 years.

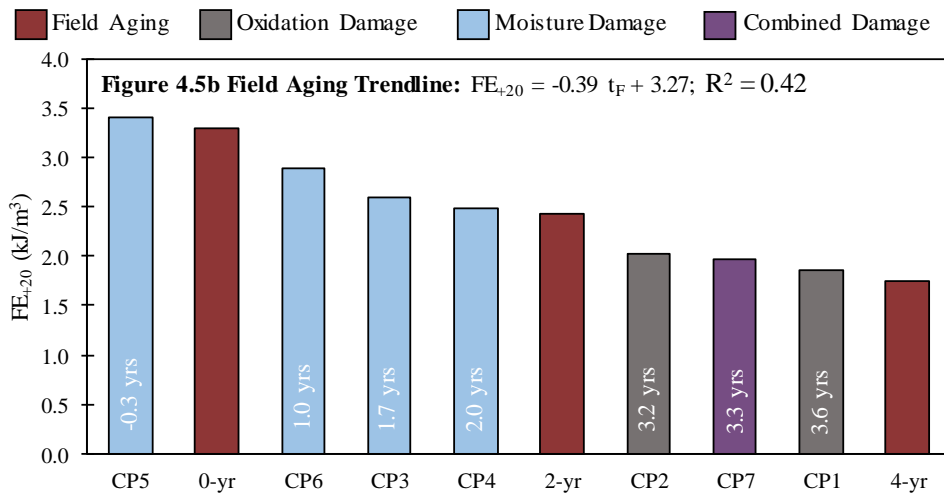


Figure 8.5. Correlating Field Aging and Laboratory Conditioning for FE_{+20} at 7% V_a

For FE_{-10} , there were two values which were believed to be outliers: 2-yr value for M18 and 0-yr value for M20. The 0-yr value of M20 was meaningfully lower than the 2-yr and 4-yr, while the 2-yr value of M18 was higher than the 0-yr value. Thus, these two values were not considered in this analysis. Figure 8.6 displays field aged and laboratory data with these values removed. As seen in Figure 8.6, FE_{-10} showed CP1 and CP2 replicated 2.9 years and 5.0 years of field aging, respectively. CP3 and CP5 simulate 1.3 years while CP6 replicate 1.6 years. CP4 replicated the most time of any moisture dominated protocol at 4.2 years of field aging; although, CP5 would be expected to have a greater simulated field aging time as it has one more FT cycle than CP4. CP7 simulated 4.7 years of field aging.

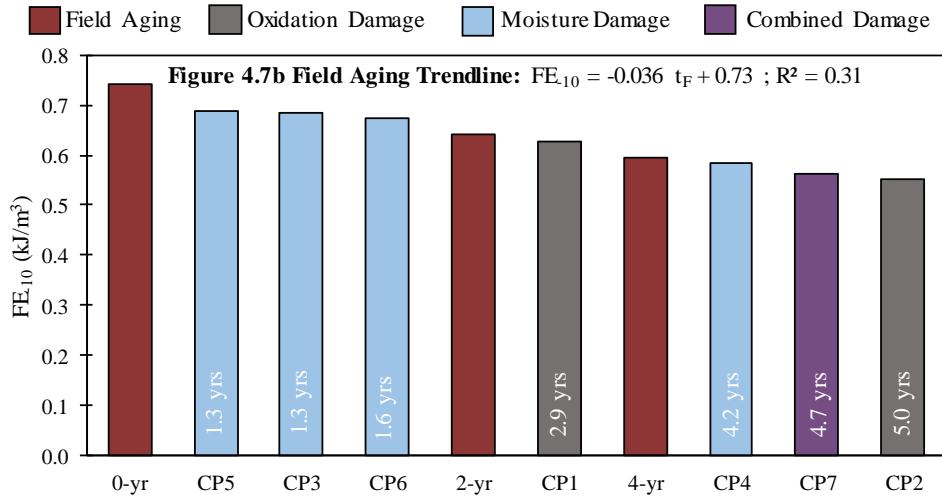


Figure 8.6. Correlating Field Aging and Laboratory Conditioning for FE-10 at 7% V_a

8.2.4 Conditioning Protocols in Conjunction with Asphalt Pavement Analyzer

Figure 8.7 summarizes 7% V_a APA data for field aged and laboratory conditioned specimens. It was observed that, on average, CP7 was the only protocol which decreased RD_{APA}. All other CPs had either no effect on rut depth or increased in rut depth. Of these, CP1 had the least effect with no change in average RD_{APA} and CP2 altered RD_{APA} more than any other protocol; however, is caused an increase with a resultant simulated field aging time of -1.6 years.

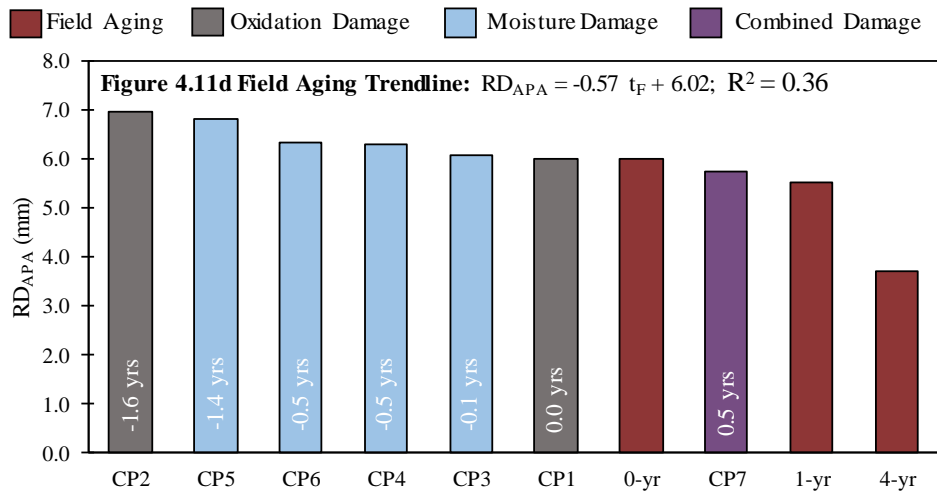


Figure 8.7. Correlating Field Aging and Laboratory Conditioning for APA at 7% V_a

8.3 Summary of Overall Field Aging Time Simulations

Figures 8.1 to 8.7 were used to develop a reasonable range of simulated field aging times for each test method at each relevant V_a level. The times that were simulated according to field

aging trendlines, which are displayed in each figure, were used as a reference point. A range was then applied based on the rankings of protocols as well as judgment based on general trendline scatter. In cases where CPs resulted in negative simulated aging times, they were assigned 0.0 years of field aging simulation. These ranges are summarized in Table 8.3.

Table 8.3. Simulation of Field Aging in Years for Asphalt Mixture Test Methods

CP	<i>ML</i>		<i>S_t</i>		<i>FE₊₂₀</i>	<i>FE₋₁₀</i> *	<i>APARD</i>
	4% V _a	7% V _a	4% V _a	7% V _a	7% V _a	7% V _a	7% V _a
CP1	1.0 to 2.0	1.0 to 2.0	0.0 to 1.0	0.5 to 1.5	3.0 to 4.0	2.5 to 3.5	0.0
CP2	1.0 to 2.0	0.0 to 1.0	0.5 to 1.0	0.5 to 1.5	2.5 to 3.5	4.5 to 5.5	0.0
CP3	3.5 to 4.5	3.0 to 4.0	0.0 to 1.0	0.0	1.0 to 2.0	1.0 to 2.0	0.0
CP4	2.0 to 3.0	1.5 to 2.5	0.0 to 1.0	0.0	1.5 to 2.5	3.5 to 4.5	0.0
CP5	2.0 to 3.0	2.0 to 3.0	1.0 to 2.0	0.0 to 0.5	0.0	1.0 to 2.0	0.0
CP6	1.5 to 2.5	1.0 to 2.0	0.5 to 1.5	0.0	0.5 to 1.5	1.0 to 2.0	0.0
CP7	4.5 to 5.5	4.0 to 5.0	0.5 to 1.5	0.0 to 1.0	3.0 to 4.0	4.0 to 5.0	0.0 to 1.0
CP8	---	4.0 to 5.0	---	2.0 to 3.0	---	---	---

*FE₋₁₀ ranges derived only from rankings after M18 and M20 outliers were removed as described in Section 8.2.3

CHAPTER 9 – SUMMARY, CONCLUSIONS, AND RECOMMENDATIONS

9.1 Summary

The main objective of this report was to characterize asphalt containing warm mix technologies at various levels of field aging and laboratory conditioning in terms of mixture and binder properties encompassing the temperature range experienced in Mississippi. Approximately 1400 mixture specimens were tested at thirteen different levels of conditioning or aging: unconditioned, one, two, three, or four years of field aging, or in one of eight laboratory conditioning protocols that included oxidation, moisture, free-thaw, and combined effects damage potential. Fifty-six binder samples were recovered from material represented within these roughly 1400 mixture specimens for complimentary properties assessment. The following mixture tests were performed: Cantabro Mass Loss (CML), Indirect Tensile (IDT), Fracture Energy (FE) at 20°C and -10°C, Asphalt Pavement Analyzer (APA), and Hamburg Loaded Wheel Tracking (HLWT). The following tests were performed on recovered binder: Penetration (*Pen.*), Dynamic Shear Rheometer at intermediate (DSR_{8mm}) and high (DSR_{25mm}) temperatures, Bending Beam Rheometer (BBR), and Fourier Transform Infrared (FTIR) spectroscopy. These tests were used to assess relative behavior of HMA to WMA over time, as well as to evaluate laboratory conditioning protocols and mixture test methods for their combined ability to reasonably simulate field aging of asphalt mixtures. The following section provides conclusions organized by chapter, which are followed by recommendations.

9.2 Conclusions

9.2.1 Chapter 5 Conclusions

- IDT strength correlated very poorly to CML and binder test results.
- IDT did not detect cumulative mixture damage from multiple environmental effects.
- Mass loss (*ML*) values related to binder properties and could reasonably detect multiple types of environmental effects.

9.2.2 Chapter 6 Conclusions

- At all temperatures, HMA and Sasobit WMA had mostly similar initial properties, indicative of stiffer mixtures and/or binders relative to Foamed and Evotherm WMA, which was supported by several sources in literature.
- HMA appeared to age at a slower rate due to long term oven aging than other mixture types, which agrees with most findings in literature.
- Cantabro *ML* results showed that moisture conditioning had approximately the same effect on HMA, Foamed WMA, and Evotherm WMA, which did not always agree with intermediate temperature findings from literature.
- Sasobit WMA fracture and durability mixture properties (i.e. anything where a stiffer mixture is detrimental) appeared much more susceptible to combined effects of oxidation, moisture, and FT damage than other mixtures.

9.2.3 Chapter 7 Conclusions

- Foam and Evotherm WMA often had improved low temperature cracking resistance relative to HMA, even after field aging; however, this was not consistent across all air void levels or test methods.
- Overall, Evotherm WMA was slightly less rut resistant than other mixtures.
- Foam and Evotherm WMA typically aged faster in the field than HMA, while Sasobit WMA's fracture and rutting properties were less affected by field aging.
- Convergence times among different WMTs appeared to be dependent on more than just the WMT, such as air void level and test method.
- Convergence of binder properties was more variable than that of mixture properties.

9.2.4 Chapter 8 Conclusions

- Oxidative conditioning typically had a greater effect on mixture fracture properties than moisture-dominated conditioning.
- In most cases, neither the increase in moisture conditioning time nor the progressive addition of FT cycles manifested in increased simulated aging times.
- Low temperature fracture and rutting testing yielded highly variable and unintuitive simulated field aging times.
- The Chapter 5 observation that CML was more suitable than IDT to capture combined environmental effects was supported when laboratory and field results were combined.
- CML was the most suitable for prediction of field aging, and was able to realistically represent 4.0 to 5.5 years of field aging after specimens were conditioned for 5 days in an 85 °C oven, followed by 14 days of 64 °C water, and one FT cycle.

9.3 Recommendations

The findings herein should be integrated with those from Volume 1 and Volume 2 of this report series for a full assessment. Specific recommendations are as follows.

- Explore implementation of Cantabro testing for assessment of environmental effects (i.e. combined oxidation, moisture, and freeze-thaw).
- Follow Table 8.3 for guidance on how to condition laboratory specimens to estimate field aging time in Mississippi. Cantabro testing is recommended for primary guidance with fracture properties used as secondary information (caution should be used with fracture properties and only oxidative or moisture conditioning). The default recommendation from the authors is to use CP7 conditioning with CML testing as it was able to simulate 4.0 to 5.5 years of field aging in this report, which was similar to Volume 2's range of 4 to 5 years.
- None of the warm mix technologies behaved holistically better or worse than the others, and their behavior relative to hot mixed asphalt was not dramatically different. There were some property differences of potential interest to some projects between warm mix technologies, and as such the overall recommendation of this report is to consider foamed, chemical, and wax technologies as potentially viable solutions that should be considered and used (or not used) on a project to project basis. It is recommended for all three technologies evaluated herein to be allowed for consideration to optimize a given project.

CHAPTER 10 REFERENCES

- Abbas, A. R., Nazzal, M., Kaya, S., Akinbowale, S., Subedi, B., Arefin, M. S., & Abu Qtaish, L. (2016). "Effect of Aging on Foamed Warm Mix Asphalt Produced by Water Injection," *Journal of Materials in Civil Engineering*, 28(11), 04016128.
- Alhasan, A., Abbas, A., Nazzal, M., Dessouky, S., Ali, A., Kim, S. S., & Powers, D. (2014). "Low-Temperature Characterization of Foamed Warm-Mix Asphalt Produced by Water Injection," *Transportation Research Record: Journal of the Transportation Research Board*, 2445, pp 1-11.
- Ali, A. W., Abbas, A. R., Nazzal, M., & Powers, D. (2012). "Laboratory Evaluation of Foamed Warm Mix Asphalt," *International Journal of Pavement Research and Technology*, 5(2), 93-101.
- Anderson, D. A., Christensen, D. W., Bahia, H. U., Dongre, R., Sharma, M. G., Antle, C., E., Button, J. (1994). *Binder Characterization and Evaluation Volume 2: Physical Characterization*. Report SHRP-A-369, Strategic Highway Research Program, Washington, D.C.
- Aschenbrener, T. (1995). "Evaluation of the Hamburg Wheel-Tracking Device to Predict Moisture Damage in Hot Mix Asphalt," *Transportation Research Record: Journal of the Transportation Research Board*, 1492, pp 193-201.
- Bańkowski, W., Horodecka, R., Gajewski, M., & Mirski, K. (2016). "The Extended Assessment of Warm Mix Asphalts Durability," *Roads and Bridges*, 15(2), 157-173.
- Bazuhair, R. W., Pittman, C. V., Howard, I. L., Jordan III, W. S., Hemsley Jr, J. M., & Baumgardner, G. L. (2018). "Conditioning and Testing Protocol Combinations to Detect Asphalt Mixture Damage," *Transportation Research Record: Journal of the Transportation Research Board*. <https://doi.org/10.1177/0361198118756631>
- Behl, A., & Chandra, S. (2017). "Aging Characteristics of Warm-Mix Asphalt Binders," *Journal of Materials in Civil Engineering*, 29(10), 04017155.
- Bell, C.A. (1989). *Summary Report on Aging of Asphalt-Aggregate Systems*. Report SHRP-A-305, Strategic Highway Research Program, Washington, D.C.
- Bell, C.A., AbWahab, Y., Christi M.E., & Sosnovske, D. (1994a). *Selection of Laboratory Aging Procedures for Asphalt-Aggregate Mixtures*. Report SHRP-A-383, Strategic Highway Research Program, Washington, D.C.
- Bell, C.A., Weider, A.J., & Fellin, M.J. (1994b). *Laboratory Aging of Asphalt-Aggregate Mixtures: Field Validation*. Report SHRP-A-390, Strategic Highway Research Program, Washington, D.C.

- Bennert, T. (2012a). *Early Age Rutting Potential of Warm Mix Asphalt (WMA)*. Report No. C-10-08, New York State Department of Transportation, Albany, NY.
- Bennert, T. (2012b). *Evaluation of Warm Asphalt Technology*. Report No. FHWA-NJ-2011-005, New Jersey Department of Transportation, Trenton, NJ.
- Bennert, T. (2014). *Laboratory Evaluation of Foamed Warm Mix Asphalt*. Report No. NJAPA RU9247, New Jersey Department of Transportation, Piscataway, NJ.
- Bernier, A., Zofka, A., Josen, R., & Mahoney, J. (2012). "Warm-Mix Asphalt Pilot Project in Connecticut," *Transportation Research Record: Journal of the Transportation Research Board*, 2294, pp 106-116.
- Bernier, A., Yut, I., Parker, F., & Dargie, D. (2017). "Long-Term Performance of Warm-Mix Asphalt Overlay on an Airport Major Taxiway: Case Study," CD-ROM, *Transportation Research Board 96th Annual Meeting*, Washington, D.C., Paper 17-06791.
- Boggs, W. (2008). "Customers warm up to green system," *Warm-Mix Asphalt: Contractor's Experiences, Information Series 134*, National Asphalt Pavement Association, Lanham, MD, pp. 16–17.
- Bower, N., Wen, H., Wu, S., Willoughby, K., Weston, J., & DeVol, J. (2016). "Evaluation of the Performance of Warm Mix Asphalt in Washington State," *International Journal of Pavement Engineering*, 17(5), 423-434.
- Branthaver, J. F., Petersen, J. C., Robertson, R. E., Duvall, J. J., Kim, S. S., Harnsberger, P. M., Mill, T., Ensley, E.K., Barbour, F. A., & Scharbron, J. F. (1993). *Binder Characterization and Evaluation. Volume 2: Chemistry*. Report SHRP-A-368, Strategic Highway Research Program, Washington, D.C.
- Bonaquist, R. F. (2011). *Mix Design Practices for Warm Mix Asphalt*. NCHRP Report 691.
- Copas, T. L., & Pennock, H. A. (1979). *Relationship of Asphalt Cement Properties to Pavement Durability*. NCHRH Synthesis 59.
- Cox, B. C. & Howard, I.L. (2015). *Cold In-Place Recycling Characterization Framework and Design Guidance for Single or Multiple Component Binder System*. Report No. FHWA/MS-DOT-RD-15-250-Volume 2, Mississippi Department of Transportation, Jackson, MS.
- Cox, B. C., Smith, B. T., Howard, I. L., & James, R. S. (2017). "State of Knowledge for Cantabro Testing of Dense Graded Asphalt," *Journal of Materials in Civil Engineering*, 29(10), 04017174.

- Cucalon, L. G., Yin, F., Martin, A. E., Arambula, E., Estakhri, C., & Park, E. S. (2016). "Evaluation of Moisture Susceptibility Minimization Strategies for Warm-Mix Asphalt: Case Study," *Journal of Materials in Civil Engineering*, 28(2), 05015002.
- Cucalon, L. G., Kassem, E., Little, D. N., & Masad, E. (2017). "Fundamental Evaluation of Moisture Damage in Warm-Mix Asphalts," *Road Materials and Pavement Design*, 18(sup1), 258-283.
- Das, P., Tasdemir, Y., & Birgisson, B. (2011). "Low Temperature Cracking Performance of Wax Modified Bitumen and Mixture," *XXIVth World Road Congress, Mexico*, 24, pp 1-11.
- Diefenderfer, S. D., & Hearon, A. J. (2008). *Laboratory Evaluation of a Warm Asphalt Technology for Use in Virginia*. Report No. FHWA/VTRC 09-R11, Virginia Transportation Research Council, Charlottesville, VA.
- Diefenderfer, S. D., & Hearon, A. J. (2010). *Performance of Virginia's Warm-Mix Asphalt Trial Sections*. Report No. FHWA/VTRC 10-R17. Virginia Transportation Research Council, Charlottesville, VA.
- Diefenderfer, S. D., McGhee, K. K., & Donaldson, B. M. (2007). *Installation of Warm Mix Asphalt Projects in Virginia*. Report No. FHWA/VTRC 07-R25, Virginia Transportation Research Council, Charlottesville, VA.
- Doyle, J. D., & Howard, I. L. (2013). "Rutting and Moisture Damage Resistance of High Reclaimed Asphalt Pavement Warm Mixed Asphalt: Loaded Wheel Tracking vs. Conventional Methods," *Road Materials and Pavement Design*, 14(sup2), pp 148-172.
- Doyle, J.D., Mejias-Santiago, M., Brown, E.R., & Howard, I.L. (2011). "Performance of High RAP WMA Surface Mixtures," *Journal of the Association of Asphalt Paving Technologists*, 80, pp 419-457.
- Doyle, J. D., Mejías-Santiago, M., & Rushing, J. F. (2013a). "Binder and Mixture Testing to Assess Rutting Performance of Warm Mix Asphalt (WMA)," *Green Streets, Highways, and Development 2013: Advancing the Practice*, pp 68-77.
- Doyle, J. D., Rushing, J. F., Mejías-Santiago, M., McCaffrey, T. J., Warnock, L. C., & Taylor, M. K. (2013b). *Laboratory Performance Testing of Warm-Mix Asphalt Technologies for Airfield Pavements*. Report No. ERDC/GSL-TR-13-41. United States Army Corp of Engineers Engineer Research and Development Center Geotechnical and Structures Lab, Vicksburg, MS.
- Elwardany, M. D., Yousefi Rad, F., Castorena, C., & Kim, Y. R. (2016). "Evaluation of Asphalt Mixture Laboratory Long-Term Ageing Methods for Performance Testing and Prediction," *Road Materials and Pavement Design*, 18(sup1), pp 28-61.

- Elwardany, M. D., Rad, F.Y., Castorena, C., Richard, & Kim, Y.R. (2018). "Climate-, Depth-, and Time-Based Laboratory Aging Procedure for Asphalt Mixtures," *Association of Asphalt Paving Technologist*, 87.
- Farshidi, F., Jones, D. J., & Harvey, J. T. (2013). *Warm-mix Asphalt Study: Evaluation of Hot-and Warm-mix Asphalt with Respect to Binder Aging*. Final Report FHWA Agreement No. CA12385A, UCPRC Research Report UCPRC-RR-2013-02, Federal Highway Administration, Washington, D.C.
- Gandhi, T., Akisetty, C., & Amirkhanian, S. (2010). "A Comparison of Warm Asphalt Binder Aging with Laboratory Aging Procedures," *Journal of Testing and Evaluation*, 38(1), pp 57-64.
- Goh, S. W., & You, Z. (2011). "Moisture Damage and Fatigue Cracking of Foamed Warm Mix Asphalt Using a Simple Laboratory Setup," *Transportation and Development Institute Congress 2011: Integrated Transportation and Development for a Better Tomorrow*, 1, pp 762-771.
- Gu, F., Zhang, Y., Luo, X., Luo, R., & Lytton, R. L. (2015a). "Improved Methodology to Evaluate Fracture Properties of Warm-Mix Asphalt Using Overlay Test," *Transportation Research Record: Journal of the Transportation Research Board*, 2506, pp 8-18.
- Gu, F., Luo, X., Zhang, Y., & Lytton, R. L. (2015b). "Using Overlay Test to Evaluate Fracture Properties of Field-Aged Asphalt Concrete," *Construction and Building Materials*, 101, pp 1059-1068.
- Hajj, E., Chia, C., Sebaaly, P., Kasozi, A. M., & Gibson, S. (2011). "Properties of Foamed Warm Mix Asphalt Incorporating Recycled Asphalt Pavement from Two Field Projects Case Studies," *Proceedings of the 2nd International Conference on Warm Mix Asphalt*, 2, pp 1-17.
- Hansen, K.R., Copeland, A., & Ross, T.C. (2017). "Recycled Materials: 2015 RAP/RAS/WMA Survey Results - Use of Recycled Materials Continues to Grow," *Asphalt Pavement Magazine*, 22(3), 26-28.
- Haggag, M., Mogawer, W., & Bonaquist, R. (2011). "Fatigue Evaluation of Warm-Mix Asphalt Mixtures: Use of Uniaxial, Cyclic, Direct Tension Compression Test," *Transportation Research Record: Journal of the Transportation Research Board*, 2208, pp 26-32.
- Harvey, J., & Tsai, B. (1997). "Long-Term Oven-Aging Effects on Fatigue and Initial Stiffness of Asphalt Concrete," *Transportation Research Record: Journal of the Transportation Research Board*, 1590, pp. 89-98.
- Hill, B., Behnia, B., Hakimzadeh, S., Buttlar, W., & Reis, H. (2012). "Evaluation of Low-Temperature Cracking Performance of Warm-Mix Asphalt Mixtures," *Transportation Research Record: Journal of the Transportation Research Board*, 2294, pp 81-88.

- Hodo, W. D., Kvasnak, A., & Brown, E. R. (2009). "Investigation of foamed asphalt (warm mix asphalt) with high reclaimed asphalt pavement (RAP) content for sustainment and rehabilitation of asphalt pavement," CD-ROM, *Transportation Research Board 88th Annual Meeting*, Washington, D.C., Paper 17-06791.
- Houston, W. N., Mirza, M. W., Zapata, C. E., & Raghavendra, S. (2005). *Environmental Effects in Pavement Mix and Structural Design Systems*. NCHRP Project 9-23.
- Harrigan, E. T. (2007). *Simulating the Effects of Hot Mix Asphalt Aging for Performance Testing and Pavement Structural Design*. NCHRP Research Results Digest 324.
- Howard, I. L., & Doyle, J. D. (2015). "Durability Indexes via Cantabro Testing for Unaged, Laboratory-Conditioned, and One-Year Outdoor-Aged Asphalt Concrete," CD-ROM, *Transportation Research Board 94th Annual Meeting*, Washington, D.C., Paper 15-1366.
- Howard, I.L., Hansen, B.S., Smith, B.T. (2018). *Columbus Mississippi Field Aging and Laboratory Conditioning Study: Air Force Base and Single Aggregate Source Reference Asphalt Mixtures*. Report FHWA/MS-DOT-RD-18-266/270-Volume 1, Mississippi Department of Transportation.
- Hurley, G. C., & Prowell, B. D. (2005a). *Evaluation of Aspha-Min Zeolite for Use in Warm Mix Asphalt*. NCAT Report 05-04, National Center for Asphalt Technology, Auburn, AL.
- Hurley, G. C., & Prowell, B. D. (2005b). *Evaluation of Sasobit for Use in Warm Mix Asphalt*. NCAT Report 05-06, National Center for Asphalt Technology, Auburn, AL.
- Hurley, G. C., & Prowell, B. D. (2006). *Evaluation of Evotherm for Use in Warm Mix Asphalt*. NCAT Report 06-02, National Center for Asphalt Technology, Auburn, AL .
- Hurley, G. C., Prowell, B. D., & Kvasnak, A. N. (2010). *Wisconsin Field Trial of Warm Mix Asphalt Technologies: Construction Summary*. NCAT Report 10-04, National Center for Asphalt Technology, Auburn, AL.
- Isola, M., Chun, S., Roque, R., Zou, J., Koh, C., & Lopp, G. (2014). "Development and Evaluation of Laboratory Conditioning Procedures to Simulate Mixture Property Changes Effectively in the Field," *Transportation Research Record: Journal of the Transportation Research Board*, 2447, pp 74-82.
- Jones, D. J., Farshidi, F., & Harvey, J. T. (2013). *Warm-Mix Asphalt Study: Summary Report on Rubberized Warm-Mix Asphalt Research*. Final Report FHWA Agreement No. CA142385C, UCPRC Summary Report UCPRC-SR-2013-03, Federal Highway Administration, Washington, D.C
- Jones, C., West, R., Julian, G., Taylor, A., Kvasnak, A., & Hurley, G. (2011). *Evaluation of Warm Mix Asphalt in Walla Walla, Washington*. NCAT Report 11-06, National Center for Asphalt Technology, Auburn, AL.

- Kanitong, K., and Bahia, H. (2008) "Evaluation of HMA Moisture Damage in Wisconsin as it Relates to Pavement Performance," *International Journal of Pavement Engineering*, 9(1), pp. 9-17.
- Kavussi, A., & Hashemian, L. (2012). "Laboratory Evaluation of Moisture Damage and Rutting Potential of WMA Foam Mixes," *International Journal of Pavement Engineering*, 13(5), 415-423.
- Kemp, G. R., & Predoehl, N. H. (1981). "A Comparison of Field and Laboratory Environments on Asphalt Durability," *Association of Asphalt Paving Technologists Proceedings*, 50, pp 492-537.
- Kim, O-K., Bell, C.A., Wilson, J., & Boyle, G. (1986). *Effect of Moisture and Aging on Asphalt Pavement Life Part 2 – Effect of Aging*. Report No. FHWA-OR-RD-86-01-2, Oregon Department of Transportation, Salem, OR.
- Kim, Y. R., Zhang, J., & Ban, H. (2012). "Moisture Damage Characterization of Warm-Mix Asphalt Mixtures Based on Laboratory-Field Evaluation," *Construction and Building Materials*, 31, pp 204-211.
- Kim, S. S., Nazzal, M., Abbas, A. R., Akentuna, M., & Arefin, M. S. (2015). *Evaluation of Low Temperature Cracking Resistance of WMA*. Report No. FHWA/OH-2015/11, Ohio Department of Transportation, Columbus, OH.
- Kumbarger, Y. S., & Biligiri, K. P. (2016). "Rational Performance Indicators to Evaluate Asphalt Materials' Aging Characteristics," *Journal of Materials in Civil Engineering*, 28(12), 04016157.
- Lavorato, S., Manolis, S., Pahalan, A., & Reid, R. (2011). "Asphalt Mix Performance Testing for Warm Mix Asphalt Field Project on Ministry of Transportation Ontario Highway 10," *Fifty-sixth Annual Conference of the Canadian Technical Asphalt Association Canadian Technical Asphalt Association*.
- Lee, J. S., & Kim, Y. (2014). "Performance-Based Moisture Susceptibility Evaluation of Warm-Mix Asphalt Concrete Through Laboratory Tests," *Transportation Research Record: Journal of the Transportation Research Board*, 2446, pp 17-28.
- Lee, S. J., Park, J., Hong, J. P., & Kim, K. W. (2013). "Fracture Resistance of Warm-Mix Asphalt Concretes at Low Temperatures," CD-ROM, *Transportation Research Board 88th Annual Meeting*, Washington, D.C., Paper 13-1858.
- Leng, Z., Gamez, A., & Al-Qadi, I. L. (2013). "Mechanical Property Characterization of Warm-Mix Asphalt Prepared with Chemical Additives," *Journal of Materials in Civil Engineering*, 26(2), 304-311.

- Li, X., Andriescu, A., Carvalho, R.L., & Youtcheff, J. (2018) "Evaluation of Recycled and Warm Mix Asphalts Using Laboratory and Full-Scale Cracking Tests," *Association of Asphalt Paving Technologists Proceedings*, 87.
- Liu, J., & Li, P. (2012). "Low Temperature Performance of Sasobit-Modified Warm-Mix Asphalt," *Journal of Materials in Civil Engineering*, 24(1), pp 57-63.
- Lottman, R. P. (1978). *Predicating Moisture-Induced Damage to Asphaltic Concrete*. NCHRP Report 192.
- Malladi, H., Ayyala, D., Tayebali, A. A., & Khosla, N. P. (2015). "Laboratory Evaluation of Warm-Mix Asphalt Mixtures for Moisture and Rutting Susceptibility," *Journal of Materials in Civil Engineering*, 27(5), 04014162.
- Mallick, R., Kandhal, P., & Bradbury, R. (2008). "Using Warm-Mix Asphalt Technology to Incorporate High Percentage of Reclaimed Asphalt Pavement Material in Asphalt Mixtures," *Transportation Research Record: Journal of the Transportation Research Board*, 2051, pp 71-79.
- Martin, A.E., Arambula, E., Yin, F., Cucalon, L. G., Chowdhury, A., Lytton, R., Epps, J., Estakhri, C., & Park, E.S. (2014). *Evaluation of the Moisture Susceptibility of WMA Technologies*. NCHRP Report 763.
- McHattie, R.L. (1983). *Estimating the Durability of Chem-Crete Modified Paving Asphalt*. Report No. AK-RD-84-04, Alaska Department of Transportation, Fairbanks, AK.
- Medeiros Jr, M. S., Daniel, J. S., Bolton, H. L., & Meagher, W. C. (2012). "Evaluation of Moisture and Low-Temperature Cracking Susceptibility of Warm-Mixture Asphalt," *International Journal of Pavement Engineering*, 13(5), pp 395-400.
- Mejías-Santiago, M., Doyle, J., Howard, I. L., & Brown, E. R. (2011). "Moisture Damage Potential for Warm Mix Asphalt Containing Reclaimed Asphalt Pavement," In *Proceedings of 2nd international warm mix conference, St. Louis, MO*, pp 1-16.
- Mejias-Santiago, M., Doyle, J. D., & Rushing, J. F. (2014). *Full-Scale Accelerated Pavement Testing of Warm-Mix Asphalt (WMA) for Airfield Pavements*. Report No. ERDC/GSL-TR-14-3. United States Army Corp of Engineers Engineer Research and Development Center Geotechnical and Structures Lab, Vicksburg, MS.
- Middleton, B., & Forfylyow, R. (2009). "Evaluation of Warm-Mix Asphalt Produced with the Double Barrel Green Process," *Transportation Research Record: Journal of the Transportation Research Board*, 2126, pp 19-26.

- Mogawer, W., Austerman, A., Kluttz, R., & Roussel, M. (2012). "High-Performance Thin-Lift Overlays with High Reclaimed Asphalt Pavement Content and Warm-Mix Asphalt Technology, Performance and Workability Characteristics," *Transportation Research Record: Journal of the Transportation Research Board*, 2293(1), pp 18–28.
- Mogawer, W. S., Austerman, A. J., Kassem, E., & Masad, E. (2011). "Moisture Damage Characteristics of Warm Mix Asphalt Mixtures," *Journal of the Association of Asphalt Paving Technologists*, 80, pp 491-526.
- Petersen, J. C., Robertson, R. E., Branthaver, J. F., Harnsberger, P. M., Duvall, J. J., Kim, S. S., Anderson, D. A., Christiansen D. W. & Bahia, H. U. (1994a). *Binder Characterization and Evaluation: Volume 1*. Report. SHRP-A-367, Strategic Highway Research Program, Washington, DC.
- Petersen, J. C., Robertson, R. E., Branthaver, J. F., Harnsberger, P. M., Duvall, J. J., Kim, S. S., Anderson, D. A., Christiansen D. W. Bahia, H. U., Dongre, R., Antle, C. E., Sharma, M. G. Button, J.W. & Glover, C. J. (1994b). *Binder Characterization and Evaluation: Volume 4*. Report. SHRP-A-370, Strategic Highway Research Program, Washington, DC.
- Porras, J., Hajj, E., Sebaaly, P., Kass, S., & Liske, T. (2012). "Performance Evaluation of Field-Produced Warm-Mix Asphalt Mixtures in Manitoba, Canada," *Transportation Research Record: Journal of the Transportation Research Board*, 2294, pp 64-73.
- Prowell, B.D., Hurley, G.C., & Crews, E. (2007). "Field Performance of Warm-Mix Asphalt at National Center for Asphalt Technology Test Track," *Transportation Research Record: Journal of the Transportation Research Board*, 1998, pp. 96-102.
- Prowell, B. D., Hurley, G.C., & Frank, B. (2012). "Warm-Mix Asphalt: Best Practices," *National Asphalt Pavement Association: Quality Improvement Publication 125, 3rd Edition*.
- Reed, J. (2010). *Evaluation of the effects of aging on asphalt rubber pavements*. Ph.D. dissertation. Arizona State University, Phoenix, AZ.
- Rushing, J., Mejías-Santiago, M., & Doyle, J. (2013a). "Assessment of warm-mix asphalt for heavy traffic airfields," *Transportation Research Record: Journal of the Transportation Research Board*, 2371, pp 41-48.
- Rushing, J. F., Mejias-Santiago, M., & Doyle, J. D. (2013b). *Comparing Production and Placement of Warm-Mix Asphalt to Traditional Hot-Mix Asphalt for Constructing Airfield Pavements*. Report No. ERDC/GSL-TR-13-35. United States Army Corp of Engineers Engineer Research and Development Center Geotechnical and Structures Lab, Vicksburg, MS.
- Safaei, F., Lee, J., Nascimento, L., Hintz, C., & Kim, Y. (2014). "Implications of Warm-Mix Asphalt on Long Term Oxidative Aging and Fatigue Performance of Asphalt Binders and Mixtures," *Road Materials and Pavement Design*, 15, pp 45-61.

- Sargand, S., Nazzal, M. D., Al-Rawashdeh, A., & Powers, D. (2012). "Field Evaluation of Warm-Mix Asphalt Technologies," *Journal of Materials in Civil Engineering*, 24(11), pp 1343-1349.
- Shen, S., Wu, S., Zhang, W., Mohammad, L., & Muhunthan, B. (2017). *Long-Term Field Performance of Warm Mix Asphalt Technologies*. Pre-publication draft of NCHRP Report 843.
- Shen, S., Zhang W., Wu, S., Mohammad L. N., & Muhunthan, B. (2018). "Long-term Field Performance of Flexible Pavements Using Warm Mix Asphalt Technologies". *Journal of the Association of Asphalt Paving Technologists*, 87, pp.
- Smith, B.T., Howard, I.L., Moore, R.A. (2018). *Columbus Mississippi Field Aging and Laboratory Conditioning Study: Plant Mixed and Field Compacted Asphalt Test Sections*. Report FHWA/MS-DOT-RD-18-266/270-Volume 2, Mississippi Department of Transportation.
- Smith, B.T., Howard, I.L. (2019). "Comparing Laboratory Conditioning Protocols to Longer-Term Aging of Asphalt Mixtures in the Southeast United States," *Journal of Materials in Civil Engineering*, 31(1), 04018346.
- Suleiman, N., & Mandal, S. (2013). "Evaluating the Rut Resistance Performance of Warm Mix Asphalts in North Dakota," CD-ROM, *Transportation Research Board 92nd Annual Meeting*, Washington, D.C. Paper 13-4855.
- Tunncliff, D. G., & Root, R. E. (1984). *Use of antistripping additives in asphaltic concrete mixtures*. NCHRP Report 274.
- Vaiana, R., Iuele, T., & Gallelli, V. (2013). "Warm Mix Asphalt with Synthetic Zeolite: A Laboratory Study on Mixes Workability," *International Journal of Pavement Research and Technology*, 6(5), 562-569.
- Vaitkus, A., Čygas, D., Laurinavičius, A., Vorobjovas, V., & Perveneckas, Z. (2016). "Influence of Warm Mix Asphalt Technology on Asphalt Physical and Mechanical Properties," *Construction and Building Materials*, 112, pp 800-806.
- Wielinski, J., Hand, A., & Rausch, D. (2009). "Laboratory and Field Evaluations of Foamed Warm-Mix Asphalt Projects," *Transportation Research Record: Journal of the Transportation Research Board*, 2126, pp 125-131.
- Wu, S., Zhang, W., Shen, S., Li, X., Muhunthan, B., & Mohammad, L. N. (2017). "Field-Aged Asphalt Binder Performance Evaluation for Evotherm Warm Mix Asphalt: Comparisons with Hot Mix Asphalt," *Construction and Building Materials*, 156, 574-583.
- Xiao, F., Amirhanian, S., & Putman, B. (2009) "Evaluation of Rutting Resistance in Warm Mix Asphalts Containing Moist Aggregate," *Transportation Research Record: Journal of the Transportation Research Board*, 2126, pp. 115-124

- Xiao, F., Zhao, W., & Amirghanian, S. N. (2011). "Laboratory Evaluation of Effects of Soaked Duration on Moisture Susceptibility of Warm Mix Asphalt Mix," *Transportation and Development Institute Congress 2011: Integrated Transportation and Development for a Better Tomorrow*, 1, pp. 472-481.
- Xiao, F., Shivaprasad, P. V., & Amirghanian, S. N. (2012). "Low-Volume Road WMA Mixtures: Moisture Susceptibility of Mixtures Containing Coal Ash and Roofing Shingle with Moist Aggregate," *Journal of Materials in Civil Engineering*, 24(1), 48-56.
- Xiao, F., Punith, V. S., Amirghanian, S. N., & Thodesen, C. (2013). "Improved Resistance of Long-Term Aged Warm-Mix Asphalt to Moisture Damage Containing Moist Aggregates," *Journal of Materials in Civil Engineering*, 25(7), 913-922.
- Yin, F., Cucalon, L.G., Martin, A.E., Arambula, E., Chowdhury, A., & Park, E.S. (2013). "Laboratory Conditioning Protocols for Warm-Mix Asphalt," *Asphalt Paving Technology, Journal of the Association of Asphalt Paving Technologists*, 82, pp 177-212.
- Yin, F., Cucalon, L.G., Martin, A.E., Arambula, E. & Park, E.S. (2014). "Performance Evolution of Hot-Mix and Warm-Mix Asphalt with Field and Laboratory Aging," *Asphalt Paving Technology, Journal of the Association of Asphalt Paving Technologists*, 83, pp 109-142.
- Yin, F., Arámbula-Mercado, E., Epps Martin, A., Newcomb, D., & Tran, N. (2016). "Long-Term Ageing of Asphalt Mixtures," *Road Materials and Pavement Design*, 18(sup1), 2-27.
- Zaniewski, J., & Viswanathan, A. G. (2006). *Investigation of Moisture Sensitivity of Hot Mix Asphalt Concrete*. Asphalt Technology Program, West Virginia University, Morgantown, WV.
- Zeleeuw, H., Paugh, C., Corrigan, M., Belagutti, S., & Ramakrishnareddy, J. (2013). "Laboratory Evaluation of the Mechanical Properties of Plant-Produced Warm-Mix Asphalt Mixtures," *Road Materials and Pavement Design*, 14(1), pp 49-70.